INVESTIGATING THE MECHANISMS OF RESISTANCE TO DUAL PI3K/MTOR INHIBITIOR IN PIK3CA MUTANT BASAL LIKE BLADDER CANCER

May F. M. Elbanna

Submitted to the faculty of the University Graduate School

in partial fulfillment of the requirements

for the degree

Doctor of Philosophy

in the Department of Pharmacology & Toxicology,

Indiana University

March 2019

Accepted by the Graduate Faculty, of Indiana University, in partial fulfillment of the requirements for the degree of Doctor of Philosophy.

Doctoral Committee

_____

Roberto Pili, M.D., Co-Chair

_____

Travis Jerde, Ph.D., Co-Chair

_____

Jian-Ting Zhang, Ph.D.

July 10, 2018

_____

Tao Lu, Ph.D.

_____

Melissa Fishel, Ph.D.

DEDICATION

This dissertation is dedicated to my exceptional mother, Naglaa Elsayed, whose continuous support and guidance led me to where I am today. She continued to believe in me despite all my shortcomings and she was always brave enough to push me to my limits. If it were not for her, this journey would have not been possible.

It is also dedicated to my amazing family, my dad who endured the absence of my mom for months so that she can be by my side, my dear husband, Ahmed, who always encouraged me to do my best, my brothers, Mohamed and Ahmed who make me a proud sister and lastly my two beautiful kids, Talia and Omar who endured days and nights of my absence to be able to accomplish this work. I hope they will be proud of me and that this journey would inspire them to be dedicated and accomplished humans themselves. For having this family, I am indeed very grateful.

Lastly, I would like to dedicate this work to cancer patients all over the world, hoping that it would contribute to improving their prognosis and alleviating their pain.

ACKNOWLEDGMENTS

First and foremost, I would like to thank my mentor, Dr. Roberto Pili for the guidance and support he has always provided me throughout my time in lab. He always encouraged me to come up with my own ideas and believed in my ability to implement them. He trained me and other lab members to be independent thinkers and gave us the courage to pursue our dreams inside and outside the lab through multiple opportunities of networking. He inspired me throughout the years as a physician scientist, a well-rounded clinician who has tremendous passion for serving patients through science. I hope one day my training under his mentorship will enable me to be a physician scientist myself.

I would like to sincerely thank my research committee members, Drs. Travis Jerde, Jian-Ting Zhang, Tao Lu, and Melissa Fishel, exceptional scientists who have given me immense support and guidance throughout my Journey. I would not have made it through my transition to Indiana University, if it were not for their help and support. I am very grateful for being part of the Pharmacology program at Indiana University, a vibrant school where bench science efficiently meets clinical practice.

I would like to thank members of the Pili lab, who all come from different backgrounds and cultures and thus created a vibrant learning environment not only with respect to science but also at the personal level. I am especially thankful to Dr. Sreenivasulu Chintala and Dr. Eric Ciamporcero for training me

through my beginnings in the lab and sharing with me some of the preliminary data that helped me start this project.

I would like to thank Dr. Melissa Fishel and members of her lab for sharing with me their three dimensional cell culture protocols and helping me set up a similar model for bladder cancer. I would also like to extend my deepest gratitude to Dr. Tao Lu and her graduate student Anjta-Voy Hartley for helping me through transfection experiments and molecular biology techniques. I am also grateful for Dr. Jun Wan at the C3B Bioinformatics core, Indiana University for the help and guidance he has offered in analyzing the DNA methylation data from our models.

It was a privilege to start my journey in the USA at Roswell Park Cancer Institute in Buffalo, NY and then move to IU. This has enabled me to experience different academic environments and cities. I am very grateful for the Roswell Park family for supporting me throughout my initial steps in the USA and for encouraging me to move to IU to follow my passion for the science in Dr. Pili's lab.

I would also like to acknowledge the Fulbright Commission for their support throughout my studies. It was indeed an honor to carry out my PhD studies in the USA as a Fulbright Scholar.

Lastly, I would like to thank my friends and family both in Egypt and the USA who have made this journey special. I am very grateful both for being able

to carry out amazing science and also for trying to create a bridge between cultures throughout an exceptional journey that made me a better person.

May F. M. Elbanna

INVESTIGATING THE MECHANISMS OF RESISTANCE TO DUAL PI3K/MTOR INHIBITOR IN PIK3CA MUTANT BASAL LIKE BLADDER CANCER

Muscle invasive bladder cancer (MIBC) carries a poor prognosis where the overall 5 year survival ranges from 48% to 66%. To date, targeted therapies, except for immune checkpoint inhibitors have not been shown to be effective in the management of this disease, where conventional chemotherapy (i.e. cisplatin) continues to be the standard of care. Therefore, the challenge lies in identifying key molecular events that can predict response to targeted therapies and thereby provide patients with maximal clinical benefit.

Using two MIBC patient derived xenograft models (PDX) that carry alterations in PI3K signaling, one of the most dysregulated signaling pathways in bladder cancer, we studied determinants of response to PI3K targeted inhibition and mechanisms of resistance.

We found that PIK3CA mutation status as well as tumor subtype (luminal-like or basal-like) play cooperative role in driving treatment response, where PIK3CA E542K mutation in basal-like tumors is associated with resistance to PI3K inhibition. Resistance is driven by feedback activation of alternative feedback signaling such as RAS-MAPK pathway.

Based on the mechanistic changes induced upon resistance, we tested different drug combinations that can overcome resistance to PI3K targeted inhibition. Interestingly, we observed bromodomain inhibition by JQ1 to be the most effective strategy to re-sensitize resistant cells to PI3K targeted therapy.

Overall, this project provides a predictive paradigm of response to PI3K targeted inhibition in PIK3CA mutant MIBC and sets the stage for future rational clinical trial design.

Roberto Pili, M.D., Co-Chair

Travis Jerde, Ph.D., Co-Chair

TABLE OF CONTENTS

LIST OF TABLES

LIST OF FIGURES

LIST OF ABBREVIATIONS

3D:	Three-dimensional
BET:	Bromodomain
BID:	Twice per day
CDK:	Cyclin-dependent kinase
CK:	Cytokeratin
Combo:	Combination
COMPASS:	Complex of proteins associated with Set1
DEGs:	Differentially Expressed Genes
DMSO:	Dimethyl sulfoxide
DMRs:	Differentially Methylated Regions
ECM:	Extracellular matrix
EGFR:	Epidermal Growth Factor Receptor
EMT:	Epithelial Mesenchymal Transition
EOT:	End of Treatment
FBS:	Fetal bovine serum
FGF:	Fibroblast growth factor
FGFR3:	Fibroblast growth factor receptor-3
GFP:	Green Fluorescent Protein
GO:	Gene Ontology
HD:	Helical domain
H&E:	Hematoxylin and eosin
hEGF:	Human epidermal growth factor

HEK:	Human Embryonic Kidney Cells
hFGF:	Human fibroblast growth factor
HIF*1α:*	Hypoxia-inducible factor 1α
IF:	Immunofluorescence
IHC:	Immuno-histochemistry
IPA:	Ingenuity Pathway Analysis
KD:	Kinase Domain
LOH:	Loss of Heterozygosity
LY-414:	LY3023414
MAPK:	Mitogen activated protein kinase
MDS:	Molecular Dynamic Simulation
MIBC:	Muscle Invasive Bladder Cancer
MTT:	3-(4,5-Dimethylthiazol-2-yl)-2,5-Diphenyltetrazolium Bromide
MUT:	Mutant
NC:	Negative control
NMIBC:	Non Muscle Invasive Bladder Cancer
PAGE:	Polyacrylamide gel electrophoresis
PBS:	Phosphate buffered saline
PDX:	Patient Derived Xenografts
PDB:	Protein Data Bank
PPAR-γ:	Peroxisome proliferator-activated receptor-γ
PPI:	Protein-Protein Interaction
PRC1/2:	Polycomb repressive complex 1 and 2

RFP:	Red Fluorescent Protein
RMSD:	Root-mean-square deviation of atomic positions
RMSF:	Root mean square fluctuation
RSK:	Ribosomal S6-Kinase
RTK:	Receptor Tyrosine Kinases
SCC:	Squamous Cell Carcinoma
SCID:	Severe Combined Immunodefeciency
SNPs:	Single Nucleotide polymorphisms
SNVs:	Single Nucleotide Variants
SV-HUC:	SV40 transformed Human Urothelial Cells
TCGA:	The Cancer Genome Atlas
TSS:	Transcription Start Site
WB:	Western Blotting
WT:	Wild Type
VAF:	Variant Allele Fraction
xCT:	Cysteine Receptor

CHAPTER I. INTRODUCTION

A. Bladder cancer overview

Bladder cancer is the fourth most common malignancy in men and the eleventh most common in women worldwide with 74000 patients diagnosed with the disease in the USA and more than 430000 patients all over the world (Howlader, Noone et al. 2012, Kamat, Hahn et al. 2016). Age is the most significant risk factor for bladder cancer where median age at diagnosis is ~70 years(Knowles and Hurst 2015, Malats and Real 2015). There is gender disparity in bladder cancer incidence where the male: female ration is 3:1. However, women tend to have more advanced disease at diagnosis and worse prognosis (Horstmann, Witthuhn et al. 2008, Zhang 2013, Dobruch, Daneshmand et al. 2016). It is still not well established whether hormonal signaling such as AR expression plays a role in this behavior with respect to both incidence as well as prognosis(Lombard and Mudryj 2015, Kashiwagi, Ide et al. 2016, Chen, Cui et al. 2017, Li, Chen et al. 2017).

Genetic predisposition is not obvious in the majority of bladder cancer cases. However, genome wide association studies have identified some single-nucleotide polymorphisms (SNPs) that are associated with increased cancer risk(Gu and Wu 2011). Interestingly, candidate genes close to the SNPs include, *MYC*; *TP63*; prostate stem cell antigen (*PSCA*); telomerase reverse transcriptase (*TERT*)–CLPTM1-like (*CLPTM1L*); fibroblast growth factor receptor 3 (*FGFR3*); apolipoprotein B mRNA-editing enzyme catalytic polypeptide-like 3A

(*APOBEC3A*). Many of these genes are well known for their key role in bladder cancer pathogenesis

Another key risk factor in this disease is smoking and other forms of environmental exposure(Malats and Real 2015). This is probably one of the reasons why bladder cancer is in a unique position, where it is only next to melanoma and lung cancer in terms of mutation burden(Kim, Akbani et al. 2015).

B. Histological subtypes of bladder cancer

Bladder cancers are predominantly urothelial carcinomas. Other histological types include squamous, adenocarcinoma, micropapillary, small cell and plasmacytoid. In regions where the incidence of schistosomiasis is high, squamous cell carcinoma is more common, and bladder cancer may be the cancer of highest incidence(Reuter 2006). The association between schistosomiasis and squamous bladder cancer have been attributed to many factors most notably are higher levels N-nitroso compounds in addition to local inflammation induced by the parasitic infestation and higher incidence of host DNA damage (Mostafa, Sheweita et al. 1999).

Urothelial carcinomas are divided into two main entities; non muscle invasive bladder cancer (NMIBC) which represents around 75% of the cases and for which grade is the main prognostic factor. The other entity is muscle invasive

bladder cancer (MIBC) which represents around 25% of the cases and is mainly prognosticated by stage (Kamat, Hahn et al. 2016).

Taking into account, the distinct histological features of both entities and the associated molecular events, a two pathway model has been proposed (Spruck, Ohneseit et al. 1994, Wu 2005, Zhu, Blenis et al. 2008). This model dominated the field for years as the key paradigm describing the key molecular events involved in bladder cancer pathogenesis (Knowles and Hurst 2015). According to this model, NMIBC and MIBC are two distinct subtypes with a distinct natural history, where NMIBC is largely composed of frequently recurring low grade papillary tumors that arise from simple hyperplasia and minimal dysplasia that are molecularly characterized by loss of heterozygosity (LOH) of chromosome 9 and gain of function mutations in fibroblast growth factor receptor 3 (*FGFR3*), *PIK3CA* (which encodes p110α of PI3K) and stromal antigen 2 (*STAG2*). On the other hand, MIBC are high grade, non-genetically stable tumors that are thought to develop from flat dysplasia and carcinoma in situ (CIS) commonly induced by TP53 mutations in addition to chromosome 9 deletions but no *FGFR3* mutations(Knowles 2008, Knowles and Hurst 2015).

C. Novel Bladder cancer molecular subtypes

The two pathway model previously described was incapable of explaining the great deal of tumor heterogeneity observed with the two main subtypes:

NMIBC and MIBC. Therefore, a lot of research was focused on identifying a better model for understanding bladder cancer pathogenesis.

Bladder cancer was therefore classified into three entities based on the standard paradigm of urothelial differentiation(Volkmer, Sahoo et al. 2012). Importantly, immune-histochemical staining (IHC) for cytokeratin14 was used to determine those distinct subtypes defined as: CK14 high, CK14 intermediate and CK14 low. Among those three groups, CK14 high group which was largely comprised of basal-like tumors; had the worst survival irrespective of stage and grade (Chan, Espinosa et al. 2009, Volkmer, Sahoo et al. 2012).

Next to the consideration of cell of origin in bladder cancer pathogenesis, a more comprehensive effort was focused on identifying key molecular and transcriptomic alterations in the disease. Sjödahl et al. (Sjödahl, Lauss et al. 2012) identified five major subtypes termed urobasal A (UroA), UroB, genomically unstable (GU), squamous cell carcinoma-like (SCCL) and ‘infiltrated’ (which is highly infiltrated with non-tumor cells). This was subsequently supported by three independent groups which focused on MIBC and identified similar subtypes, that specially overlapped with respect to the two major subtypes; basal like and luminal like (Sjödahl, Lauss et al. 2012, Choi, Porten et al. 2014, Damrauer, Hoadley et al. 2014, Network 2014, Robertson, Kim et al. 2017).

Luminal MIBCs were found to be enriched for uroplakins, KRT20, ERBB2 forkhead box A1 (FOXA1; also known as HNF3α), GATA-binding protein 3 (GATA3), tripartite motif-containing protein 24 (TRIM24) and peroxisome proliferator-activated receptor-γ (PPARγ). Luminal MIBCS were largely of papillary morphology and harbored FGFR3 alterations (amplification and/or mutation).

On the other hand, basal MIBCs expressed basal markers (KRT5, KRT6, KRT14, CD44 and CDH3). They were either of squamous pathology or had a high degree of squamous differentiation. In all studies cited(Choi, Porten et al. 2014, Damrauer, Hoadley et al. 2014, Network 2014, Eriksson, Rovira et al. 2018), patients with this subtype had the worst prognosis. Transcription factors implicated in this subtype were those known to be active in the basal/stem cell compartment of the normal urotheilum, including: signal transducer and activator of transcription 3 (STAT3), nuclear factor-κB (NF-κB), hypoxia-inducible factor 1 (HIF1) and p63. This finding echoes the preliminary subtype focused studies which utilized normal differentiation paradigm of the bladder as guide for bladder cancer subtyping.

It is important to note that Damraeur et al. (Damrauer, Hoadley et al. 2014) proposed a link between the transcription profile of bladder and breast cancer subtypes. Interestingly, they also proposed a classifier of 47 genes (Base47) that can be applied to stratify tumors according to subtype. However,

the clinical utility of this classifier is yet to be determined (Kamat, Hahn et al. 2016).

D. Molecular alterations in bladder cancer

D.1.1. Genomic instability and chromosomal alterations

MIBCs are characterized by high degree of genomic instability and chromosomal alterations in comparison to NMIBC. MIBC is known to harbor inactivating mutations in genes involved with DNA damage/repair pathway such as: excision repair cross-complementation group 2 (*ERCC2*), ataxia-telangiectasia mutated (*ATM*) and Fanconi anaemia complementation group A (*FANCA*). Such alterations in addition to mutations in the cohesin complex which is known to play key role in chromosome segregation plays a role in the high degree of genomic instability of bladder cancer(Knowles 2008, Knowles and Hurst 2015).

Chromosome 9 deletion in MIBC is associated with loss of key tumor suppressor genes such as cyclin-dependent kinase inhibitor 2A (*CDKN2A*; which encodes p16 and p14ARF) and *CDKN2B* (which encodes p15) at 9p21 and tuberous sclerosis 1 (*TSC1*) at 9q34(Platt, Hurst et al. 2009, Sjödahl, Lauss et al. 2011). TSC1 is part of the TSC1–TSC2 complex which negatively regulates the PI3K/mTOR signaling, a key deregulated pathway in bladder cancer. Loss of heterozygosity (LOH) of 9p, homozygous deletion of *CDKN2A* and loss of

expression of p16 in NMIBC are predictors of reduced recurrence-free interval (Bartoletti, Cai et al. 2007, Ploussard, Dubosq et al. 2010).

D.1.2. Mutation load in bladder cancer and signaling alterations

As previously stated, the mutation frequency in bladder cancer is only exceeded by melanoma and lung cancer which accounts for the immense heterogeneity in this disease that cannot be readily explained through the molecular two pathway model(Kim, Akbani et al. 2015). While tobacco smoking is a very strong environmental risk factor for bladder cancer; a smoking related mutation signature has not been found in the disease(Kim, Mouw et al. 2016).

The most frequently mutated pathways in bladder cancer include:

FGFR signaling alterations (mutations or upregulation) are predominantly found in low grade papillary tumors (Ta) with much less frequency in T1 tumors and MIBC. Although Ta tumors are generally associated with a good prognosis, the presence of FGFR mutations is associated with higher recurrence(Brooks, Kilgour et al. 2012, Knowles and Hurst 2015).

PI3K signaling is one of the key pathways that are highly deregulated in bladder cancer (Shah, McConkey et al. 2011, Network 2014, Robertson, Kim et al. 2017). Aberrant activation of PI3K signaling can occur either indirectly through alterations in tyrosine kinases (EGFR/FGFR) or directly through alterations in the pathway itself(Knowles, Platt et al. 2009, Platt, Hurst et al. 2009).

Aberrant PI3K signaling is driven by activating PIK3CA mutations in 25% of bladder cancer cases(Network 2014). The most common PIK3CA activating mutations are single amino acid substitutions that occur either in the helical domain (HD) (E545K, E542K) or kinase domain (KD) (H1047R)(Knowles, Platt et al. 2009, Platt, Hurst et al. 2009). Functional studies have shown different mechanisms of activation by helical and kinase domain mutations, where H1047R KD mutation is dependent on P85 binding but not on RAS binding for the enzymatic activation of PI3K, however the opposite holds true for HD mutations (Zhao and Vogt 2008).

Unlike most solid tumors, bladder cancer holds a unique position where PIK3CA HD mutations are more common compared to KD mutations; accounting for 80% of cases driven by PIK3CA activating mutations(Platt, Hurst et al. 2009, Network 2014). In Bladder cancer, the selective pressure for HD mutations is not yet understood and therefore a possible role of distinct HD mutations in predicting response to PI3K pathway targeted therapy is yet to be determined (Knowles, Platt et al. 2009, Platt, Hurst et al. 2009).

Interestingly, in bladder cancer PIK3CA helical domain mutations are not exclusively coexistent with RAS mutations; therefore RAS activation cannot always explain resistance to therapy targeting this pathway. In some instances, double mutations were identified in PIK3CA; one case with a HD and a KD domain mutation, and one case with two mutations in the HD domain (E542K

E545K); indicating an additive, non-redundant effect of multiple PIK3CA mutations in this disease(Sjödahl, Lauss et al. 2011).Other alterations in PI3K signaling in bladder cancer involve: LOH in the lipid and protein phosphatase PTEN which negatively regulates PI3K and *TSC1* mutation(Knowles and Hurst 2015).

MAPK signaling in bladder cancer, its role in disease pathogenesis and its cross talk with other key altered pathways in the disease (i.e. PI3K signaling), are still not clear (Knowles and Hurst 2015).

For instance, FGFR3 mutations have been shown to activate MAPK but not PI3K signaling in urothelial cells(Di Martino, L'hôte et al. 2009). This finding resonates with the mutual exclusivity of RAS (*HRAS* or *KRAS*) and *FGFR3* mutations in bladder cancer. On the other hand, *FGFR3* mutation and *PIK3CA* mutation commonly co-occur in NMIBC (Kompier, Lurkin et al. 2010, Juanpere, Agell et al. 2012); suggesting a cooperative cross talk between MAPK and PI3K pathways. It is yet to be determined whether the PI3K-MAPK cross talk is preferentially activated by distinct PIK3CA mutations in bladder cancer.

E. Epigenetic alterations in bladder cancer

E.1. Histone modifications and chromatin modifying genes

The heterogeneity of bladder cancer and the high incidence of mutations stresses the importance of taking into account not only the cooperative cross talk

between aberrant signaling pathways, but also the possible cooperative role between aberrant signaling and epigenetic modifications (Kim, Akbani et al. 2015).

Epigenetic balance is crucial to orchestrating gene expression and therefore plays a key role in development, neoplastic pathogenesis and resistance to therapy(Kim, Akbani et al. 2015, Piunti and Shilatifard 2016).

Interestingly, MIBC has the highest incidence of mutations in chromatin modifying genes among all tumors (89%)(Gui, Guo et al. 2011). Loss of function mutations in a large number of chromatin modifying genes are highly enriched in bladder cancer; most notably are mutations in Lysine Methyltransferase 2D (KMT2D) and Lysine Demethylase 6A (KDM6A) which were interestingly found to be mutually exclusive, indicating either redundant downstream effects or a synthetically lethal effect of combined loss (Gui, Guo et al. 2011, Network 2014).

Both KMT2D and KDM6A are members of the complex of proteins associated with Set1 (COMPASS) family where KMT2D acts as H3K4 methyl transferase while KDM6A acts as a H3K27 demethylase. Opposing roles played by the members of COMPASS family and members of other epigenetic families such as the polycomb repressive complex 1 and 2 (PRC1 and PRC2) maintain epigenetic balance(Piunti and Shilatifard 2016).

KMT2D (MLL3/4) mono-methylates enhancers at lysine 4 of histone 3 in coordination with the demethylation function of KDM6A (UTX) at lysine 27 of histone 3 which counteracts the H3K27 me2/3 repressive mark deposited by PRC2 and thus possibly favors H3K27 acetylation by histone acetyltransferases (HATs) CBP/P300. H3K27 acetylation is thought to induce expression of transcriptionally poised genes when added. However, the role of transcriptional co-regulation undertaken by histone methyltransferases (KMT2D) and demethylases (KDM6A) in carcinogenesis remains largely unknown (Kim, Sharma et al. 2014, Piunti and Shilatifard 2016).

Earlier reports have suggested possible significant prevalence of KMT2D mutations in non-papillary high grade bladder cancer as opposed to papillary low grade tumors where mutations in demethylases (KDM6A) are more prevalent (Gui, Guo et al. 2011, Kim, Akbani et al. 2015, Kamat, Hahn et al. 2016). This dichotomy resonates with the mutual exclusivity observed in the TCGA data with regard to mutations in those two chromatin modifying genes(Network 2014). However, a conclusive relation between KMT2D and KDM6A mutations and basal and luminal subtypes of bladder cancer respectively is yet to be determined.

Overall, the role of genetically determined phenotypic variation in bladder cancer in driving resistance to therapy remains underexplored. It is therefore important to understand how mutations in chromatin modifying genes could

influence bladder carcinogenesis and subsequently influence therapeutic response.

E.2. DNA methylation

Bladder cancer is known for extensive DNA methylation changes, many of which have clinic-pathological associations (Sánchez-Carbayo 2012). DNA methylation pattern is distinct between NMIBC and MIBC (Wolff, Chihara et al. 2010, Lauss, Aine et al. 2012), where NMIBC is characterized by distinct patterns of hypomethylation in non-CpG islands; while MIBC is characterized by widespread CpG island hypermethylation. This provides a proof of concept that epigenetic alterations in addition to other molecular alterations previously discussed play a key role in bladder cancer pathogenesis that has not been explained by the simplistic two pathway model.

Interestingly, the distinct DNA methylation pattern is not only characteristic of MIBC VS NMIBC, but also related to distinct MIBC subtypes that have recently been proposed (i.e. basal VS luminal)(Network 2014).

The dogma is that hypermethylation in promoters is associated with silencing of gene expression; on the other hand hypomethylation within gene bodies is usually associated with upregulated expression(Lauss, Aine et al. 2012). Gene body hypomethylation in some tumors such as medulloblastoma have been linked to histone H3 lysine 4 (H3K4) trimethylation, a marker of open chromatin; that is known to be deposited by KMT2D, an enzyme that is

significantly altered in bladder cancer(Knowles and Hurst 2015). This mandates further research into the multiple layers of gene regulation at the epigenetic level.

F. Management of bladder cancer

Patients with NMIBC are mainly managed by trans-urethral tumor resection followed by intravesical chemotherapy in low/intermediate risk categories or immunotherapy (i.e. Bacillus Calmette-Guerin (BCG)) in high risk NMIBC(Kamat, Hahn et al. 2016). BCG is made from a weakened strain of Mycobacterium bovis, a vaccine for tuberculosis. Whereas, the standard of care in MIBC is comprised of neoadjuvant cisplatin based chemotherapy followed by radical cystectomy and bilateral pelvic lymphadenectomy(Kamat, Hahn et al. 2016).

To date, besides anti PD-1/PD-L1 therapies(Sundararajan and Vogelzang 2015), specific targeted therapies have not been approved for the management of this disease; where conventional platinum-based chemotherapy continues to be the standard of care(Leow, Martin-Doyle et al. 2014, Lobo, Mount et al. 2017).

Recently, efforts aimed at improving the understanding of the disease at the molecular level have led to a spur in preclinical drug development research focused on various significant targets in the disease such as: EGFR, VEGF, FGFR, androgen receptor and CD24(Van Kessel, Zuiverloon et al. 2015).

Interestingly, EGFR targeted therapy which once failed to show significant improvement in patient survival in clinical studies(Philips, Halabi et al. 2009, Pruthi, Nielsen et al. 2010, Wong, Litwin et al. 2013) was shown to provide significant therapeutic response in basal-like but not luminal-like bladder tumors in a recent preclinical study that was informed by the novel genetically guided stratification of bladder cancer patients. This was predominantly attributed to overexpression of EGFR in basal-like but not luminal-like MIBC (Rebouissou, Bernard-Pierrot et al. 2014).

Taken together, this highlights the gap in the bladder cancer field that shall benefit from current novel molecular findings which would ultimately improve the outlook for targeted therapy in this disease setting.

F.1. PI3K targeted therapy in bladder cancer

A recent attempt at comprehensive molecular characterization of bladder cancer has identified PI3K pathway as one of the most frequently dysregulated signaling pathways in this disease (25% of cases). PIK3CA (HD) mutations are the most frequent alterations in this pathway (20% of cases with PI3K pathway activation) in comparison to other alterations (i.e. TSC mutations, PTEN mutations, AKT amplification) (Network 2014, Robertson, Kim et al. 2017). There is also extensive cross talk between PI3K/mTOR signaling and other key signaling pathways in bladder cancer such as MAPK and Wnt signaling(Knowles and Hurst 2015). Additionally, it has been shown to be involved in resistance to

cisplatin-based chemotherapy(Peng, Wang et al. 2010); therefore it is considered to be an attractive therapeutic target.

Despite the centrality of this pathway to bladder cancer pathogenesis, few trials have investigated the utility of PI3K/mTOR inhibitors in bladder cancer management. Most of the existing trials investigated mTOR inhibitor, everolimus. Retrospective analysis of everolimus specific responses found a TSC1 inactivating mutation in most of the responders. This finding stresses the promise of PI3K/mTOR targeting agents in the clinic when used in molecularly susceptible patients (Iyer, Hanrahan et al. 2012, Seront, Rottey et al. 2012).

It is important however to note that TSC1 inactivating mutations in bladder cancer are far less common than PI3KCA HD mutations(Knowles, Platt et al. 2009, Platt, Hurst et al. 2009). Nonetheless, only two bladder cancer trials have been found to utilize novel PI3K inhibitors (Munster, Aggarwal et al. 2015) and (NCT01551030) which utilized GSK2126458 (dual PI3K/mTOR inhibitor) and BKM120 (PI3K inhibitor) respectively**.** Therefore, the significance of PIK3CA HD mutations in terms of predicting therapeutic response is yet to be determined.

There is indeed anecdotal data that suggest that PIK3CA mutation status can predict response to PI3K targeted therapy. Patients with wide range of solid tumors who were treated with PI3K targeted therapy concluded that patients with a PIK3CA H1047R mutation had a higher partial response (PR) rate (38% vs.

10%; p=0.018) and a trend towards having a longer median progression free survival (PFS) (5.7 months vs. 2 months; p=0.06) compared to patients with helical PIK3CA mutations treated on the same protocols. On the other hand, patients with E542K HD mutations had a trend towards worse PFS compared to patients with E545K HD mutations (Janku, Tsimberidou et al. 2011, Janku, Wheler et al. 2013).

However, it is important to interpret retrospective data cautiously and to take into account the innate tumor heterogeneity that provides another layer of complexity and has shown in many studies to play a role in driving response to treatment irrespective of mutation status (Guo, Chekaluk et al. 2013).

F.2. Resistance to PI3K targeted therapy

PI3K/mTOR signaling is involved in highly complex signaling networks in both tumorigenic and non-tumorigenic cells which hampered the clinical utility of PI3K targeting agents. Dose limiting toxicities such as stomatitis, noninfectious pneumonitis, rash, hyperglycemia, and immunosuppression have been a major issue with PI3K targeting agents(Chia, Gandhi et al. 2015). In addition; the centrality of this pathway led to resistance through feedback signaling (Brown and Toker 2015).

One of the key resistance mechanisms to PI3K targeted inhibition is feedback reactivation of PI3K signaling. Studies have shown that PI3K inhibition

is associated with activation of multiple receptor tyrosine kinases in a FOXO-dependent manner (Chakrabarty, Sánchez et al. 2012). Similarly, mTOR inhibition is associated with feedback activation of PI3K signaling through stimulations of receptor tyrosine kinases(O'Reilly, Rojo et al. 2006).

Although dual PI3K/mTOR inhibition was proposed in order to overcome the previously mentioned mechanisms of resistance that have been reported when targeting either PI3K or mTOR separately; it was not optimal. A study has reported JAK2/STAT5 activation which promoted feedback AKT activation in the context of dual PI3K/mTOR inhibition (Britschgi, Andraos et al. 2012).

Additionally, chronic exposure of a breast cancer cell line to PI3K inhibitor GDC-0941 was associated with PIK3CA amplification and therefore feedback activation of PI3K signaling (Huw, O'brien et al. 2013). Whether this happens in patient treated with PI3K inhibitors is not yet known. However, it has been reported that patients treated with mTOR inhibitor everolimus develop mTOR mutations that lead to resistance (Wagle, Grabiner et al. 2014).

Another mechanism by which resistance to PI3K targeted inhibition develops is the concurrent activation of alternative signaling pathways. It has been shown that PI3K inhibition leads to feedback activation of MAPK signaling and therefore better therapeutic outcome upon combined MAPK-PI3K inhibition (Carracedo, Ma et al. 2008, Serra, Scaltriti et al. 2011). This highlights the

importance of understanding the PI3K-MAPK cross talk bladder cancer which is not yet well characterized. Similarly, ribosomal S6-Kinase (RSK) has been shown to be an alternative signaling route upon PI3K inhibition(Serra, Eichhorn et al. 2013).

MYC amplification has also been proposed as a mechanism of resistance specifically in the context of PIK3CA mutant tumors (Zhu, Blenis et al. 2008, Ilic, Utermark et al. 2011, Liu, Cheng et al. 2011, Muellner, Uras et al. 2011, Dey, Leyland-Jones et al. 2015) which is important to consider in bladder cancer given the high incidence of therapeutic resistance in basal-like bladder cancer where MYC is amplified(Choi, Porten et al. 2014).

Recent reports have also shown that MYC-driven resistance to PI3K pathway targeted therapy can be epigenetically driven through sustained bromodomain (BRD4) binding at chromatin regulatory regions of insulin receptor, EGFR family RTKs and MYC driving their expression and thus signaling (Stratikopoulos and Parsons 2016).

F.3. Overcoming resistance to PI3K targeted therapy: rational drug combinations

PI3K driven preclinical models such as genetically engineered mouse models or patient derived xenograft models have continuously provided an invaluable tool for testing drug combination regimens to develop rational treatment strategies that would improve treatment outcomes in the clinic.

A wide range of combinations have been proposed to sensitize cancer cells to PI3K targeted inhibition. These combinations include: combined PI3K/MAPK inhibition(Carracedo, Ma et al. 2008), combined PI3K/CDK4/6 inhibition (Bonelli, Digiacomo et al. 2017) and combined targeting of PI3K signaling and DNA damage response (i.e. PARP) in genetically susceptible tumors (i.e. BRCA deficient)(Juvekar, Burga et al. 2012). The choice of the optimal combination would therefore be dependent on the molecular make up of each cancer diagnosis either with respect to site or subtype.

More recently, studies have looked at the possibility of combining PI3K inhibitors with bromodomain (BET) inhibitors; an approach that target the epigenome in an attempt to have a more global effect. Bromodomain targeting has been shown to suppress MYC expression which is either induced upon resistance to PI3K targeted therapy (Zhu, Blenis et al. 2008, Ilic, Utermark et al. 2011, Dey, Leyland-Jones et al. 2015, Stratikopoulos, Dendy et al. 2015) or inherently amplified in a subset of tumors (Dey, Leyland-Jones et al. 2015). A dual PI3K-BET inhibitor that can overcome resistance to PI3K targeted therapy that is usually multi-factorial and therefore difficult to tackle has been developed (Stratikopoulos, Dendy et al. 2015, Stratikopoulos and Parsons 2016, Andrews, Singh et al. 2017).

In summary, PI3K signaling is central to bladder cancer pathogenesis which poses this pathway as an attractive therapeutic target. However,

therapeutic resistance eventually develops. A better understanding of the molecular determinants of this resistance in bladder cancer is key to proposing rational drug combinations that would ultimately provide a better therapeutic outcome for patients.

G. Overview of drugs utilized in this study

G.1. LY3023414, a novel dual PI3K/mTOR inhibitor

LY3023414 is a novel imidazoquinolinone based complex designed to inhibit class I PI3K isoforms and mTOR kinase potently and selectively in an ATP competitive manner (LoRusso 2016, Smith, Mader et al. 2016). The compound was tested both *in vitro* and *in vivo* using a wide range of cancer cells lines and PDX models.

In vitro, LY3023414 was found to inhibit PI3K/mTOR signaling leading to G1 cell-cycle arrest and anti-proliferative activity in wide range of cell lines that included; PTEN deficient U87MG glioblastoma cell line, breast cancer cell lines and mesothelioma cell lines. It is important to note that no obvious correlation between LY3023414 sensitivity and any particular aberration known to activate the PI3K/AKT/mTOR pathway was detected whether this aberration was mutation, amplification or deletion (Smith, Mader et al. 2016).

LY3023414 was tested in combination with standard of care drugs such as: cisplatin, docetaxel, doxorubicin, erlotinib, gemcitabine, irinotecan, paclitaxel,

pemetrexed, rapamycin, and tamoxifen) and found to have either an additive or synergistic effect. The most significant combination effect was observed with erlotinib in pancreatic cancer and rapamycin in lung and renal cancer cell lines.

In vivo, LY3023414 showed high bioavailability and efficient modulation of downstream targets in the PI3K/mTOR signaling, i.e. dephosphorylation of AKT, S6K, S6RP, and 4E-BP1 for 4 to 6hours. Additional, daily oral administration of the drug to mice was associated with an anti-tumor effect in wide range of xenograft models tested that represented various tumor pathologies. The anti-tumor effect observed was thought to be a strong indicator of drug therapeutic effect despite non sustained target inhibition (i.e. 4-6 hours).

Currently, LY3023414 is being clinically tested in a phase I first in human dose study in patients with advanced cancer (NCT01655225), and phase II double blinded, placebo-controlled randomized phase II study of Enzalutamide with or without LY3023414 in patients with metastatic castration resistant prostate cancer (NCT02407054).

G.2. LY3214996, a novel ERK1/2 inhibitor

LY3214996 is a novel highly selective ERK1/2 inhibitor with IC50 in the nanomolar range for both ERK1 and ERK2 in biochemical assays. In an ATP competitive manner; it has been shown to potently inhibit phospho-RSK1 in BRAF and RAS mutant cancer cell lines(Bhagwat, McMillen et al. 2017).

In vitro, cells carrying MAPK pathway alterations (BRAF, NRAS or KRAS mutation) have been shown to be highly sensitive to LY3214996. *In vivo,* target modulation induced by LY3214996 (inhibition of phospho-p90RSK1), correlated with the anti-tumor effect observed in xenograft models with MAPK alterations (i.e. BRAF or NRAS mutant melanoma, BRAF or KRAS mutant colorectal, lung and pancreatic cancer xenografts or PDX models). Importantly, LY3214996 showed a significant anti-tumor effect in a model of melanoma where resistance to vemurafenib was driven by MAPK reactivation. This finding supports our rationale for testing LY3023414 (PI3K inhibitor)-LY3214996 (ERK1/2 inhibitor) combination where we found resistance to LY3023414to be partly driven by MAPK reactivation.

Interestingly, LY3214996 was previously tested in combination with investigational and standard of care drugs (i.e. CDK4/6 inhibitor abemaciclib) and was found to be well tolerated and to have a potent anti-tumor effect in wide range of human malignancies (particularly KRAS mutant tumors)(Bhagwat, McMillen et al. 2017).

LY3214996, is currently in phase I clinical trial (NCT02857270) being tested in patients with advanced and metastatic cancers.

G.3. (+)-JQ1, a BRD4-directed small-molecule inhibitor (bromodomain inhibitor)

The bromodomain and extraterminal domain (BET) family of adaptor proteins play diverse roles in transcription regulation by RNA polymerase II (Pol II) through its members; Brd2, Brd3, Brd4, and Brdt. Transcription regulation carried out by this family of epigenetic readers is done through their ability to recognize acetylated lysines on histone tails and other nuclear proteins (Dhalluin, Carlson et al. 1999, Filippakopoulos, Qi et al. 2010).

Brd4 is a well characterized member of this family. Through its interaction with TEFb, it regulates transcriptional elongation in conjunction with the acetylation state of chromatin (Jang, Mochizuki et al. 2005). Brd4 has also been shown to regulate transcription through interaction with alternative histone modifiers such as arginine demethylase Jmjd6 and the lysine methyltransferaseNsd3 and the SWI/SNF complex(Liu, Ma et al. 2013).

In 2010, (+)-JQ1, a compound with high affinity to the BET family of bromodomains (i.e. Brd4) was characterized alongside with I-BET, a similar compound developed by an independent group (Filippakopoulos, Qi et al. 2010, Nicodeme, Jeffrey et al. 2010) . (+)-JQ1 functions by displacing BET proteins (most notably, Brd4) from chromatin and thereby modulating transcription.

The therapeutic rationale for using (+)-JQ1 was first provided by a rare tumor known as NUT midline carcinoma which is driven by Brd4-NUT

oncoprotein(Filippakopoulos, Qi et al. 2010). In this disease, treatment with (+)-JQ1 led to the dissociation of Brd4-NUT complex from chromatin, inhibiting tumor growth in mice and interestingly inducing terminal squamous cell differentiation in a highly undifferentiated tumor. The observed differentiation induced by (+)-JQ1 treatment stresses the role of epigenetic changes in controlling tumor differentiation and therapeutic response.

Therapeutic benefit associated with the use of (+)-JQ1 in models of more common malignancies such as hematological malignancies shed the light on alternative oncogenic transcriptional programs that can be effectively suppressed by BET inhibition, such as MYC and BCL2 expression (Dawson, Prinjha et al. 2011, Delmore, Issa et al. 2011, Mertz, Conery et al. 2011).

However, it is important to note that transcriptional effects of bromodomain inhibitors have been proposed to be context dependent. For example, while (+)-JQ1 was found to significantly suppress MYC in leukemia cells, this was not the case in fibroblasts where (+)-JQ1 has minimal effect on MYC(Zuber, Shi et al. 2011).

Therefore, it is thought that for (+)-JQ1 to be therapeutically effective, the chromatin/epigenetic state of tumor to be treated should be taken into account. Brd4 occupancy has been shown to correlate with specific histone acetylation marks such as: H4K5, H4K8, H3K9, and H3K27 (Lovén, Hoke et al. 2013).

Additionally, tumors where (+)-JQ1 treatment is most effective in suppressing MYC are those where there is high Brd4 occupancy at nearby enhancers (Delmore, Issa et al. 2011). While MYC is expressed ubiquitously in most proliferating cell types, the enhancers that regulate this gene are highly cell type specific, therefore therapeutic outcome to bromodomain inhibition can be driven by different enhancer configurations at the MYC locus (Hnisz, Abraham et al. 2013).

Bladder cancer is unique in its epigenetic landscape with respect to DNA hypermethylation (Sánchez-Carbayo 2012) observed in advanced basal-like tumors in addition to the high load of mutations in chromatin modifying genes(Kim, Akbani et al. 2015). This sets bladder cancer as a model where (+)-JQ1 could be an attractive therapeutic agent.

Additionally, the fact that resistance to PI3K targeted therapy was attributed to MYC overexpression (Zhu, Blenis et al. 2008, Liu, Koul et al. 2009, Ilic, Utermark et al. 2011, Matkar, Sharma et al. 2015) in a wide range of tumors specifically those either driven by PI3KCA mutations or of basal subtype (i.e. triple negative breast cancer) provided rationale for testing the ability of (+)-JQ1 in overcoming resistance induced upon PI3K inhibition(Stratikopoulos, Dendy et al. 2015). More recently a dual PI3K-Brd4 inhibitor was developed to be tested for that purpose(Andrews, Singh et al. 2017).

Overall, it is important to stress that unlike MAPK inhibitors, the allure of (+)-JQ1 lies in its ability to modify epigenetically altered transcription that not only influence MYC expression but also RTKs in a more global manner.

H. Summary, Hypothesis and Specific Aims

Muscle invasive bladder cancer (MIBC) carries a poor prognosis where the overall 5 year survival ranges from 48% to 66% (Howlader, Noone et al. 2012). To date, besides anti PD-1/PD-L1 therapies (Sundararajan and Vogelzang 2015), specific targeted therapies have not been approved for the management of this disease and conventional platinum-based chemotherapy continues to be the standard of care(Leow, Martin-Doyle et al. 2014). Therefore, the challenge lies in identifying key molecular events that can constitute new targets for therapeutic interventions, and predictors of response to targeted therapies, and thereby providing patients with greater clinical benefit.

The PI3K/AKT/mTOR pathway is among the most frequently dysregulated pathways in bladder cancer (Knowles, Platt et al. 2009, Platt, Hurst et al. 2009, Knowles and Hurst 2015). Our lab has recently established two human patient-derived xenograft (PDXs) models from bladder cancer (RP-B-01 and RP-B-02). The sequencing of these two PDXs has shown that each carries distinct activating PIK3CA mutations in the helical domain HD, E542K and E545K, respectively). Both PDXs also carry the mutually exclusive mutations in two histone modifier genes, KMT2D and KDM6A, respectively. Interestingly, these

two models are biologically distinct, where one model displays a basal-like phenotype (RP-B-01) while the other is luminal-like (RP-B-02) (Ciamporcero, Shen et al. 2016, Wei, Chintala et al. 2016).

We found that therapeutic resistance to dual PI3K/mTOR inhibitors (i.e. LY3023414) occurred in the context of the basal like RP-B-01 (E542K mutant) but not in the E545K mutant model. In RP-B-01 models, resistance was associated with feedback activation of MAPK signaling (ERK phosphorylation) and stabilization of MYC.

The oncogenic transformation induced by PI3K HD mutations is known to be RAS dependent (Zhao and Vogt 2008). However, it is not yet clear whether feedback RAS-MAPK activation induced upon therapeutic resistance is preferentially driven in the context of E542K but not the E545K mutations.

The heterogeneity and high mutation burden in bladder cancer (Kim, Akbani et al. 2015) should also be taken into account as another layer of complexity that can predict therapeutic resistance to PI3K targeted therapy in the context of distinct PIK3CA mutations and distinct tumor subtypes.

The overall objective of the proposed study is to fully dissect the mechanisms of resistance to PI3K targeted therapy in PI3KCA driven basal-like bladder cancer which carries a worse prognosis and to provide a mechanistic

rationale for alternative combinatorial treatment strategies that can overcome resistance to single agent therapy.

Our central hypothesis (Figure 1) is that sensitivity or resistance to PI3K targeted therapy in bladder cancer is genetically and epigenetically driven by activation of the RAS-PI3K-MYC axis.

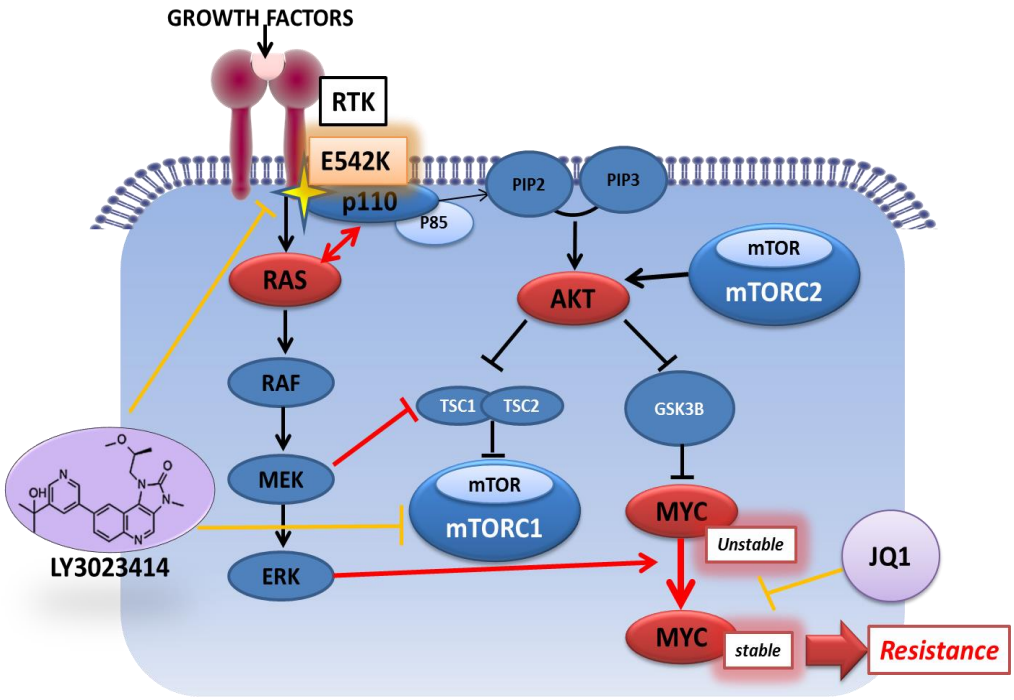

Figure 1: Proposed mechanism of resistance to dual PI3K/mTOR targeted therapy in PIK3CA *E542K MUT* Bladder cancer. Drug binding to the p110 subunit of PI3K is predicted to be less efficient with *E542K* but not *E545K* mutation leading to feedback MAPK activation which eventually leads to stabilization of MYC. This feedback signaling leads to resistance and could potentially be overcome either by combining ERK-PI3K inhibition or using a bromodomain inhibitor JQ1 through the suppression of MYC.

We tested this hypothesis by pursuing the following Specific Aims:

Specific Aim I: Determine the role of PIK3CA hotspot helical domain mutations in predicting response to PI3K pathway targeted therapy

Based on the differential response to dual PI3K/mTOR inhibitor (LY3023414) that we observed in two bladder cancer PDX models (RP-B-01/RP-B-02) that carry distinct PIK3CA HD mutations (E542K, E545K respectively), We tested whether distinct PIK3CA mutations can drive differential proliferative potential in isogeneic HEK cells transfected with the mutations of interest. Next, we examined the response of PIK3CA transfected HEK cells to treatment both in monolayer and 3D culture. We also evaluated whether resistance in PIK3CA E542K transfected HEKs was associated with inefficient target modulation compared to the PIK3CA E545K transfected cells. Lastly, we tested therapeutic response in additional PIK3CA mutant basal like bladder cancer cell lines to determine whether treatment response is function of solely mutation status or both mutation and subtype.

Specific Aim II: Investigate the role of activation of RAS-MAPK signaling in driving resistance to PI3K targeted therapy in a mutation dependent manner

Based on the key role of RAS in interacting with PIK3CA HD mutations to induce signaling, we tested whether feedback RAS-MAPK signaling is preferentially activated in the context of PIK3CA E542K mutation (RP-B-01) but not the E542K mutation (RP-B-02). Activation of MAPK signaling in RP-B-01

cells was associated with stabilization of MYC. However, this was that the case in RP-B-02 cells. Therefore, we subsequently tested multiple drug combinations that included LY3023414 with either ERK1/2 inhibitor or bromodomain inhibitor (JQ1). The purpose was to identify a therapeutic strategy that can overcome resistance to PI3K targeted inhibition in PIK3CA driven basal like bladder cancer. An ongoing effort in this project is to screen additional bladder cancer PDX models currently under development for PIK3CA mutation status to validate our findings with further *in vivo* studies.

Taken together, this study is translationally important because it will enable us to better understand the determinants of response to PI3K pathway targeted therapy in bladder cancer. The proposed research is innovative because it represents an unprecedented attempt to evaluate the combined role of PIK3CA mutational status and cancer subtype in driving therapeutic response. Ultimately, this project is intended to pave the way for more mechanistic studies in order to achieve a more personalized therapeutic approach in this disease.

I. Dissertation Overview

This dissertation describes experiments directed towards testing the above specific aims. Chapter II discusses the methodology undertaken to carry out the proposed studies. Chapter III presents the genomic characterization of two novel bladder cancer PDX models which were found to carry distinct PIK3CA HD mutations. It also provides an overview of the *in vitro* and *in vivo experiments*

that provided preliminary evidence for differential response to PI3K targeted inhibition in both models. This sets the stage for testing whether distinct PIK3CA HD mutations indeed drive distinct therapeutic response to treatment in Chapter IV. This central hypothesis was tested using isogeneic HEK cells transfected with the mutations of interest. Additionally, in Chapter IV, the potential role of feedback RAS-MAPK signaling in driving therapeutic resistance is discussed. Rational drug combinations based on the predicted mechanisms of resistance are discussed. Since subtype-specific therapeutic response is also a point of interest in this work, Chapter V discusses detailed characterization of DNA methylation profile in RP-B-01 and RP-B-02 (basal and luminal, respectively) and how mutations in chromatin modifying genes could play a role in predicting response/resistance to PI3K targeted inhibition. Finally Chapter VI discusses the major findings and limitations of the study as well as the proposed future experiments that are needed to fully dissect the mechanisms of resistance to PI3K targeted therapy in PIK3CA mutant bladder cancer.

CHAPTER II: MATERIALS AND METHODS

A. Genomic Profiling of MIBC PDX models (RP-B-01 and RP-B-02)

A.1. Whole Exome Sequencing

Individual exome capture of each DNA sample was carried out using the SureSelectXT Reagent kit as per manufacturer's recommendation (Agilent Technologies, Inc.). 3 µg of genomic DNA was fragmented to a size range of 150-200 bp followed by end repair, adaptor ligation, and low cycle (5) PCR. Libraries were purified and validated for appropriate size (225-275 bp) on a 2100 Bioanalyzer High Sensitivity DNA chip (Agilent Technologies, Inc.). 750 ng of purified library was then hybridized to the SureSelectXT Human All Exon 50 Mb library for 18 hours at 65°C. The captured regions were then bound to Streptavidin T1 magnetic beads (Life Technologies, Inc.) and washed to remove any non-specific bound products. Eluted library underwent a second 11 cycle PCR amplification using Herculase II Fusion Polymerase (Agilent Technologies, Inc.) to add sample specific barcodes necessary for multiplexing. Final libraries were purified, validated for size by a BioAnalyzer (250-350 bp), and quantitated using KAPA qPCR. Individual libraries were pooled (3-plex) in equimolar 2 nM final concentration. Each pool was normalized to 10 pM, loaded and clustered to individual lanes of a HiSeq Flow Cell using an Illumina cBot (TruSeq PE Cluster Kit v3), followed by 2 x 101 PE sequencing on a HiSeq2000 sequencer according to the manufacturer's recommended protocol (Illumina Inc.).

A.2. Mutation Detection in Primary tumors

High quality paired-end reads passing Illumina RTA filter were aligned to the NCBI human reference genome (GRCh37) using BWA (Li and Durbin 2009). PCR duplicated reads were marked using Picard (Li, Handsaker et al. 2009). Putative SNVs and Indels were identified by running variation detection module of Bambino(Edmonson, Zhang et al. 2011). All putative SNVs were further filtered based on a standard set of criteria to remove the following common types of false calls: (1) the alternative allele was present in the matching normal sample and the contingency between the tumor and normal samples was not statistically significant; (2) the mutant alleles were only present in one stand and the strand bias was statistically significant; (3) the putative mutation occurred at a site with systematically reduced base quality scores; (4) the reads harboring the mutant allele were associated with poor mapping quality. Ambiguous calls were manually inspected to ensure accuracy. Putative indels were evaluated by a re-alignment process to filter out potential false calls introduced by unapparent germline events, mapping artifacts and homopolymer. All mutations were annotated using ANNOVAR(Wang, Li et al. 2010) with NCBI RefSeq database.

A.3. Mutation Detection in Xenograft Tumors

To filter out reads caused by mouse stromal contamination in PDX, all reads from the PDXs were run through an *in silico* approach to determine the species of origin. More specifically, we first created a combined reference sequence containing the sequences of all chromosomes in the NCBI genome

assemblies of human (GRCh37) and mouse (GRCm38), and then aligned reads from PDX to the combined reference sequence using BWA. Only reads classified as human but not mouse origin were kept in downstream analyses. Afterwards, standard somatic mutation calling was performed on PDX with the matched normal as described previously. For testing purpose, we also performed somatic mutation calling on the uncleaned PDX data to evaluate the effect of mouse contamination on the somatic mutation calling.

A.4. Comparison of Mutation in Primary versus Xenograft Tumors

All unique somatic mutations identified from the primary tumor or PDX were re-visited in both the primary tumor and matched PDX BAM files. The number of mutant and non-mutant reads at the site of each mutation in all BAM files was extracted using Mutation Reads Extractor to calculate coverage and variant allele fraction (VAF).

A.5. Sanger Validation

PCR amplicons targeting the PIK3CA and CASP8 regions were generated with gene specific primers using a touchdown PCR protocol with the following parameters: 94°C for 15 min, followed by 45 cycles of 94°C for 20 seconds, 68°C initial annealing for 30 seconds (followed by 1°C reduction of temperate per cycle to a final annealing temperature of 58°C for remaining 35 cycles), and 72°C for 1 min. Amplicons were purified using the QIAquick® PCR Purification Kit (QIAGEN Inc., Valencia, CA) as per manufacturer instructions. Ten microliter aliquots for

each sample were run on a 2% agarose gel for 1 hour at 100V to confirm the correct amplified length (~250 bp). The products were tagged using Big Dye Terminator v3.1 Master Mix Kit (Life Technologies™, Carlsbad, CA) as per manufacturer instructions, and purified over hydrated Sephadex-G50 from Sigma-Aldrich (Sigma-Aldrich®, St. Louis, MO), in Multiscreen HV Plates (Thermo Fisher Scientific Inc., Waltham, MA). The eluted samples were placed on a 3130xl ABI Prism Genetic Analyzer and run on the default settings for 50 cm Array using POP-7 Polymer. The data was analyzed with Sequencing Analysis 5.2 software (Life Technologies™, Carlsbad, CA).

A.6. RNA-Seq Analysis

Raw reads that passed quality filter from Illumina RTA were first pre-processed by using 1) FASTQC for sequencing base quality control and 2) cutadapt to remove adapter sequences if applicable. Those reads were then mapped to the latest mouse reference genome (mm10) and ENSEMBLE annotation database using Tophat (Trapnell, Pachter et al. 2009) or STAR(Dobin, Davis et al. 2013). A second round of QC using RSeQC(Wang, Wang et al. 2012) was applied to mapped bam files to identify potential RNA-Seq library preparation problems. From the mapping results, reads that matched a single unique location in the genome were kept, allowing up to two mismatches for further analysis. The number of reads aligning to each gene was calculated using HTSeq(Anders, Pyl et al. 2015). Differentially expressed genes were identified using DESeq2 (Love, Huber et al. 2014), a variance-analysis package developed

to infer the statically significant difference in RNASeq data. A biological hypothesis was also tested using a generalized linear model implemented in DESeq2 by construct corresponding contrasts. Multiple testing corrections were applied. The list of differentially expressed genes (DEGs) were analyzed for enriched Gene Ontology and/or KEGG pathway term with the GAGE (Luo, Friedman et al. 2009) Bioconductor package. GSAASeqSP(Xiong, Mukherjee et al. 2014) was also applied for pathway analysis that utilizes p-values from all genes instead of only DEGs.

B. *In-Silico* Modeling of PI3K protein and Protein-Drug (LY3023414) interactions

B.1. Structure Modeling

The crystallographic structure of the proteins PI3K (*E542K MUT/* RP-B-01) and PI3K (*E545K MUT/* RP-B-02) were not found in the Protein Data Bank (PDB) of Research Collaboratory for Structural Bioinformatics (RCSB) (Berman, Westbrook et al. 2000). Hence, the protein structures were modelled for further studies. Homology modeling is a very powerful tool for the design of 3D structure of a protein. The homology search for the two mutant sequences were performed through NCBI BLASTp against PDB database to obtain templates for the structure modeling(Johnson, Zaretskaya et al. 2008). The molecular modeling of the mutants was performed with MODELLER 9.16 (Fiser and Šali 2003). It applies spatial restraints of probability density functions than the energy utilization. The python commands were specified to produce five mutant models.

The mutant model with minimum DOPE score was chosen as the best model. The composed models were approved by SAVES server.

B.2. Ligand

The structure of the ligand molecule LY3023414 was obtained from Chem-IDplus, a TOXNET database maintained by the U.S National Library of Medicine (NLM) (Hochstein, Arnesen et al. 2007). LY3023414 is highly soluble at pH 2-7. In biochemical testing against approximately 266 kinases, LY3023414 inhibited class I PI3K isoforms, mTORC1/2, and DNA-PK at low nanomolar concentrations. *In vitro*, inhibition LY3023414 inhibited PI3K signaling resulting in G1 cell-cycle arrest and arresting cancer cell proliferation in wide range of cancer cell lines. *In vivo*, LY3023414 was highly bioavailable and was capable of inducing dose-dependent transient dephosphorylation of PI3K/AKT/mTOR pathway downstream substrates such as AKT, S6K, S6RP, and 4E-BP1 that lasted 4-6 hours which is related to the drug half-life of 2 hours. In mice, LY3023414 was given either once or twice daily. In both dosing methods, antitumor activity was observed despite non sustained target modulation. However, the intermittent inhibition of downstream targets was not thoroughly addressed and it was not clear whether it can lead to feedback activation or resistance in select cancer diagnoses as opposed to others. LY3023414 was tested in combination with standard of care drugs such as cisplatin and was found to have an additive effect, however a thorough understanding of whether this additive effect was influenced by cancer subtype was not addressed.

LY3023414 is currently being tested in Phase I and II trials in wide range of human malignancies(Smith, Mader et al. 2016).

B.3. Molecular Docking

The protein-ligand intercommunication was computationally analyzed by molecular docking. We have adopted surflex-dock method, Sybyl-X 2.0 (Jain 2003). This study act as an important platform to explain the significant interactions that makes the protein-ligand complex more stable. Before the initiation of docking, the mutant proteins PI3K (E542K MUT/ RP-B-01) and PI3K (E545K MUT/ RP-B-02) were processed by the standard procedures of surflex-dock program namely, the elimination of heteroatoms related to the protein, fixing of side chain, bumps relaxation and inclusion of hydrogen (H) atoms. The AMBER7 F99 force field was used to assign charge and atom types for each atom of the protein (Pearlman, Case et al. 1995). The Gasteiger-Huckel charges were computed for small molecules. Energy minimization of the protein was executed by the conjugate gradient method (Powell's method) (Fletcher and Powell 1963) in association with tripos force field. The protomol was created with specific active site residues, where LY3023414 can go and bind. Surflex-dock uses an empirical scorings function that discloses the various interaction energies involved between protein and ligand (Paulsen and Anderson 2009). The scores are Dock score, Chem score, Gold score, Crash score, PMF score, Polar score and Consensus score (C-score). This C-score combines all other scores (Dock score, Chem score, Gold score, Crash score, PMF score, Polar score) and

rank the complex based on the binding energy. The high binding energy complexes were identified by their C-score as well as the H-bond formations. All the interacting energy values are mentioned in kcal/mol.

B.4. Molecular Dynamic Simulation

MD simulation was executed to examine the stability of the PI3K E542K MUT -LY3023414 and PI3K E545K MUT-LY3023414 complexes after 45000 ps. The Gromacs 4.5.5 package was employed for the MD simulation(Hess, Kutzner et al. 2008). The mutant proteins PI3K (E542K MUT/ RP-B-01) and PI3K (E545K MUT/ RP-B-02) topology was generated by the Gromacs standard parameters along with Gromos96 53a6 force field(Oostenbrink, Villa et al. 2004). Then the ligand LY3023414 topology was created by an online PRODRG server(SchuÈttelkopf and Van Aalten 2004). The solvation of the system was carried out by simple-point-charge models placed in a cubic box(Berendsen, Postma et al. 1981). The complexes were located 1.2 nm gap away from the cubic box. The total system was made neutral by the addition of Na^+ or Cl^-. The steepest descent algorithm was used for energy minimization for 50000 steps. The position restraining of the protein was performed in constant number of particles, volume and temperature (NVT) for 100 ps at 300 K and followed by simulation in constant number of particles, pressure and temperature (NPT) for 100 ps at 300K. Linear Constraint Solver algorithm was used to restrain the bond length(Hess, Bekker et al. 1997). The electrostatic communications were determined by the Particle Mesh Ewald Method (Darden, York et al. 1993). The

production simulation was executed for 45000 ps simulation. After the end of the simulation, trajectory run was performed and the generated graphs were visualized through Xmgrace tool (Turner 2005).

C. *In-Vitro* Experiments

C.1. Materials

DMEM and Ham's/F-10 media were purchased from Thermo Scientific (Waltham, MA, USA). For 3D culture, growth factor reduced. Phenol-red free matrigel was purchased from Corning (Corning, NY, USA). Collagen was provided by Dr. Sherry Harbin at Purdue University, West Lafayette (Indiana, USA). Matrigel based 3D culture was carried out in 96-well Black/Clear Round Bottom Ultra Low Attachment Spheroid Microplate (#4515) supplied by Corning (Corning, NY, USA).

Immortalized urothelial cells (SV-HUC) were purchased from ATCC. HEK-293T cells and bladder cancer cell lines (253J and TCCSUP) were provided by collaborators at Roswell Park Cancer Institute (Buffalo, NY). Both HEK and SV-HUC cells were selected for overexpression of PIK3CA. HEK cells are well known for being readily transfectable which makes them an invaluable tool for testing the function of specific proteins including PI3K (Nakanishi, Walter et al. 2016). Similarly, we chose SV-HUC cells for being a physiologically relevant cell line that we can use to assess the impact of specific PIK3CA mutation in bladder/urothelial background. 253J and TCCSUP cell lines were selected for

being PIK3CA mutant bladder cancer cell lines (Earl, Rico et al. 2015). All cell lines used in this project were grown in DMEM medium containing 10% FBS and 1% penicillin-streptomycin (pen-strep).

LY3023414 was kindly provided by Eli Lilly and Company. Other drugs used in this study (BEZ235, BKM123, LY996 and JQ1) were purchased from Selleck Inc (Selleckchem, Houston, TX).

For transfection purpose, HA-PIK3CA wild-type and mutant (E545K) (Addgene plasmids 12522, 12525) from Dr. Jean Zhao (Dana-Farber Cancer Institute, Boston, MA)(Zhao, Liu et al. 2005) were used. HA-PIK3CA E542K was generated by Quick Change site-directed mutagenesis from Agilent Technologies (Santa Clara, CA). Following transfection, cells were selected using Puromycin at concentration of 2ug/ml for HEK-293T cells and 0.25 ug/ml for urothelial cells.

For Western blotting, monoclonal antibodies against GAPDH, AKT (total and P-AKT), mTOR (total and P-mTOR), ERK1/2 (total and P-ERK), PPRAS40, P-4EPB1, P-S6, Cleaved PARP, Cleaved Caspase-3, LC3B, HA-tag, c-MYC, P110α were purchased from Cell Signaling (Danvers, MA). For Immunohistochemical (IHC) analysis, antibodies against CK20 (Clone Ks20.8) and against CK5/6 (Clone D5/16 B4) were purchased from DAKO (Glostrup, Denmark). Antibodies against E-cadherin, Vimentin and IHC specific P-mTOR were purchased from Cell Signaling (Danvers, MA). Secondary antibodies were

from Thermo Fisher Scientific (Pittsburgh, PA, USA). For IHC, DAP was purchased from DAKO (Glostrup, Denmark) and Immpress HRP anti-mouse/rabbit were purchased from vector laboratories (Burlingame, CA).

The Trizol, TaqMan probes, and qPCR master mix were procured from Life Technologies (Carlsbad, CA). The iScript reverse transcriptase was from Bio-Rad (Hercules, CA).

C.2. Isolation and Propagation of cells from PDX tumors

RP-B-01 and RP-B-02 cells were isolated from MIBC PDX tumors developed from original patient tumors by subcutaneous implantation in SCID mice. Cells were authenticated by chromosome karyotyping (Ciamporcero, Shen et al. 2016). Cells were cultured using enriched F-medium (2:1 mixture of Ham's/F-10 medium and DMEM medium) supplemented with ROCK inhibitor and insulin growth factor as described previously(Liu, Ory et al. 2012). These cells were confirmed to be of human origin with the detection of the human specific *Alu* gene by RT-PCR.

C.3. Cell Proliferation and Metabolic activity assays

The proliferation of cells with and without addition of drugs was monitored either by crystal violet staining, an alamarBlue based fluorescence assay or MTT absorbance assay. Either urothelial cells or HEK293-T cells were used. For urothelial cells, 4000 cells in 100 µL growth medium were incubated in 96-well

clear bottom black plates for 24 hours followed by incubation with different drug concentrations (range: 60 nM to 2 µM) at different time points ranging from 48 to 96 hours. For HEK293-T cells 1000 cells were seeded in 100 µL growth medium. At the end of incubation, 10 µL of alamarBlue reagent (AbD Serotec, Kidlington, UK) was added and after overnight incubation, fluorescence readings were taken at excitation and emission wavelengths of 544 nm and 590 nm respectively. If MTT was used, 20 µL of MTT reagent (Biovision, Milpitas, CA) was added and after 4 hour incubation, wells were washed, 100 µL of methanol was added/well and absorbace was measured at 570 nm. Data were analyzed and dose response curves generated using GraphPad Prism software (v. 7.0).

C.4. Three Dimensional growth assays

Three dimensional (3D) growth assay was adapted based on a previously described method used from pancreatic cancer cell lines(Arpin, Mac et al. 2016). Briefly, bladder cancer cells (RP-B-01, RP-B-02, TCCSUP, 253J) and PIK3CA transfected HEK293-T cells were resuspended in DMEM media containing 3% Matrigel (Corning, NY) at a cell density of 2000 cell/well and plated in 75 µL of Matrigel containing media in 96-well round bottom ultra low attachment spheroid microplates (Corning #4515). Cells were treated on days 4 and 8 following establishment of 3D spheres. alamarBlue based fluorescence assay was used for quantification as previously described. Alternatively, cells were made stably fluorescent by TdTomato or GFP via lentivirus and gowth/drug response was quantified using Thermo ArrayScan high-content imaging system. Images of 3D

structures were captured by ArrayScan using a 2.5× objective for either TdTomato or GFP; then two-dimensional (2D) projections were processed to quantify differences in total intensity and total area. At least 3 repeats of cell proliferation were carried out for each cell line both in monolayer and in 3D to monitor proliferation over time and differential drug response *in vitro.*

C.5. Western Blot analysis

Protein extracts were isolated from tumor tissue using a polytron homogenizer and cells were extracted by sonication in lysis RIPA buffer (Biovision, Milpitas, CA) supplemented with phosphatase and protease inhibitors. Forty micrograms of protein were separated by gel electrophoresis followed by transfer on to a nitrocellulose membrane. Western blot analysis was performed using the primary antibodies previously described by overnight incubation of membranes in 4°C at 1:1000 dilution. All dilutions were made in Tris Buffered Saline-0.05% Tween-20 buffer containing 5% bovine serum albumin (BSA).Next, membranes were probed with secondary HRP conjugated antibody (rabbit or mouse) and incubated for 1 hour at room temperature at 1:5000 dilution.

C.6. Immuno-histochemical (IHC) analysis

I used IHC analysis to determine the expression of various molecular markers in the original cystectomy specimens in comparison to their PDX counterparts (RP-B-01 and RP-B-02). Standard immunohistochemical protocols were followed as previously described by our lab (Ciamporcero, Shen et al. 2016,

Wei, Chintala et al. 2016). Briefly, formalin fixed paraffin embedded tumors were used to prepare (5 μm) sections. Sections were deparaffinized followed by rehydration and antigen unmasking in sodium citrate buffer (pH 6.0) for all antibodies used in IHC experiments except for CK20 and CK5/6 where EDTA buffer (pH 8.0) was used. Primary antibodies p-AKT, IHC specific p-mTOR, and cytokeratin 5/6/20 were applied to sections overnight at 4°C, followed by their respective horseradish-conjugated secondary antibody (Immpress HRP anti-mouse/rabbit vector laboratories (Burlingame, CA)) for 1hr at room temperature. Photomicrographs were captured using a Zeiss Axio (Peabody, MA) microscope.

C.7. Quantitative RT-PCR

Gene expression at the mRNA level was determined by performing quantitative RT-PCR (qRT-PCR). Trizol reagent was used to isolate RNA from tumor tissue and cells. cDNA was prepared using the high efficiency iScript cDNA synthesis kit from Bio-Rad (Hercules, CA). Gene specific primers were designed in Primer3 software(Rozen and Skaletsky 2000) then utilized to determine gene specific expression levels using a SYBR Green PCR Master Mix from Bio-Rad (Hercules, CA). CFX96 Touch Real-Time PCR Detection system (Bio-Rad) was used for quantification of gene amplification peaks. GAPDH was used as an internal control. Normalized fold expression of genes was determined using the CFX Manager Software utilizing the $\Delta\Delta C_t$ method.

C.8. *In-Vitro* Testing of Drug Combination Synergy

The growth/metabolic activity of bladder cancer cell lines used was monitored by an alamarBlue fluorescence assay as described previously. Cells seeded at density of 4000 cells in 100 µL of DMEM media were treated with single agent or combination treatment at different concentrations ranging from (60 nM to 2 µM). 48 hour post incubation with drugs, 10 µL of alamarBlue was added. After overnight incubation with alamarBlue, growth inhibition was determined by measuring fluorescence using a Synergy™ H1 plate reader (Biotek, Winooski, VT) with excitation and emission wavelengths of 544 nm and 590 nm respectively.

Fluorescence readings were used to determine the fraction of cells affected under each treatment condition. Fraction affected was plugged in Compusyn™ Software to generate isobologram and determine the combination index for each combination tested based on the mathematical model developed by Chou and Talalay (Chou 2010, Leow, Martin-Doyle et al. 2014).

D. *In-Vivo* Experiments

Two patient derived tumor xenografts (PDXs), RP-B-01 and RP-B-02, were generated by subcutaneous implantation of fresh primary tumors from bladder cancer patients in SCID mice (Ciamporcero, Shen et al. 2016). RP-B-01 was developed from a treatment naïve female patient diagnosed with T4b N1 Mx tumor. The tumor was grade III, infiltrating urothelial carcinoma with 98%

squamous differentiation. On the other hand, RP-B-02 was developed from a female patient who received cisplatin based neoadjuvant chemotherapy. The tumor was diagnosed as T2b N0 Mx, grade III tumor with squamous differentiation.

For evaluation of tumor drug response *in vivo*, small pieces of PDXs were subcutaneously implanted in SCID mice and allowed to establish. When the tumors reached approximately 100-200 mm3, mice were randomized into groups of 5-8 mice and treated with either vehicle or LY3023414 (10 mg/kg BID by oral gavage). Tumor sizes were blindly measured weekly along with the body weight of mice. At the end of the treatment, tumors were collected, weighed, and processed for formalin fixation and small pieces were frozen for protein extraction.

E. Statistical Analysis

Statistical analyses were performed with GraphPad Prism 7 software. For the continuous outcomes such as tumor growth, I performed the two-sample t-test for two-arm comparison and analysis of variance (ANOVA) for multiple-arm comparison. When ANOVA is used, the ad hoc Tukey test followed to determine the mean differences of interest. The assumption of normality was checked using histograms and normal probability plot. When normality was questionable, the non-parametric Wilcoxon rank test was used. Two-sided P values < 0.05 were considered statistically significant.

CHAPTER III: DIFFERENTIAL RESPONSE TO A DUAL PI3K/MTOR INHIBITOR IN PI3KCA MUTANT UROTHELIAL CANCER

A. Chapter Summary

Genomic profiling of different tumor subtypes is increasingly used in order to identify valid therapeutic targets and improve outcome for patients. In our lab, we developed two muscle invasive bladder cancer (MIBC) patient-derived xenograft (PDX) models; RP-B-01 and RP-B-02. We used genomic profiling (whole exome sequencing and RNA sequencing) to characterize both models(Wei, Chintala et al. 2016). Based on a newly proposed RNA-Seq based molecular classification of MIBC (Choi, Porten et al. 2014, Damrauer, Hoadley et al. 2014, Network 2014), we found that each model belongs to a biologically distinct subtype, where RP-B-01 was basal like; while RP-B-02 was luminal like. We found RP-B-01 to be enriched in cisplatin resistance markers; which include Caspase 8 truncating mutation and over expression of cysteine transporter xCT. Indeed, we found RP-B-01 to be significantly resistant to cisplatin compared to RP-B-02 both *in vitro* and *in vivo*.

Genomic analysis also revealed that both RP-B-01 and RP-B-02 carry PIK3CA helical domain (HD) mutations; E542K and E545K respectively. Despite the biological similarity between the two PIK3CA HD mutations; the two models respond differently to multiple dual PI3K/mTOR inhibitors (i.e. LY3023414) *in vivo* as well as *in vitro*; where RP-B-02 is responsive while RP-B-01 is resistant. Preliminary in *silico* analysis of drug (LY3023414) binding to each mutation revealed more potent binding in the context of the E545K mutation which could

potentially lead to the better therapeutic response that we have observed in the RP-B-02 model. This finding provided the rational for testing the role of distinct PIK3CA HD mutation in determining response to PI3K targeted therapy. Overall, we found that while genomic profiling was predictive of therapeutic response to cisplatin; the mutation status of PIK3CA was not predictive of response to PI3K targeted therapy. This suggests that comprehensive profiling in the context of newly characterized bladder cancer subtypes (Basal; Luminal), rather than solely mutational analysis, may predict response to PI3K/mTOR targeted therapies in bladder cancer. Importantly; this sets the stage for dissecting the role of distinct mutations in predicting therapeutic response as well as understanding the complex role of alternative pathways and epigenetic changes in driving response to treatment.

B. Background and Rationale

Bladder cancer is the 4th most common malignancy in men and the 9th most common in women, with 81,190 new cases and 17,240 deaths expected in 2018 (Siegel, Miller et al. 2018). Muscle invasive bladder cancer (MIBC) carries a poor prognosis where the overall 5 year survival ranges from 35% to 70% (Siegel, Miller et al. 2018). To date, besides anti PD-1/PD-L1 therapies (Sundararajan and Vogelzang 2015), specific targeted therapies have not been approved for the management of this disease, where conventional platinum-based chemotherapy continues to be the standard of care (Leow, Martin-Doyle et al. 2014). However, patients eventually develop cisplatin resistance(Galluzzi,

Senovilla et al. 2012, Drayton, Dudziec et al. 2014), thus there is a dire need to develop novel therapeutic options for those patients.

PI3K/mTOR signaling is altered in 40% of bladder cancer cases (Network 2014). However, targeting this pathway bladder cancer patients has not been successful so far either due to the toxicity encountered in heavily treated patients who usually receive PI3K targeted therapy on clinical trials or due to lack of responsiveness (Carneiro, Meeks et al. 2015, Houédé and Pourquier 2015). Interestingly however, in a phase II clinical trial where patients were treated with everolimus; only patients with mutation in Tuberous Sclerosis Complex 1 (TSC1) showed significant response to treatment compared to other patients (Seront, Rottey et al. 2012), which highlights the importance of patient selection in clinical trial design in order to achieve therapeutic benefit. It is important to point out that most of the conducted clinical trials so far are focused on mTOR targeting agents (i.e. Everolimus), including a currently ongoing trial at Indiana University (NCT01215136). Only two trials are testing agents that target other factors in the PI3K/mTOR pathway; one of them is using a dual PI3K/mTOR inhibitor (GSK2126458) and the other is investigating the specific PI3K inhibitor buparlisib (BKM-120) in metastatic transitional cell carcinoma of the urothelium (NCT01551030). Therefore; So far, a correlation between PIK3CA helical domain mutation status and response to treatment has not been determined.

More clinically and molecularly relevant models are necessary to better understand the molecular alterations associated with drug response, and to develop more effective personalized therapies for MIBC. Patient derived tumor xenografts (PDX) have become an increasingly attractive model for preclinical drug development because of their retained original tumor heterogeneity and genetic make- up, suggesting a more reliable drug development tool as compared to tumor cell lines(Bernardo, Costa et al. 2014, Cirone, Andresen et al. 2014). To date, there are a limited number of established bladder cancer PDX models that are molecularly characterized and available for testing drug resistance and sensitivity (Pan, Zhang et al. 2015, Inoue, Terada et al. 2017, Suh, Jeong et al. 2017).

In this study, we characterized two PDX tumors recently established in our lab by genomic profiling. As previously reported, RP-B-01 is less cisplatin responsive as compared to RP-B-02 (Ciamporcero, Shen et al. 2016), and carries specific cisplatin resistance markers, such as a caspase 8 mutation and over expression of the cystine transporter xCT. Genomic analysis also revealed that both RP-B-01 and RP-B-02 carry PIK3CA HD mutations; E542K and E545K respectively. However, the RP-B-0-1 has been found to be significantly resistant to treatment with dual PI3K/mTOR inhibitor LY3023414 (LY414) suggesting the presence of alternative resistance pathways that warrant further investigation.

C. Results

C.1. Genomic profiling of two MIBC PDX models (RP-B-01/RP-B-02)

In our lab, we developed two MIBC PDX models (RP-B-01 and RP-B-02) from two female patients undergoing cystectomy for urothelial carcinoma by subcutaneous implantation of tumors pieces from cystectomy specimens in SCID mice (Table 1, Page 85) (Ciamporcero, Shen et al. 2016). In order to create a predictive model for response to cisplatin (mainstay of therapy in bladder cancer) as well as elucidate alternative targeted therapies; we decided to perform genomic profiling of the original tumors and the derived PDXs. Using a high throughput paired-end sequencing approach, we generated 84 to 330 million of 100-bp reads per sample. For non-PDX samples, over 98% of the reads were successfully mapped to the human reference by using BWA. For PDX samples, the mapping rates were 94.5% and 86.6% with human reference. After mapping to the human and mouse combined reference, the mapping rates for these two PDXs increased to 99.1% and 99.2%. All samples reached the designed goal of 80% of the targeted regions covered with at least 30X coverage.

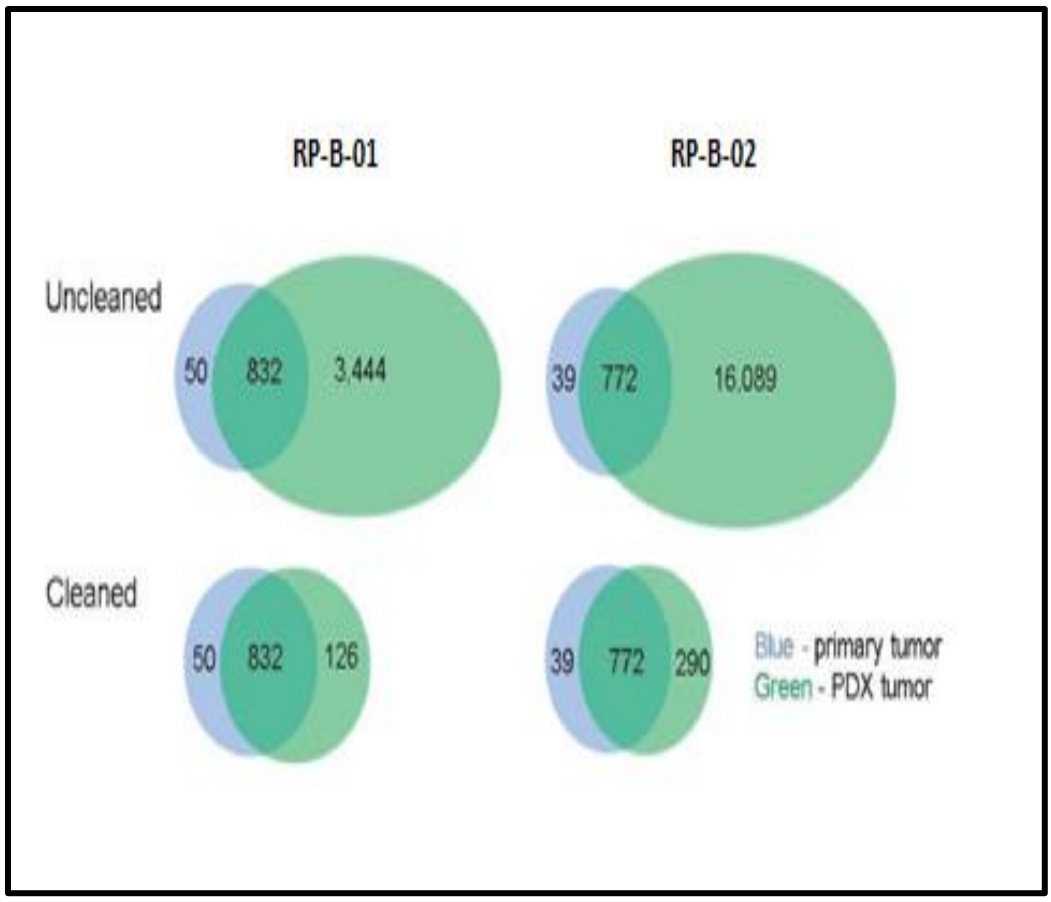

Figure 2: Effects of mouse contamination on somatic mutation in MIBC PDX models. Before ("Uncleaned") and after ("Cleaned") filtering out mouse contamination, the initial single nucleotide variation (SNV) calls from PDX samples (green) were compared with the matched primary tumor (blue). Top: "Uncleaned", bottom: "Cleaned"; Left: RP-B-01, right: RP-B-02. The excessive amount of SNV calls in the "Uncleaned" PDX data likely reflects artifacts introduced by mouse contamination. *A previous version of this figure was published in (Wei, Chintala et al. 2016).*

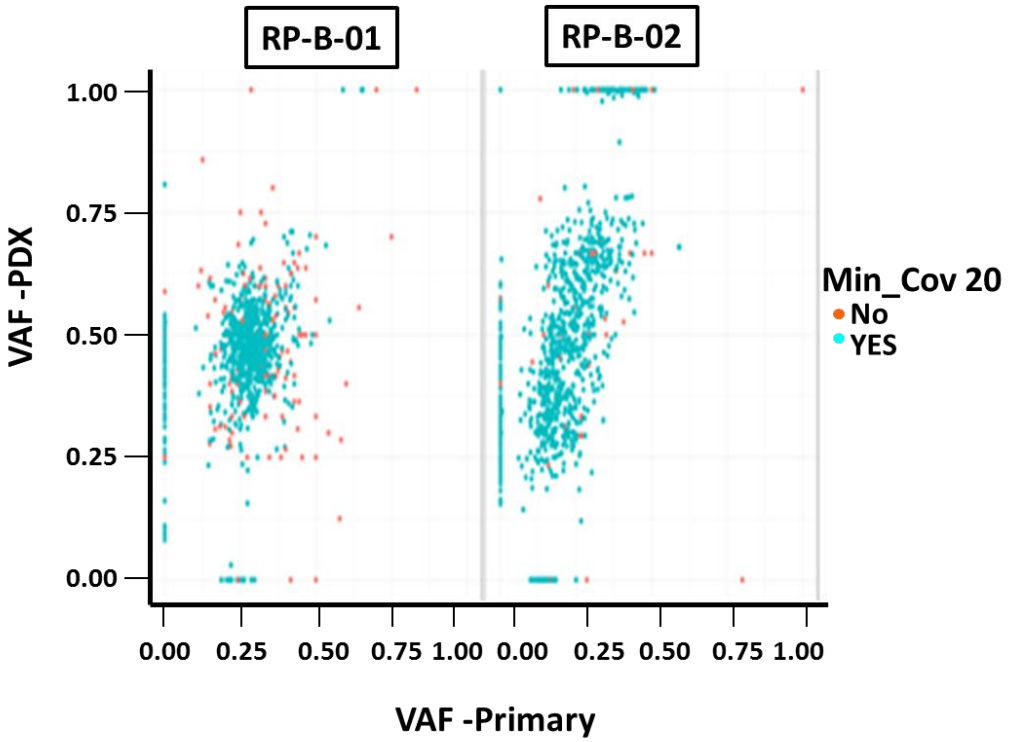

Figure 3: Variant allele fraction in primary tumor and matched PDX. Variant allele fraction (VAF) defined as the fraction of reads harboring mutant allele for each mutation in the primary tumor and matched PDX. The mutations with less than 20X coverage in primary or PDX tumor are highlighted in red. *A previous version of this figure was published in (Wei, Chintala et al. 2016).*

In a test run on the unfiltered data, we identified 4,276 and 16,861 SNVs in RP-B-01 and RP-B-02 respectively (Figure 2). The majority of these SNVs was not identified in the primary tumor and was likely caused by mouse contamination. After filtering out mouse reads, most of these suspicious mutation calls disappeared and the remaining mutations were highly consistent with the matched primary tumor.

Following sequencing, we identified 1,008 SNVs and five Indels from the primary and PDX in RP-B-01 and 1,101 SNVs and 14 Indels from RP-B-02. The

identified mutations were then manually reviewed to ensure accuracy. After manual review, there were 919 mutations (917 SNVs and 2 Indels) left in RP-B-01 and 980 mutations (973 SNVs and 7 Indels) in RP-B-02. The mutation profiles were compared between the primary and PDX to determine similarity. In both cases, majority (91% in RP-B-01 and 82% in RP-B-02) of all mutations was shared by primary and PDX samples (Figure 3). There also existed smaller numbers of sample-specific mutations (2% primary-unique and 7% PDX-unique in RP-B-01, 3% primary-unique and 15% PDX-unique in RP-B-02), which may reflect the tumor progression from primary to PDX tumors. In RP-B-01, the frequency of variant alleles (VAFs) of the shared mutations were centered near primary = 0.25 and PDX = 0.5, which may indicate higher tumor purity in PDX than the primary tumor. Similarly, in RP-B-02, most shared mutations were around primary= 0.25 and PDX = 0.5. Additionally, there was a small group of mutations near primary = 0.4 and PDX = 1.0, which were likely to be homozygous in the PDX (Figure 3). Of note, VAF=1.0 is indicative of 2 alleles being mutant (i.e. homozygous mutation) while VAF=0.5 is indicative of one allele being mutant (i.e. heterozygous mutation). Along with tumor evolution as well as subsequent tumor passaging in mice VAF can change for each mutation.

Among the identified somatic mutations, 13 alterations were previously found clinically relevant according to ClinVar or mutated in other cancers as summarized by COSMIC (Figure3, Table 1). Most of these mutations were present in both primary and PDXs except for CFTR R1066C, which was only

present in the PDX. For other novel nonsynonymous mutations, 57 mutations occurred in Cancer Gene Census genes or other genes known to be recurrently mutated in bladder cancer genes (Morrison, Liu et al. 2014, Network 2014), including 10 predicted loss-of-function mutations summarized in Table 1. The majority (55/57) of these potentially loss of function mutations were present in both the primary and PDX. Only two mutations, RANBP2 P1380R in RP-B-01, and RYR2E1859K in RP-B-02, were present in the PDXs but not in the primary tumor.

Table 1: Somatic Mutations identified in RP-B-01 and RP-B-02

Somatic mutations identified in RP-B-01 and RP-B-02		
Reported in COSMIC ***(Clinically relevant according to ClinVar)***		
	RP-B-01	RP-B-02
	RS1 R209H	CREBBP W1472C
	PIK3CA E542K	PIK3CA E545K
	MLL3 R199*	NCSTN S389C
	LRIG3 E576K	MYD88 S219C
	KLHL3 S410L	CFTR R1066C,
	FANCD2 L1134V	CDKN2A E69*
	DNAH7 R1957*	
Novel nonsynonymous loss of function mutations		
	MLL2 Q1361	ZFP36L1 F253fs
	ARID2 L47fs	MYST4E1398fs
		MLL S2663*
		KRAS E3_splice
		KDM6A Q958*
		ETV4 Q170*
		ELF3 D223fs
		BMPR1A R361*

C.2. MIBC patient-derived xenografts recapitulate original tumors biology

Table 2: Characteristics of primary patient tumors

Name	Grade	Stage	Description	Therapy
RP-B-01	Infiltrating urothelial carcinoma	T4b N1 Mx	Grade III tumor with 98% Squamous differentiation with venous, lymphatic and perineural invasion	Left untreated, deceased
RP-B-02	Infiltrating urothelial carcinoma	T2b N0 Mx	Grade III tumor with squamous differentiation	Neoadjuvant Gemcitabine and cisplatin followed by paclitaxel/carboplatin after surgery

In addition to using genomic profiling in order to confirm the similarity between primary tumors derived from cystectomy specimens (Table 2: Patient characteristics) and PDX tumors; I used standard histological techniques in order to confirm that PDX tumors phenocopied the original tumors.

Hematoxylin and eosin staining (Figure 4) demonstrated that PDX tumors maintained similar morphology to original tumors. Immunohistochemical (IHC) staining for both E-cadherin and Vimentin (Figure 5) showed that both PDX models maintained the epithelial phenotype of original tumors. This confirms our

models as valid tools for preclinical drug development that can faithfully recapitulate the complexity and heterogeneity of patient tumors.

Recently, a novel classification (W. Choi et al., 2014; Damrauer et al., 2014; Network, 2014) has been introduced in the bladder cancer field in an attempt to better stratify the disease into distinct subtypes which would ultimately revolutionize bladder cancer therapy into a more personalized approach. Using, IHC staining for cytokeratin 5/6 (CK 5/6) and cytokeratin 20 (CK 20); I found RP-B-01 to express CK 5/6 while RP-B-02 expressed mainly CK 20 (Figure 5). This staining pattern confirms distinct subtypes; where RP-B-01 is basal-like while RP-B-02 is luminal-like. Importantly, we validated this with gene expression analysis which showed basal-like genes to be upregulated in RP-B-01 compared to RP-B-02; while luminal-like genes were significantly upregulated in RP-B-02 (Figure 6, 7).

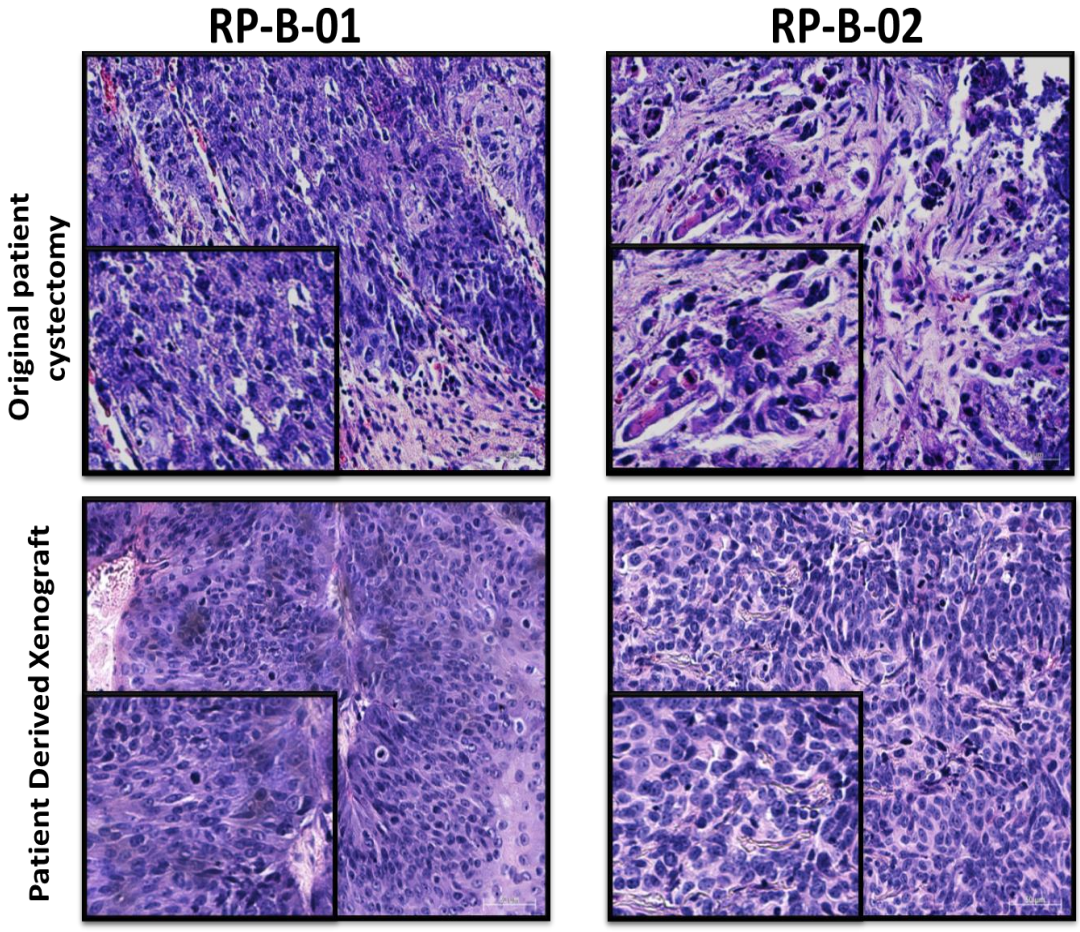

Figure 4: Patient derived bladder xenograft models. Xenografts established from two different patient tumor samples phenocopy the original tumors when observed by H&E. RP-B-01 and RP-B-02 are classified as high grade tumors with squamous differentiation. *A previous version of this figure was published in (Ciamporcero, Shen et al. 2016).*

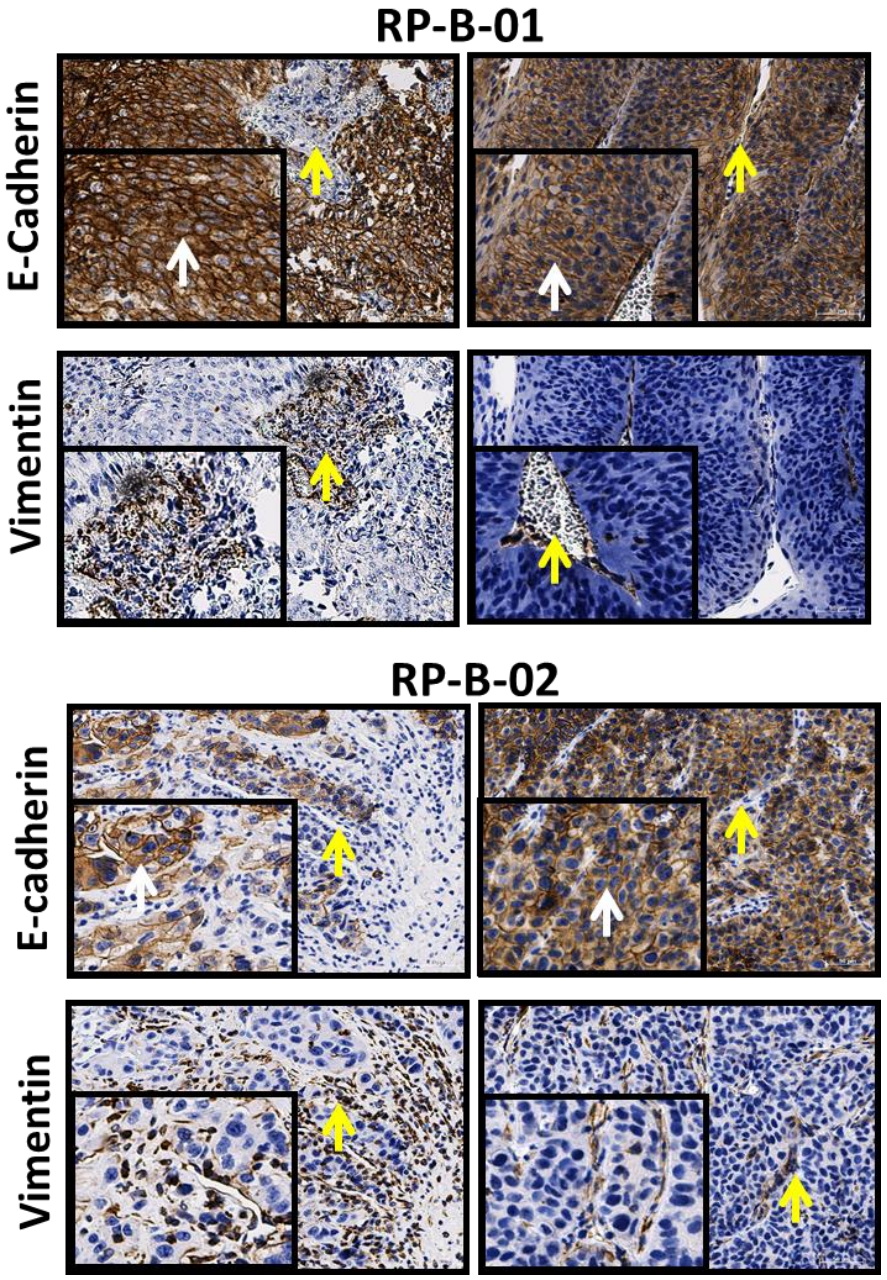

Figure 5: Characterization of MIBC PDX tumors. Representative IHC staining for both E-cadherin and Vimentin show that both models maintain an epithelial phenotype similar to original patient tumors. Left panel shows representative images of original cystectomy specimens and right panel shows representative images of PDX tumors. White arrows point to E-Cadherin staining while yellow arrows point to Vimentin staining.

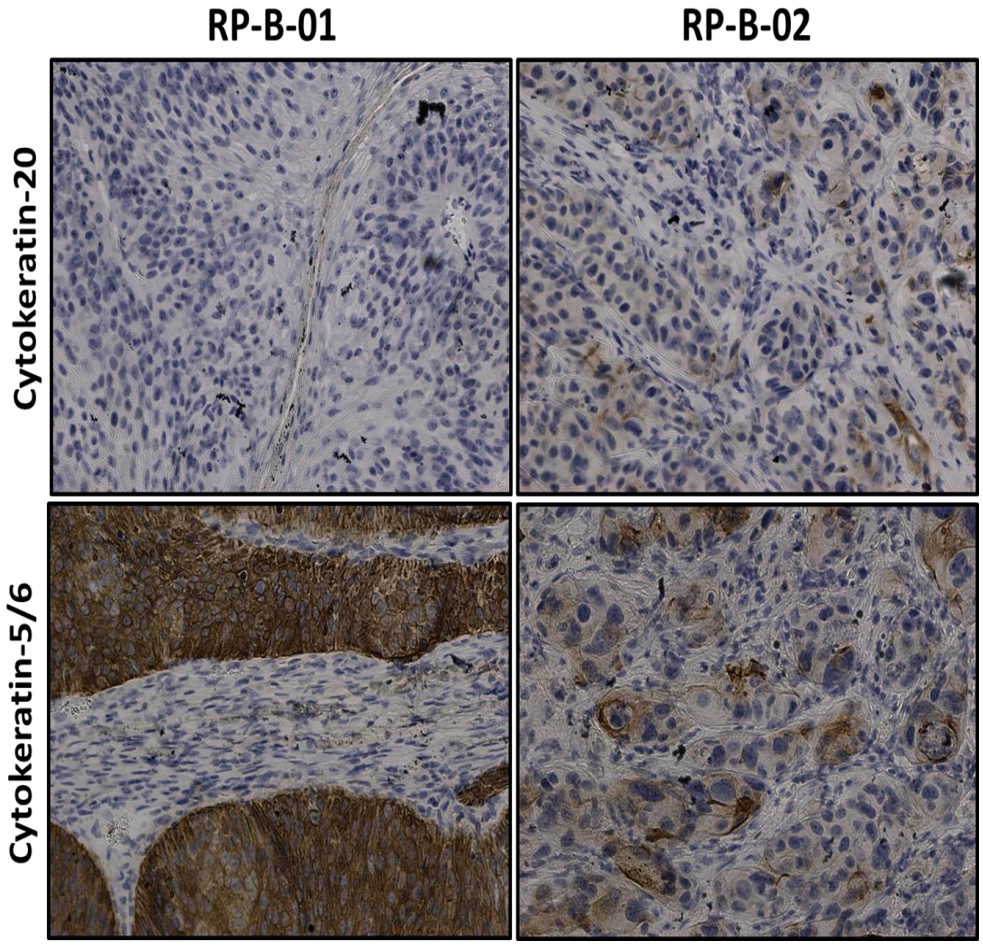

Figure 6: MIBC PDX models (RP-B-01) and (RP-B-02) are of distinct subtype. IHC staining of both models showing RP-B-01 to be positive for CK 5/6 and negative for CK 20 indicating a basal-like phenotype. RP-B-02 is positive for both CK 5/6 and CK 20 indicating a luminal-like phenotype. *A previous version of this figure was published in (Wei, Chintala et al. 2016).*

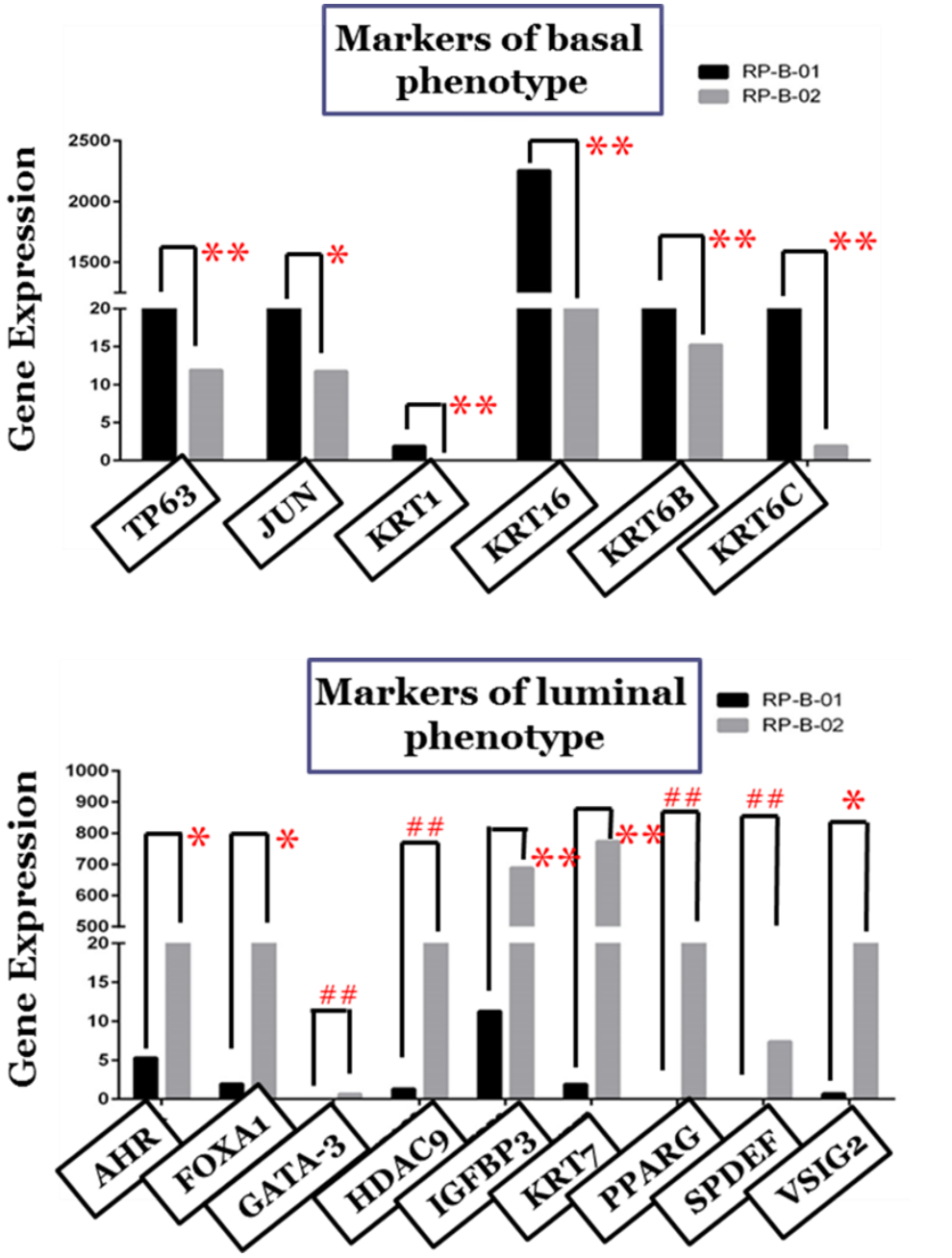

Figure 7: Gene expression analysis support distinct subtypes. Genes associated with basal-like phenotype (per TCGA data) are significantly upregulated in RP-B-01 compared to RP-B-02 (i.e. TP63: The master regulator of the basal-like phenotype. Genes associated with luminal-like phenotype are significantly upregulated in RP-B-02 compared to RP-B-01 (i.e. PPARG, The master regulator of the luminal like phenotype) (Choi, Porten et al. 2014).

C.3. MIBC patient derived xenografts (RP-B-01&RP-B-02) respond differently to a dual PI3K/mTOR inhibitor LY3023414 *in vivo*

Aberrant PI3K signaling (Figure 8) is driven by activating PIK3CA mutations in 25% of bladder cancer cases (Network 2014). The most common PIK3CA activating mutations are single amino acid substitutions that occur either in the helical (E545K, E542K) or kinase domain (H1047R) (Zhao and Vogt 2008). Unlike most solid tumors, bladder cancer holds a unique position where PIK3CA HD mutations are more common compared to KD mutations; accounting for 80% of cases driven by PIK3CA activating mutations (Network 2014). Interestingly, through comprehensive genomic profiling, we found our bladder PDX models to carry distinct PIK3CA HD mutations; where RP-B-01 was E542K mutant, while RP-B-02 was E545K mutant. Based on this finding, I tested the response of those two models to dual PI3K /mTOR inhibitor *in vivo.* Interestingly, I found the RP-B-02 model to be significantly sensitive to treatment; while RP-B-01 was resistant (Figure 9, 10).

Importantly; the anti-tumor effect observed in RP-B-02 was associated with inhibition of downstream PI3K/mTOR signaling (i.e. P-AKT &P-S6). However, in RP-B-01, I observed upregulation of AKT phosphorylation that coincided with therapeutic resistance and absence of significant anti-tumor effect (Figure 11).

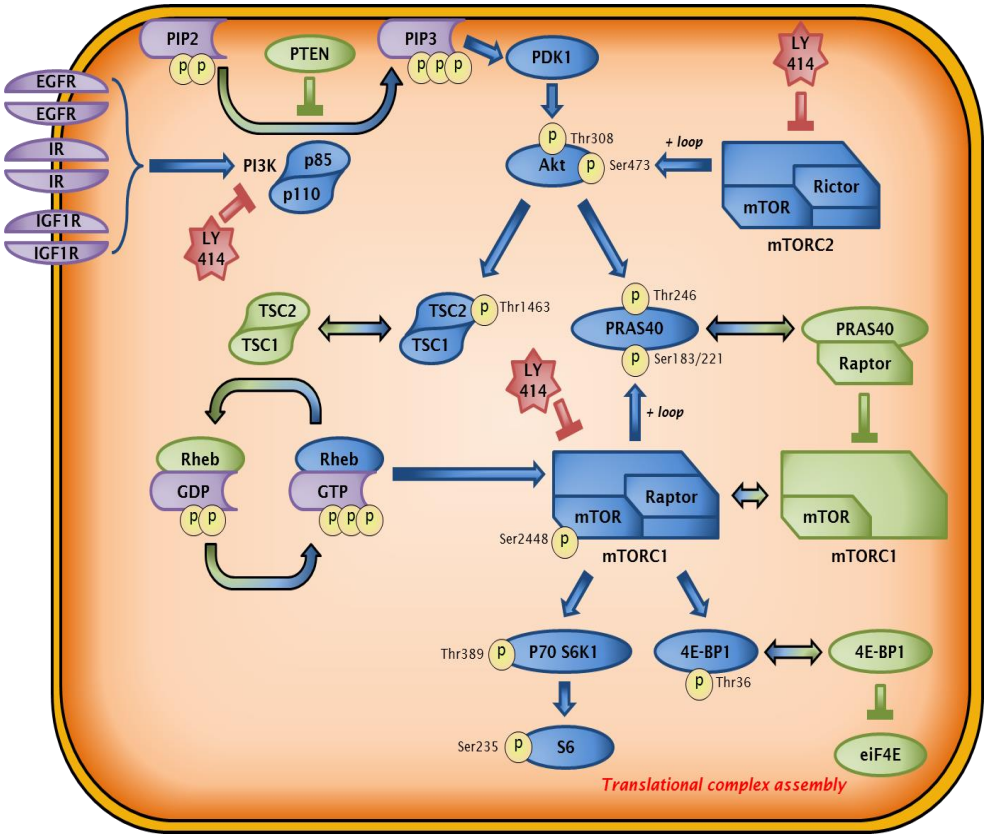

Figure 8: PI3K Signaling Pathway. The PI3K/AKT signaling pathway is activated by receptor tyrosine kinases such as (EGFR. IR), integrins, B and T cell receptors, cytokine receptors, G-protein-coupled receptors and other stimuli that induce the transformation of phosphatidylinositol di phosphate (PIP2) into (3,4,5) trisphosphates (PIP3) by phosphoinositide 3-kinase (PI3K). These lipids serve as plasma membrane docking sites for proteins that harbor pleckstrin-homology (PH) domains (i.e. AKT). At the membrane PDK1 phosphorylates AKT at Thr308 leading to partial activation of AKT, which is then fully activated by being phosphorylated at Ser473 by the help of mTORC2. PTEN (a tumor suppressor) inhibits AKT activity by dephosphorylating PIP3.

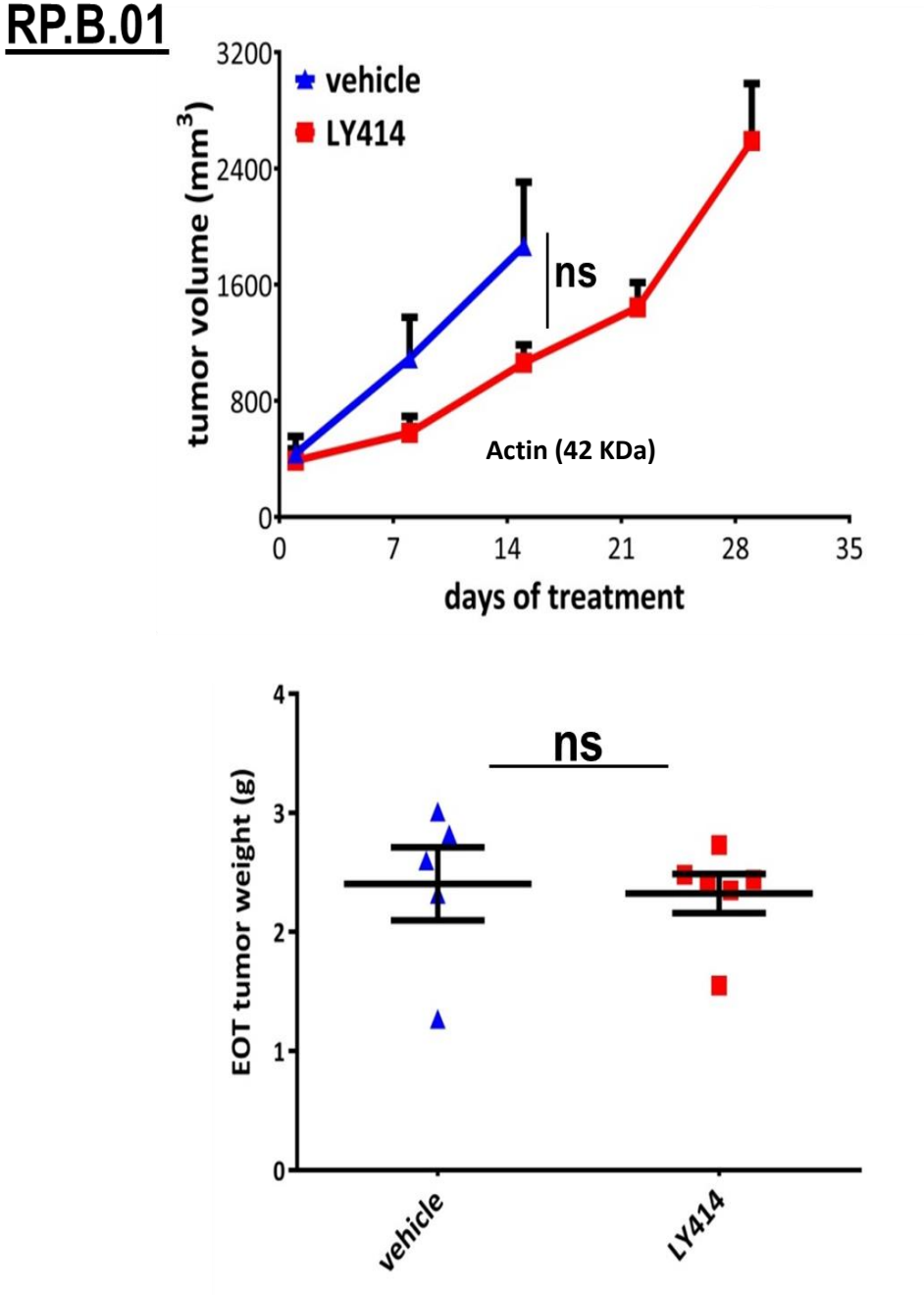

Figure 9: Differential response of PIK3CA mutated RP-B-01 and RP-B-02 to LY3023414. RP-B-01 (PIK3CA E542K MUT) is not sensitive to LY414. Top panel shows tumor volume blindly measured throughout treatment. Lower panel shows tumor weight blindly measured at the end of treatment (EOT*). A previous version of this figure was published in (Wei, Chintala et al. 2016) .*

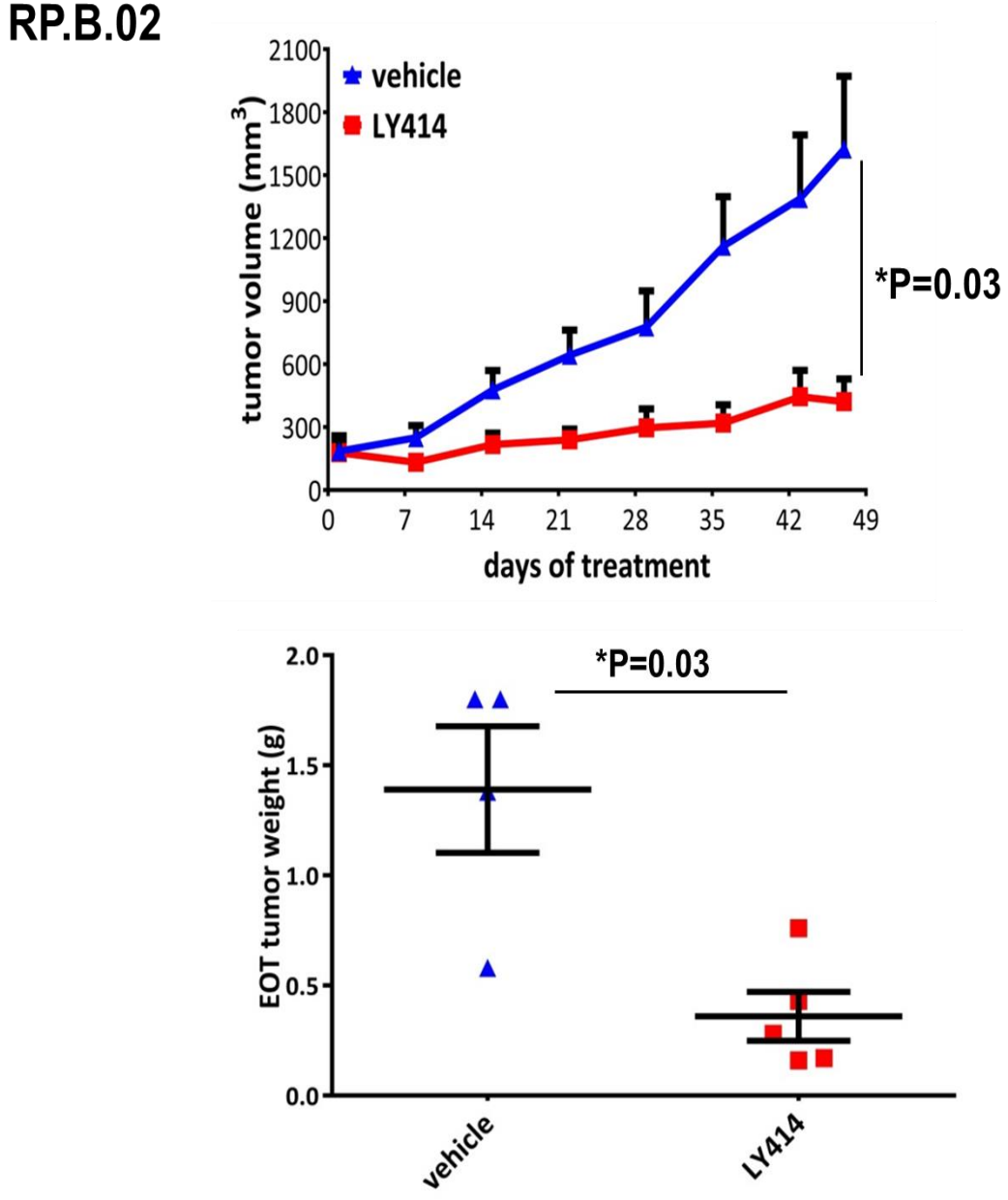

Figure 10: Differential response of PIK3CA mutated RP-B-01 and RP-B-02 to LY3023414. RP-B-02 (PIK3CA E545K MUT) is sensitive to LY414. Top panel shows tumor volume blindly measured throughout treatment. Lower panel shows tumor weight blindly measured at the end of treatment (EOT). *A previous version of this figure was published in (Wei, Chintala et al. 2016).*

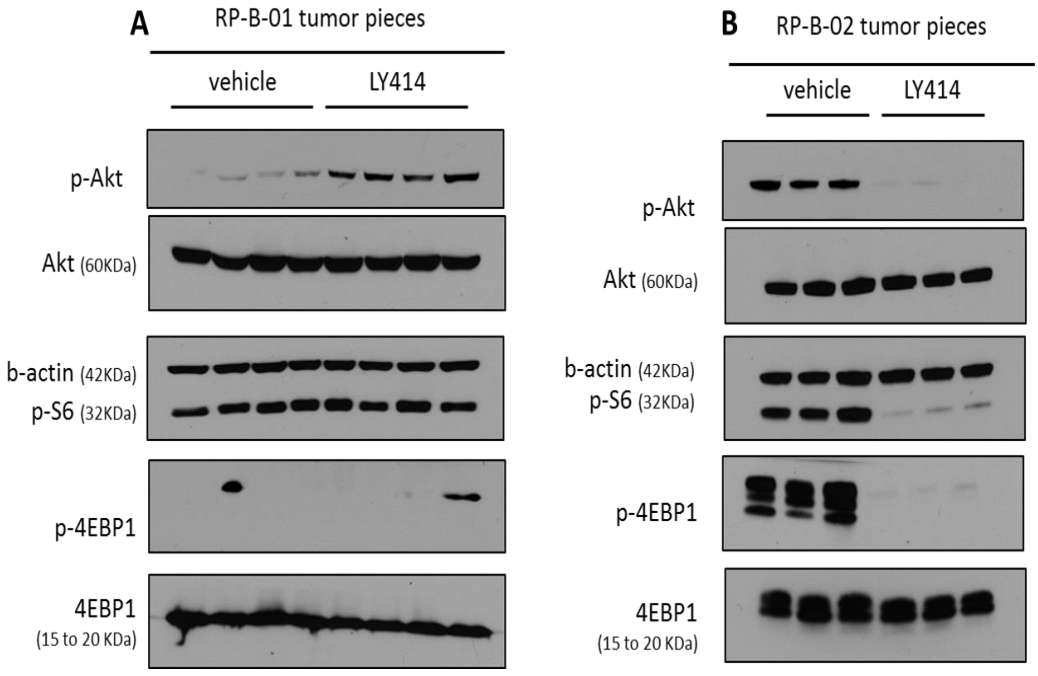

Figure 11: Resistance to LY3023414 in RP-B-01 is associated with feedback activation of AKT signaling *in vivo*. A. In RP-B-01, activation of AKT phosphorylation and absence of p-S6 inhibition in LY3023414 treated tumors compared to vehicle control. B. RP-B-02 treated tumors demonstrate inhibition of downstream targets (p-AKT, p-S6, p-4EBP1) compared to mice treated with vehicle control. *A previous version of this figure was published in (Wei, Chintala et al. 2016).*

C.4. Isolation and characterization of PDX derived cell lines

In our lab, we were able to isolate epithelial cells from PDX tumors (Figures 9,10) and subculture them on plastic using growth factor enriched media in addition to a feeder system of 3T3 irradiated fibroblasts (Liu, Ory et al. 2012). Cell lines derived from PDX tumors were morphologically distinct both in 2D and 3D culture reflecting the morphological differences between those two tumors (Figure 12, 13). Interestingly, I observed that cells growing on plastic underwent epithelial to mesenchymal transition. Using western blotting, I was able to show that e-cadherin expression was lost and cells started to express vimentin (Figure 14). When cells were cultured in 3D, they re-expressed E-cadherin similar to what we observed in original PDX tumors (Figure 15). Therefore; we considered our 3D culture model to be more representative of tumor complexity and thus a more valid tool for drug testing *in vitro*.

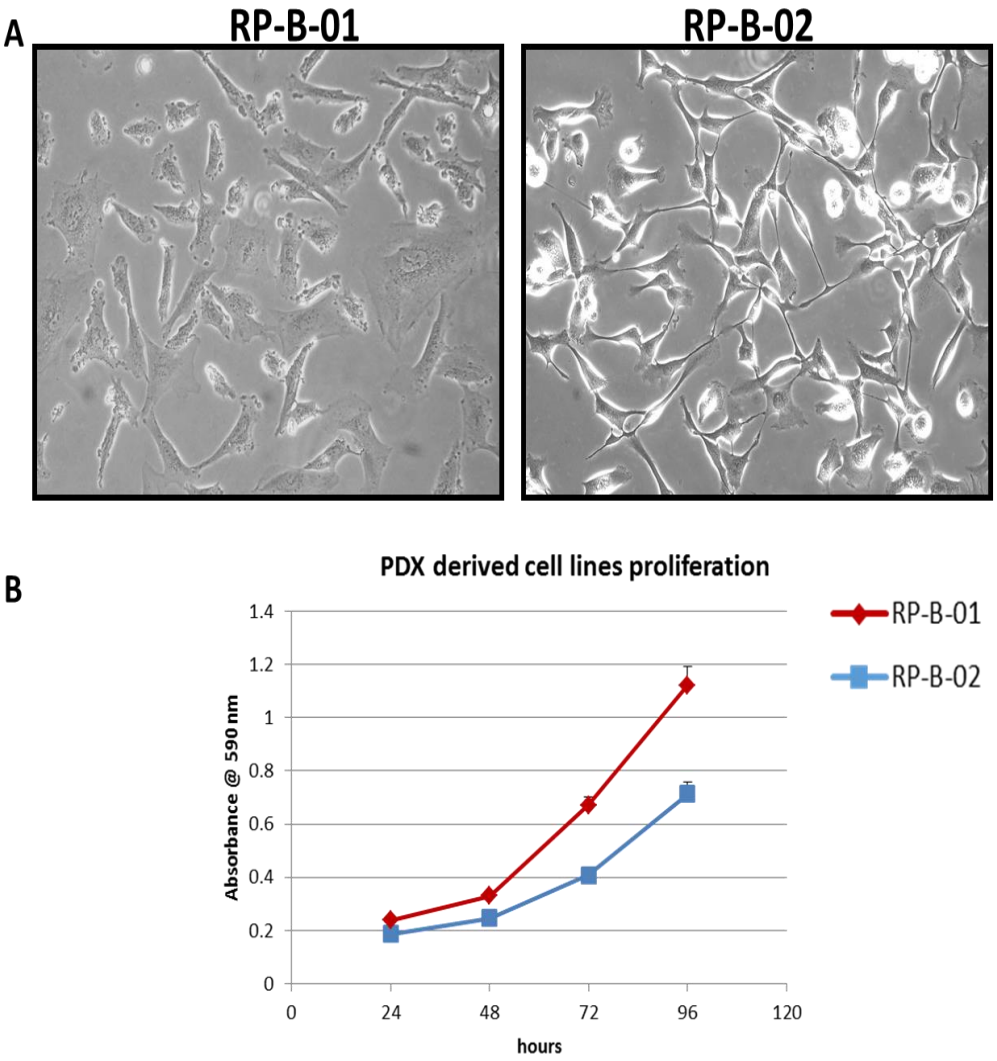

Figure 12: Isolation and characterization of PDX derived cell lines. A. epithelial cells from PDX tumors were isolated and propagated *in vitro (Liu, Ory et al. 2012)* Cell lines derived from PDX indicate difference in morphology between the two models. RP-B-01 appears to be flatter as compared to RP-B-02. B. Proliferation assay shows that RP-B-02 cell line grows slower compared to RP-B-01. *A previous version of this figure was published in (Ciamporcero, Shen et al. 2016).*

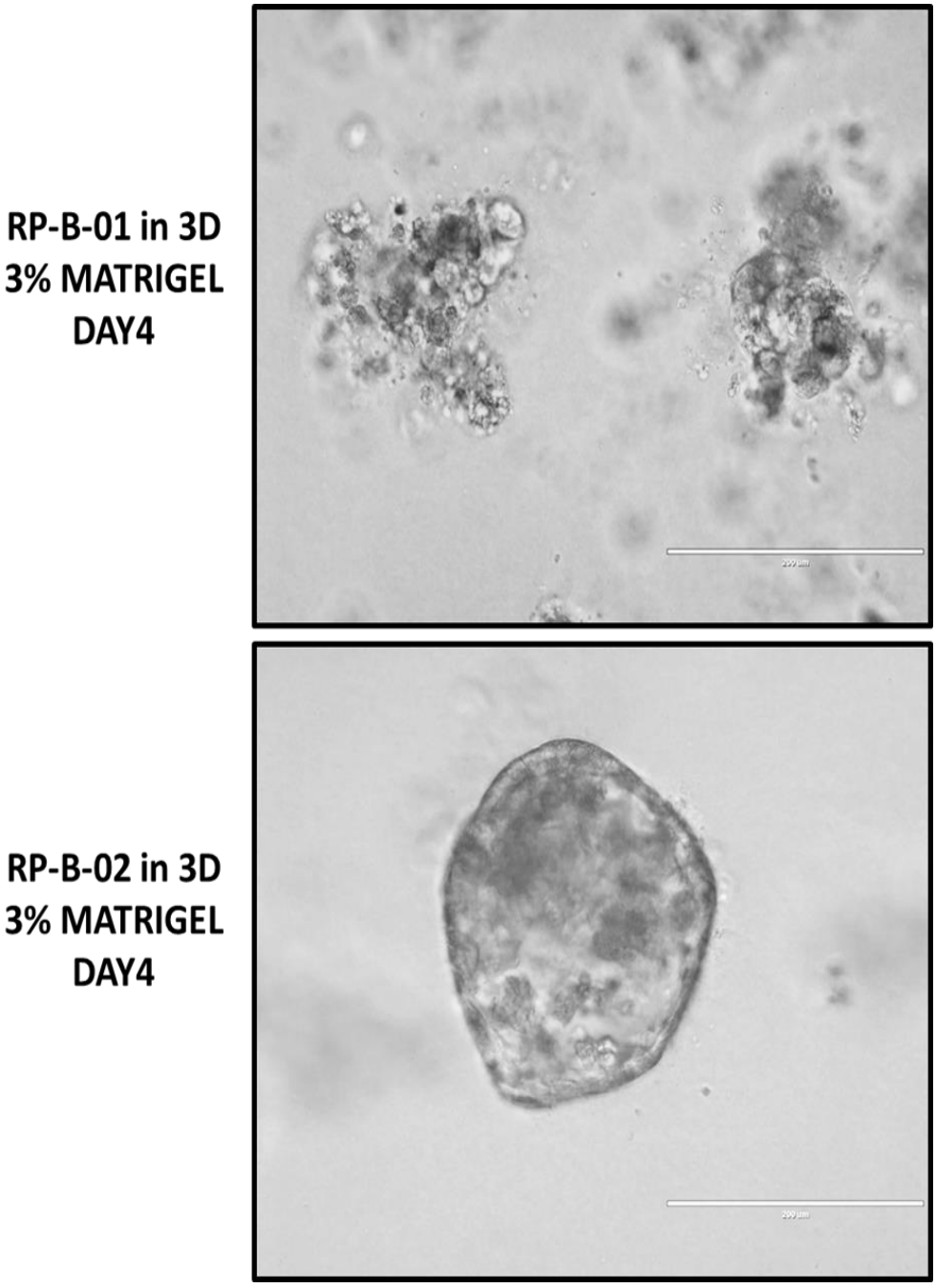

Figure 13: PDX derived cell lines are morphologically distinct in 3D culture. In media supplemented with 3% growth factor reduced matrigel, RP-B-01 cells (Top panel) form less coherent spheres while RP-B-02 (bottom panel) form coherent round spheres.

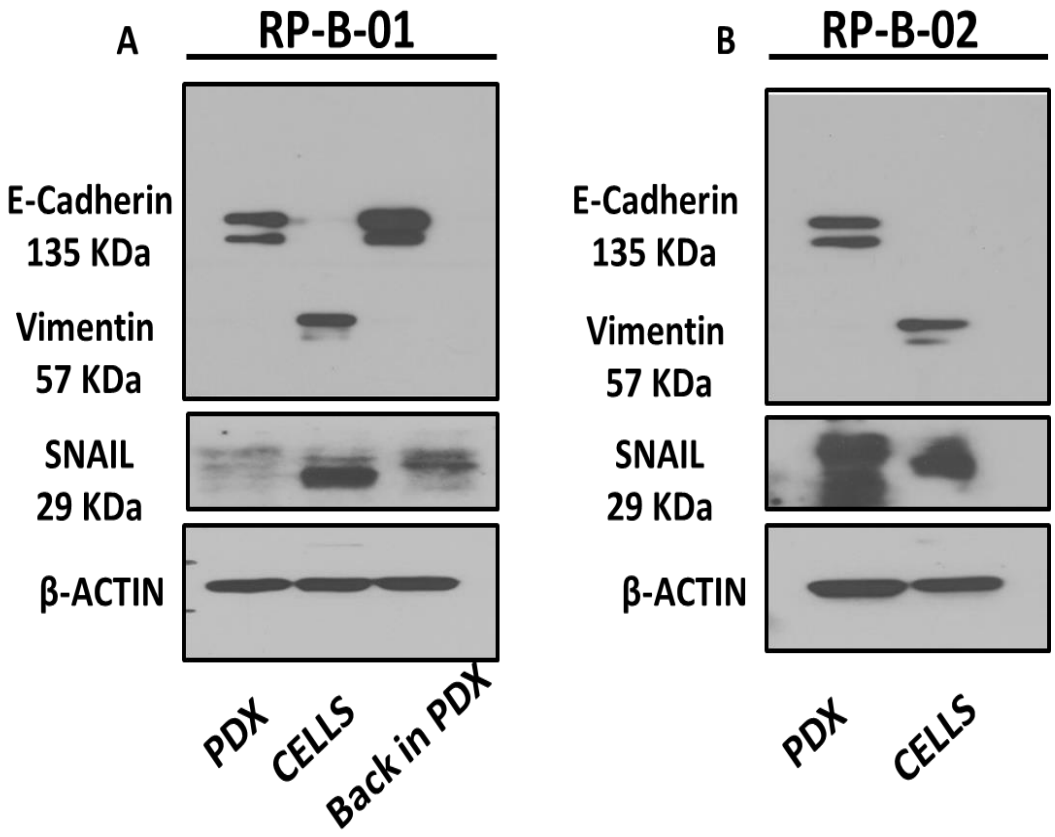

Figure 14: Epithelial-mesenchymal (EMT) transition in PDX derived cell lines. Western blot showing EMT in PDX derived cells compared to original tumors. Transplanting (RP-B-01) cells back in the mouse was associated with re-expression of E-cadherin

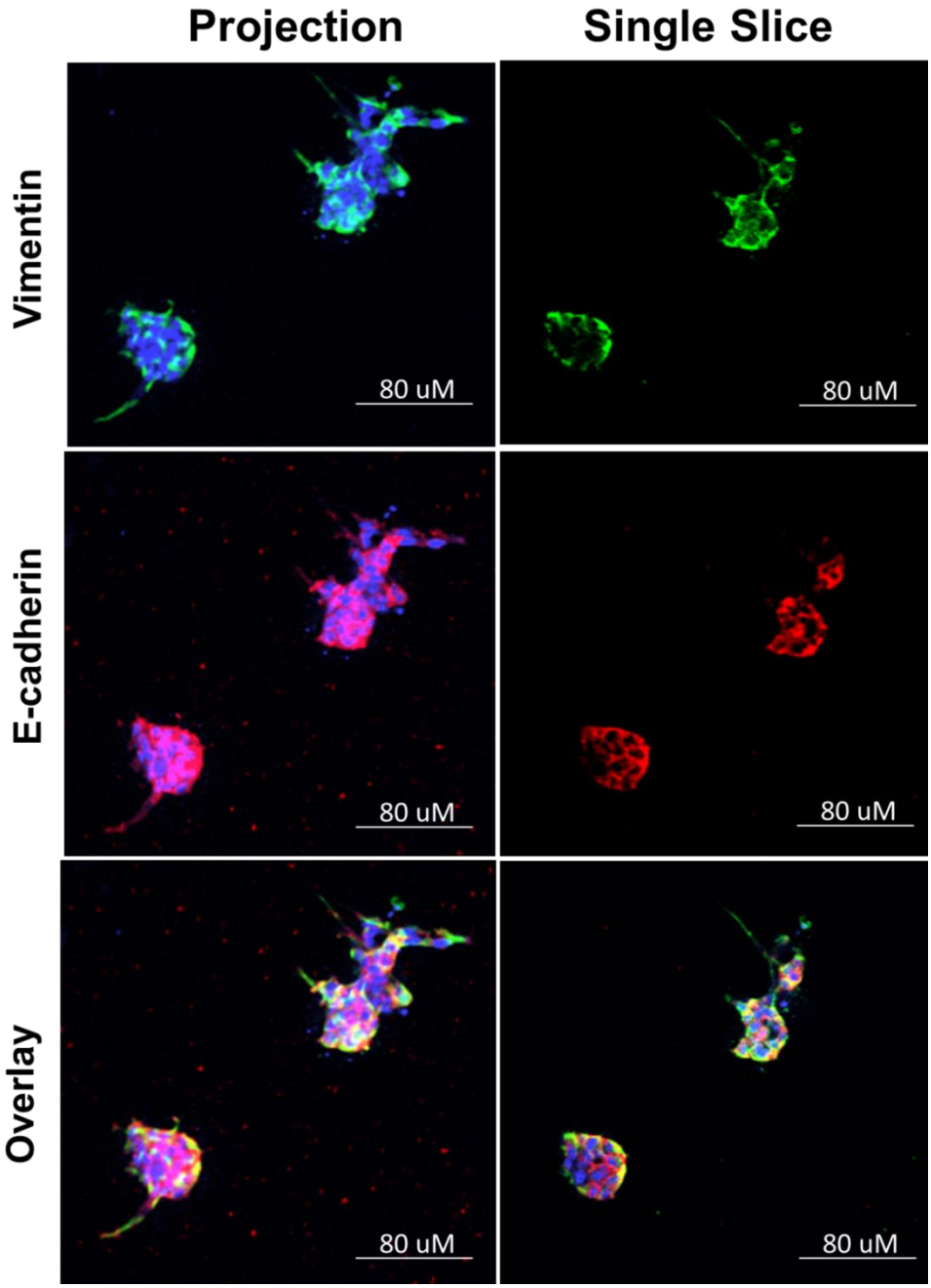

Figure 15: Re-expression of E-cadherin in 3D model of RP-B-02 PDX-derived cell line. RP-B-02 cells in 3D culture re-express E-Cadherin (red) and are more representative of the original tumor epithelial phenotype.

C.5. PDX derived cell lines (RP-B-01&RP-B-02) corroborate the *in vivo* response to LY3023414 *in vitro*

Based on the differential response to dual PI3K/mTOR inhibitor (LY3023414) that we observed when testing drug response for each model *in vivo;* I hypothesized that a similar response shall be observed *in vitro.* Interestingly however, when I tested drug response in growth factor enriched media that we used to isolate the cells, I was not able to see the differential drug response that I observed *in vivo.* When I switched to treatment in regular DMEM media I was able to observe a therapeutic response that corroborates our *in vivo* data; where RP-B-01 cells were significantly resistant to LY3023414 compared to RP-B-02. The IC50 for RP-B-01 was more than 3- fold the IC50 for RP-B-02 cell line (144 nM and 45 nM respectively) ($p<0.001$, Figure 16).

Next; I assessed *in vitro* target modulation by looking at phosphorylation signal of downstream target in the PI3K/mTOR signaling pathway (i.e. P-AKT and S6). Interestingly, while the phosphorylation signal was efficiently inhibited in both models upon short drug exposure (i.e. 30 and 90 min); longer drug exposure was associated with up regulation of AKT phosphorylation in the RP-B-01 but not the RP-B-02 model which coincided therapeutic resistance (Figure 17)

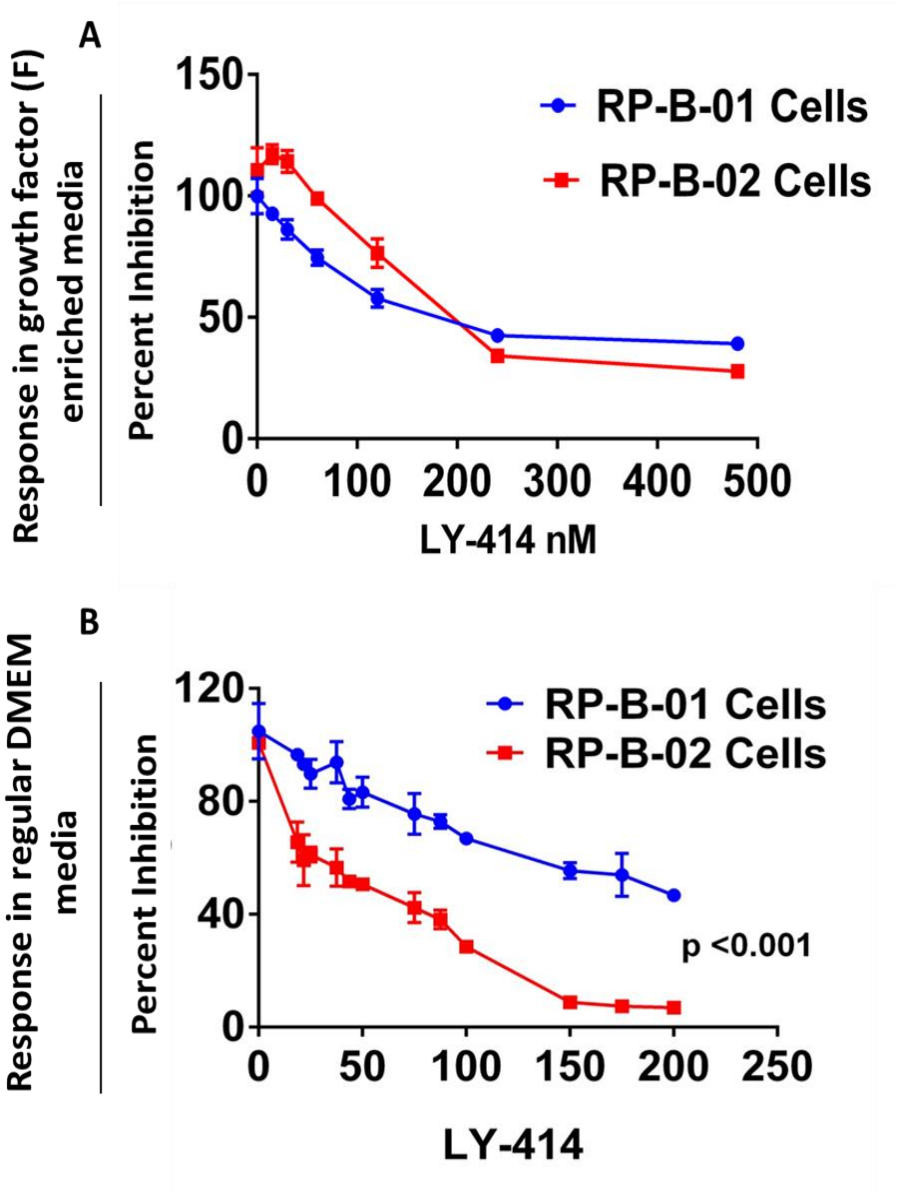

Figure 16: Differential response of PIK3CA mutated RP-B-01 and RP-B-02 to LY3023414 *in vitro.* A. In growth factor enriched media, response to LY3023414 is similar. B. In DMEM media, RP-B-01 cells are significantly resistant to LY3023414 compared to RP-B-02. Mean ± SD, n =3, representative results from at least triplicate experiments. One way ANOVA, Tukey's multiple comparisons test, ***P<0.001. *A previous version of this figure was published in (Wei, Chintala et al. 2016).*

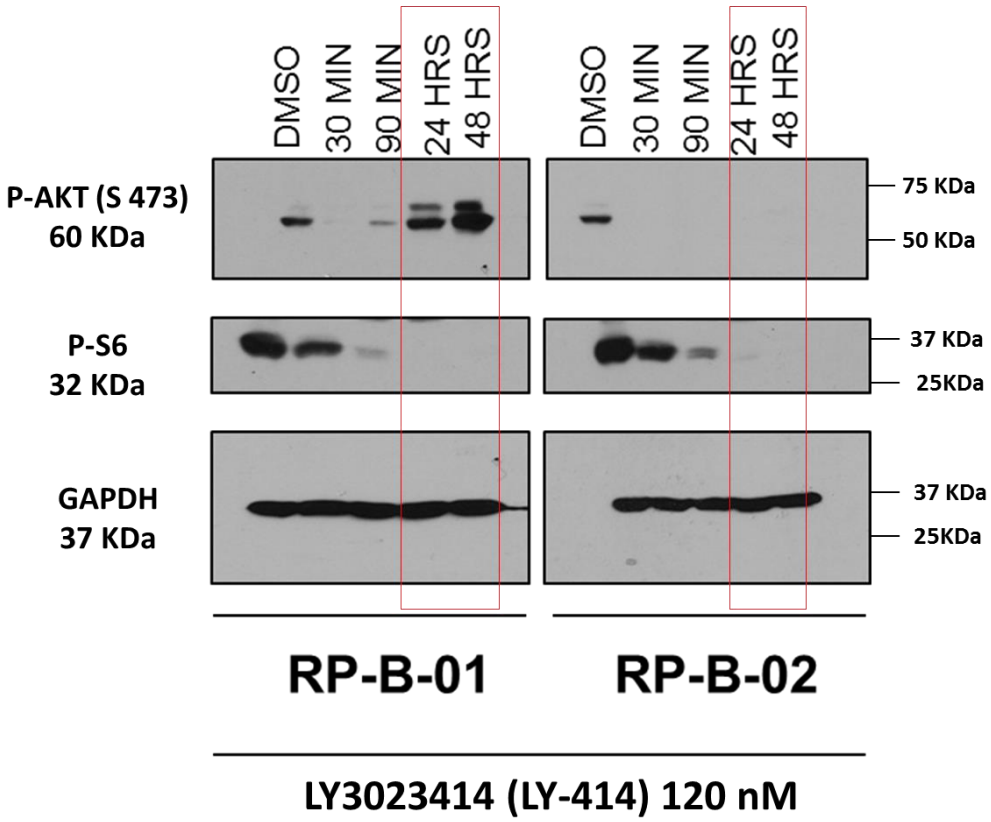

Figure 17: Resistance to LY3023414 in RP-B-01 is associated with feedback activation of AKT signaling in vitro**.** Prolonged drug exposure (24H and 48H) is associated with feedback activation of AKT signaling in RP-B-01 cells. PI3K signaling inhibited at all treatment time points in RP-B-02 cells treated with LY3023414. Drug concentration for all time points=120 nM. *A previous version of this figure was published in (Wei, Chintala et al. 2016).*

C.6. Validation of differential drug response in a 3D culture system of PDX derived cell lines

Drug screening is a key component for drug development and optimizing anti-tumor therapies. Traditionally, *in vitro* drug testing has been conducted in monolayer systems that are not capable of recapitulating the tumor complexity. Recently, the field has witnessed the rise of interest in 3D culture systems which are capable of reproducing tumor complexity while circumventing the cost associated with *in vivo* drug testing (Choi, Lin et al. 2014, Kenny, Lal-Nag et al. 2015, Elbanna, Chintala et al. 2017). In order to validate our therapeutic response data in a more complex system that we can later use for screening of further additional compounds or combinations, I was able to develop a novel matrigel based 3D culture system consisting of bladder cancer patient derived cell lines(Elbanna, Chintala et al. 2017). Using fluorescently labeled cells (GFP or RFP), I was able to monitor the growth dynamics of RP-B-01/02 derived 3D spheroids under different matrix conditions over nine days in high throughput fashion via Thermo ArrayScan XTI (Figure 18).

Interestingly at higher matrigel concentration (10%) and higher cell seeding density (16,000 cell/well), we did not observe significant growth in sphere size when comparing day 4 (solid bar, Figure 19B) to Day 8 (shaded bar, Figure 19B). However this was not the case at lower cell seeding density (2000-8000 cell/well) irrespective of matrigel concentration (Figure 19). Nevertheless, at lower cell density, no significant increase in sphere size was observed overtime.

Taking into account that RP-B-02 cells grow more favorably in 3D culture (Figure 13) in comparison to RP-B-01 cells, I selected 4000 cell/well as an optimal seeding condition for both cell lines that would allow for adequate growth overtime in culture and accurate interpretation of drug treatment experiments.

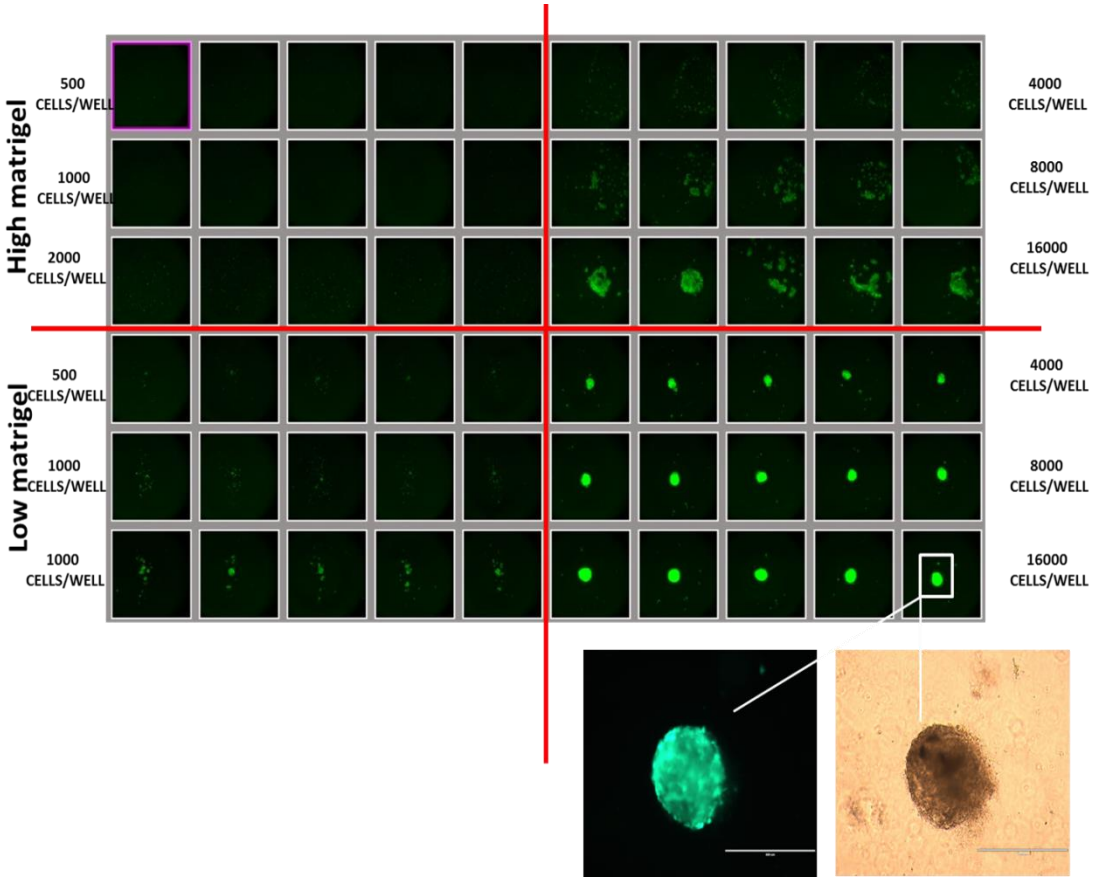

Figure 18: Development of 3D culture system of PDX- derived cell lines for in vitro drug testing. Representative image of Thermo ArrayScan XTI platform used to monitor growth of fluorescently labeled PDX- derived cells over time.

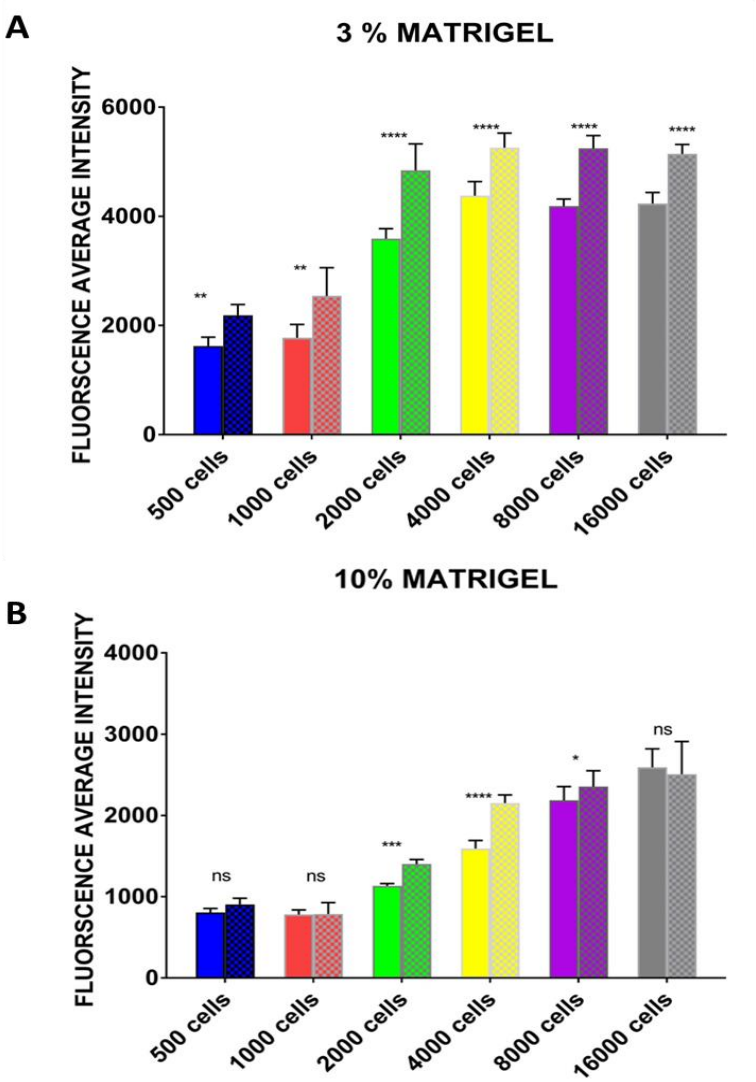

Figure 19: Growth dynamics of different seeding densities of RP-B-01 cells in different Matrigel concentrations**.** A. RP-B-01 cells seeded at different densities in media supplemented with 3% Matrigel. Solid bar represents GFP fluorescence intensity on DAY4 as detected by Thermo ArrayScan XTI. Shaded bar represents GFP fluorescence intensity on DAY8. B. RP-B-01 cells seeded at different densities in media supplemented with 10% Matrigel.

Therapeutic response to PI3K pathway targeted agents (i.e. LY LY3023414) was assessed in the same way, using fluorescence as an endpoint (Figure 20). RP-B-02 derived 3D spheroids were more sensitive to PI3K pathway inhibitors as compared to RP-B-01. This drug response profile was reminiscent of what we observed *in vivo* using patient derived xenograft models derived from the same tumors as well as *in vitro* in 2D monolayer. Ultimately, the goal of this approach is to improve the accuracy with which promising therapeutic leads can be found as well as decrease the cost that comes with drug development.

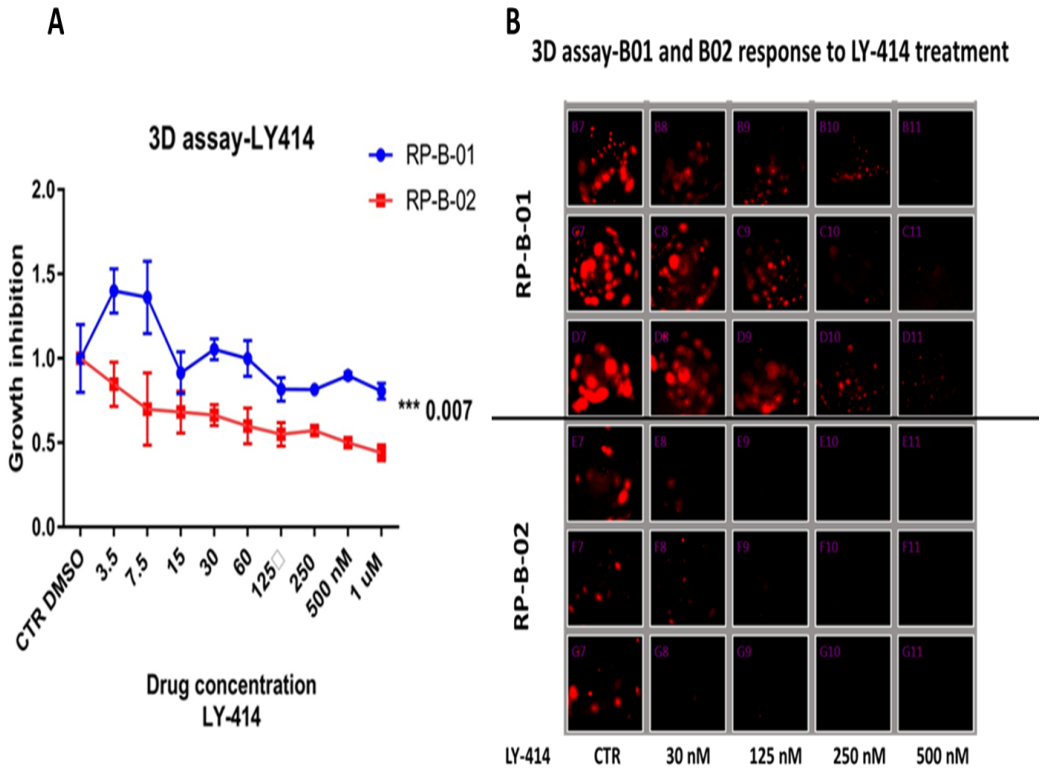

Figure 20: Drug response in 3D culture. A. RP-B-01 and RP-B02 cells were plated into 3D cultures, and cell growth in these spheroids was measured via fluorescence intensity on days 4, 8, and 12 after plating. 3D cultures were treated with increasing concentrations of LY414 following measurements on days 4 and 8. Fluorescence intensity data within each experiment were normalized to D12 CTR DMSO, and D12 readings were compared. Testing response to LY3023414 (dual PI3K/mTOR inhibitor) in 3D shows RP-B-02 derived spherorganoids to be significantly more sensitive to LY414 compared to RP-B-01; similar to the response observed in vivo. B. A representative image of ArrayScan based high throughput drug testing done in 96 well plates using fluorescence as readout for drug response. Mean ± SD, n =3, representative results from at least triplicate experiments. Student's t test *p<0.05, ***p<0.01.

D. Discussion

Cisplatin based conventional chemotherapy continues to be the mainstay of treatment for patients with MIBC. Nonetheless, recent efforts aiming at better molecular characterization of this disease set the stage for a more targeted approach to treatment that could provide patients with better outcomes and less toxicity(Kamat, Hahn et al. 2016). The challenge however lies in the ability of genomic profiling in accurately predicting valid therapeutic targets. In the light of this challenge, PDX models provide an invaluable tool for preclinical drug development (Jäger, Xue et al. 2015, Lai, Wei et al. 2017).

In our genomic profiling study, the PDXs models maintained the same genetic make-up as the original tumors; where 80-90% of all somatic mutations were present in both the primary and PDX tumors. However, a small percentage (7% and 15% in RP-B-01 and RP-B-02, respectively) of mutations were PDX-specific and a smaller percentage of mutations (2% and 3% in RP-B-01 and RP-B-02, respectively) were specific to original patient tumor . These minor differences may reflect the changes that happen during tumor progression from primary to PDXs as well as the changes that are charactersitic of innate tumor heterogeneity. Overall, our results confirm the high similarity between original and PDX tumors which validates the clinical utility of our platform for preclinical drug development.

Due to the importance of cisplatin in management of MIBC, cisplatin resistance has been a major challenge in the field. Cisplatin resistance has been thought to be either intrisnic or acquired (Galluzzi, Senovilla et al. 2012, Dasari and Tchounwou 2014). Several mechanisms have been proposed as mediators of cisplatin resistance, including reduction of intracellular drug accumulation either by decreased uptake or increase efflux(Galluzzi, Senovilla et al. 2012), upregulation of DNA damage repair (Martin, Hamilton et al. 2008) as well as lysosomal sequestration(Zhitomirsky and Assaraf 2016). Importantly, RP-B-01, which was shown to be cisplatin resistant both *in vivo* and *in vitro*, did harbor significant genomic alterations in an array of well known cisplatin resistance associated genes, such as *Casp8, SLC7A11, TLE4*, and *IL1A*. This shows that our genomic profiling was indeed predictive of cisplatin resistance in RP-B-01 PDX model.

On the other hand, whole exome sequencing of our MIBC PDX models, predicted two canonical PIK3CA HD mutations (E5452K and E545K in RP-B-01 and RP-B-02 respectively). However, when I tested therapeutic response to PI3K targeted therapy both *in vivo* and *in vitro*; I found RP-B-01 to be resistant while RP-B-02 is sensitive. Additionaly, targeting of the PI3K/mTOR pathway did not result in sustained target modeulation in RP-B-01 (PIK3CA E542K mutant model) implying that existence of an alteration in the PI3K/mTOR pathway is not predictive of response to PI3K targeted therapy per se. Based on this finding, we set out to examine the role of distinct mutation in being predictive of differential

response to PI3K targeted therapy. Our hypothesis is partly supported by a retrospective study of wide range of solid tumors that have been treated with PI3K targeted therapy that has shown that PIK3CA E542K mutant tummors; but neither H1047R nor E545K mutant tumors have a trend towards worse progression free survival(Janku, Tsimberidou et al. 2011, Janku, Wheler et al. 2013). Interestingly, when I switched *in vitro* treatment with LY3023414 in growth factor (insulin and EGF) enriched media, the differential response we observed *in vivo* as well as with DMEM media was overcome. Also, when I treated with MK2206, an AKT inhibitor the re-induction of AKT phosphorylation we observed with dual PI3K/mTOR inhibitor LY3023414 upon therapeutic resistance in RP-B-01 was not observed. Collectively, these observations point to alternative feedback signaling that is active in RP-B-01 but not RP-B-02. Whether altrenative signaling is driven soley by distinct PIK3CA mutations or also by different subtypes (i.e. basal-like VS luminal-like) remains to be better understood.

Taken together, our comprehensive genomic profiling of two MIBC PDX models is predictive of response to cisplatin but not PI3K tageted therapy(Wei, Chintala et al. 2016). Distinct PI3KCA muations in addition to distinct molecular subtypes in our models are two key points that require further investigation in order to derive a better predictive algorithm for response to targeted therapy in patients with MIBC. Ultimately our goal is to guide the clinical implementation of targeted therapy in the management of bladder cancer.

CHAPTER IV: PIK3CA E542K MUTATION IN BLADDER CANCER CONFERS RESISTANCE TO PI3K TARGETED THERAPY

A. Chapter Summary

The current goal of precision medicine is to develop more tailored treatments for cancer patients in order to improve prognosis and limit toxic side effects. However the challenge is to identify molecular aberrations that are predictive of response. Genomic profiling of two MIBC PDX models developed in our lab (Wei, Chintala et al. 2016) (RP-B-01 and RP-B-02) identified two distinct PIK3CA HD mutations in each model (E542K and E545K respectively). Additionally they were found to be of distinct molecular subtypes (basal-like and luminal-like respectively). Despite the existence of PIK3CA mutations in both models, I found them to respond differently to PI3K targeted therapy both *in vivo* and *in vitro;* where RP-B-01 was resistant while RP-B-02 was sensitive. Based on this finding, I set out to compare the role of distinct PIK3CA HD mutations in driving differential response to treatment by transfecting isogeneic HEK cells with the mutations of interest. Interestingly, PIK3CA E542K mutation conferred a significant growth advantage to HEK cells specifically in 3D culture. HEK cells transfected with E542K but neither WT nor E545K mutant PIK3CA were significantly resistant to dual PI3K/mTOR inhibitor LY3023414 both in 2D and 3D culture. Similar to what we observed in RP-B-01, resistance observed in PI3KCA E542K transduced HEK cells was associated with lack of efficient target modulation in comparison to PI3KCA E545K transduced HEK cells where AKT phosphorylation was adequately inhibited at all treatment time points. Next, to

showing the role of distinct PIK3CA mutations in driving differential treatment response; I examined potential alternative signaling that can drive feedback resistance. Interestingly, I found ERK phosphorylation to be induced upon resistance to PI3K inhibition in RP-B-01 and associated with MYC stabilization. Additionally, I found combining LY3023414 treatment with JQ1; a bromodomain inhibitor that is known to inhibit MYC and its downstream targets(Mertz, Conery et al. 2011) to be significantly synergistic in RP-B-01 but not RP-B-02. Synergy found with JQ1 was specific to LY3023414 but not helpful with resistance induced upon cisplatin treatment in RP-B-01. Taken together, this chapter reports a novel predictive role for distinct PI3KCA HD mutations in driving response to PI3K targeted inhibition. It also provides a mechanistic rationale for drug combinations that can potentially override resistance to PI3K targeted therapy and improve its clinical outcomes.

B. Background and Rationale

The field of bladder cancer management is lagging behind in comparison to other solid tumors were targeted therapy is currently the standard of care. In this disease, cisplatin; which is a conventional chemotherapeutic agent continues to be the mainstay of therapy (Leow, Martin-Doyle et al. 2014, Kamat, Hahn et al. 2016). The lack of predictive molecular stratification has impeded the success of targeted therapy (Shah, McConkey et al. 2011).

A recent attempt at comprehensive molecular characterization of bladder cancer has identified PI3K/mTOR pathway as one of the most frequently deregulated signaling pathways in this disease where PI3K signaling is deregulated in 42%of bladder cancer cases, 25 % of these cases are due to PIK3CA activating mutations (Platt, Hurst et al. 2009, Network 2014). PIK3CA activating mutations are single amino acid substitutions that occur either in the helical (E545K, E542K) or kinase domain (H1047R). Functional studies have shown different mechanisms of activation by helical and kinase domain mutations, where H1047R is dependent on P85 binding but not on RAS binding, however the opposite holds true for helical domain mutations which are so far thought to be functionally similar (Miled, Yan et al. 2007, Zhao and Vogt 2008).

Preclinical data and data from phase I and II clinical trials suggest that PIK3CA mutation status can predict response to PI3K targeted therapy (Janku, Tsimberidou et al. 2011). A recent retrospective non randomized study that analyzed data from patients with wide range of solid tumors who were treated with PI3K targeted therapy concluded that patients with wide range of solid tumors who were treated with PI3K targeted therapy who harbored a PIK3CA H1047R mutation had a higher partial response (PR) rate (38% vs. 10%; p=0.018) and a trend towards having a longer median progression free survival (PFS) (5.7 months vs. 2 months; p=0.06) compared to patients with helical domain PIK3CA mutations treated on the same protocols. The fact that PIK3CA H1047R mutation is predictive of response compared to helical domain mutations

was attributed to the coexistence KRAS mutations with helical but not kinase domain mutations (Janku, Wheler et al. 2013).

However; unlike most solid tumors, bladder cancer holds a unique position where PIK3CA helical domain mutations are more common compared to kinase domain mutations; accounting for 80% of cases driven by PIK3CA activating mutations (Network 2014). The selective pressure for helical domain mutations in bladder is not yet understood (Knowles, Platt et al. 2009, Knowles and Hurst 2015); however it might indicate that PIK3CA mutations have different roles in different histological backgrounds and therefore a different capacity of predicting response to therapy. A similar phenomenon has been reported for BRAF mutations; where a BRAF V600E mutation is predictive for response to BRAF inhibitors in melanoma, but not in colorectal cancer (Janku, Wheler et al. 2013). It is therefore important to interpret data from retrospective clinical studies cautiously and take into account the distinctive biology of each tumor as well as the inherent weakness of retrospective as opposed to randomized controlled prospective trials.

Nonetheless; it is important to note that in bladder cancer PIK3CA helical domain mutations are not exclusively coexistent with RAS mutations; therefore RAS activation cannot always explain resistance to therapy. In some instances, double mutations were identified in PIK3CA; one case with a HD and a KD domain mutation, and one case with two mutations in the HD domain (E542K

E545K); indicating an additive non redundant effect of multiple PIK3CA mutations in this disease (Sjödahl, Lauss et al. 2011); and therefore potentially a differential therapeutic potential.

Although the rate of PIK3CA activating HD activating mutations in bladder cancer is high; mTOR inhibitors were exclusively used in bladder cancer trials despite the absence of mTOR mutations in this disease(Houédé and Pourquier 2015). Only two bladder cancer trials are utilizing novel PI3K inhibitors (Munster, Aggarwal et al. 2015), (NCT01551030). Therefore, the significance of PIK3CA HD mutations in terms of predicting therapeutic response is yet to be determined.

We have previously reported that two MIBC PDX models (RP-B-01 and RP-B-02) that carry distinct PIK3CA helical domain (HD) mutations (E542K and E545K respectively) respond differently to dual PI3K/mTOR inhibitor (LY3023414), where one model is sensitive (RP-B-02, PIK3CA E545K MUT) while the other is resistant (PIK3CA, E542K MUT) (Figures 9,10) (Wei, Chintala et al. 2016). Additionally, our comprehensive genomic analysis showed that each model is of distinct subtype; where RP-B-01 is basal like while RP-B-02 is luminal like.

In this chapter, I explore the role of distinct PI3KCA HD mutations in driving differential response to PI3K targeted therapy by transfecting isogeneic cells (HEK cells) with either WT or mutant PIK3CA. Using transfected HEK cells,

I examine the oncogenic potential of each mutation and its role in driving differential response to treatment. We also performed a comprehensive gene set enrichment analyses (GSEA) on gene expression data from our PDX models and publicly available data from The Cancer Genome Atlas (TCGA) in order to identify distinct signaling mechanisms downstream of those two mutations that can play a role in therapeutic resistance. Subsequently, I tested rational drug combinations capable of overriding resistance to PI3K targeted therapy (i.e. bromodomain inhibitor). Taken together, this chapter is focused on dissecting molecular mechanisms of resistance to PI3K targeted therapy in PIK3CA E542K mutant bladder cancer and providing a rationale for novel drug combinations that can override resistance to therapy.

C. Results

C.1. PIK3CA HD mutations drive distinct signaling irrespective of tumor subtype

The differential therapeutic response that I observed in our bladder PDX models (Wei, Chintala et al. 2016), could be mutation dependent, subtype related or a combination of both. To determine, the mutation-specific signaling pathways that could play a role in therapeutic resistance irrespective of tumor subtype, we performed a comprehensive gene set enrichment analyses (GSEA) on gene expression data from our PDX models and publicly available data from The Cancer Genome Atlas (TCGA). We separated the gene expression data sets into different categories based on the PIK3CA mutation status and the molecular

subtype to identify pathways that were consistently enriched in cells with E542K mutation versus cells with E545K mutation in a subtype independent fashion.

Interestingly, this analysis identified differential metabolic pathways between *E542K* and *E545K* mutant tumors. *E542K* mutant tumors are highly enriched with alternative pathways that are often utilized in hypoxic conditions (Figure 21) while *E545K* mutant tumors have enrichment for oxygen dependent metabolic pathways (Figure 22).

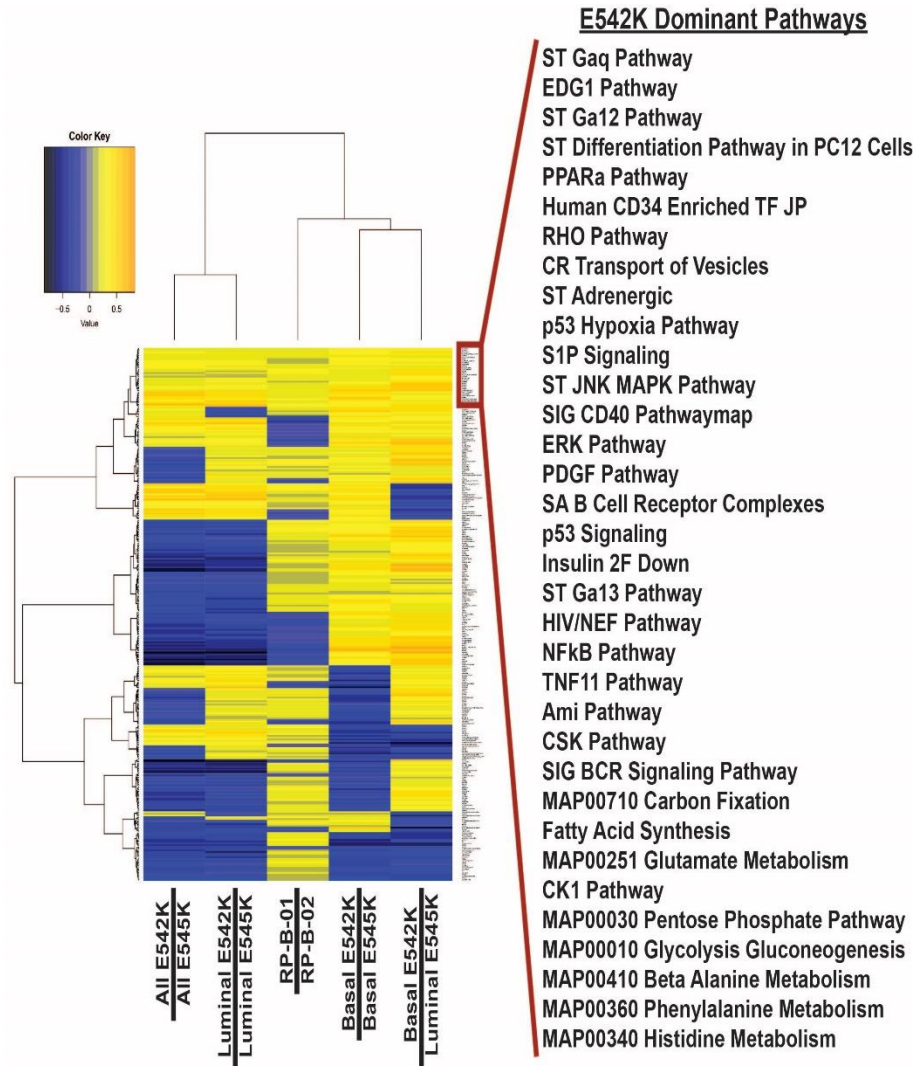

Figure 21: PIK3CA *E542K MUT* dependent pathways. Heatmap comparing E542K and E545K mutated samples using RNA-sequencing data from the TCGA Bladder Cancer (BLCA) data set and from RNA-sequencing of RP-B-01 and RP-B-02 cells. Each column represents a different comparison of samples with E542K mutations and E545K mutations. The heatmap values represent GSEA enrichment scores (ES) utilizing the C2: curated gene sets database with positive values (yellow/orange) representing enrichment in the E542K condition and negative values (black/blue) representing enrichment in the E545K condition. The callout box outlined in red highlights the C2 gene sets that are enriched for E542K samples in all of the comparisons.

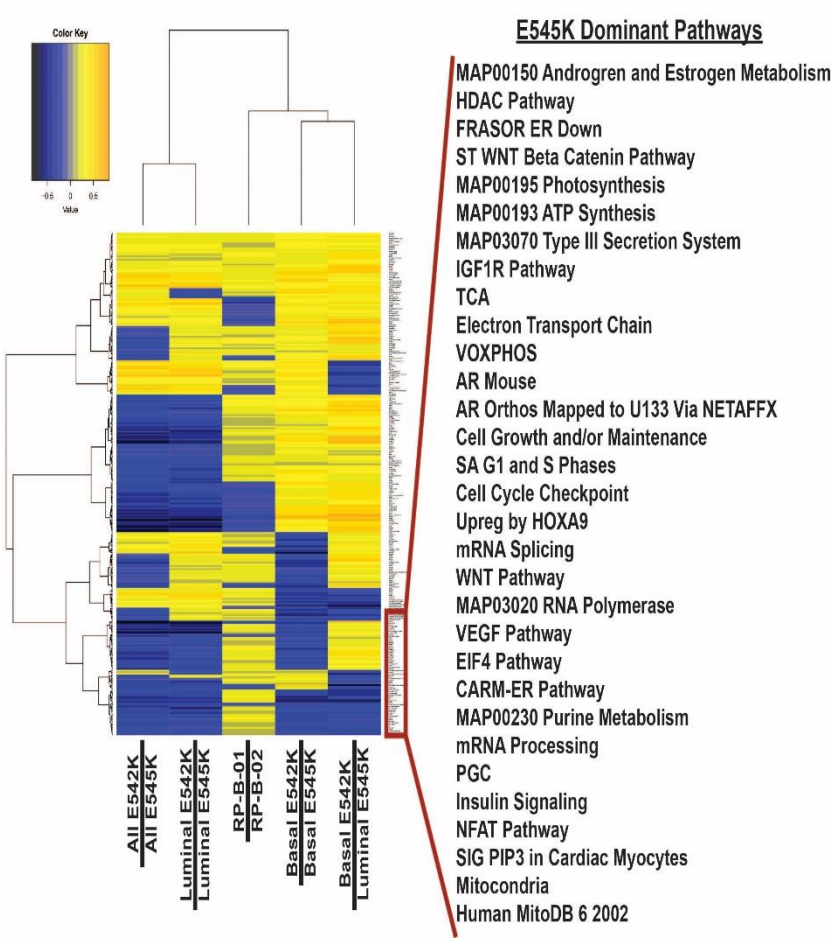

Figure 22: PIK3CA *E545K MUT* dependent pathways. Heatmap comparing E542K and E545K mutated samples using RNA-sequencing data from the TCGA Bladder Cancer (BLCA) data set and from RNA-sequencing of RP-B-01 and RP-B-02 cells. Each column represents a different comparison of samples with E542K mutations and E545K mutations. The heatmap values represent GSEA enrichment scores (ES) utilizing the C2: curated gene sets database with positive values (yellow/orange) representing enrichment in the E542K condition and negative values (black/blue) representing enrichment in the E545K condition. The callout box outlined in red highlights the C2 gene sets that are enriched for E545K samples, the listed gene sets to the right show enrichment for at least 4 out of the 5 comparisons.

C.2. *E542K* mutational status is associated with distinct metabolic behavior in urothelial cells

Altered metabolism in urothelial cells has been implicated in bladder cancer development where cancer progression is linked to glycolytic switch (anaerobic breakdown of glucose) and increased expression of genes related to the pentose phosphate pathway (glucose-6-phosphate dehydrogenase [G6PD]) and fatty-acid synthesis (fatty acid synthase [FASN]). Interestingly PI3K/mTOR signaling is known to be central to this switch (Massari, Ciccarese et al. 2016, von Rundstedt, Rajapakshe et al. 2016). Nonetheless, our analysis shown in figures 21 and 22 supports the idea that this switch is more likely favored by an E542K mutation rather than an E545K mutation.

It is not ideal to test this observation in urothelial cancer cells conventionally cultured in monolayer because of the uniform exposure of cells to non-physiologic oxygen tension. However, the 3D culture model that I have developed (Figures 13, 18-20) would provide a very attractive tool in this setting where cancer cells can spontaneously generate a multi-cellular 3D structure. This culture system can more faithfully mimic the tumor complexity in comparison to cells cultured in monorlayer since it allows for testing oxygen tension which is a surrogate marker for distinct tumor microenvironment that influences drug response(Park, Jeong et al. 2016). In order to test this hypothesis more thoroughly, I wanted to include more PIK3CA mutant bladder cancer cell lines to my panel in addition to RP-B-01 and RP-B-02 PDX derived cell lines.

Recently, a panel of 40 bladder cancer cell lines have been characterized with respect to subtype as well as recurring mutations in bladder cancer (i.e. PIK3CA, FGFR, RAS mutations) (Earl, Rico et al. 2015). This invaluable resource included 8 bladder cancer cell lines that harbor PIK3CA HD mutations. Of those eight cell lines, I was able to get hold of two additional cell lines to add to my panel: TCC-SUP which is basal-like and carries PIK3CA *E545K* mutation in addition to 253J which is basal-like and carries PIK3CA *E545G* mutation (Figure 23A).

First, I tested response to LY3023414 in those additional cell lines in comparison to my original PDX derived cell lines. Importantly, I found TCC-SUP to be significantly sensitive to LY3023414 and to behave like RP-B-02 in comparison to RP-B-01 and 253J which were less sensitive. This strengthens the idea that PIK3CA *E545K* (TCC-SUP, RP-B-02) mutation is inherently more sensitive to treatment compared to *E542K* mutation. It would be interesting to see whether *E545G* mutation (253J) clusters with *E542K* (RP-B-01) mutation, hence the similar therapeutic response. However, the lack of patient samples that carry this rare mutation in TCGA data hinders against investigating this observation more thoroughly.

A

RESISTANT	RP-B-01	Basal	PIK3CA E542K
RESISTANT	253J	Basal	PIK3CA E545G
SENSITIVE	TCCSUP	Basal	PIK3CA E545K
SENSITIVE	RP-B-02	Luminal	PIK3CA E545K

B

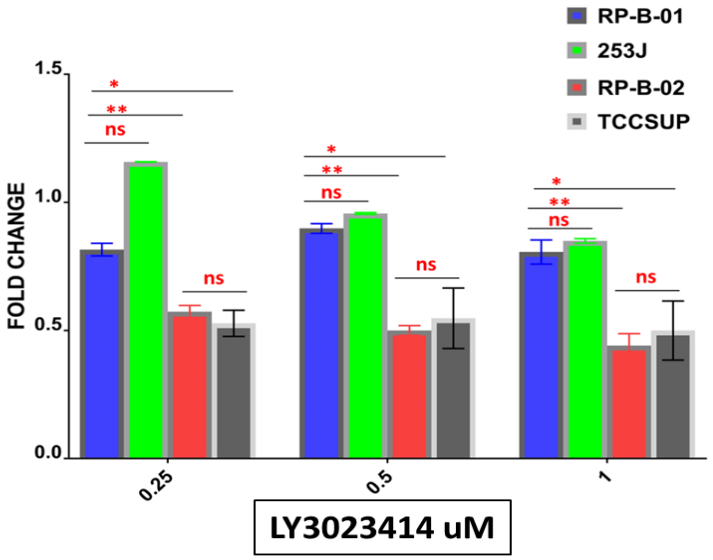

Figure 23: PIK3CA E545K MUT cell lines are more sensitive to PI3K targeted inhibition. A. Table highlighting the subtype and PIK3CA mutation status of bladder cancer cell lines used in the experiment. B. PIK3CA *E545K* mutant TCCSUP and RP-B-02 are both sensitive to LY3023414 single agent compared to basal-like RP-B-01 (*E542K MUT*) and 253J (*E545G MUT*). Fold change refers to degree of inhibition in comparison to vehicle (DMSO) control. Mean ± SD, n =3, representative results from at least triplicate experiments. One way ANOVA, Tukey's multiple comparisons test, *P= 0.01, **P<0.01, **P<0.001.

Next, I plated equal number of cells from all four cell lines (Figure 23A), and allowed them to form 3D structures per optimized conditions for 3D culture formation and growth (Figures 18-20). On Day 12, I incubated well established bladder cancer spheres with a spheroid permeable hypoxia probe, LOX-1 (Zhang, Hosaka et al. 2010, Park, Jeong et al. 2016) for 24 hours. On the next day, LOX-1 red fluorescence was measured by H1 Synergy microplate reader(Sada, Nishikawa et al. 2016). Absorption and phosphorescence peaked at 483 nm and 616 nm respectively (Zhang, Hosaka et al. 2010). Interestingly, I found the fluorescence intensity to be significantly higher in RP-B-01 (*E542K MUT*) compared to both RP-B-02 and TCC-SUP (*E545K MUT)*, while both *E545K MUT* spheres (RP-B-02 and TCC-SUP) behaved similar (Figure 24).

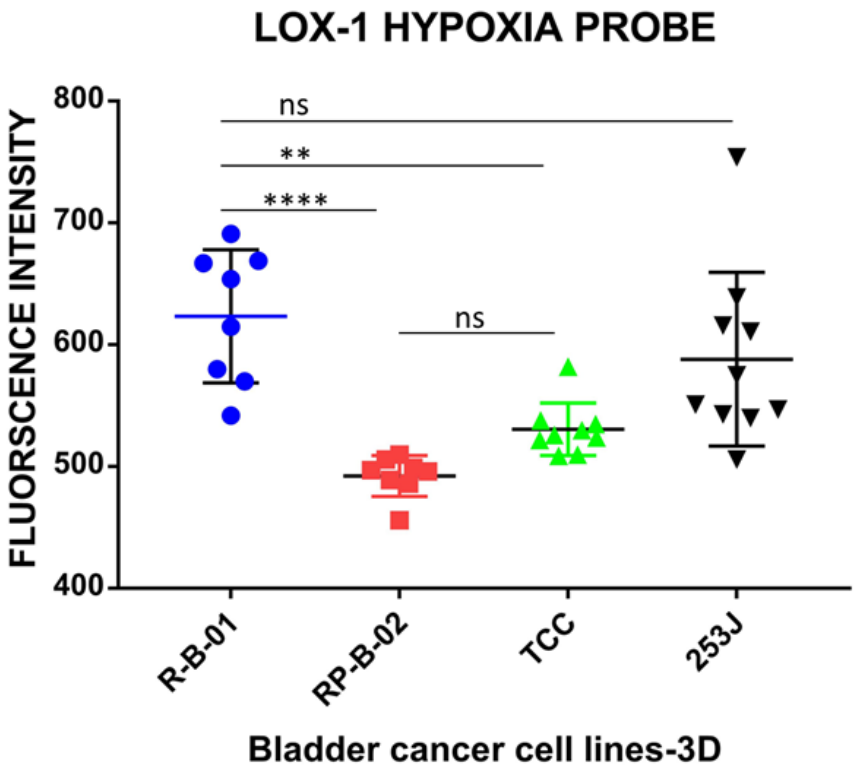

Figure 24: Uptake of LOX-1 hypoxia probe in bladder cancer spheroids. Each type of spheroid was incubated with 3D permeable hypoxia probe, LOX-1, for 24 hours on Day 12 of 3D formation. The mean fluorescence intensity was measured by h1 Synergy microplate reader. Each dot represents one well. Mean ± SD, n =3, representative results from at least triplicate experiments. One way ANOVA, Tukey's multiple comparisons test, *P= 0.01, **P<0.01, ***P<0.001, ****P<0.0001.

For a more accurate evaluation of the distribution and uptake of LOX-1 hypoxia probe in bladder cancer spheroids, I further evaluated the hypoxic regions within spheroids by confocal microscopy in order to take into account the different shape/size of spheres (Figure 13). In order to reach that goal, I co-stained the spheres with blue nuclear stain Hoechst to uniformly stain all nuclei in the sphere 30 min prior to imaging which was done 24 hours after incubation with LOX-1.

Interestingly, I found the uptake of LOX-1 red signal indicative of hypoxia to show a higher trend in RP-B-01 spheres compared to RP-B-02 spheres. The fluorescence was normalized to the nuclei within the sphere as indicated by positive Hoechst stain (Figures 25, 26). The RP-B-02 spheres has seemingly less hypoxic regions despite the compactness of the RP-B-02 spheres in comparison to RP-B-01 spheres (Figure 13) which is thought to be a key player in driving hypoxia in the core of the sphere (Park, Jeong et al. 2016). Using q-PCR I tested the expression of fatty acid synthase (FASN), one the genes that is induced upon the glycolytic switch in bladder cancer (Massari, Ciccarese et al. 2016, von Rundstedt, Rajapakshe et al. 2016) and is associated with progression and therapeutic resistance in bladder cancer(Jiang, Li et al. 2012, Zheng, Gao et al. 2016). FASN significantly overexpressed in RP-B-01 compared to RP-B-02 and was induced in a time dependent manner upon prolonged exposure of RP-B-01 cells to LY3023414 which coincides with resistance.

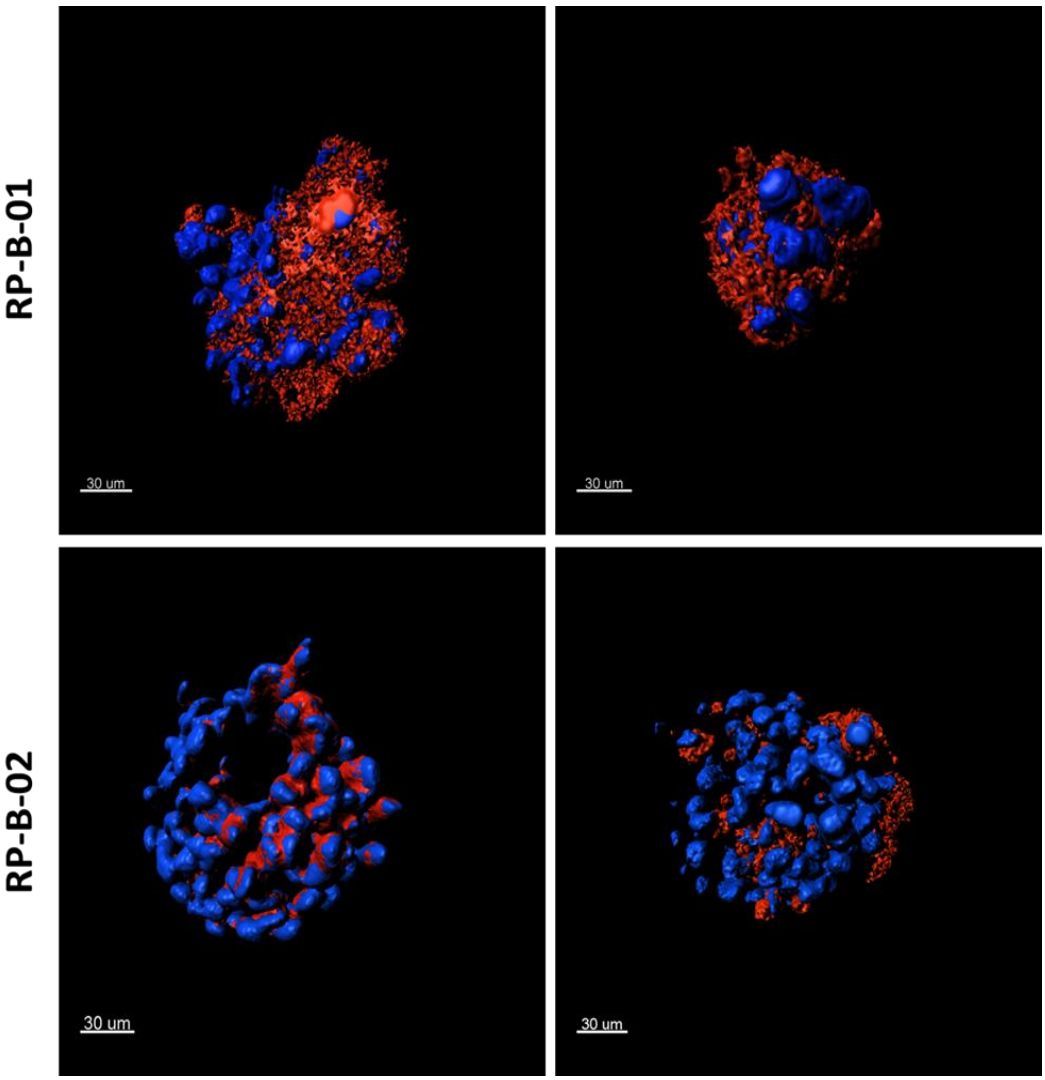

Figure 25: Confocal based evaluation of the hypoxic status of PDX derived spheroids. Imaris ™ based reconstruction and segmentation of PDX derived spheroids for visualization of the distribution of Red (LOX-1) and blue (Hoechst) signals. *The images are representative of at least 5 replicates of each condition done in 3 technical replicates.*

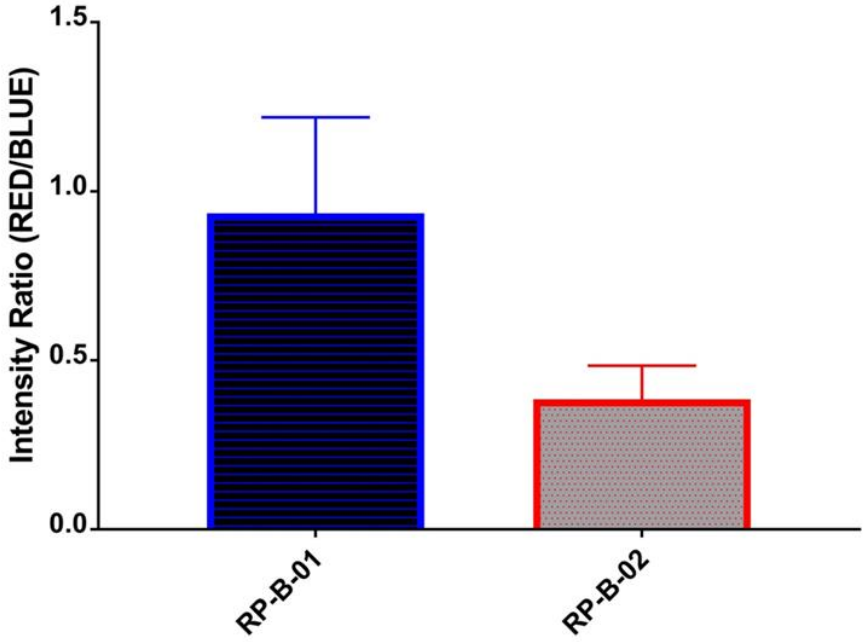

Figure 26: Quantification of the LOX-1 fluorescence intensity in PDX derived spheroids. LOX-1 uptake was quantified as ratio between red signal (LOX-1) and blue signal (Hoechst). This ratio allows for accounting for sphere variability in shape and size which was accounted for using Hoechst which stains all nuclei. B0-1 trended towards higher uptake of LOX-1 in comparison to RP-B-02. However the results were not statistically significant.

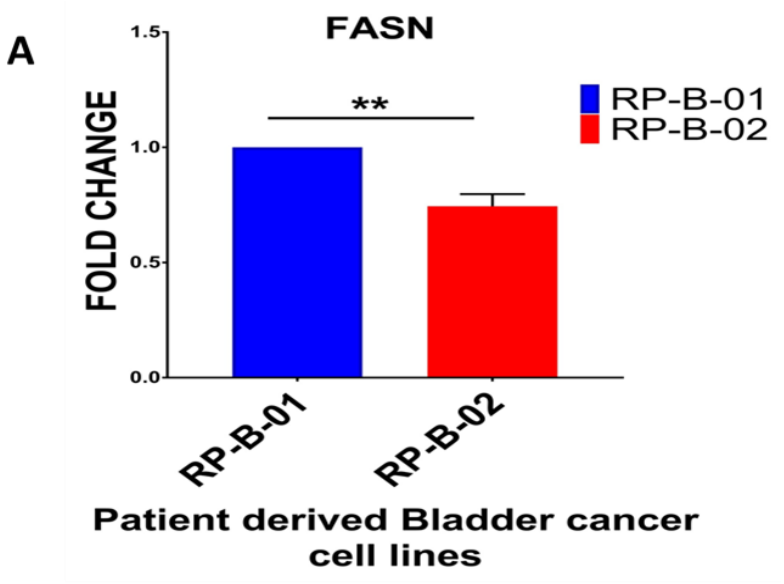

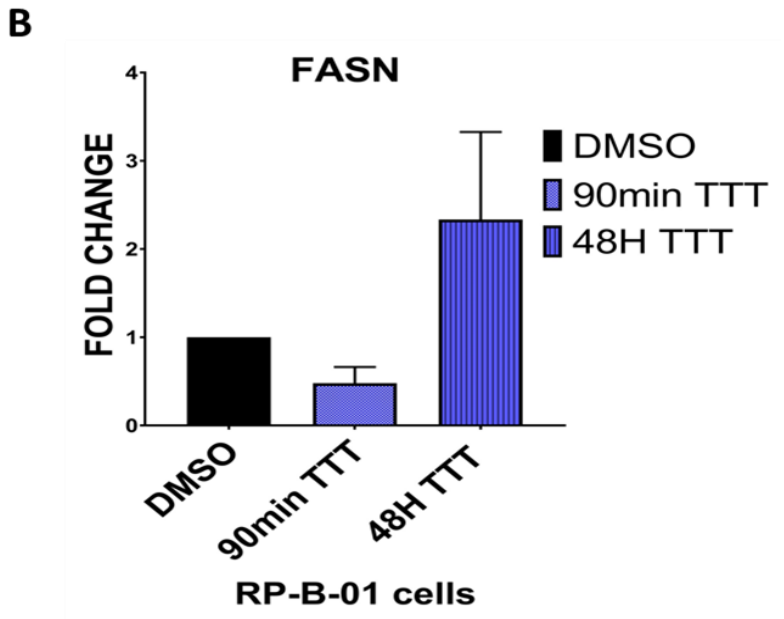

Figure 27: FASN is overexpressed in RP-B-01 and induced upon resistance to LY3023414. A: qPCR confirms significantly more FASN in RP-B-01 compared to RP-B-02 similar to the RNA-Seq analysis. B. FASN is downregulated at 90 min treatment (TTT) of RP-B-01 cells with LY3023414, a time point where P-AKT is efficiently inhibited by the drug. However, it is induced upon prolonged drug exposure (48 hours) which coincided with upregulation of P-AKT and resistance to LY3023414.

C.3. *E542K* mutant PI3K protein confers significant growth advantage to HEK cells

In order to validate the distinct growth and metabolic behavior of the two PIK3C HD mutations (PIK3CA *E542K* & *E545K*); I transfected isogeneic HEK293T cells with either *WT* or *MUT* PIK3CA plasmids. Although HEK cells do not represent an ideal biologically relevant background, they are readily transfectable cells that express WT PI3K protein and that have been previously used to test the behavior of different PI3K isoforms(Nakanishi, Walter et al. 2016).

Using western blotting, I confirmed the expression of protein of interest (WT or Mutant) in transfected cells by probing for HA-tag expression. Overexpression of PI3K protein was associated with upregulation of P-AKT in comparison to non-transfected control (empty vector); which shows that the overexpressed protein is functional and thus mechanistically testable (Figure 28). Next, using Alamar blue proliferation based assay, I monitored the growth of HEK cells expressing WT and mutant PI3K protein over time both in monolayer and in 3D culture. Both forms of mutant PI3K protein conferred a growth advantage to HEK cells compared to WT protein in monolayer (~20% on days 2 and 3) (Figure 29A). Interestingly however; in 3D culture, I found that E542K mutant protein conferred a significant growth advantage to HEK cells (~50-100%) in comparison to the E545K mutant (~30-70%) (Figure 29B).

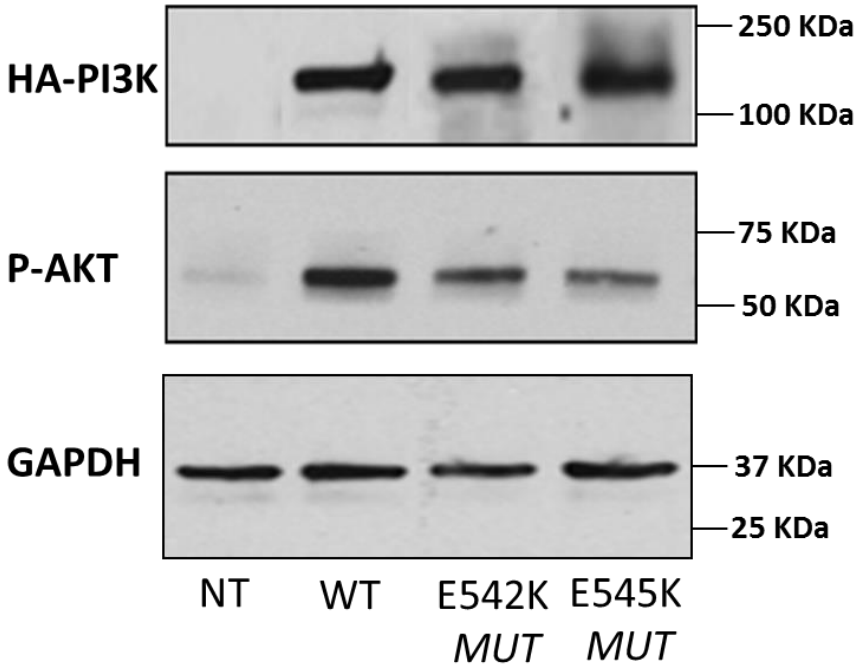

Figure 28: Development of isogenic HEK cells that are either WT or carry the PIK3CA HD mutation *(E542K; E545K)*. Overexpression of PI3K protein was associated with upregulation of P-AKT in comparison to non-transfected control (NT); which shows that the overexpressed protein is functional and thus mechanistically testable.

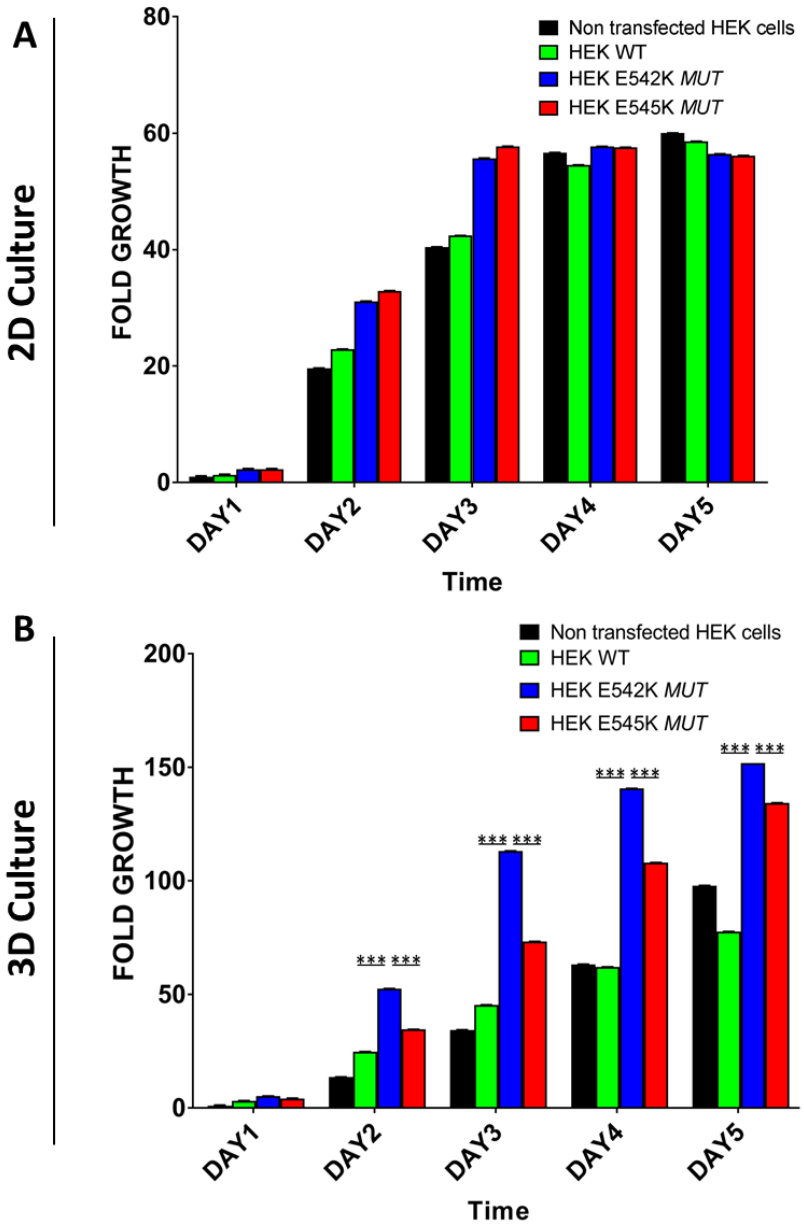

Figure 29: PIK3CA *E542K* mutation confers significant growth advantage to HEK cells. A. Growth of HEK cells (WT/MUT) monitored in monolayer overtime using Alamar blue fluorescence proliferation-based assay. Mutant protein conferred growth advantage to cells (average of 3 replicates). B. In 3D Matrigel-based system, HEK PIK3CA *E542K MUT* cells grew significantly faster than E545K mutants. Mean ± SD, n =3, representative results from at least triplicate experiments. One way ANOVA, Tukey's multiple comparisons test, ***P<0.001.

Next, using q-PCR, I tested the expression of FASN in transfected HEK cells to examine whether over expression of distinct PIK3CA mutations would influence gene expression and mirror the overexpression of FASN in RP-B-01 cells. Interestingly, in PIK3CA *E545K* transfected HEKs , I found FASN, one of the markers of altered metabolism in urothelial cancer to be significantly downregulated in comparison to *E542K* mutant and WT cells (Figure 30).This finding mirrors the differential metabolic behavior that I observed in bladder cancer PDX derived cell lines (RP-B-01 and RP-B-02 respectively).

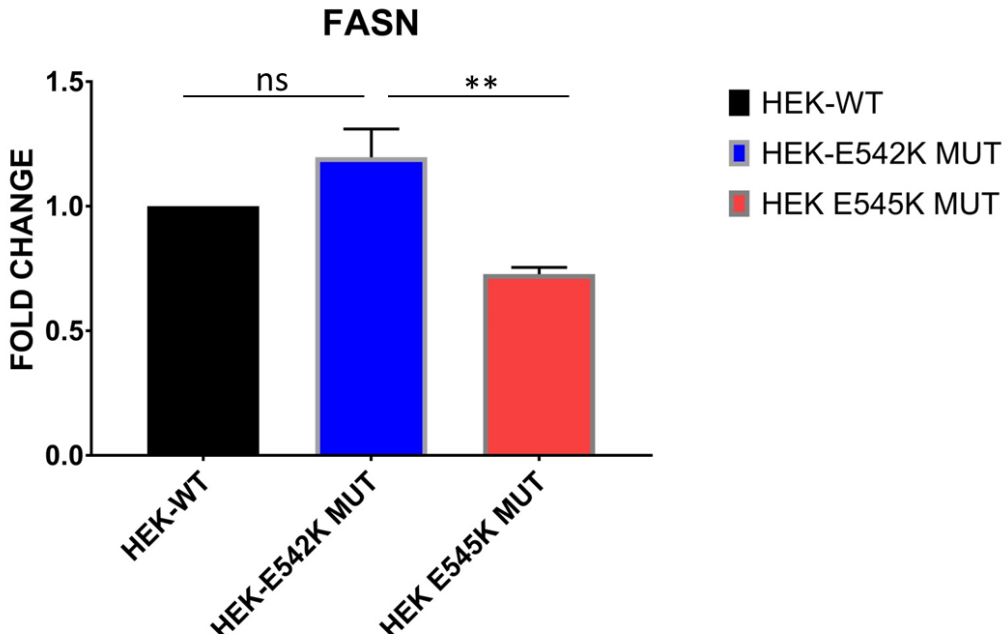

Figure 30: FASN is reduced in PIK3CA *E545K MUT* cells. q-PCR show significant downregulation of FASN in *E545K MUT* cells compared to *E542K MUT* cells. Mean ± SD, n =3, representative results from at least triplicate experiments. One way ANOVA, Tukey's multiple comparisons test, **P<0.01.

In 3D culture, I assessed the distribution and fluorescence intensity of Mitotracker signal in PIK3CA transfected HEK cells as an alternative tool for assessing the metabolic changes associated with HD PIK3CA mutations(Fijalkowska, Xu et al. 2010) . Similar to what I observed with the hypoxia probe LOX-1 (Figures 24-26), I found a distinct uptake and distribution of the Mitotracker in E542K and E545K mutant HEK spheroids (Figure 31). Interestingly, I found the Mitotracker fluorescence signal to be significantly less in both E542K and E545K mutant HEK spheroids compared to their WT counterpart after being normalized to the Hoechst blue signal to account for the striking difference in spheroid sizes (Figure 32). However, there was no significant difference between E542K and E545K mutant spheroids (Figure 32). Therefore, for further validation my goal is complement this experiment with LOX-1 staining to overcome the limitations associated with Mitotracker as a tool for measuring hypoxia/metabolic changes(Mitra and Lippincott‐Schwartz 2010).

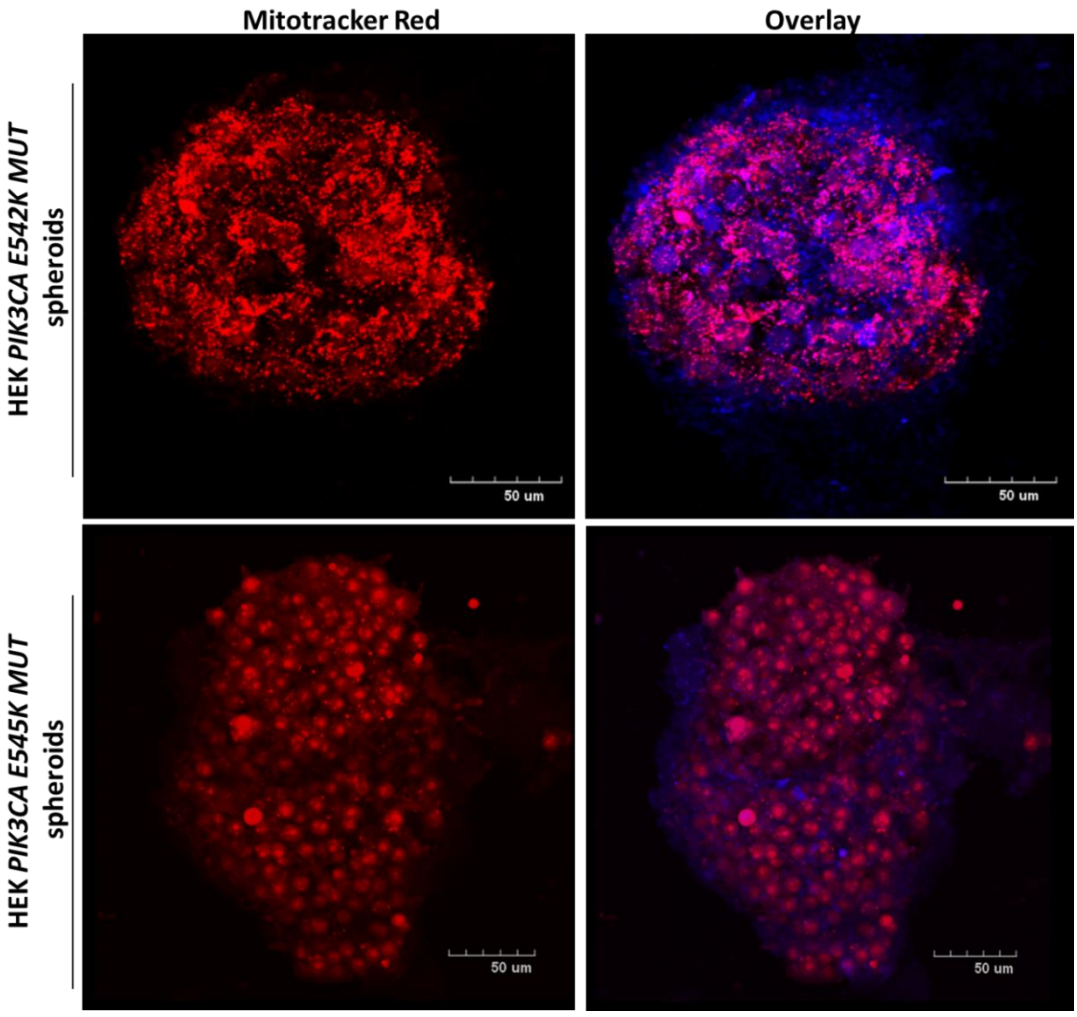

Figure 31: Uptake and distribution of Mitotracker Red in *PIK3CA MUT* HEK spheroids. projected image of multi-slice confocal imaging of PIK3CA mutant s spheres show distinct uptake and distribution of Mitotracker Red signal in *E542K MUT* in comparison to *E545K MUT* spheres. *The images are representative of at least 5 replicates of each condition done in 3 technical replicates.*

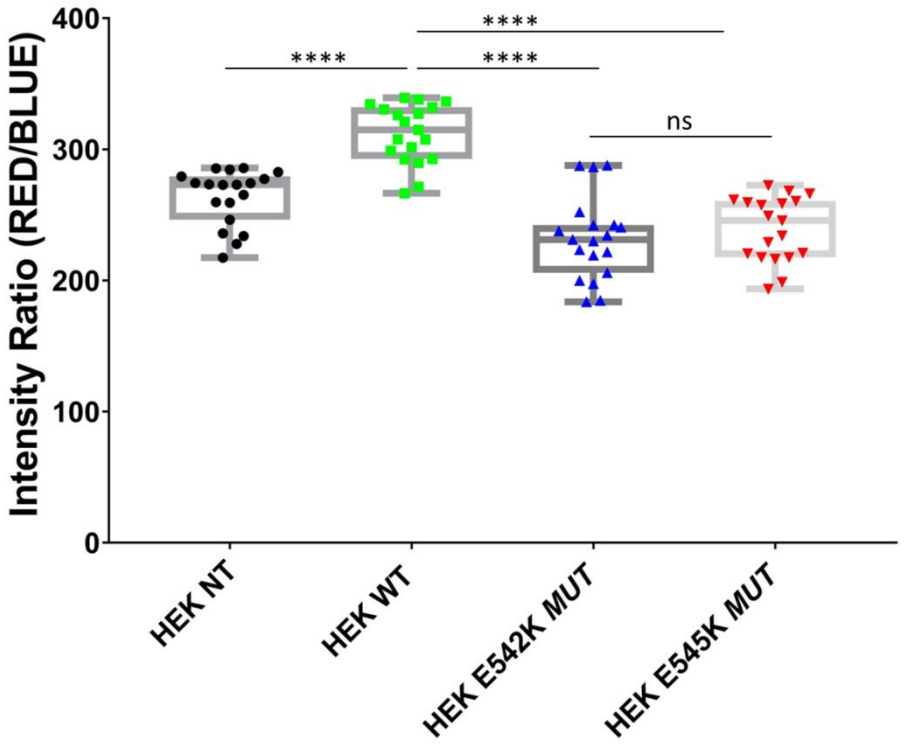

Figure 32: PIK3CA mutation status influence Mitotracker signal intensity in HEK spheroids. Confocal imaging-based quantitative analysis of the Red (Mitotracker)/Blue (Hoechst) signal in images slices taken per spheroid per condition show that over expression of WT PIK3CA in HEK cells is associated with significantly higher mitotracker signal in comparison to both non transfected (NT) and mutant (MUT) conditions. No significant difference in the intensity of the red signal was detected in *MUT* HEK spheroids. *. Mean ± SD, n =6, representative results from at least triplicate experiments. One way ANOVA, Tukey's multiple comparisons test, **P<0.01.*

C.4. PIK3CA E542K mutation is associated with weaker binding of LY3023414

Thus far, I have shown that PIK3CA HD mutations drive distinct mutation dependent signaling in bladder cancer that is reflected in the behavior of PDX derived spheroids as well as in PIK3CA mutant HEK cells/spheroids. These findings provide a solid foundation for testing whether differential response to PI3K targeted inhibition is mutation dependent.

First, I sought out collaboration with the department of biotechnology, VIT University, Vellore, India in order to investigate whether the mutation type could influence the affinity of the compound (LY3023414) to the substrate (PI3K protein) in a distinct manner. *In silico* analysis of the binding affinity of LY3023414 to WT and mutant PI3K protein started with computationally deriving the crystal structure of Phosphoinositide-3-kinase (PI3K) alpha lipid kinase. Using NCBI BLASTp homology search(Johnson, Zaretskaya et al. 2008) the crystal structure of Phosphoinositide-3-kinase (PI3K) alpha lipid kinase (PDB ID: 4YKN with 2.9 Å resolution) was built with 99% sequence identity and 99% query coverage against the target mutant sequences (E542K and E545K respectively) and it was used as a template for the homology modeling. The structural quality of the model produced by MODELLER(Fiser and Šali 2003) was verified by the Ramachandran plot, which reveals that phi/psi angles of the residues are located in favored regions (97.7% and 97.9% respectively). 3D verification revealed that the compatibility of the residues are 80.73% and 81.59% respectively and the structures have the average score of >0.2, which indicates the excellent

compatibility among the residues. The ERRAT confirmed non-bonded contacts between the diverse atoms. The quality factor of the modeled mutants was found to be 85.12 and 83.64 respectively. The ProSA module projected the Z-score of -9.22 and -9.89 for RP-B-01 and RP-B-02 respectively. The complete analysis of the results supported the great quality of the modelled protein.

Using the predicted in silico model for both forms of mutant PI3K protein (*E542K* and *E545K* mutant); molecular docking for both mutations (found in RP-B-01 and RP-B-02 respectively) with the PI3K/mTOR pathway inhibitor LY3023414(Fiser and Šali 2003) was done. The docking in the context of the *E545K* mutation resulted in higher binding energy compared to the *E542K* mutation with the C-score of 4.23 and 2.21 respectively. Moreover, H-bond interaction with Glu237 (distance 3.2 Å) and Lys678 (distance 3.3 Å) was detected in the context of the *E545K mutation* while found 2 H-bond formation with Cys838 (distance 3.4 Å) and Ser312 (distance 3.2 Å) were detected with the *E542K* mutant. Overall, *E545K* mutation was found to be associated with improved interaction of LY3023414 with PI3K protein (Figure 33). On the other hand; *E542K* mutation was associated with poor binding of LY3023414 to the PI3K protein (Figure 34) (Wei, Chintala et al. 2016).

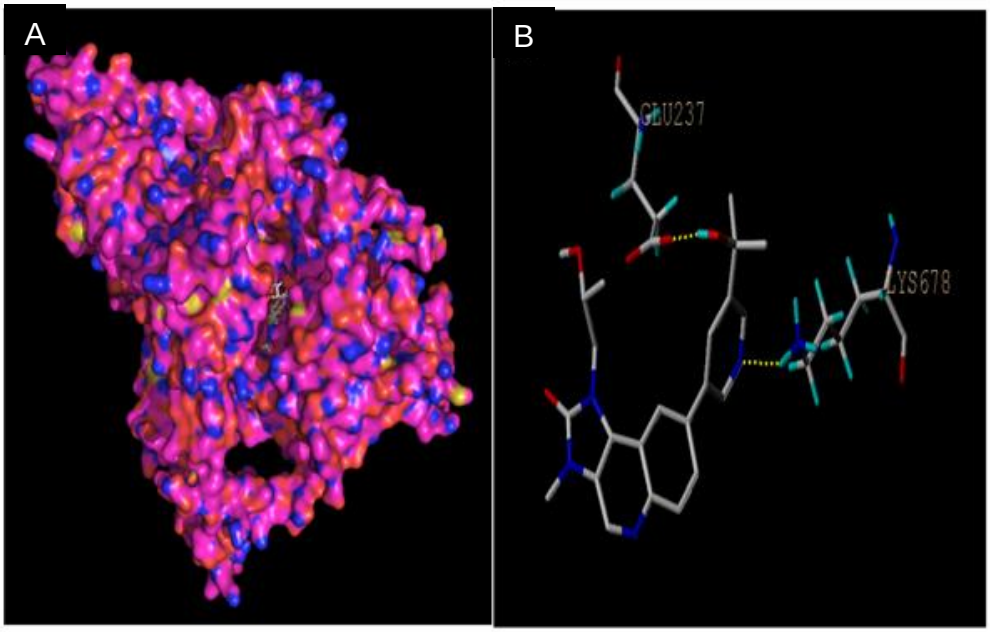

Figure 34: Docking results of PI3K E545K *MUT* and LY3023414. A. Binding mode of LY3023414 with E545K *MUT.* B. E545K *MUT* residues involved in H-bond formation with LY3023414

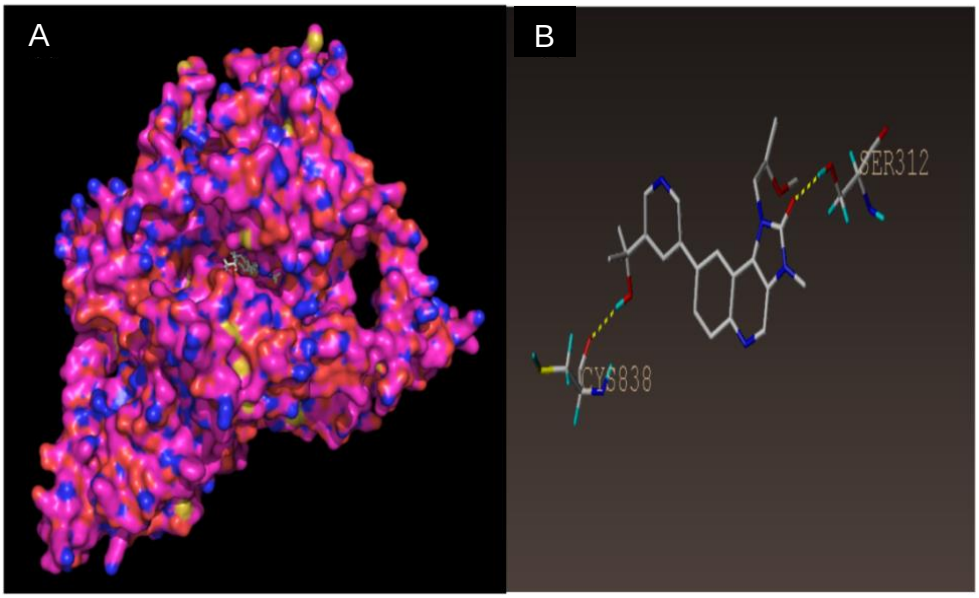

Figure 33: Docking results of PI3K E542K MUT and LY3023414**.** A. Binding mode of LY3023414 with PI3K E542K MUT. B. PI3K E542K MUT residues involved in H-bond formation with LY3023414.

To figure out the stability of the complexes PI3K (*E542K*-LY3023414) and PI3K (*E545K*-LY3023414), molecular dynamic simulation (MDS) was implemented and the generated graphs were analyzed(Turner 2005, Hess, Kutzner et al. 2008). The first thing tested in the MDS study was Root-mean-square deviation of atomic positions (RMSD). The displacement of heavy atoms after 45000 ps of MD simulation was determined by g_rms of GROMACS package. The RMSD of the complexes PI3K (*E542K*)-LY3023414 and PI3K (*E545K*) - LY3023414 are shown in (Figure 35). As illustrated in the figure, the PI3K (*E545K*) - LY3023414 complex has sudden rise in the beginning and after 5000 ps RMSD value stabilized at 0.65 nm. Whereas, the PI3K (*E542K*)-LY3023414 complex has gradual increase in the RMSD value from 0.42 nm to 0.62 nm till 35000 ps. Later the value gets stabilized after 35000 ps at 0.68 nm. The complete analysis of RMSDs of the complexes PI3K (*E542K*)-LY3023414 and PI3K (*E545K*) - LY3023414 reveals that the PI3K (*E545K*) - LY3023414 complex has higher stability than PI3K (*E542K*)-LY3023414 complex.

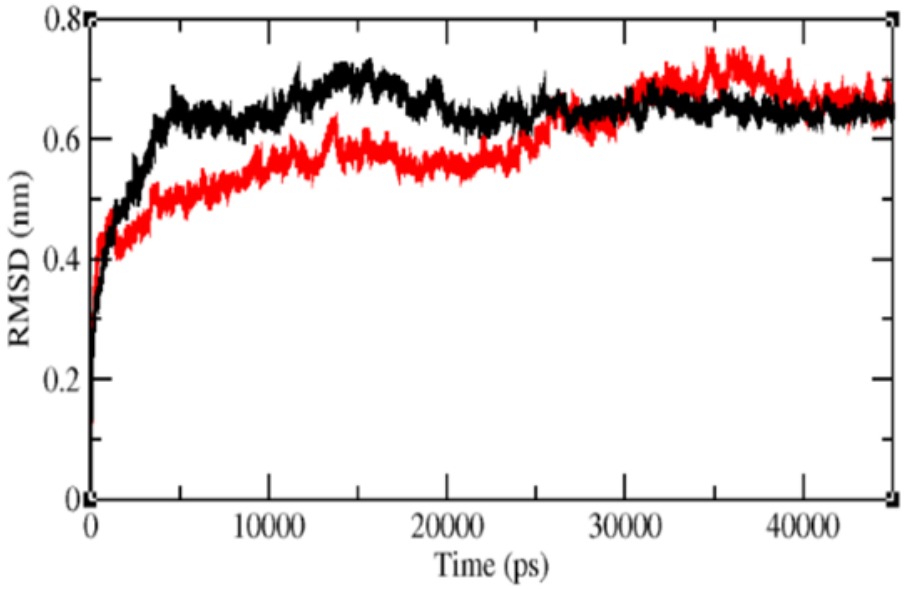

Figure 35: RMSD Plot. Backbone RMSD plots of PI3K *E545*K *MUT* -LY3023414 complex (black) and PI3K *E542K MUT*-LY3023414 complex (red).

Next, root mean square fluctuation (RMSF) was measured to predict the average movement of the atoms on binding of LY3023414 with PI3K protein that carries either the *E542K* or *E545K* mutation after 45000 ps using the g_rmsf. The PI3K (*E542K*)-LY3023414 complex was found to have fluctuations ranging from 0.08 nm to 1.05 nm (Figure 36A). The LY3023414 binding site residues Cys838 and Ser312 in the context of the *E542K* mutant PI3K protein have 0.09 nm and 0.22 nm variation. Similarly, the LY3023414 binding site residues of *E545K* mutant PI3K protein, Cys678 and Glu237 have the fluctuation of 0.07 nm to 0.21 nm. As depicted in (Figure 36B), the Lys545 of RP-B-02 model has the variation of 0.12 nm and the residue Lys542 in the RP-B-01 treatment resistant model has the fluctuation of 0.16 nm. The complete observation of the fluctuation ranges

reveals that the *E545K* mutation influences some structural changes in PI3K protein and cause increased binding affinity of LY3023414 towards PI3K and makes the complex more stable.

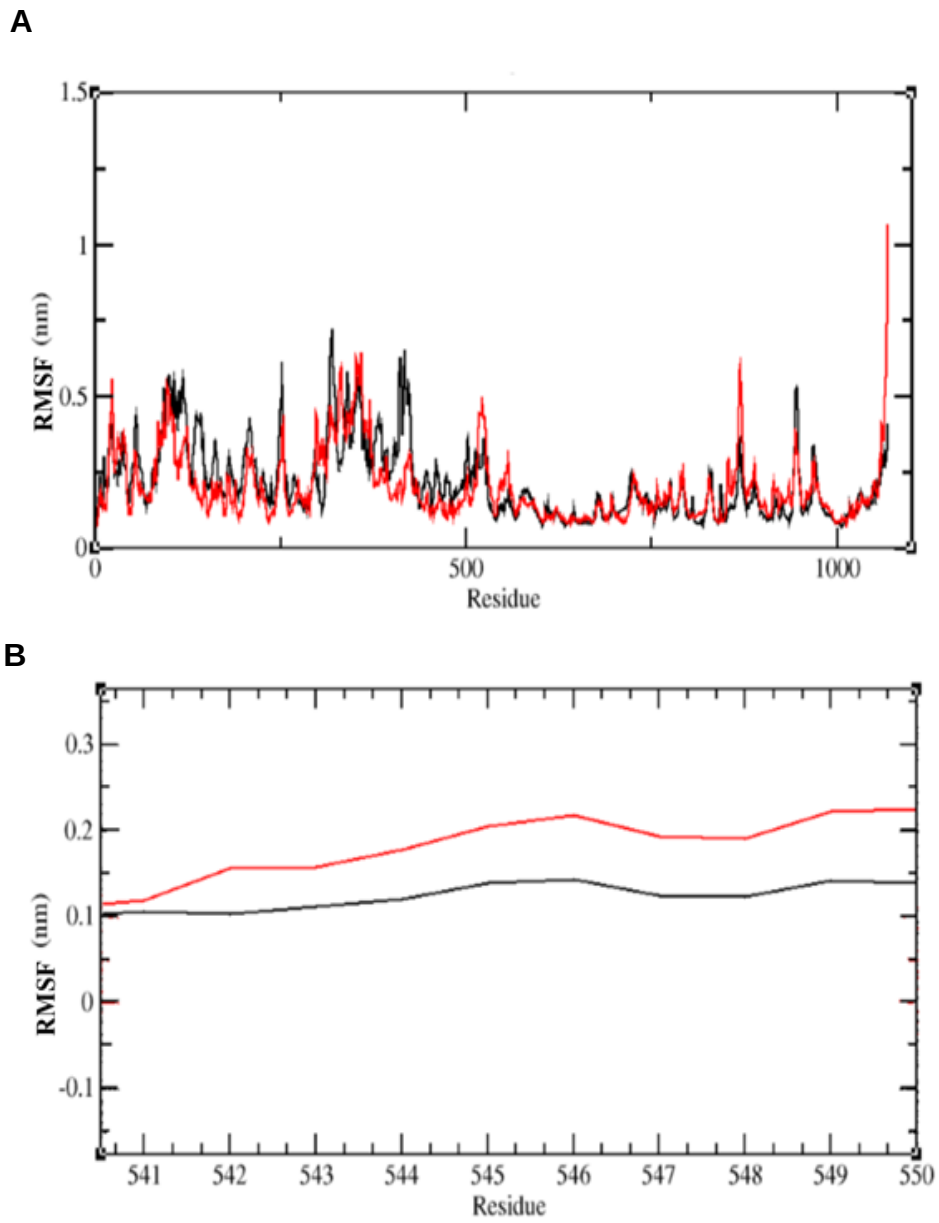

Figure 36: RMSF Plot. A. RMSF plot for backbone atom of PI3K *E545K MUT* -LY3023414 complex (black) and PI3K *E542K MUT* -LY3023414 complex (red) showing distinct fluctuations of atoms in both conditions. B. RMSF plot for specific Lysine residues at the 542 and 545 positions in *E542K (red*) and *E545K* mutants (black).

To further confirm that distinct missense mutations in the PI3K protein helical domain drive distinct conformational changes in the PI3K treatment which influence the affinity between the protein and the drug; the radius of gyration (Rg); a measure of the compactness of protein, was calculated after 45000 ps. The Rg plot of the two different complexes is depicted in (Figure 37). The PI3K (*E542K*)-LY3023414 complex shows minor deviation at the start of the simulation. After 25000 ps, the Rg value started rising till 3.25 nm. Then, there is sudden decrease in the Rg value which gets stabilized at 3.23 nm. The PI3K (*E545K*) - LY3023414 complex showed rapid increase at the beginning , then the Rg value started decreasing gradually then it reached 3.15 nm till 30000 ps. Then the Rg value is stable at 3.15 nm after 30000 ps. The difference in the stability status of the two complexes indicates that the binding of LY3023414 with *E545K* mutant is influenced by distinct conformational changes in the protein.

Lastly, the H-bond distances of PI3K (*E542K*)-LY3023414 and PI3K (*E545K*)-LY3023414 complexes (Figure 38); showed that the PI3K (*E542K*)-LY3023414 complex had fluctuating H-bond distances of 3 nm till 10000 ps and 3.2 nm distances from 10000 ps to 27000 ps. After 30000 ps the H-bond distance decreases from 3.4 nm to 3.2 nm. Whereas the PI3K (*E545K*)-LY3023414 complex had a more stable H-bond distance overall (average of 3.28 nm). Taken together, the PI3K (*E545K*)-LY3023414 complex interaction is found to be more stable that the PI3K (*E542K*)-LY3023414 complex.

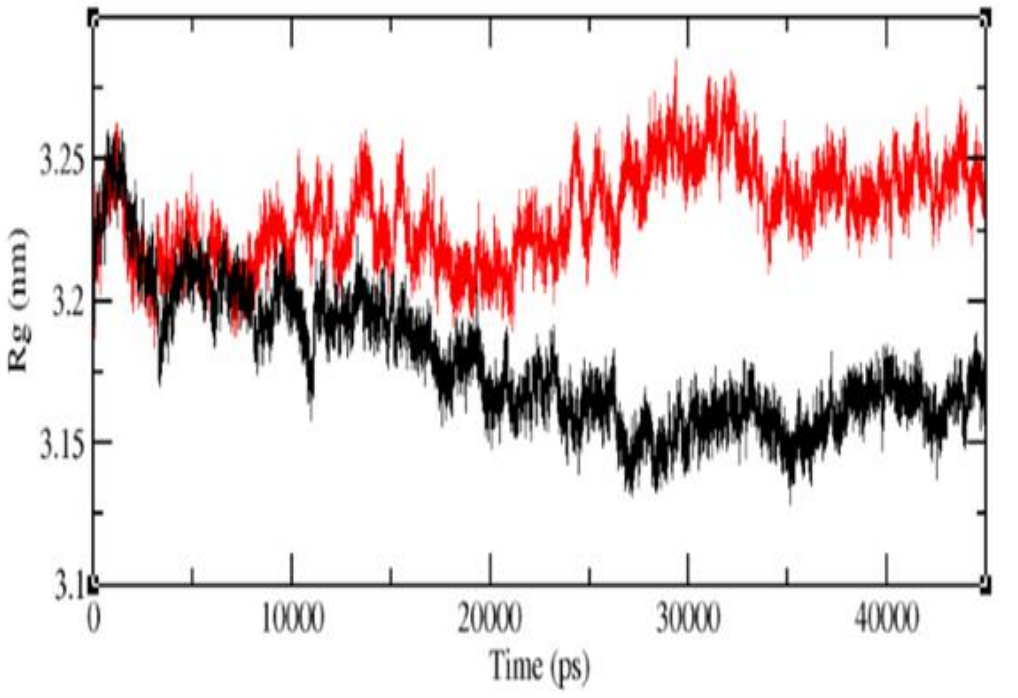

Figure 37: Rg Plot of Cα atoms. Rg plots of Cα atoms of PI3K E545K-LY3023414 complex (black) and PI3K E542K-LY3023414 complex (red). Radius of gyration (Rg) is a measure of protein compactness, the higher the Rg score (red/*E542K*), the less stable the protein conformation.

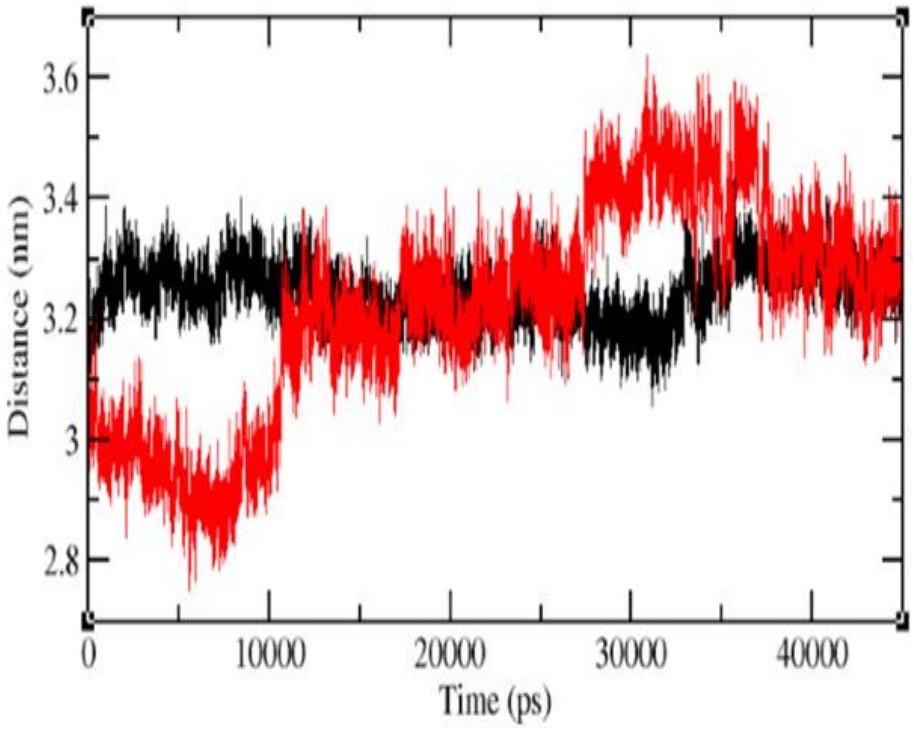

Figure 38: H-bond plot. H-bond distances between the PI3K *E545K*-LY3023414 complex (black) and PI3K *E542K*-LY3023414 complex (red).

Overall preliminary *in silico* analysis supports the idea that distinct PIK3CA mutations drive distinct conformational changes in the protein that influence protein-drug binding and stability of the formed complex in a manner that could potentially affect therapeutic response.

It is therefore important to test whether this is functionally translated in a manner where distinct mutations influence the protein kinase activity. Using ADP-Glo assay we tested the effect of LY3023414 on the kinase activity of the two mutant forms of PI3K protein (*E542K* and *E545K* mutants). Interestingly, we did

not find a significant difference between the two mutations (Figure 39), implying that resistance associated with distinct conformational changes induced by the *E542K* mutation are not driven by direct effect on the protein kinase activity but more globally by alterative drug-protein and protein-protein interactions.

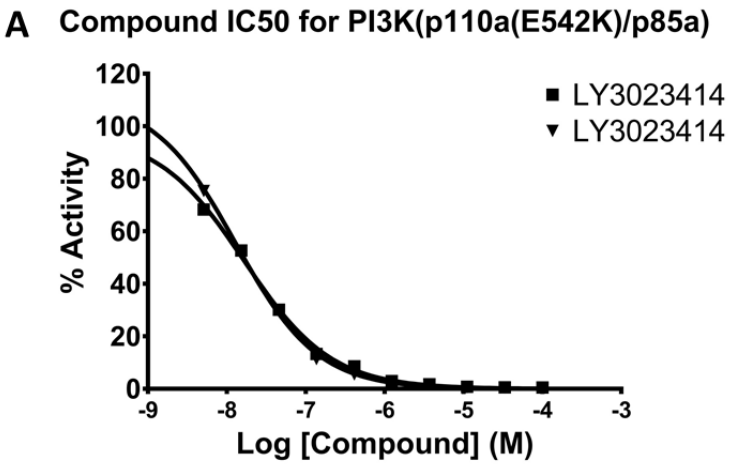

	LY3023414	LY3023414
HillSlope	-0.7865	-0.8392
EC50	1.651e-008	1.293e-008

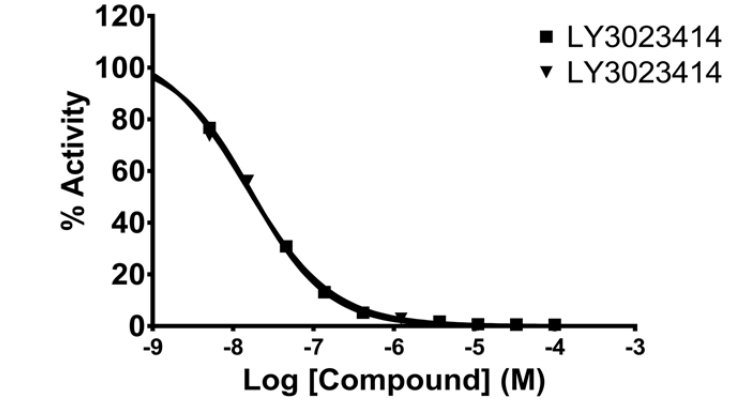

	LY3023414	LY3023414
HillSlope	-0.9146	-0.8197
EC50	1.687e-008	1.468e-008

Figure 39: LY3023414 does not have differential effects on kinase activity of PI3K protein carrying distinct HD PIK3CA mutations. A. IC50 of LY3023414 with respect to kinase activity of PI3K E542K *MUT* is 1.65E-08 and 1.29E-08 (duplicates). B. IC50 of LY3023414 with respect to kinase activity of PI3K E545K MUT is 1.69E-08 and 1.47E-08 (duplicates)

C.5. HEK cells harboring the *E542K* mutant PI3K protein are resistant to LY3023414

Next to investigating the distinct LY30234314-PI3K interactions induced by PIK3CA HD mutations *in silico*, I tested whether response to LY3023414 is indeed mutation specific using PIK3CA transfected HEK cells. Cells transfected with the *E542K* mutant protein were significantly more resistant to LY3023414 when treated in monolayer at all treatment time points compared to *E545K* mutant cells ($P<0.001$) (Figure 40A). Similarly, when treated in 3D, *E542K* mutant spheroids were strikingly resistant to treatment compared to their *E545K* mutant counterparts, yet at a lower concentration range (Figure 40B). Collectively, these data provide a proof of concept that there is a potential independent role of distinct PIK3CA mutations in driving differential response to PI3K targeted therapy.

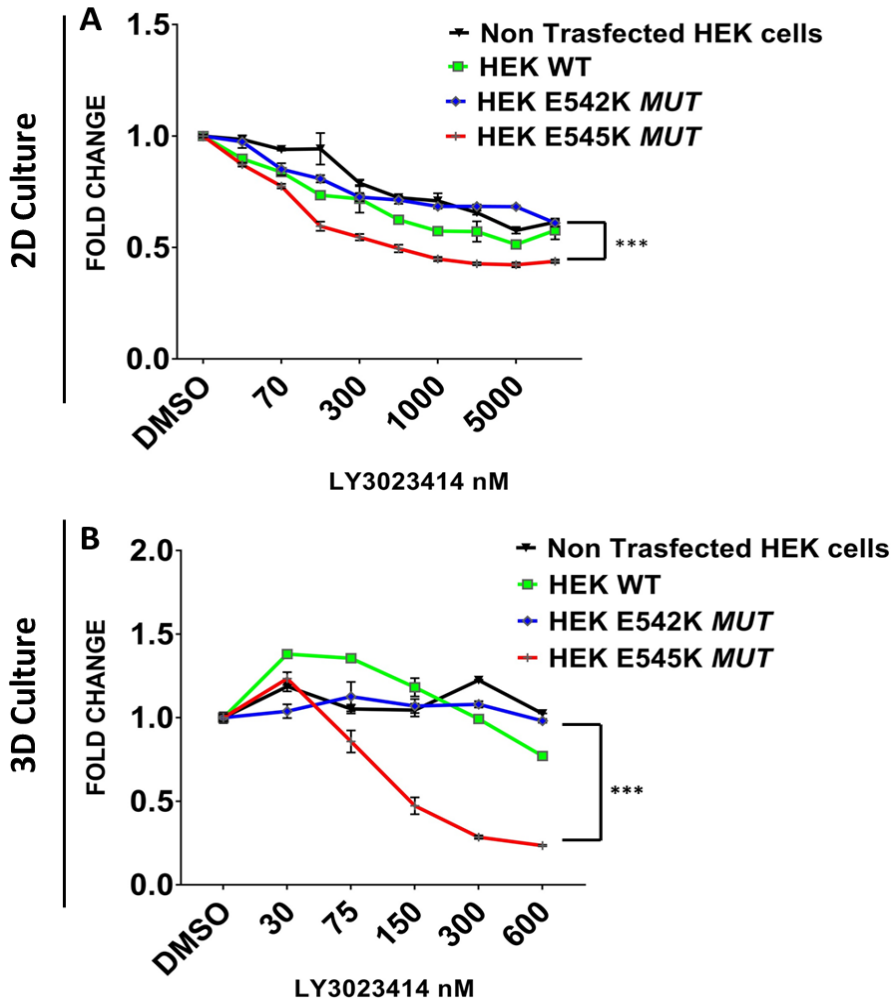

Figure 40: HEK cells harboring the E542K mutant PI3K protein are resistant to dual PI3K/mTOR inhibitor LY3023414. A. Cells treated in monolayer with LY3023414 at different concentration and time points (72 hour treatment time point shown). HEK *E545K MUT* cells are significantly sensitive to treatment compared to other clones. B. Cells treated in matrigel based 3D culture with LY3023414 on Days 4 and 8. HEK *E545K MUT* cells are significantly sensitive to treatment compared to other clones. Mean ± SD, n =3, representative results from at least triplicate experiments. One way ANOVA, Tukey's multiple comparisons test, ***P<0.001.

C.6. Resistance to LY3023414 in *E542K* mutant HEK cells is associated with inefficient target modulation

Therapeutic resistance observed in RP-B-01 is associated with upregulation of AKT phosphorylation upon extended exposure to LY3023414 *in vitro* (24H and 48H) as well as *in vivo.* Therefore I tested the effect of LY3023414 treatment on downstream PI3K/mTOR signaling in PIK3CA transfected HEK cells. Interestingly, at 24 and 48H, AKT phosphorylation was inhibited in PIK3CA *E545K* mutant HEK cells but not in PIK3CA *E542K* mutant cells (Figure 41). These data corroborates our findings in the resistant *E542K* mutant RP-B-01 model and further strengthens the rationale behind a mechanistic role of distinct PI3KCA mutations in driving response to treatment.

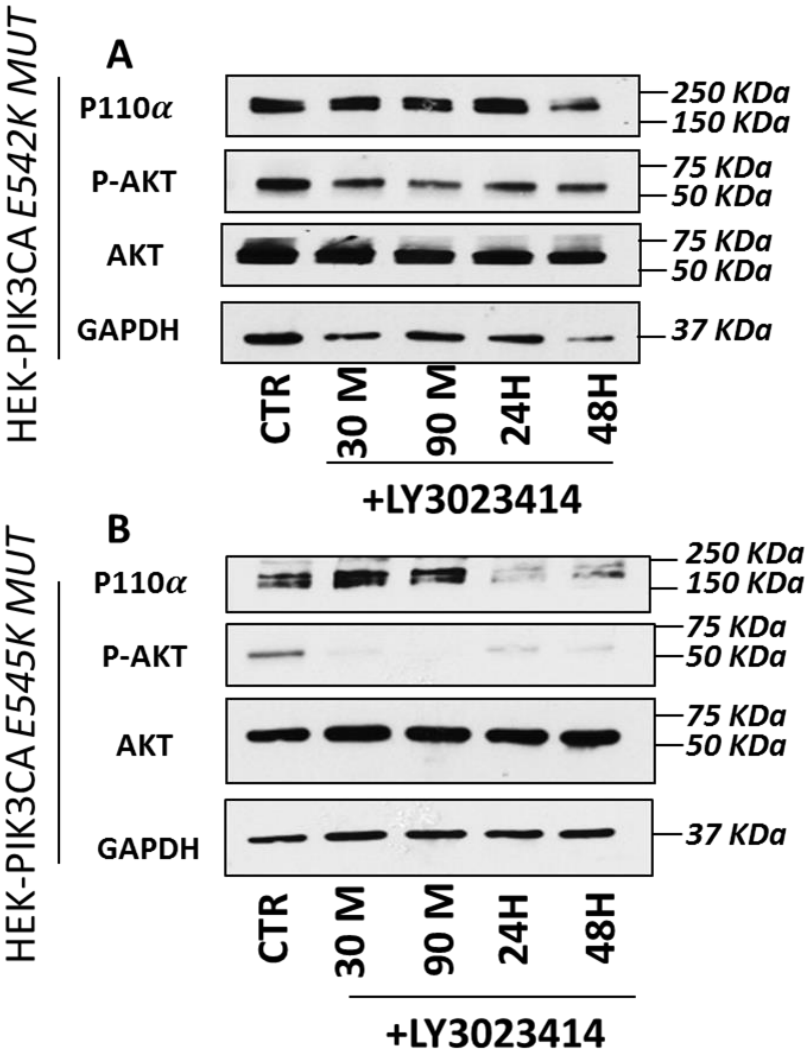

Figure 41: Resistance to PI3K targeted inhibition in *E542K* mutant HEK cells is associated with inefficient target modulation. A. HEK cells transfected with PIK3CA E542K MUT treated with LY3023414 at different time points. AKT phosphorylation was not inhibited compared to B. PIK3CA E545K transfected cells were both AKT phosphorylation and total PI3K protein were decreased upon exposure to LY3023414 at different time points tested.

C.7. RAS-MAPK signaling is activated in RP-B-01 and associated with stabilization of MYC

The ultimate goal of studying therapeutic resistance is to identify alternative signaling pathways that are activated in resistant tumors and that are potentially targetable. In addition to the hypoxia driven metabolic pathways that we found to be significantly enriched in *E542K* mutant bladder tumors (Figures 21,22), This analysis identified ERK/MAPK/growth factor signaling pathways as being significantly activated in *E542K* mutated cells, including RP-B-01 cells (Figure 21) in comparison to their *E545K* mutant counterparts. Interestingly, this corroborates with previous research that has looked at potential cross talk between PI3K/mTOR and MAPK signaling in driving therapeutic resistance (Zhu, Blenis et al. 2008, Dey, Leyland-Jones et al. 2015). Indeed when I looked at downstream signaling in RP-B-01 cells treated with LY3023414 at different time points; I found that feedback activation of AKT phosphorylation that is induced at 24 and 48 hours of treatment is associated with up-regulation of ERK phosphorylation and stabilization of MYC compared to control non treated condition (Figure 42). At the gene expression level, I found MYC to be significantly upregulated in RP-B-01 compared to RP-B-02 and to be two-fold higher in HEK-*E542K* mutant cells in comparison to their *E545K* mutant counterparts. Additionally resistance to LY3023414 in RP-B-01 cells trended towards time dependent induction of MYC (Figure 43).

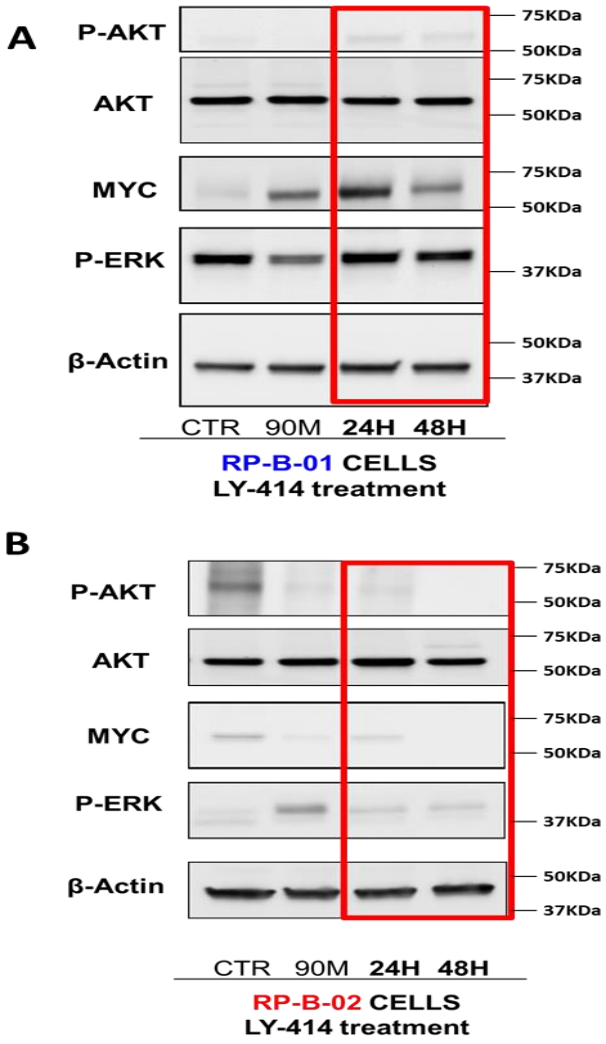

Figure 42: Resistance to LY3023414 in RP-B-01 is associated with activation of MAPK signaling and stabilization of MYC. A. AKT and ERK phosphorylation were inhibited upon 90 minute treatment of RP-B-01 cells with LY3023414. Feedback activation of AKT phosphorylation upon extended exposure to LY3023414 (24 and 48 hour) is associated with feedback ERK phosphorylation and stabilization of MYC in comparison to non-treated control condition. B. RP-B-02 cells were responsive to LY3023414 are all time points tested. AKT and ERK phosphorylation were inhibited at all time points tested. MYC levels at 24 and 48 hours were similar to non-treated control condition.

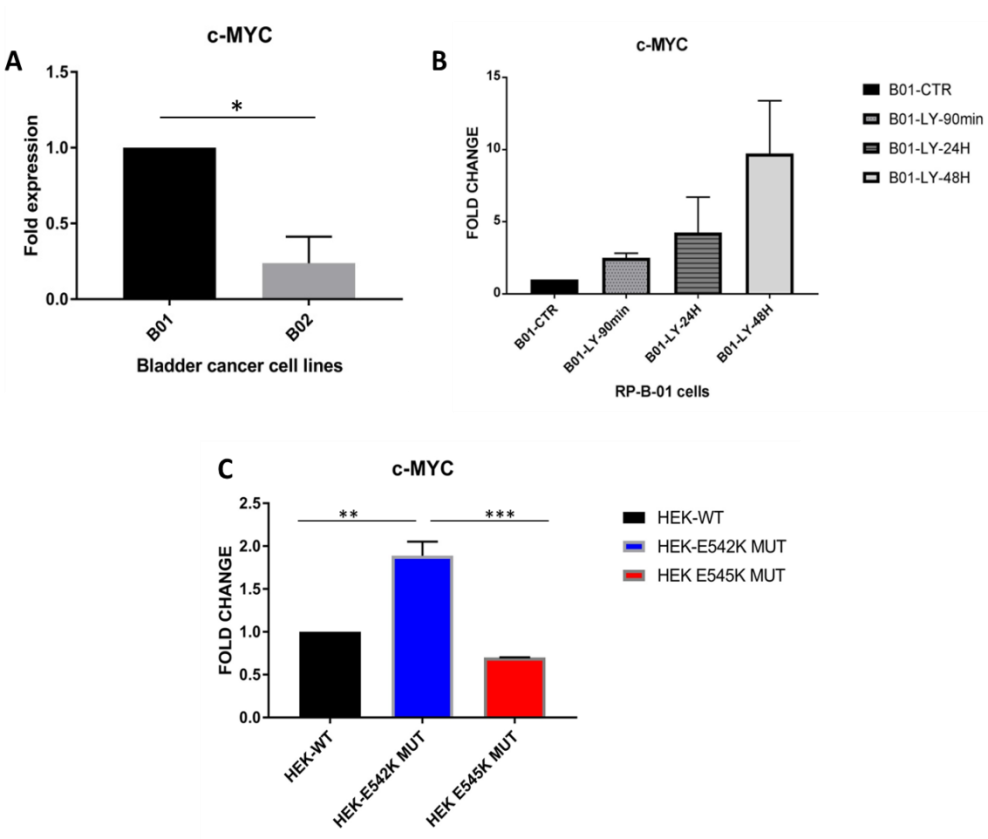

Figure 43: PIK3CA E542K mutation status is associated with induction of MYC RNA levels. A. MYC RNA levels are significantly higher in RP-B-01 (*E542K MUT*) in comparison to RP-B-02 *(E545K MUT)*. B. MYC gene expression is induced in a time dependent manner upon exposure to LY3023414 which coincides with treatment resistance and stabilization at the protein level as assessed by WB. C. Overexpression of PIK3CA *E542K MUT* is associated with significant induction of MYC at the RNA level in comparison to both WT and *E545K MUT* conditions. Mean ± SD, n =3, representative results from at least triplicate experiments. One way ANOVA, Tukey's multiple comparisons test, *P<0.05, **P<0.01.

C.8. Combined PI3K/mTOR and BET inhibition sensitizes RP-B-01 to LY3023414

The cross talk between PI3K and MAPK signaling which impinges downstream on MYC has been previously proposed as a potential mechanism of resistance in PIK3CA mutant (Dey, Leyland-Jones et al. 2015) and MYC driven metastatic breast cancer (Stratikopoulos, Dendy et al. 2015).

Bromodomain inhibitors are drugs that target the bromodomains which act as readers that bind acetylated lysines in histone tails and thus regulate gene transcription through the recruitment of other molecular partners(Pérez-Salvia and Esteller 2017). One of the earliest bromodomain inhibitors that have been developed is (+)-JQ1(Filippakopoulos, Qi et al. 2010), a drug that is well known for its ability to downregulate transcription of MYC and its genome wide dependent target genes through interfering with chromatin-dependent signal transduction to RNA polymerase by interfering with the acetyl-lysine recognition domains (bromodomains) of putative coactivator proteins involved in gene transcription(Delmore, Issa et al. 2011). Interestingly, the ability of (+)-JQ1 to target MYC epigenetically has put it forward as a promising drug that can override resistance to PI3K targeted inhibition (Stratikopoulos, Dendy et al. 2015, Stratikopoulos and Parsons 2016, Andrews, Singh et al. 2017).

Therefore, I tested whether (+)-JQ1 would sensitize RP-B-01 cells to PI3K targeted inhibition. I tested different concentrations of LY3023414 and (+)-JQ1 combination *in vitro* both in RP-B-01 and RP-B-02 cell lines. Using ComboSyn™,

a drug combination analysis program based upon the Chou-Talalay method for drug combination analysis (Chou 2010). I found the combination of LY3023414 and (+)-JQ1 to be synergistic at all concentrations tested for both drugs with log combination index less than zero (Figure 44). Indeed combined LY3023414 (+)-JQ1 treatment was associated with suppression of feedback AKT phosphorylation and MYC stabilization that were induced upon therapeutic resistance in cells exposed to single agent LY3023414 for prolonged duration (i.e. 90 minute treatment VS 24/48 hour treatment) (Figure 45).

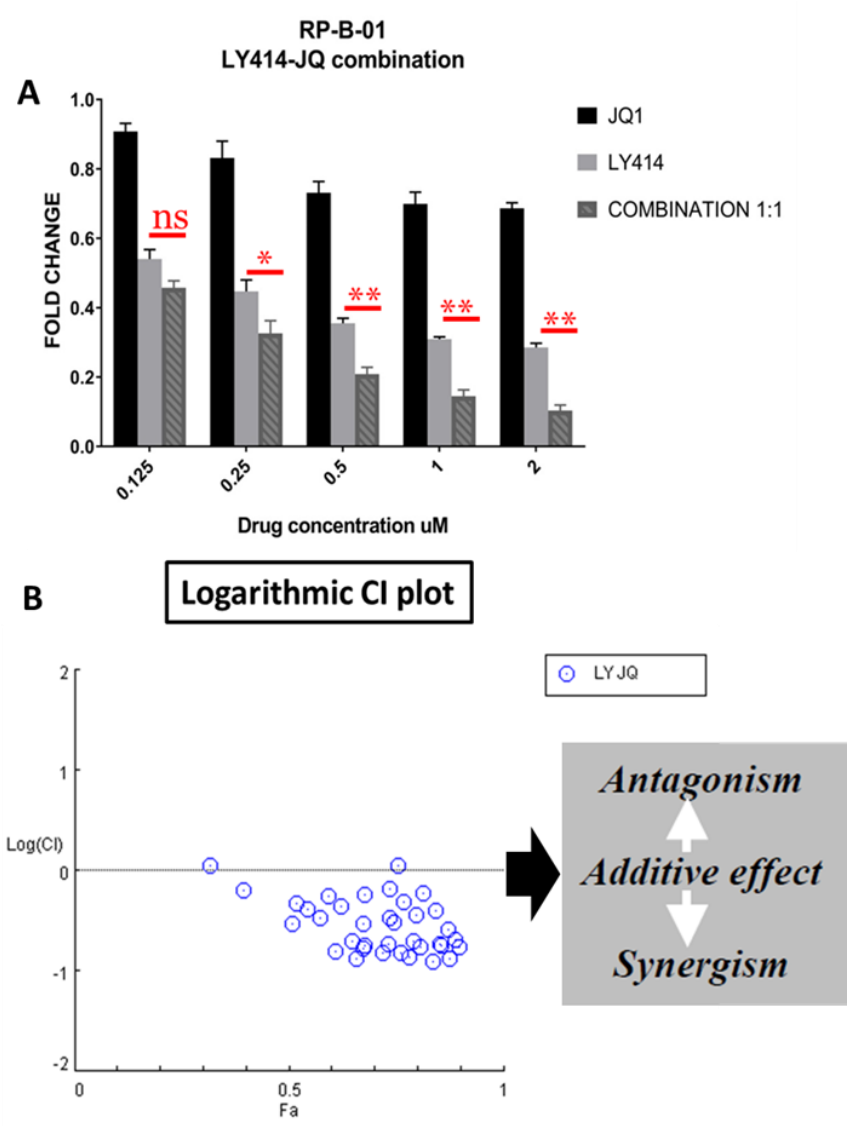

Figure 44: Combined PI3K/mTOR and BET inhibition sensitizes RP-B-01 to LY3023414. A. RP-B-01 cells were treated with LY3023414 and (+)-JQ1 in either as single agent or in combination in (1:1) ratio. At most concentrations tested the combination significantly sensitized cells to treatment in comparison to single agent. Mean ± SD, n =3, representative results from at least triplicate experiments. One way ANOVA, Tukey's multiple comparisons test, **P<0.01. B. The logarithmic CI index plot show most concentrations tested to have log CI less than zero indicative of synergy.

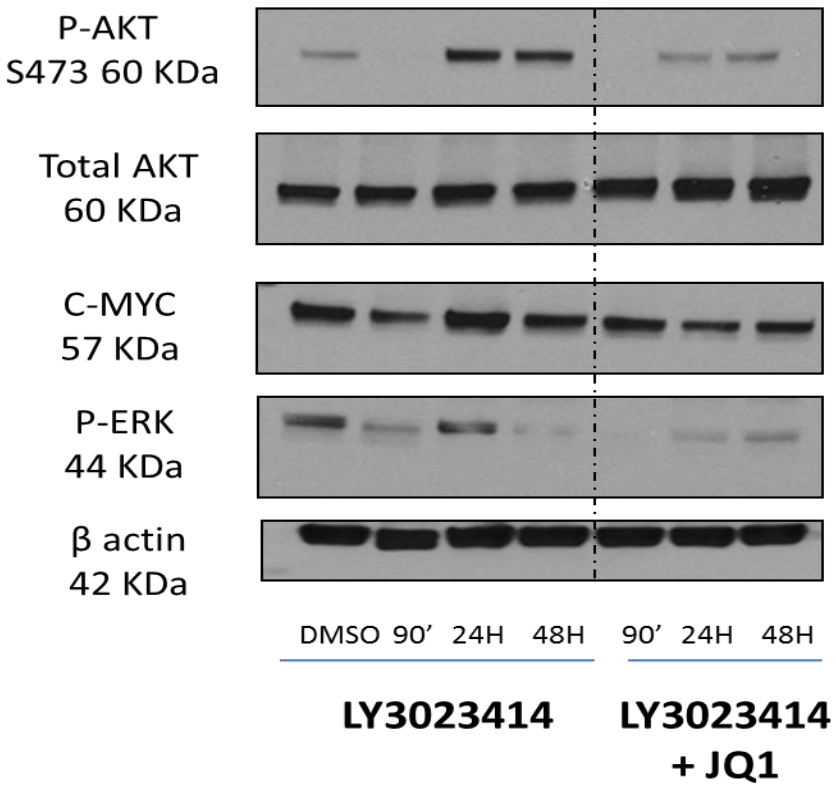

Figure 45: Combined PI3K/mTOR and BET inhibition is associated with downregulation of feedback AKT phosphorylation in RP-B-01 cells. Feedback AKT phosphorylation is induced in RP-B-01 cells treated with single agent LY3023414 upon prolonged drug exposure (24H). When RP-B-01 cells are treated with LY3023414 combination, feedback AKT phosphorylation is attenuated along with MYC level.

However, this was not the case in the RP-B-02 cell line which is sensitive to LY3023414 as single agent. In this cell line, the combination of two drugs had either an additive or antagonistic effect for most of the concentrations tested with log combination index equal to zero (Figure 46).

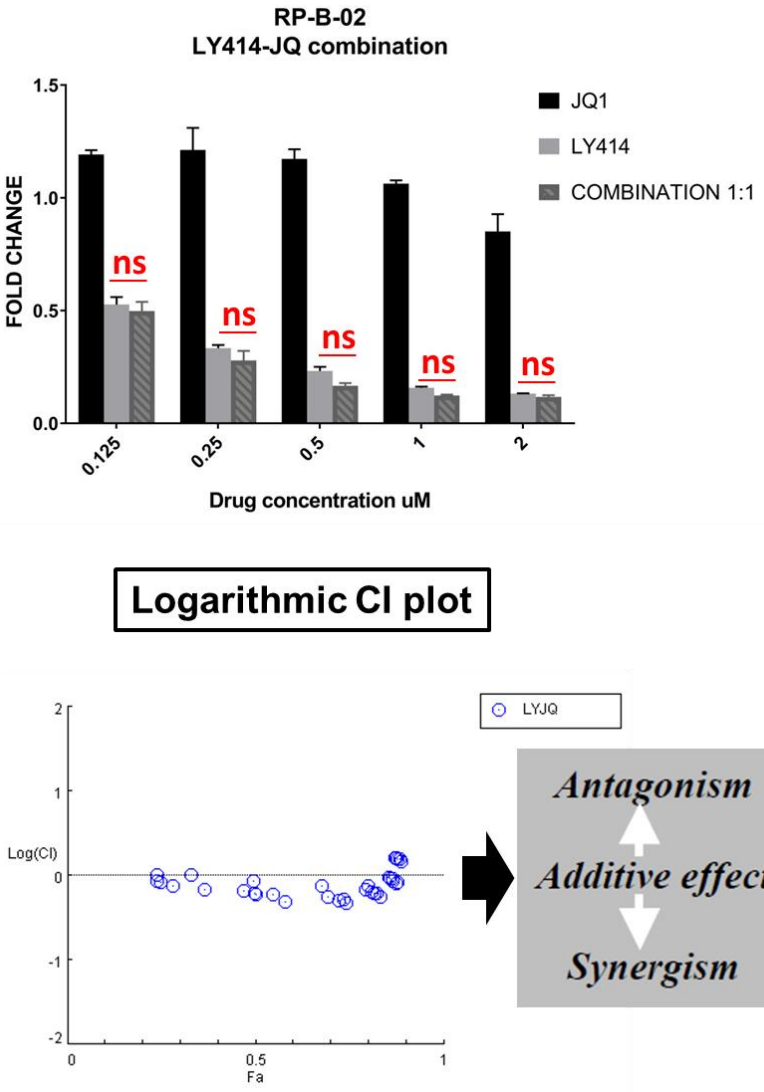

Figure 46: Combined PI3K/mTOR and BET inhibition is not synergistic in RP-B-02. A. RP-B-02 cells were treated with LY3023414 and (+)-JQ1 in either as single agent or in combination in (1:1) ratio. At most concentrations tested the combination did not provide RP-B-02 cells with significant therapeutic benefit. *Mean ± SD, n =3, representative results from at least triplicate experiments.* One way ANOVA, Tukey's multiple comparisons test, **P<0.01. B. The logarithmic CI index plot show most concentrations tested to have log CI equal to or more than zero indicating either an additive or antagonistic effect.

C.9. BET inhibition sensitizes RP-B-01 to LY3023414 but not cisplatin

Next I wanted to test whether the ability of (+)-JQ1 to sensitize RP-B-01 to treatment is specific to PI3K targeted inhibition or relevant to alternative treatments such as cisplatin. RP-B-01 is also resistant to cisplatin (Ciamporcero, Shen et al. 2016, Wei, Chintala et al. 2016); the mainstay of therapy in bladder cancer patients (Kamat, Hahn et al. 2016, Lobo, Mount et al. 2017). Interestingly, I did not find the cisplatin- (+)-JQ1 combination to be synergistic at any concentrations tested (Figure 47), indicating that bromodomain targeting by (+)-JQ1 sensitizes RP-B-01 to LY302414 but not cisplatin. This provides a proof of concept that the benefit conferred to RP-B-01 cells by bromodomain targeting is specific to resistance to PI3K targeted inhibition.

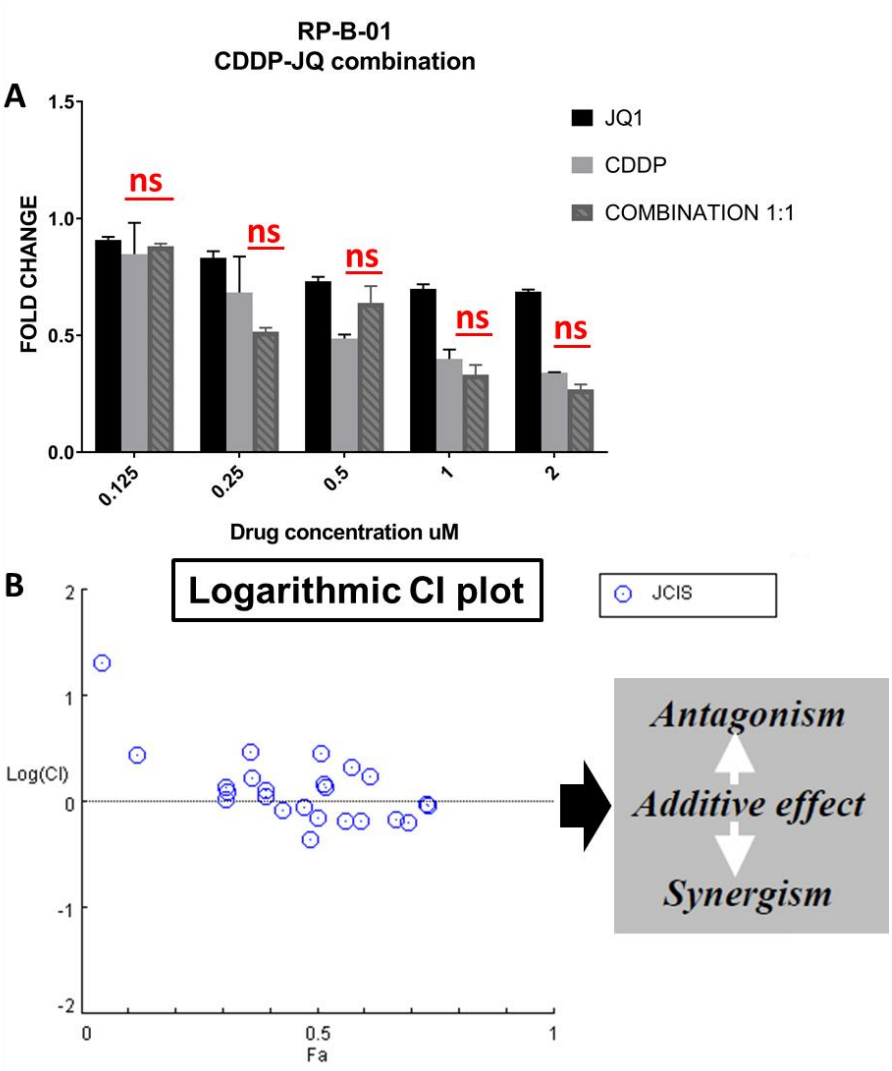

Figure 47: BET inhibition sensitizes RP-B-01 to LY3023414 but not cisplatin. A. RP-B-01 cells were treated with cisplatin and (+)-JQ1 either as single agent or in combination in (1:1) ratio. At all concentrations tested the combination was not better than cisplatin single agent. Mean ± SD, n =3, representative results from at least triplicate experiments. One way ANOVA, Tukey's multiple comparisons test, P> 0.5. B. The logarithmic CI index plot show most concentrations tested to have log CI equal to or more than zero indicating either an additive or antagonistic effect

C.10. ERK inhibition does not sensitize RP-B-01 to LY3023414 treatment

Since we found MAPK signaling to be significantly activated in RP-B-01 in comparison to RP-B-02, I wanted to determine whether combined ERK (LY3214996) (Bhagwat, McMillen et al. 2017, Zhao, McMillen et al. 2017, Kidger, Sipthorp et al. 2018) and PI3K inhibition (LY3023414)(Smith, Mader et al. 2016) would overcome resistance to PI3K targeted therapy in RP-B-01 similar to what I observed with (+)-JQ1. Interestingly however, the synergy that I observed with (+)-JQ1 was not evident with ERK inhibitor LY3214996 (Figure 48) despite feedback activation that I have observed upon therapeutic resistance (Figure 42A). This implies that while RP-B-01 cells escape PI3K inhibition by MAPK activation, it is probably stabilization of MYC that plays the key role in driving resistance and therefore the main event that is worth co-targeting to provide a better therapeutic outcome.

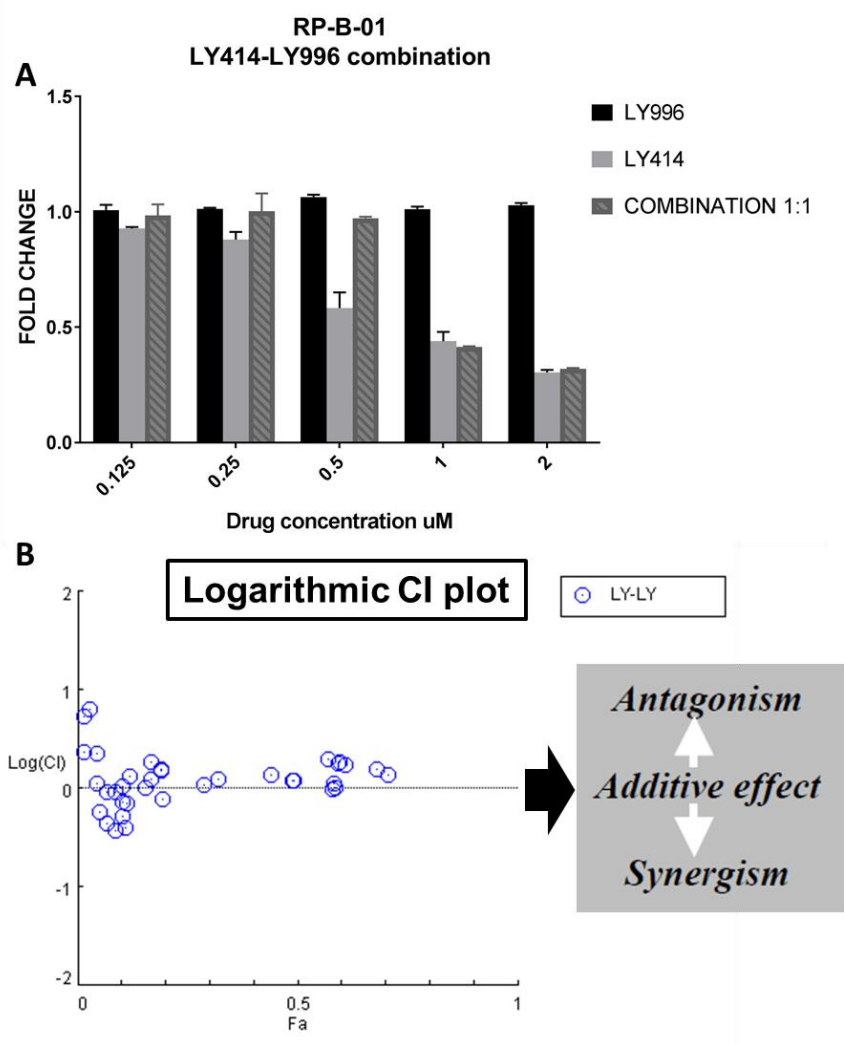

Figure 48: ERK inhibition does not sensitize RP-B-01 to LY3023414 treatment. A. RP-B-01 cells were treated with LY3023414 and LY3214996 either as single agent or in combination in (1:1) ratio. At all concentrations tested the combination was not better than LY3023414 single agent. Mean ± SD, n =3, representative results from at least triplicate experiments. One way ANOVA, Tukey's multiple comparisons test, P> 0.5. B. The logarithmic CI index plot show most concentrations tested to have log CI equal to or more than zero indicating either an additive or antagonistic effect.

C.11. Development of alternative MIBC PDX models for drug testing

In order to validate our data in alternative models *in vivo*; I developed and characterized 9 additional PDX models (Table 3). Using cytokeratin staining (Cytokeratin 20 and 5/6), I identified the subtype of each model (Figure 49). The use of Cytokretain staining to identify subtype was verified by comprehensive genomic analysis in collaboration with Dr. David McConkey at the Johns Hopkins school of Medicine (Figure 50). Next, using Taqman™ PCR based mutation detection assay, I screened the models for PIK3CA mutation status. Interestingly I found IU68T to be a luminal-like model that carries a missense PIK3CA mutation (E545K) similar to RP-B-02 (Figure 51).

Table 3: List of novel bladder cancer PDX models developed in Indiana University (IU)

IU PDX LABEL	PATHOLOGY
IU-3T	Urothelial Carcinoma
IU-5T	Squamous Cell Carcinoma, NOS tumor configuration: invasive
IU-16T	Urothelial Carcinoma, Papillary
IU-25T	Urothelial carcinoma; glandular differentiation (10%)
IU-37T	Metastatic Urothelial Carcinoma
IU-68T	Papillary Urothelial Carcinoma
IU-80T	Urothelial Carcinoma
IU-104T	Urothelial Carcinoma, SCC
IU-105T	Urothelial Carcinoma

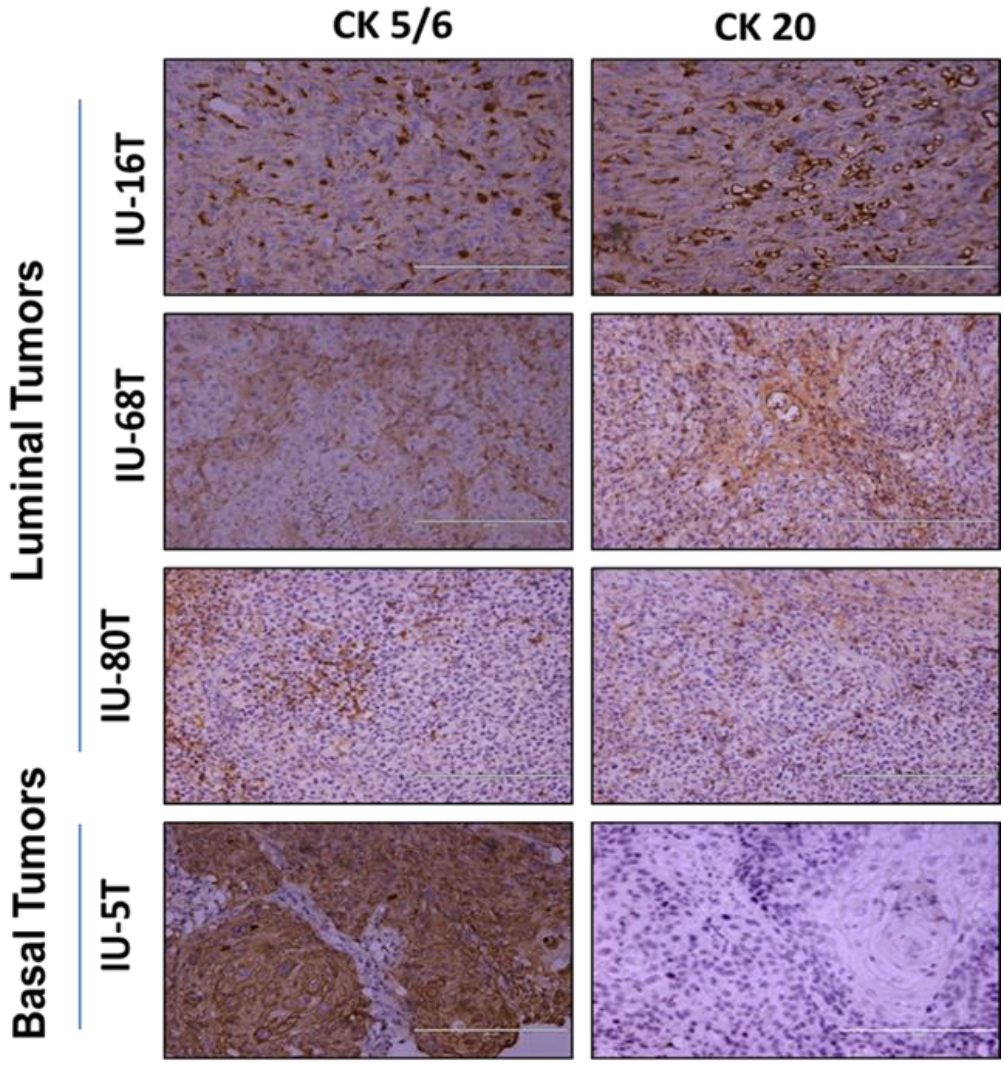

Figure 49: Development and characterization of basal-like MIBC PDX models. Representative IHC for Cytokeratins 20 and 5/6. Cytokeratin staining identified IU-5T as novel basal-like MIBC PDX models while IU-80T, IU68T and IU-16T behaved as luminal-like tumors. Scale bars = 200 µm.

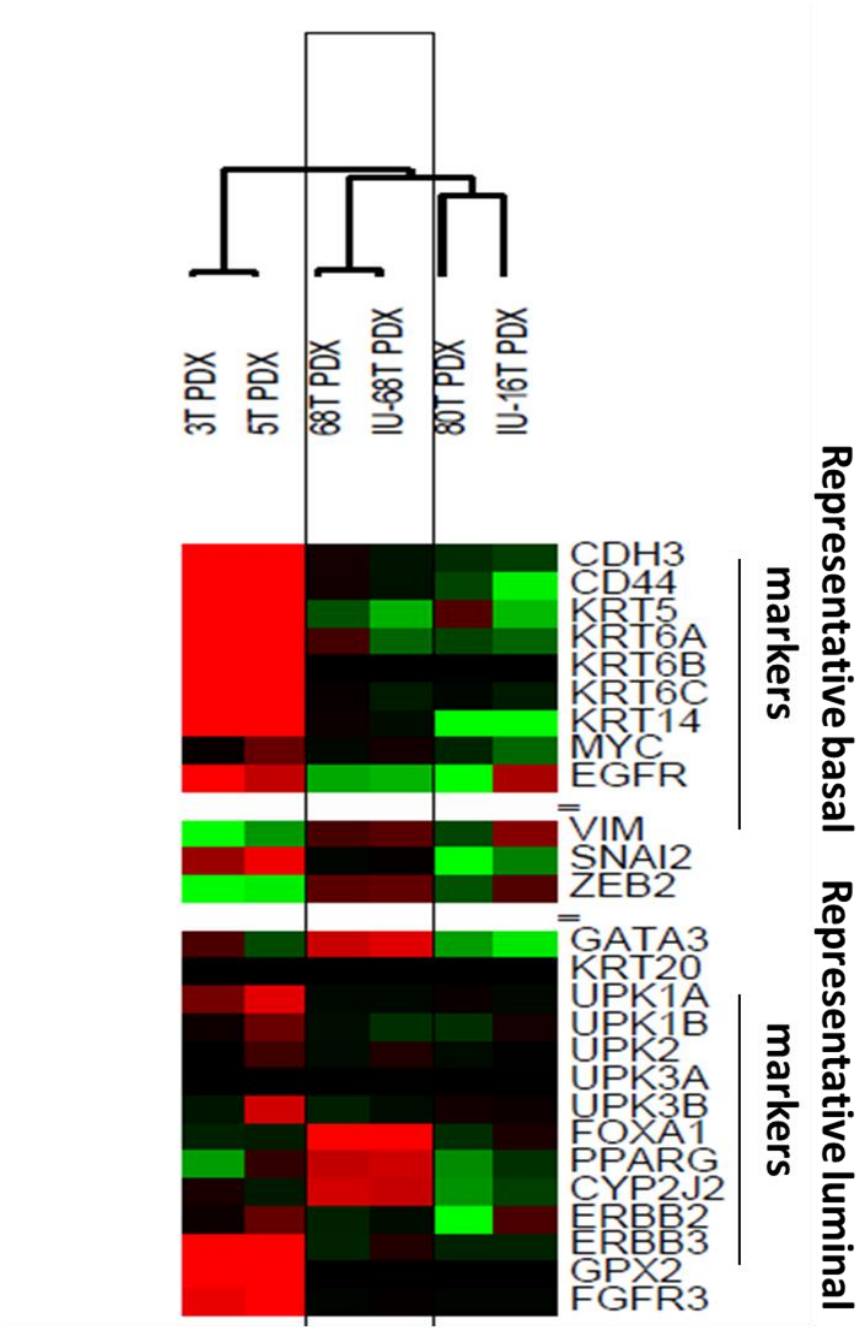

Figure 50: RNA-Seq analysis confirms IHC detected subtype of novel IU PDX models. Representative heat map depicting expression levels of select basal and luminal markers in novel IU bladder cancer PDX models. RNA-seq analysis confirms IU-3Tand IU-5T to behave as basal-like tumors while IU-68T/16T/80T are luminal-like

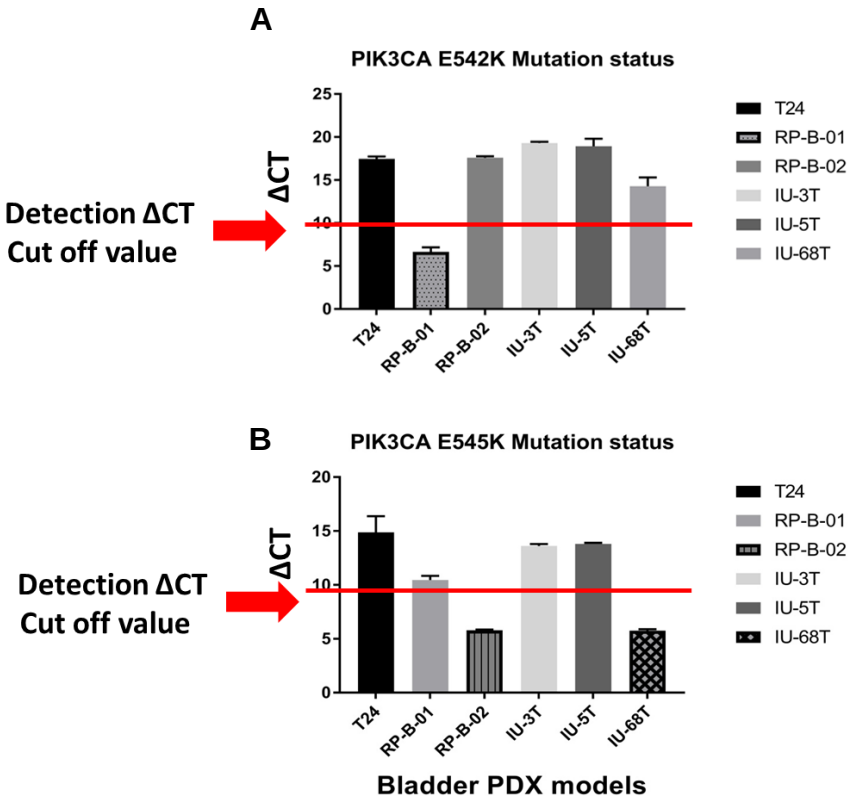

Figure 51: IU-68T is a novel Luminal like PIK3CA E545K mutant Bladder PDX model (RP-B-02 like). A. Screening of IU PDX mdoels for PIK3CA *E542K* mutation. Red solid line represents ΔCT cut off value for detection of mutation. B. Screening of IU PDX mdoels for PIK3CA *E545K* mutation. Red solid line represents ΔCT cut off value for detection of mutation. CT value below cutt off is indicative of positive mutation status. Both RP-B-02 and IU68-T are PIK3CA *E545K* mutants.

D. Discussion

Targeted therapy provides select patients with maximal therapeutic benefit with fewer side effects compared to conventional chemotherapy. However, so far targeted therapy has not found its way in the management of bladder cancer where conventional chemotherapy (i.e. cisplatin) continues to be the standard of care (Kamat, Hahn et al. 2016). This is largely attributed to the lack of predictive molecular stratification of patients in bladder cancer clinical trials (Shah, McConkey et al. 2011). A recent attempt at comprehensive molecular characterization of bladder cancer has identified PI3K pathway as one of the most frequently dysregulated signaling pathways in this disease; where PIK3CA (HD) mutations are the most significant (Knowles, Platt et al. 2009, Platt, Hurst et al. 2009, Shah, McConkey et al. 2011, Network 2014). Despite the high rate of mutations in this pathway in bladder cancer as well as other tumors, therapies targeting this pathway are still facing key challenges in the clinical setting (Fruman & Rommel, 2014; Massacesi et al., 2016). While PIK3CA HD mutations are the most significant alterations in this pathway in bladder cancer, largely mTOR inhibitors were exclusively used in clinical trials despite the absence of mTOR mutations in this disease (Houédé and Pourquier 2015). Only two bladder cancer trials are utilizing novel PI3K inhibitors (Munster, Aggarwal et al. 2015) and (NCT01551030). Therefore, the significance of PIK3CA HD mutations in terms of predicting therapeutic response is yet to be determined.

Bladder cancer however is a highly complex disease with high incidence of mutations that is only exceeded by melanoma and lung cancer (Kim, Akbani et al. 2015). In the light of the recent comprehensive characterization of bladder cancer into distinct molecular subtypes(Choi, Porten et al. 2014, Damrauer, Hoadley et al. 2014, Network 2014, Robertson, Kim et al. 2017), it is crucial to understand the therapeutic significance of PIK3CA HD mutations in the context of distinct molecular subtypes (i.e. basal-like and luminal-like tumors).

Preclinical data and data from phase I and II clinical trials suggest that PIK3CA mutation status can predict response to PI3K targeted therapy (Janku, Tsimberidou et al. 2011, Janku, Wheler et al. 2013). However, there is also data to suggest that either response or resistance to PI3K targeted inhibition is rather a function of tumor subtypes as is the case of triple negative basal-like breast cancer. In basal-like breast cancer PI3K/mTOR signaling has been suggested to play a key role(Massihnia, Galvano et al. 2016) in therapeutic resistance to PI3K targeted inhibition which was linked to subtype specific alterations such as MYC amplification, alternative feedback signaling and innate tumor heterogeneity(Dey, Leyland-Jones et al. 2015, Matkar, Sharma et al. 2015, Massihnia, Galvano et al. 2016). Interestingly, classification of MIBC into distinct molecular subtypes was carried out in the light of well-established gene expression profiles of breast cancer subtypes (Damrauer, Hoadley et al. 2014); suggesting that subtype can also be a player in driving resistance to PI3K targeted inhibition.

We characterized two MIBC PDX models developed in our lab (RP-B-01 and RP-B-02) which are of distinct molecular subtypes (basal-like and luminal-like respectively) and carry distinct PIK3CA HD mutations (E542K and E545K respectively) to respond differently to multiple dual PI3K/mTOR inhibitors (i.e. LY3023414) where RP-B-01 was resistant while RP-B-02 was sensitive to treatment. To pinpoint whether resistance to PI3K targeted inhibition is a function of PIK3CA mutation status, subtype or a combination of both, we underwent comprehensive GSEA of TCGA data in conjunction with RNA-seq data from our two PDX models to determine the signaling pathways that are significantly distinct between E542K and E545K mutant tumors irrespective of subtype.

We found *E542K* mutant tumors to be enriched with glycolytic pathways that are known to have a much higher turnover of intermediates for macromolecular biosynthesis and redox homeostasis despite being less efficient than oxidative phosphorylation (OXPHOS)(Wong, Qian et al. 2017). In 3D culture, we found that *E542K* mutant bladder cancer spheroids trended towards a higher uptake of hypoxia marker LOX-1. Moreover, when we transfected isogenic HEK cells with either *E542K* or *E545K* mutant PI3KCA and found the E542K mutation status to be associated with therapeutic resistance similar to what we have observed in our RP-B-01 model implying that mutation status can play a key role in determining treatment response.

We found that resistance to PI3K targeted inhibition in RP-B-01 PIK3CA *E542K* mutant model coincided with stabilization of MYC which is known to mediate the transcription of almost all the genes involved in glycolysis and glutaminolysis where it promotes the shuttling of glycolytic intermediates to macromolecular biosynthetic pathways (Osthus, Shim et al. 2000, Priolo, Pyne et al. 2014, Stine, Walton et al. 2015). Recent reports investigating resistance to PI3K targeted therapy have proposed sustained bromodomain (BRD4) binding at chromatin regulatory regions of receptor tyrosine kinases and MYC as key drivers of therapeutic resistance (Stratikopoulos, Dendy et al. 2015, Stratikopoulos and Parsons 2016). Indeed when we combined dual PI3K/mTOR inhibitor (LY3023414) and bromodomain inhibitor (JQ1), we found significant synergy and we were able to overcome resistance to PI3K targeted inhibition.

Importantly, we were not able to harness this therapeutic benefit when we combined JQ1 with cisplatin or when MAPK and PI3K signaling pathways were co-targeted. Taken together, this provides proof of concept that the synergy was specific to overcoming resistance to PI3K targeted inhibition induced downstream by activation of MYC. Although our GSEA and confirmatory q-PCR experiments in HEK and bladder cancer cells show that *E542K* mutation induce MYC expression and its downstream glycolytic metabolic rewiring significantly more than *E542K* mutation, it is not yet mechanistically clear why that is the case. Our future goal is to investigate whether this is driven by differential RAS binding affinity to the PI3Kα protein that harbors HD mutations.

A key limitation of our study is lack of further confirmatory *in vivo data* in alternative PDX models in order to provide a stronger predictive rationale for selection of patients who can benefit from PI3K targeted therapy in clinical trials. However, it is our current goal to develop and screen further models for that purpose.

CHAPTER V: CHARACTERIZATION OF THE EPIGENETIC SIGNATURE OF TWO BIOLOGICALLY DISTINCT BLADDER CANCER MODELS

A. Chapter Summary

Two bladder patient derived xenograft (PDX) models developed in our lab carry PIK3CA activating HD mutations. One model is responsive to treatment with dual PI3K/mTOR inhibitor LY3023414 (RP-B-02; PIK3CA *E545K* mutant) while the other model (RP-B-01; PIK3CA *E542K* mutant) is resistant, as previously described in chapters III and IV. Interestingly, these two models are of distinct bladder cancer subtypes, where RP-B-01 is basal-like compared to RP-B-02 which is luminal-like. We hypothesized that distinct PIK3CA HD mutations (*E545K* and *E542K*) could play a potential role in driving resistance to therapy, driven by two mutually exclusive epigenetic loss of function mutations; KMT2D and KDM6A, which were detected in RP-B-01 and RP-B-02 respectively(Wei, Chintala et al. 2016). Therefore we set out to compare the differential DNA methylation profiles between two models and investigate whether it influences gene expression through protein-protein interaction (PPI) network in association with mutated genes detected in each PDX model. DNA methylation analysis recognized 14,944 differentially methylated regions (DMRs) ($q < 0.05$) locating within 4 kb upstream to 500 bp downstream of gene transcription start sites (TSSs). About one third (35.3%) DMRs were hypermethylated in B01 compared to B02. Interestingly; most differentially expressed genes (DEGs) (64.5%) associated with DMRs exhibited positive correlation between gene expression change and corresponding DNA methylation variation. However, DMRs

negatively correlated with expression of associated genes were overrepresented in proximity to TSS. Importantly, PPI network of genes with nonsense mutation specific to RP-B-01 and RP-B-02 (i.e. KMT2D and KDM6A respectively) were distinct with little overlap observed. They showed significantly different ratios of DEGs and DMRs, suggesting a potential role in driving phenotypic distinction and differential therapeutic response. Overall, we found that both models have distinct gene expression and DNA methylation profile. In the previous chapter we proposed potential role of distinct PIK3CA mutations in predicting response to treatment. However, taking into account the complexity of subtype related signaling and other key mutations in both PDX models; we propose that resistance could potentially be predicted by the complex interplay of distinct PIK3CA mutations with distinct gene expression profile that is epigenetically driven in PIK3CA mutant bladder cancer.

B. Background and Rationale

Epigenetic alterations, which include aberrant DNA methylation as well as mutations in chromatin remodeling genes, occur in 89% of cases (Network 2014). Global and gene specific alterations in DNA methylation in MIBC have been extensively studied primarily to better diagnose and prognosticate patients(Mikeska and Craig 2014). However, in the light of the newly proposed MIBC subtypes, the role of epigenetic changes, mainly alterations in DNA methylation, in driving the fate of the basal bladder cancer cell that could partly

lead to distinct subtypes and possibly predict treatment response remain to be understood (Mikeska and Craig 2014, Kitchen, Bryan et al. 2016).

Two bladder cancer patient derived xenograft (PDX) models developed in our lab (RP-B-01 and RP-B-02) carry distinct PIK3CA activating HD mutations. We previously reported gene expression profile for those models(Wei, Chintala et al. 2016) and found them to be representative of basal-like and luminal-like subtypes respectively. Importantly; they are also distinct in terms of treatment response, where one model is responsive to treatment with either dual PI3K/mTOR inhibitor LY3023414 (RP-B-02; *PIK3CA E545K* mutant) or cisplatin while the other model (RP-B-01; *PIK3CA E542K* mutant) is resistant to both. Here we set out to compare the differential DNA methylation profiles between two models and investigate how it influences gene expression through protein-protein interaction (PPI) network in association with mutated genes detected in each PDX model. The purpose is to identify potential players that drive resistance to treatment.

C. Results

C.1. A significant number of DMRs exist between RP-B-01 and RP-B-02

In previous genome wide profiling of RP-B-01 and RP-B-02 models, we identified differentially expressed genes (DEGs) between these two models and found them to be equivalent to 6.18% of expressed genes. Looking at genome wide DNA methylation in this study, we identified total 354,493 differentially

methylated regions (DMRs) by MethylAction ($q < 0.05$), 42.5% of which were hypermethylated in B01 compared to B02. 14,944 DMRs locate from upstream 4 kb to downstream 500 bp of 9,663 genes, 35.3% of which were hypermethylated in B01 (Figure 52A). Interestingly, a significant number of genes had mixed signals within different regions in the gene body; that are yet to be functionally interrogated (Figure 52B). We subsequently integrated the DNA methylation dataset with gene expression dataset to determine the ratio between DEGs and DMRs in both models. We identified a total of 369 genes with DMRs and we found DEGs to be significantly hypermethylated in RP-B-01 compared to RP-B-02 (Figure 53); which highlights the role of DNA methylation in driving differential gene expression.

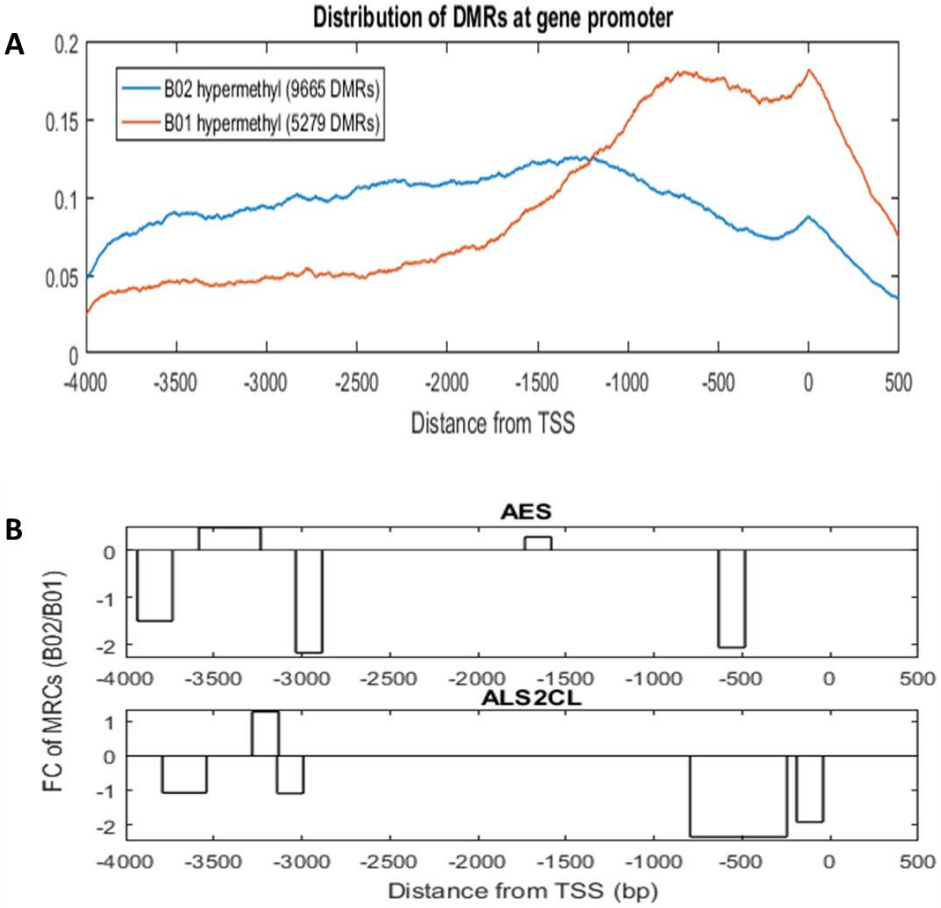

Figure 52: Significant number of differentially methylated regions exists in bladder cancer PDX models. A. 14,944 DMRs locate from upstream 4 kb to downstream 500 bp of 9,663 genes, 35.3% of which were hypermethylated in B01. B. Signals of differential methylation between two models were mixed and not exclusive to the Transcription start site (TSS) (i.e. promoter region).

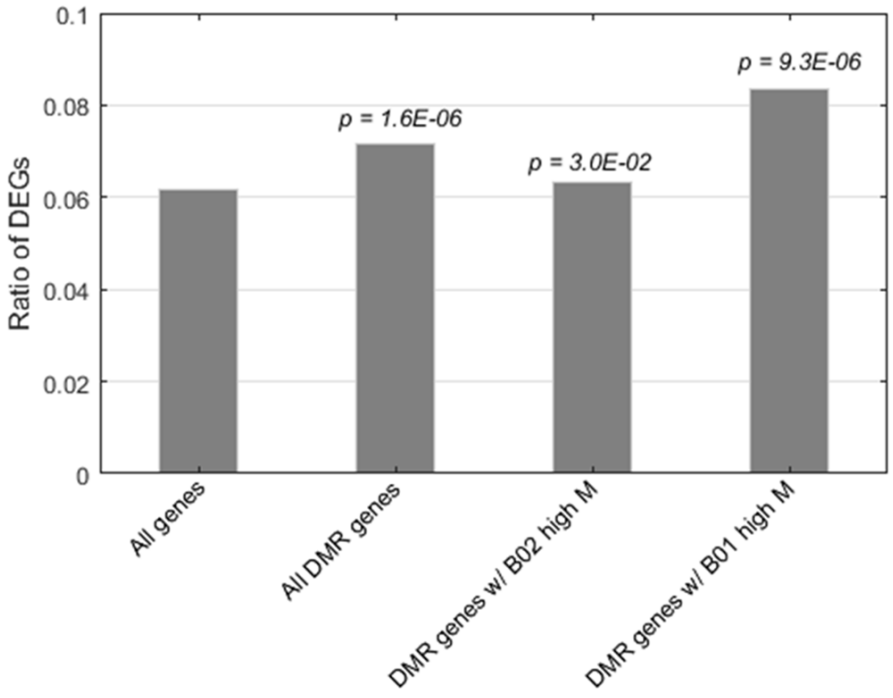

Figure 53: Ratio of DEGs in different groups of genes. Genes enriched with DMRs show significant differential expression between two models when compared to overall gene expression. In RP-B-01, DEGs with DMRs are significantly hypermethylated (High M) compared to RP-B-02.

The dogma in the field is that CpG island methylation generally correlates with gene repression and regulation of tissue specific gene expression (Deaton and Bird 2011). However, recent reports challenge this concept and show that both positive and negative correlation between DNA methylation and gene expression exist and provide multiple levels of regulation of gene expression(Wan, Oliver et al. 2015). We investigated the methylation status of well recognized genes that have been proposed to be markers of basal-like (i.e. TP63, KRT6) and luminal like (i.e. PPARG, FOXA1, HDAC9) subtypes(Choi, Porten et al. 2014, Damrauer, Hoadley et al. 2014, Eriksson, Rovira et al. 2018).

We found those genes to be generally negatively regulated by methylation, where basal genes were hypermethylated in RP-B-02 in comparison to RP-B-01 and suppressed (Figure 54) while luminal genes were hypomethylated in RP-B-02 compared to RP-B-01 and overexpressed (Figure 55). Interestingly, this pattern was not exclusive to methylation at the promoter region of each gene, but also included methylation signals that were detected in gene body (Figure 54, 55).

However, looking globally at DEGs between the two models, we found that most DEGs (64.5%) with DMRs show positive correlation between gene expression change and methylation change (Figure 56). In RP-B-01 model, DMRs with higher methylation level and lower gene expression level were enriched in proximity to TSS (Figure 56B).

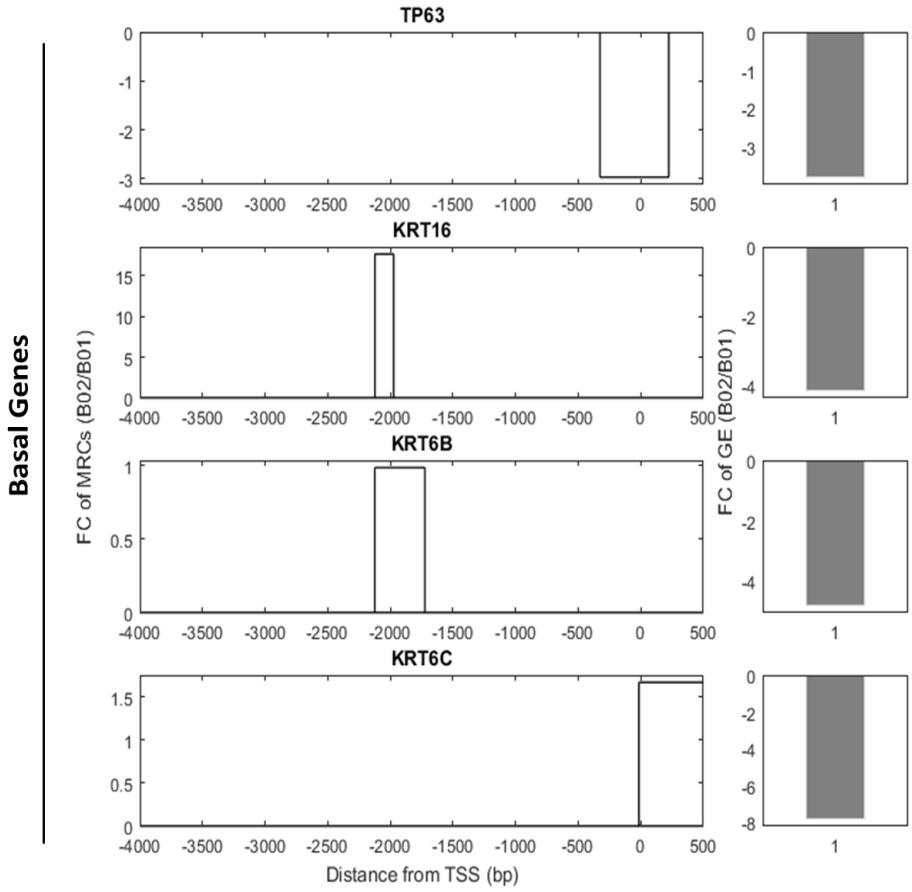

Figure 54: Methylation status of genes that define basal subtype of bladder cancer. CK6 and CK16; markers of basal like subtype of bladder cancer are hypermethylated in RP-B-02 compared in RP-B-01 and gene expression is lower; however P63 which is expressed at lower level in RP-B-02 is hypomethylated.

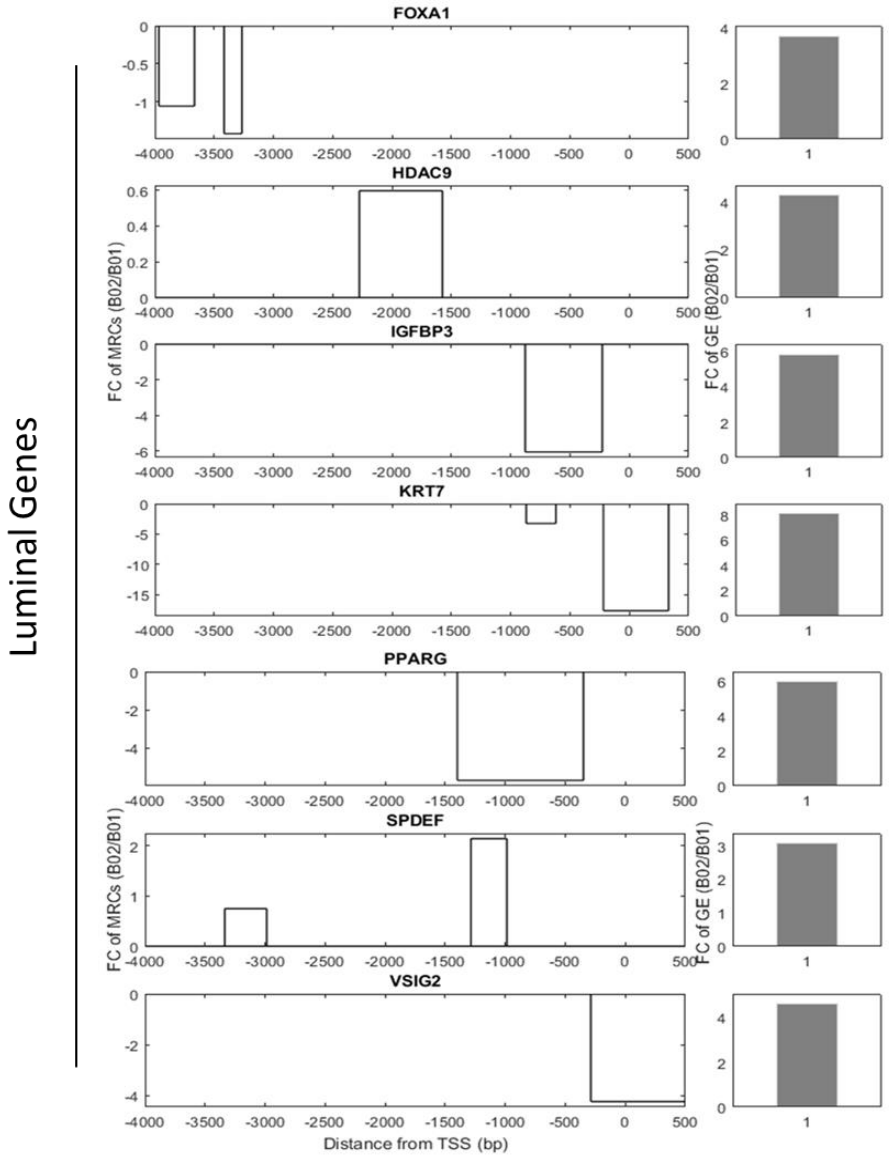

Figure 55: Methylation status of genes that define luminal subtype of bladder cancer. Markers of luminal like subtype in bladder cancer (i.e. FOXA1, PPARG) are hypomethylated in RP-B-02 compared to RP-B-01 and gene expression is higher.

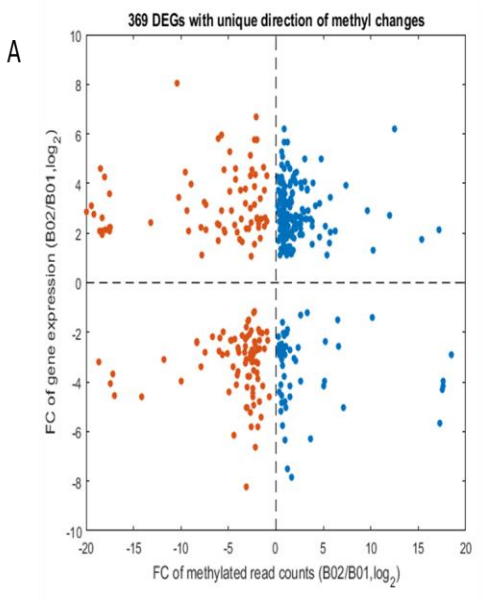

Total 369 DEGs with DMRs	M: B01 high	M: B02 high
GE: B02 high	76	154
GE: B01 high	84	55

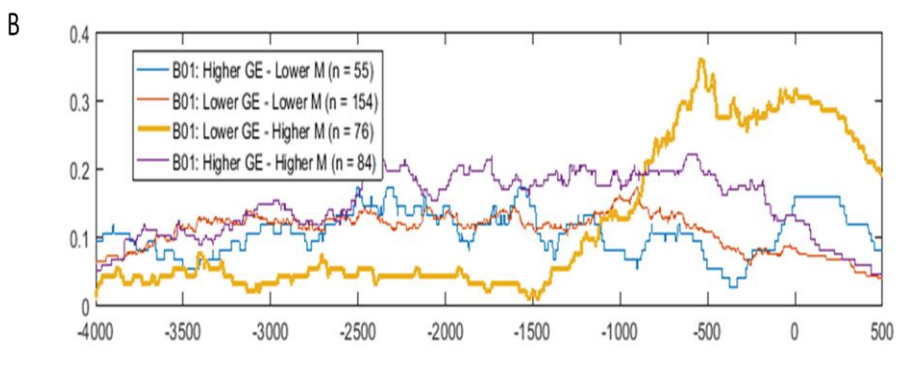

Figure 56: Significant percentage of DEGs with DMRs show positive correlation between methylation change and gene expression. A. Scatter plot of fold change (FC) in gene expression (B02/B01) and FC of methylation changes (B02/B01). The table is showing unique direction of methylation changes in 369 DEGs. 154 and 84 genes in RP-B-01 and RP-B-02 respectively show positive correlation between gene expression and DNA methylation. B. Graphical representation of methylation changes in RP-B-01 in relation to gene expression. DMRs with higher methylation level and lower gene expression level in B01 were enriched in proximity to TSS. GE= gene expression, M= methylation, FC= fold change. DEGs= differentially expressed genes, DMRs= differentially methylated regions.

C.2. Positive DMRs play a key role in bladder differentiation and development

Genes associated with positive DMRs are enriched with negative regulators of key developmental and regulatory functions(Wan, Oliver et al. 2015). Therefore, we performed Gene ontology (GO) analysis on genes associated with positive or negative DMRs. We identified four functionally distinct groups of genes in both bladder cancer models (Figure 57); interestingly we detected consistent findings with a previous report(Wan, Oliver et al. 2015); where positive DMRs were enriched with negative regulation of cell activation/cell-cell adhesion/cellular process/cell differentiation/leukocyte activation/biological process . This supports the idea that a novel model of gene expression regulation exists, where DNA methylation indirectly suppresses the expression of certain genes by inducing the expression of specific repressors.

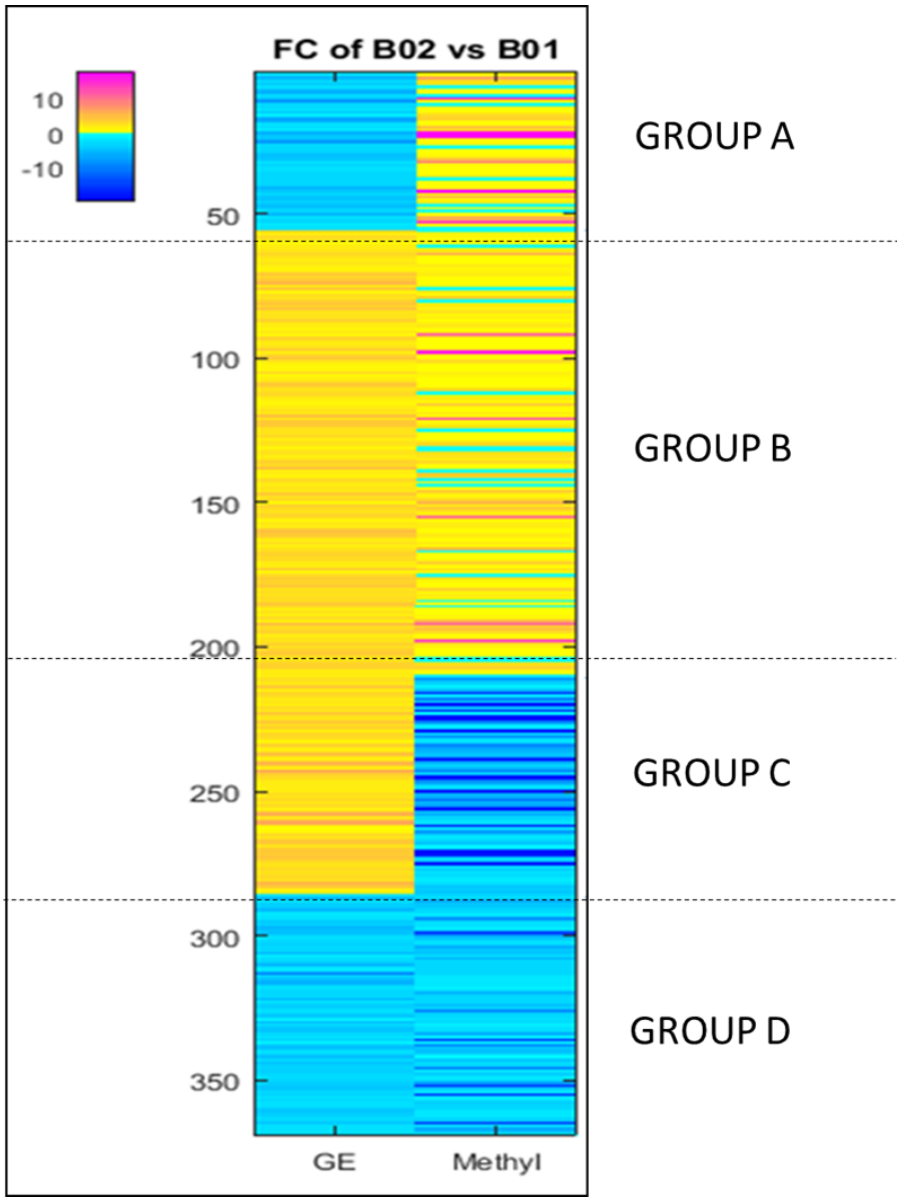

Figure 57: Four groups of DEGs identified based on correlation between gene expression and methylation changes. Representative heat map of 4 groups of DEGs

C.3. Genes interacting with mutated genes are more enriched in DEG, DMRs, and DEG with DMR sets than others

In order to understand the functional significance of DEGs and DMRs between two models, we sought to investigate the complex interaction network of DEGs with DMRs in relation to mutant genes in both models. Out of total 1,899 somatic mutations identified in our previously published analysis (Wei, Chintala et al. 2016), 919 (48%) were B01-specific.1,324 mutations matched to expressed genes, 675 (51%) of which were B01-specific ($p = 1.1E-4$, compared to all mutations). In line with the distinct subtype and therapeutic response of each model, we found the mutant genes to be functionally distinct, where B01 specific mutant genes were enriched with abnormalities in DNA repair while RP-B-02 specific mutations were enriched with cell-adhesion and morphogenesis related pathways (Figure 58A). While no mutation was covered by DMR; PPI network showed significantly stronger perturbation when taking into account the difference of gene expression and methylome between model specific mutations (Figure 58B).

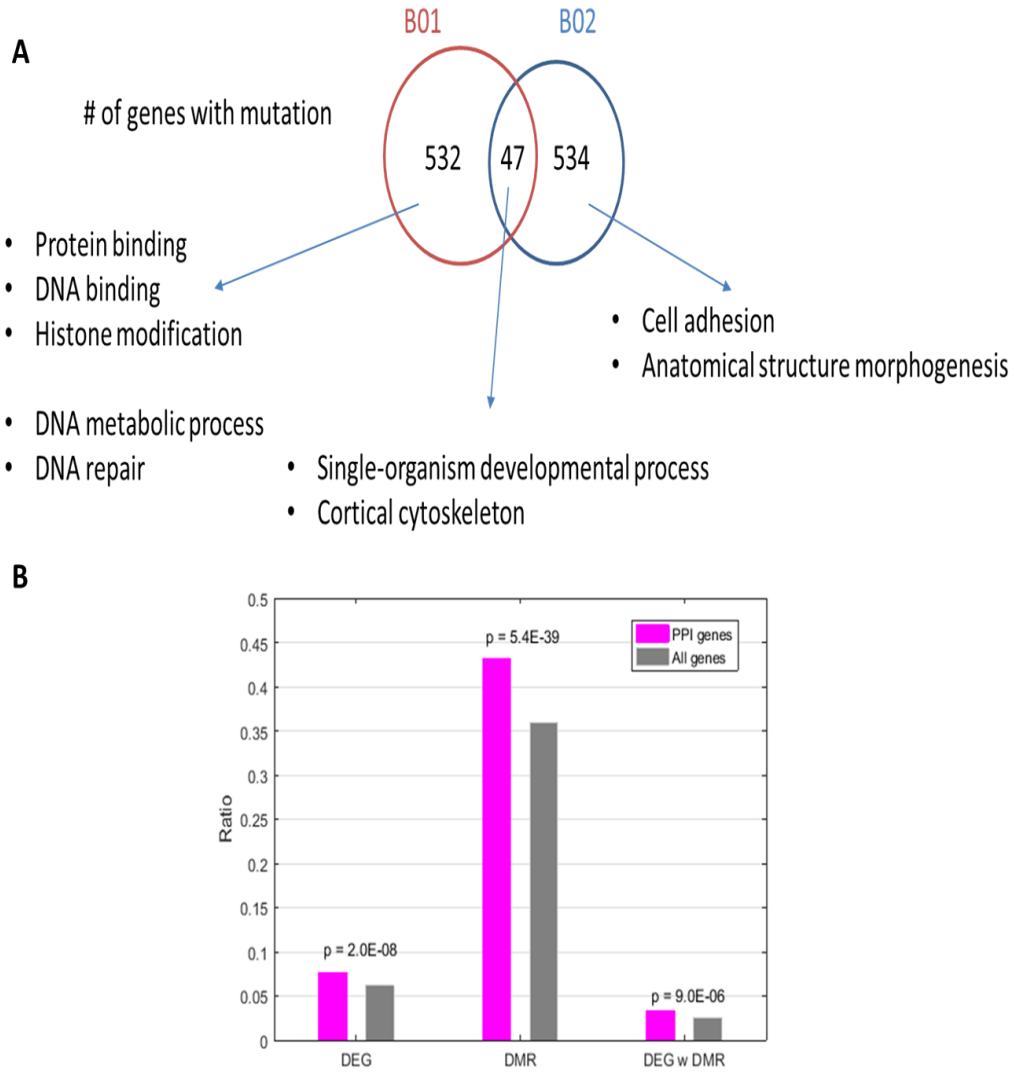

Figure 58: Genes with mutations in each model have distinct functions. A. Representative graph of the common and distinct mutations between both models and their functional relevance. B. PPI network with stronger perturbation on difference of gene expression and methylome between two types of mutations

C.4. Nonsense and Missense mutations drive distinct PPI interaction network with DEGs and DMRs

Loss of function mutations in a large number of chromatin modifying genes are highly enriched in bladder cancer (89% of cases). Most notably are mutations in *KMT2D* and *KDM6A* which are mutually exclusive, indicating either a redundant or a synthetically lethal effect of combined loss (Gui, Guo et al. 2011, Kim, Sharma et al. 2014, Network 2014). Both KMT2D and KDM6A are members of the complex of proteins associated with Set1 (COMPASS) family, where KMT2D acts as H3K4 methyl transferase while KDM6A acts as a H3K27 demethylase (Figure 59). Opposing roles played by the members of COMPASS family and members of other epigenetic families such as the polycomb repressive complex 1 and 2 (PRC1 and PRC2) maintain the epigenetic balance (Piunti and Shilatifard 2016)**.** Earlier reports have suggested significant prevalence of *KMT2D* mutations in non-papillary high-grade bladder cancer as opposed to papillary low-grade tumors where mutations in demethylases (i.e. *KDM6A*) are more prevalent (Gui, Guo et al. 2011, Kim, Akbani et al. 2015, Kamat, Hahn et al. 2016)**.** This dichotomy resonates with the mutual exclusivity observed in the TCGA data with regard to mutations in those two chromatin modifying genes (Network 2014). However, a conclusive relation between *KMT2D* and *KDM6A* mutations and basal and luminal subtypes of bladder cancer, respectively, is yet to be determined.

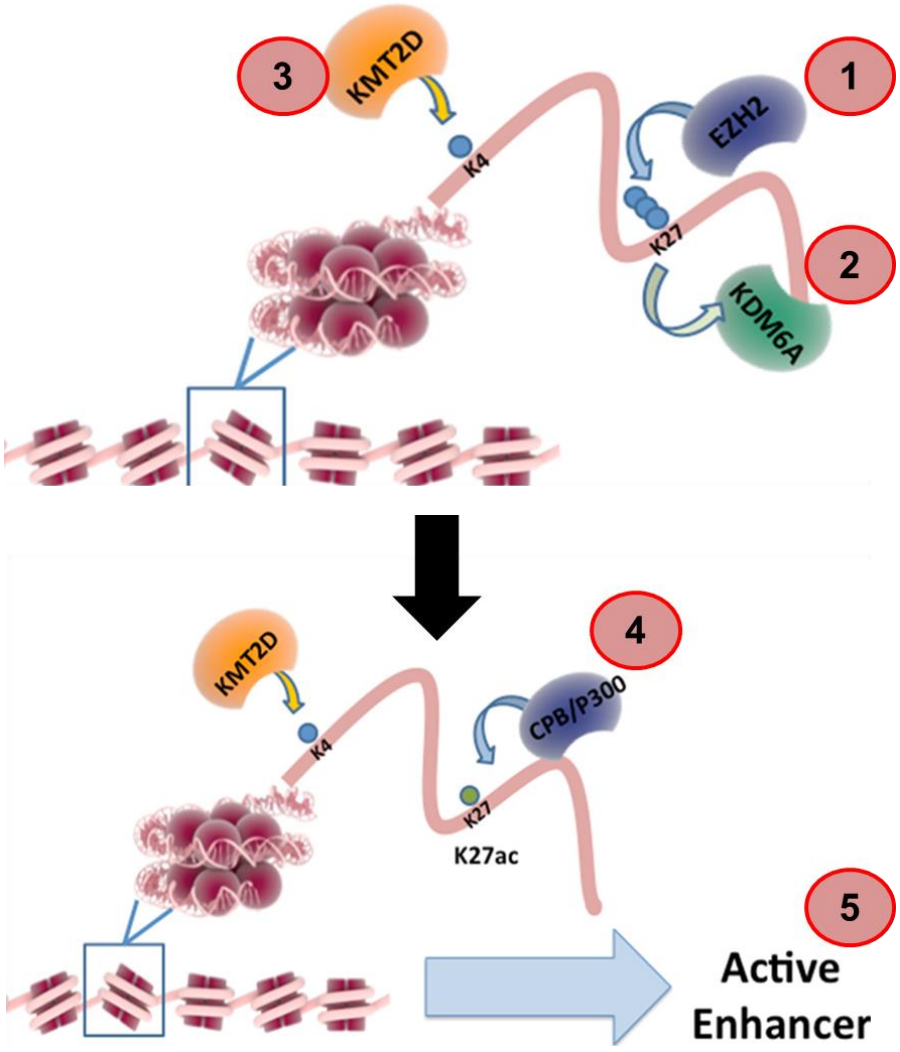

Figure 59: The coordinated function of COMPASS and PRC family members to maintain epigenetic balance. KDM6A (COMPASS family member) counteracts the H3K27me2/3 repressive marks deposited by PRC2 (i.e. EZH2). Subsequently, KMT2D (COMPASS family member) can function as a methyltransferase toward lysine 4 on histone H3, which subsequently favors the H3K27ac deposition by the histone acetyltransferases (HATs) CBP/p300. This is thought to positively regulate, when stimulated, the expression of genes transcriptionally poised because of the restrictive presence of PRC2 activity. The numbered circles are intended to highlight the coordination of steps. *Adapted from (Piunti and Shilatifard 2016)*.

On our end, when we closely examined missense mutations in both models, we found overlapping mutations that involved the histone methytransferase complex (ACTB/CHD8/KMT2D) (Figure 60). Interestingly however; nonsense mutations were mutually exclusive in both models; where RP-B-02 was enriched with nonsense mutations in both protein acetylation complex (KMT2A/NAA15/SRCAP/TRRAP) and histone methyltransferase complex (KDM6A/KMT2A/TAF6) (Figure 62).While this observation resonates with the distinct subtypes of both models that could partly be epigenetically driven; its functional significance in terms of distinct therapeutic response is yet to be determined.

The dichotomy was also clear when we compared the PPI network of each mutation subset. While the PPI network of missense mutations was enriched with DMRs in RP-B-01 (Figure 61), the opposite was true for nonsense mutations where RP-B-02 had significantly higher DMRs and lower DEGs in comparison to RP-B-01(Figure 63).

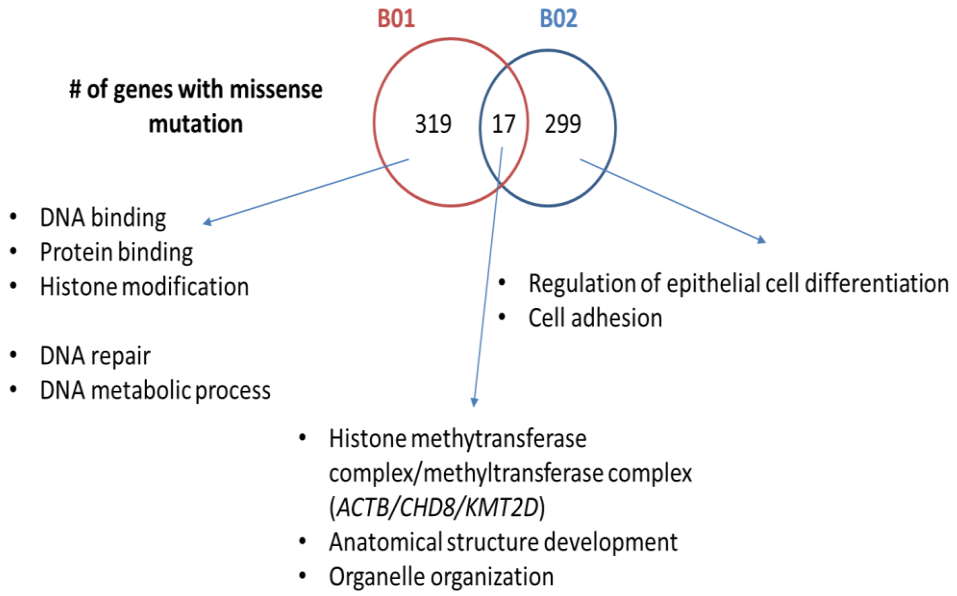

Figure 60: Genes with missense mutation in two models have distinct functions. Graphical representation of the functional relevance of missense mutations in each model. Missense mutations in the histone methytransferase complex (ACTB/CHD8/KMT2D) overlapped between two models.

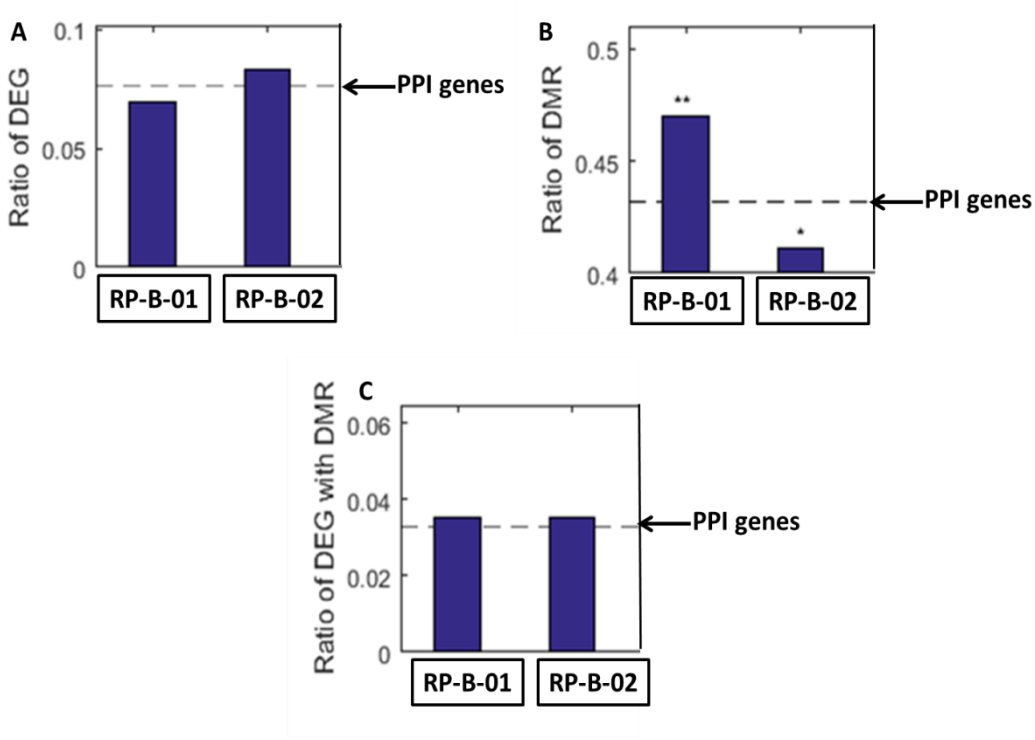

Figure 61: Differential enrichment for PPI network of genes with missense mutations. Proteins interacting with genes carrying missense mutations are more enriched in DEGs in RP-B-B02; however they are significantly more enriched in DMRs in RP-B-B01. *<0.05, **<0.01.

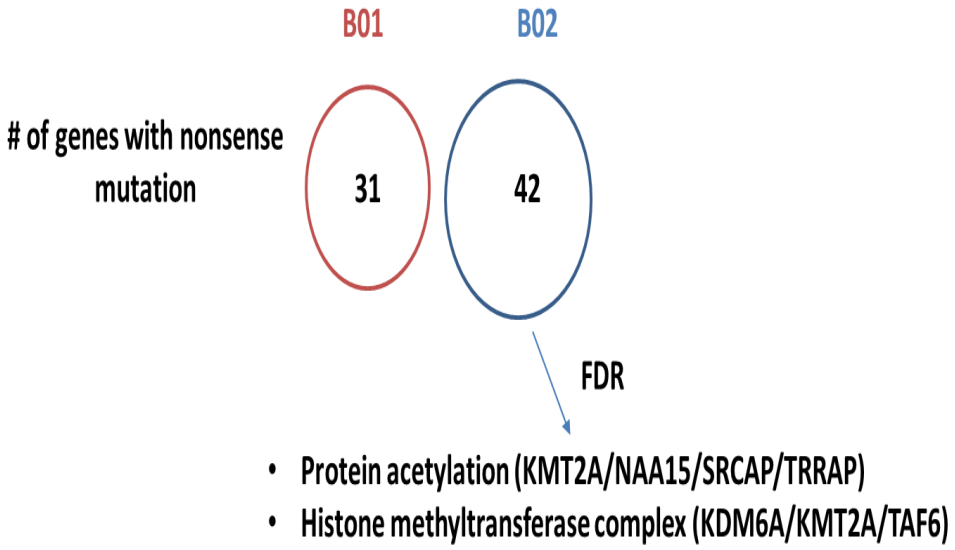

Figure 62: Genes with nonsense mutation in two groups have distinct functions. Graphical representation of the functional relevance of nonsense mutations in each model. No overlap exists between two models with respect to nonsense mutations. RP-B-02 is enriched in nonsense mutations in histone methyltransferase complex.

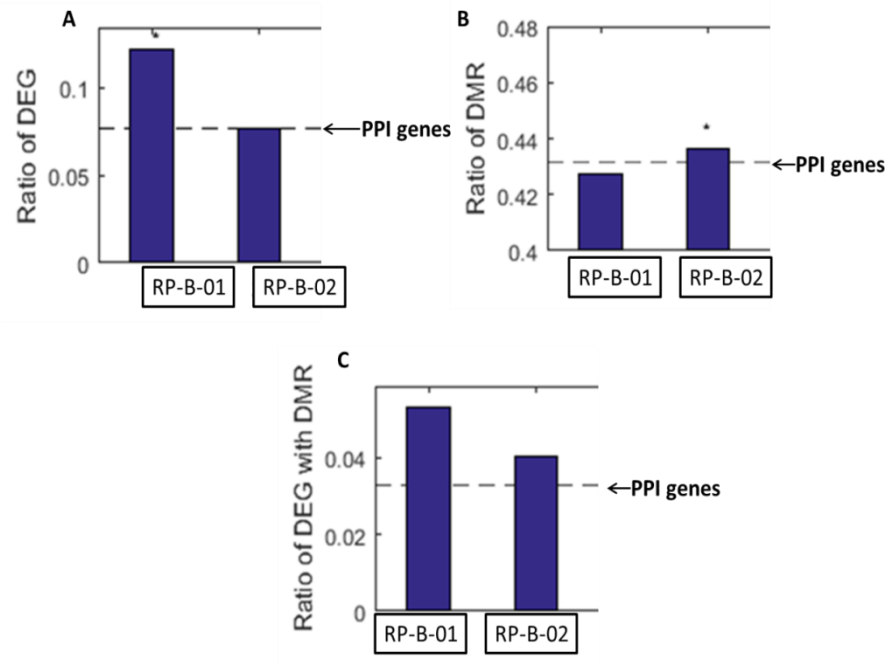

Figure 63: Differential enrichment for PPI network of genes with nonsense mutations. Opposite to the trend observed in figure 61; proteins interacting with genes carrying nonsense mutations are enriched with DMRs in B02 yet enriched with DEGs in B01.

C.5. KMT2D/KDM6A PPI network is subtype related

We subsequently interrogated the PPI network for genes that specifically interact with KMT2D and KDM6A mutations in RP-B-01 and RP-B-02 model respectively. KDM6A nonsense mutation in RP-B-02 mostly interacted with genes at their enhancer regions; which are known to be crucial for cell type specific gene expression and regulation of differentiation (Ong and Corces 2011, Lee, Wang et al. 2013, Lee, Park et al. 2017). This resonates with our GO analysis; which showed that RP-B-02 specific mutations are enriched with differentiation and morphogenesis related pathways (Figure 58, 60).

On the other hand the PPI network for KMT2D showed significant interaction with Nuclear Receptor Subfamily 1 Group H Member 3 (NR1H3) (also known as LXRA)(Figure 64). NR1H3 is known to regulate fatty acid synthase (FASN) expression(Joseph, Laffitte et al. 2002); which plays a key role in regulation of lipid homeostasis. FASN is overexpressed in RP-B-01 compared to RP-B-02 and is induced upon resistance to LY3023414 in a time dependent manner (Figure 27). Collectively, these findings support the role of metabolic shift influenced by both subtype and mutation status in driving resistance to PI3K targeted therapy in the RP-B-01 model.

A

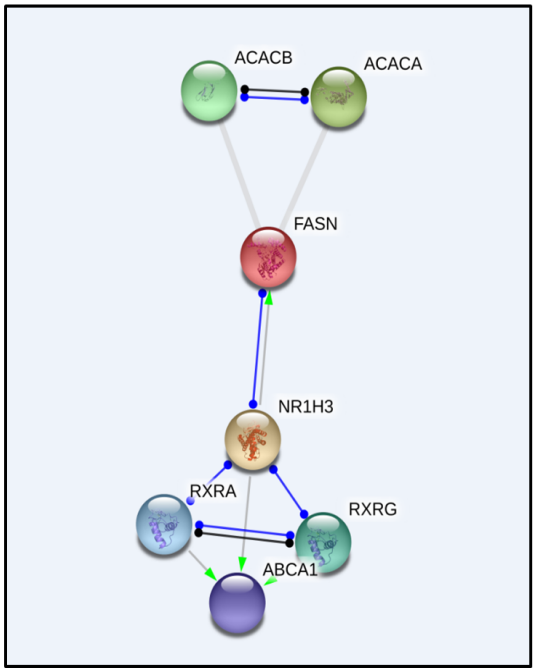

B

KMT2D (B01)

CENPA	HIST1H3G	HIST1H4I	NR1H3 **
H3F3A	HIST1H3H	HIST1H4J	RXRA
H3F3B	HIST1H3I	HIST1H4K	RXRB
H3F3C	HIST1H3J	HIST1H4L	
HIST1H3A	HIST1H4A	HIST2H3A	
HIST1H3B	HIST1H4B	HIST2H3D	
HIST1H3C	HIST1H4C	HIST2H4A	
HIST1H3D	HIST1H4D	HIST4H4	
HIST1H3E	HIST1H4E	NFYB	
HIST1H3F	HIST1H4H	NR1H2	

C

KDM6A (B02)

mainly enhancer region

ANAPC1	DNAJA1	HIST1H3D
ANAPC10	DNAJA2	HIST1H3E
ANAPC2	DNAJA4	HIST1H3F
ANAPC4	FZR1	HIST1H3G
ANAPC5	H3F3A	HIST1H3H
BUB1B	H3F3B	HIST1H3I
CDC16	H3F3C	HIST1H3J
CDC20	HIST1H3A	HIST2H3A
CDC23	HIST1H3B	HIST2H3D
CENPA	HIST1H3C	

Figure 64: PPI network of mutated chromatin modifying genes in RP-B-01 and RP-B-02**.** A. PPI network of NR1H3 (*STRING DATABASE*) shows that NR1H3 activates FASN. The interaction score is set at high confidence (0.7). KEGG pathway analysis related to this interaction network predicts the following pathways (in order of significance) as the most significantly involved pathways in this interaction (Fatty acid biosynthesis, Fatty acid metabolism, PPAR signaling, AMPK signaling) B. Most significantly interacting proteins with KMT2D which are predicted to carry missense mutation in basal-like RP-B-01. NR1H3 is predicted to have the most significant interaction. **P<0.01. C. PPI network of KDM6A which is predicted to carry nonsense mutation in luminal-like RP-B-02.

D. Discussion

DNA methylation has been previously investigated in bladder cancer mainly to enable early detection and monitoring of disease recurrence in urine sediments in order to avoid the economic and clinical burden associated with routine cystoscopy(Barocas, Globe et al. 2012). However, in our study we are proposing a novel insight into bladder cancer DNA methylome in conjunction with newly characterized chromatin modifying genes that are highly prevalent in bladder cancer. Novel subtypes have been recently proposed for MIBC; therefore our novel subtype distinct bladder cancer PDX models represent an invaluable tool to test subtype specific epigenetic signature.

Previous research has shown that high grade bladder cancer is enriched with DNA hypermethylation in comparison to lower grade tumors(Olkhov-Mitsel, Savio et al. 2017). We observed a similar trend in basal-like treatment resistant RP-B-01 model; where DEGs with DMRS were significantly hypermethylated compared to luminal-like RP-B-02 model. However, in this study we propose a novel concept; where we show that a significant fraction of the hypermethylated DMRs observed in the RP-B-01 model positively correlate with gene expression.

This corroborates a previous report that showed that a significant fraction of tissue specific DMRs positively correlate with gene expression level and are enriched with negative regulators of gene expression(Wan, Oliver et al. 2015). While they were not able to predict this 2-layer regulation when they analyzed

cancer specific DMRs in colon cancer(Irizarry, Ladd-Acosta et al. 2009, Wan, Oliver et al. 2015); our bladder cancer study showed that positive DMRs were significant and also enriched in negative regulators of pathways involved with cell differentiation and tissue development. This could possibly be explained by RP-B-02 specific nonsense mutations in both protein acetylation complex (KMT2A/NAA15/SRCAP/TRRAP) and histone methyltransferase complex (KDM6A/KMT2A/TAF6) which were found to preferentially interact with enhancer regions that are known to play key role in tissue specific development. However this observation warrants further investigation in order to better understand the complex interplay between histone and DNA methylation and how this guides subtype specific development.

We also interrogated the PPI network specific to distinct mutant chromatin modifying genes identified in both models and we found a strong interaction with genes involved in lipid homeostasis; mainly (NR1H3; PPARG). These genes were significantly upregulated in RP-B-02 compared to RP-B-01 model, which had a higher level of fatty acid synthase (FASN). Interestingly, upon prolonged treatment with dual PI3K/mTOR inhibitor LY414 which coincided with resistance; FASN was induced pointing toward a metabolically driven mechanism of resistance that we proposed as mechanism of resistance to PI3K therapy in PIK3CA *E542K* mutant bladder cancer. The novelty however, lies in the possibility that this could be driven by cross talk between highly prevalent

mutations in chromatin modifying genes and PIK3CA which frequently co-occur together.

Overall, our findings present a novel concept of multilayered regulation of gene expression by DNA methylation. A main limitation of our study is lack of DNA methylation data from normal bladder tissue which would provide deeper insight into the functional significance of this regulation. While targeting specific molecular perturbations has not been successful in the bladder cancer field so far, a better understanding of specific bladder cancer subtypes that could be driven by an epigenetic signature can eventually lead to the long awaited advancement in the management of this disease.

CHAPTER VI: DISCUSSION

A. Summary and Discussion

A.1. MIBC: Current management and its limitations.

The standard of care in MIBC is comprised of neoadjuvant cisplatin based chemotherapy followed by radical cystectomy and bilateral pelvic lymphadenectomy (Kamat, Hahn et al. 2016).

However, cisplatin based treatment is associated with high dose-limiting toxicities including; increased risk of hematological adverse events and renal adverse events. Additionally, many patients eventually develop resistance to cisplatin and become cisplatin–refractory(Chou, Selph et al. 2016).

Several immune checkpoint inhibitors that target programmed cell death protein 1 (PD1), its ligand PDL1, and cytotoxic T lymphocyte-associated protein 4 (CTLA4) have already been approved for first or second line use in bladder cancer management (Sundararajan and Vogelzang 2015). With respect to targeted therapy, agents targeting different pathways (i.e. VEGF, EGFR, and PI3K/mTOR) were used, albeit in small nonrandomized trials. Modest to non-survival benefit was seen with these agents. This unfavorable outcome was attributed to lack of adequate patient population selection on trials (Sverrisson, Espiritu et al. 2013).

Recently however, novel molecularly based classification for muscle invasive bladder cancer was proposed classifying MIBC into different subtypes(Choi, Porten et al. 2014, Network 2014, Robertson, Kim et al. 2017) that are thought to reflect the hallmarks of breast cancer biology(Damrauer, Hoadley et al. 2014). Additionally, key molecular aberrations in the disease were identified. The goal is to ultimately guide better patient selection on clinical trials to decrease attrition and provide patients with new personalized treatment options. Interestingly, anti-EGFR therapy which has previously failed in clinical trials (Petrylak, Tangen et al. 2010, Wong, Litwin et al. 2011) was associated with significant therapeutic benefit in basal-like MIBC in a pre-clinical study that was guided by novel bladder cancer subtypes (luminal-like and basal-like) (Rebouissou, Bernard-Pierrot et al. 2014).

The PI3K/AKT/mTOR is dysregulated in 42% of bladder cancer cases, 25% of these cases are due to activating *PIK3CA* mutations(Network 2014, Robertson, Kim et al. 2017). PI3Ks are heterodimeric lipid kinases in which 2 main gain of function mutations have been characterized, either kinase domain (KD) mutations (H1047R) or helical domain (HD) mutations (E545K, E542K)**.** HD mutations are the most common activating PIK3CA mutations in bladder cancer, unlike other solid tumors where KD mutations are more common(Knowles, Platt et al. 2009, Platt, Hurst et al. 2009) However, the role of these mutations in determining response to therapy remains to be elucidated. Understanding the molecular determinants of response to PI3K pathway targeted therapeutics will

pave the way for a more personalized therapeutic approach that will improve success rates in clinical trials.

A.2. Development and Characterization of two PIK3CA mutant MIBC PDX models

The centrality of PI3K/mTOR signaling to bladder cancer pathogenesis (Knowles, Platt et al. 2009, Platt, Hurst et al. 2009) highlights the need for developing MIBC models which harbor common pathway aberrations in order to develop effective treatment for targeting this pathway in patients.

In our lab, we developed PDX models from patient cystectomy specimens. Using high through put genomic profiling in conjunction with patient characteristics and unique histological features of each tumor used, we characterized two MIBC PDX models. Interestingly, we found the two models to harbor distinct PIK3CA HD mutations, where RP-B-01 was *PIK3CA E542K MUT*, while RP-B-02 was *PIK3CA E545K MUT*. Additionally, I found the models to be representative of two distinct bladder cancer subtypes, basal-like and luminal-like respectively. This sets those models as valuable tools for testing the interplay between mutation status and subtype in driving resistance/response to PI3K targeted inhibition.

Interestingly, I found the two models not only distinct with respect to mutation status and subtype, but also distinct in therapeutic response, where

basal-like *PIK3CA E542K MUT* RP-B-01 was resistant to dual PI3K/mTOR targeted inhibition while luminal-like *PIK3CA E545K MUT* RP-B-02 was sensitive. These findings provided the rationale for dissecting determinants of response to PI3K targeted inhibition.

A.3. PIK3CA *E542K* mutation confers resistance to PI3K targeted therapy

In order to determine whether resistance to PI3K targeted therapy is a function of mutation status or more complexly driven by cross talk between PIK3CA mutation status and unique genetic/epigenetic signature of each subtype; we analyzed publicly available RNA-seq data from TCGA in conjunction with RNA-seq data from our models (RP-B-01/02) to determine the pathways that are significantly enriched in PIK3CA *E542K* mutant tumors in comparison to *E545K* mutant tumors irrespective of subtype. Our analysis confirmed a differential signaling pattern that is driven by each mutation and which is mainly involved with a distinct metabolic profile where *E542K* mutant tumors are better equipped to undergo a glycolytic switch and utilize alternative nutrients to glucose such as fatty acids and amino acids.

Next to confirming that mutation status per se drives distinct signaling pattern, we tested whether they are similarly distinct with respect to drug interaction. Predictive *in-silico* analysis of *LY3023414-PIK3CA* binding predicted a differential mode of binding with each *PI3KCA HD* mutation. Using a scoring system that ranks multiple forces that are known to be involved in ligand-

substrate interaction such as hydrogen bonds and electromagnetic forces, we found that drug-protein binding is tighter with the *PIK3CA E545K* mutation as opposed to the *E542K* mutation which behaved more similar to the *WT* protein.

In order to confirm that *PIK3CA* mutation status can independently predict response to PI3K targeted therapy, I developed isogenic HEK cells that express either WT or mutant (*E542K; E545K*) *PIK3CA*. I monitored the oncogenic potential of each mutation by observing cell growth in monolayer and 3D culture and interestingly found that *E542K* mutation confers a significant growth advantage to HEK cells in comparison to *E545K* mutation. I tested therapeutic response to LY3023414 and found cells transfected with *E542K* mutant PIK3CA to be significantly more resistant to treatment compared to cells transfected with *E545K* mutant PIK3CA. Therapeutic resistance was associated with sustained AKT phosphorylation in *PIK3CA E542K* mutant cells.

PIK3CA *HD* mutations are thought to behave similarly since they are both RAS dependent unlike PIK3CA kinase domain *(H1047R)* mutation which is dependent on P85 binding (Miled, Yan et al. 2007, Zhao and Vogt 2008). However our data show that they induce distinct downstream signaling pattern as well as characteristic interaction profile with the drug that induces resistance with PIK3CA *E542K* but not the *E545K* mutation. This also opens the possibility not only for distinct interaction with LY3023414 but also for differential capacity in

protein-protein interaction and therefore in their ability to induce feedback signaling.

Providing a proof of concept that distinct PIK3CA HD mutation can be predictive of therapeutic response to PI3K targeted therapy is very significant for the bladder cancer field where HD mutations represent that majority of mutations found in PIK3CA mutant bladder tumors unlike other tumors where kinase domain mutations are more common(Knowles, Platt et al. 2009, Platt, Hurst et al. 2009).

A.4. Promising drug combinations to overcome resistance to PI3K targeted inhibition

The main goal of dissecting mechanisms of therapeutic resistance is to identify better combinatorial treatment approaches that can target alternative feedback signaling induced upon resistance.

Our mutation specific TCGA based pathway analysis showed that E542K mutation status is associated with significant upregulation of G- protein coupled signaling in addition to activation of MAPK-ERK signaling. Indeed I found that in RP-B-01 (*PIK3CA E542K MUT*) but not in RP-B-02 cells (*PIK3CA E545K MUT),* ERK phosphorylation is induced upon resistance to LY3023414. Interestingly, feedback activation of MAPK signaling was associated with stabilization of MYC. MYC is a well-known player in resistance to PI3K targeted therapy especially in

the context of *PIK3CA* mutation(Dey, Leyland-Jones et al. 2015). Moreover, it is known to be play a key role in the metabolic rewiring of cancer cells in order to switch to glycolytic signaling and more efficiently utilize intermediates for macromolecular biosynthesis (Stine, Walton et al. 2015, Wong, Qian et al. 2017)as is observed in *E542K* mutant tumors.

Based on the distinct signaling that is associated with *E542K* mutation status, I tested a number of drug combinations to identify a promising approach that can overcome resistance to PI3K targeted inhibition. Interestingly, I only found bromodomain (BET) targeting (Brd4) by JQ1 to sensitize RP-B-01 cells to LY3023414, where the JQ1-LY3023414 combination was synergistic at all concentrations tested. However, bromodomain inhibition did not sensitize RP-B-01 cells to cisplatin treatment. This indicates that the therapeutic benefit associated with BET inhibition is specific to resistance induced upon PI3K targeted inhibition which is associated with the stabilization of MYC.

On the other hand, when I tested a combination of LY3023414 and LY3214996, which target PI3K/mTOR and ERK1/2 respectively, I did not find synergy. Therefore, despite feedback ERK phosphorylation induced upon resistance, co-targeting ERK phosphorylation did not sensitize cells to treatment. This indicates a more central role for MYC in driving resistance.

A.5. Subtype distinct epigenetic signature predicts resistance to PI3K targeted inhibition

Bladder cancer is a highly complex disease with high mutation burden that is only second to melanoma and lung cancer (Kim, Akbani et al. 2015). Although, we provided evidence that mutation status can predict response to treatment per see, we also think that other factors play a role such as molecular subtype.

Therefore, using our comprehensive genomic and DNA methylathion data from our bladder cancer PDX models, we were able to show that R-B-01 and RP-B-02 which are of basal-like and luminal-like subtype respectively have a distinct gene expression and DNA methylation profile.

Interestingly, we found basal-like RP-B-01 to be enriched with DNA hypermethylation compared to luminal-like RP-B-02. It would be interesting to further study whether this behavior could be linked to the CpG Island Methylator Phenotype (CIMP) which was first described in colon cancer (Hughes, Melotte et al. 2013).

In colon cancer, BET inhibition with JQ1 was found to preferentially inhibit the growth of a subset of epigenetically dysregulated colon cancer that exhibited the CIMP phenotype. Interestingly, this response in colon cancer was attributed to a distinct super enhancer region in CIMP positive colon cancer that regulates

MYC transcription (McCleland, Mesh et al. 2016). Therefore it would be interesting to know whether the therapeutic benefit we observed with JQ1 in basal-like RP-B-01 but not in RP-B-02 is linked to the hyper-methylator epigenetic signature we identified in this tumor.

Moreover, we identified two mutually exclusive chromatin modifying mutations in RP-B-01 and RP-B-02 (KMT2D and KDM6A respectively). These two enzymes are involved with histone methylation and are thought to be subtype specific (Gui, Guo et al. 2011, Kim, Sharma et al. 2014, Network 2014). Yet it remains to be known, whether the distinct DNA CpG hypermethylation we found in RP-B-01 is linked to those mutations.

Overall, we uncovered a distinct epigenetic signature for each model. DNA hypermethylation is a well characterized phenomenon in a multitude of cancers that is thought to be prognostically and therapeutically relevant (Hughes, Melotte et al. 2013). Although still controversial, therapeutic benefit associated with BET inhibition was shown to be linked to CIMP phenotype (McCleland, Mesh et al. 2016, Tögel, Nightingale et al. 2016). Therefore, herein we provide rationale for role of subtype specific-epigenetic signature in driving resistance to PI3K targeted inhibition in the context of distinct PIK3CA mutations.

B. Limitations of the Study

This study provides proof of concept that PIK3CA mutation status is predictive of response to PI3K targeted inhibition. However, a key limiation of this study is that we used only two bladder cancer PDX models (RP-B-01 and RP-B-02) in order to test treatment response *in vivo.* However I am currently in the process of developing further PDX models in order to validate our studies *in vivo*. I successfully developed and characterized 9 alternative bladder cancer PDX models that represent a wide range of histologies. As shown in Chapter IV (Figures 49, 50 and 51), I found two models (IU3T and IU5T) to be basal-like while 3 models (IU16T, IU80T and IU68T) to be luminal like. I screened for PIK3CA mutation status in those models and found IU68T to harbor a PIK3CA *E545K* mutation indicating that it behaves like RP-B-02 and thus would be a valuable tool to continue validation of our findings.

Transfecting isogenic HEK cells with PIK3CA *WT* and mutants was key to determining the signficance of mutation status in predicting response to treatment. However, ideally another cell line would be important to strenghthen the validity of our findings. While HEK cells are readily transfectable and are well known for being used in wide range of settings to test the biological significance of various proteins (Thomas and Smart 2005, Nakanishi, Walter et al. 2016), it would be more physiologically relevant to use a urothelial cell line in order to monitor the oncogenic and therapeutic effect of HD PIK3CA mutations such as SV-HUC cells (Christian, Loretz et al. 1987). I tried to express PIK3CA

(WT/MUT) in SV-HUC cells however overexpression of PIK3CA in those cells, which naturally express high levels of PIK3CA and P-AKT, has been associated with inhibition of downstream AKT phosphorylation. Therefore, despite being physiologically relevant, SV-HUC cells were not optimal for testing the downstream effects of PIK3CA HD mutations.

Another key limitation of the study is the lack of direct evidence regarding the mechanistic rationale behind the ability of PIK3CA *E542K* but not *E545K* mutation to drive distinct down stream signaling and drug interactions that play a role in therapeutic resistance. PIK3CA HD mutations are well established in the field to be RAS dependent. Yet, It is not clear whether interaction efficiency with RAS is distinct with each mutation in a manner that could influence feedback signaling. I did see therapeutic resistance with PIK3CA *E542K* but not the *E545K* mutation in addition to feedback activation of MAPK signaling in *E542K* mutant RP-B-01 but not in *E545K* mutant RP-B-02,. However I don't currently have direct evidence to show that the RAS-MAPK activation that is specific to RP-B-01 is mutation dependent. To test this possibility, ideally I would like to run a Co-IP experiment to examine whether RAS more strongly interact with PIK3CA *E542K* mutant protein in compariosn to its *E545K* mutant counterpart. Ultimately, this would provide stronger evidence that patients who carry the PIK3CA *E542K* mutation are more likey to develop resistance to PI3K targeted inhibition.

Additionally I was able to propose BET inhibition as an additional tool that can be used in conjunction with PI3K targeted inhibition to overcome resistance to PI3K targted inhibition specifically in bladder cancer that harbors the PIK3CA *E542K* mutation. Although, I did study the epigenetic signature in each model, I was not able to identify so far a unique DNA hypermethylation signature in basal-like RP-B-01 that could provide a direct mechanistic rationale for the synergy between LY3023414-JQ1 combination in *E542K* mutant RP-B-01 but not the *E545K* mutant RP-B-02.

Taken together, this study provides a predictive paradigm for mutation response to PI3K targeted inhibition in bladder cancer patients. Therefore, my stuidoes lay the foundation for better selection of pateint population on clinical trials, provide patients with more personalized treatment and therefore improved treatment outcome.

C. Future directions

This study lays the foundation for molecularly driven patient selection on bladder cancer clinical trials testing PI3K targeted therapy. Further future studies are needed to strengthen the mechanistic rationale behind this predictive model and to provide more solid evidence for future clinical trial design.

While our *in silico* predictive analysis of drug-PI3K interaction showed that PIK3CA *E545K* mutation is associated with more stable binding with

LY3023414 compared to the PIK3CA *E542K* mutation, ideally we would like to run surface plasmon resonance spectroscopy (SPR) (Patching 2014) in order to calculate association ('on rate', ka) and dissociation rates ('off rate', kd), the equilibrium dissociation constant ('binding constant', KD) for LY3023414 in the context of each distinct PIK3CA mutations. We expect that LY3023414 will have faster dissociative off rate (Koff) in the presence of the E542K mutated PIK3CA protein; suggesting a shorter drug residence time and weaker inhibitory effect. Ultimately, this would strengthen our MDS studies and provide a potential mechanism underlying the therapeutic resistance in tumors harboring the E542K mutation compared to those harboring the E545K mutation.

As previously mentioned, ideally we would like to validate our mutation dependent drug response data in alternative cell lines. We believe that immortalized urothelial cells (SV-HUCs) are ideal for that purpose since they are physiologically relevant. They could also provide a tool for testing the differential effect of mutation not only on drug response but also cell proliferation, morphology and migration/invasion.

Further PIK3CA mutant bladder cancer PDX models should be tested for mutation-induced drug response in the context of distinct subtype (i.e. basal vs luminal). If it is not feasible to develop a suitable number of PDX models in order to adequately power our studies, an alternative tool would be to use CRISPR-CAS-HDR system (Liang, Potter et al. 2017) to edit the mutation in RP-B-01

from PIK3CA *E542K* to PIK3CA *E545K* mutation. Then we would test whether mutation change would be associated with reversal of therapeutic resistance. This would provide powerful evidence that treatment response is indeed mutation dependent.

The complexity of bladder cancer as well as determinants of therapeutic response compelled us to look at the role of epigenetic changes in driving drug resistance. Thus in the future we would like to investigate this hypothesis in more depth. The epigenetic/DNA methylome signature of bladder cancer would potentially provide a more mechanistic rationale for the synergy we observed between JQ1 and LY3023414. Similar to the DNA hypermethylation signature we found in RP-B-01; hypermethylator phenotype has been proposed in other tumors, such as colon cancer (Issa 2003, Barault, Charon-Barra et al. 2008, Irizarry, Ladd-Acosta et al. 2009, Sánchez-Carbayo 2012). In colon cancer, it was shown that in association with DNA hypermethylation, MYC is activated through super enhancers. In this context bromodomain inhibition (JQ1) was indeed very beneficial and capable of curbing tumor growth (McCleland, Mesh et al. 2016). Therefore, it would be interesting to see if a similar signature is associated with the benefit associated with bromodomain inhibition in bladder cancer.

Overall, this study provides an unprecedented paradigm for prediction of treatment response to PI3K targeted inhibition in MIBC. Cross talk between hot spot PIK3CA mutation and tumor subtype has been investigated for its role in

therapeutic response/resistance. The future goal of this piece of work is to provide mechanistic rationale for better clinical trial design in a disease where an effective targeted therapy has not yet found its way to the clinic.

REFERENCES

SEER

Cancer Statistics Review, 1975-2013, National Cancer Institute.

Anders, S., P. T. Pyl and W. Huber (2015). "HTSeq—a Python framework to work with high-throughput sequencing data." Bioinformatics **31**(2): 166-169.

Andrews, F. H., A. R. Singh, S. Joshi, C. A. Smith, G. A. Morales, J. R. Garlich, D. L. Durden and T. G. Kutateladze (2017). "Dual-activity PI3K–BRD4 inhibitor for the orthogonal inhibition of MYC to block tumor growth and metastasis." Proceedings of the National Academy of Sciences **114**(7): E1072-E1080.

Arpin, C. C., S. Mac, Y. Jiang, H. Cheng, M. Grimard, B. D. Page, M. M. Kamocka, S. Haftchenary, H. Su and D. P. Ball (2016). "Applying small molecule signal transducer and activator of transcription-3 (STAT3) protein inhibitors as pancreatic cancer therapeutics." Molecular cancer therapeutics **15**(5): 794-805.

Barocas, D. A., D. R. Globe, D. C. Colayco, A. Onyenwenyi, A. S. Bruno, T. J. Bramley and R. J. Spear (2012). "Surveillance and treatment of non-muscle-invasive bladder cancer in the USA." Advances in urology **2012**.

Bartoletti, R., T. Cai, G. Nesi, L. R. Girardi, G. Baroni and M. Dal Canto (2007). "Loss of P16 expression and chromosome 9p21 LOH in predicting outcome of patients affected by superficial bladder cancer." Journal of Surgical Research **143**(2): 422-427.

Berendsen, H. J., J. P. Postma, W. F. van Gunsteren and J. Hermans (1981). Interaction models for water in relation to protein hydration. Intermolecular forces, Springer**:** 331-342.

Berman, H. M., J. Westbrook, Z. Feng, G. Gilliland, T. Bhat, H. Weissig, I. N. Shindyalov and P. E. Bourne (2000). "The Protein Data Bank." Nucleic Acids Research **28**(1): 235-242.

Bernardo, C., C. Costa, T. Amaro, M. Goncalves, P. Lopes, R. Freitas, F. Gaertner, F. Amado, J. A. Ferreira and L. Santos (2014). "Patient-derived sialyl-Tn-positive invasive bladder cancer xenografts in nude mice: an exploratory model study." Anticancer research **34**(2): 735-744.

Bhagwat, S. V., W. T. McMillen, S. Cai, B. Zhao, M. Whitesell, L. Kindler, R. S. Flack, W. Wu, K. Huss and B. Anderson (2017). Discovery of LY3214996,

a selective and novel ERK1/2 inhibitor with potent antitumor activities in cancer models with MAPK pathway alterations, AACR.

Bonelli, M. A., G. Digiacomo, C. Fumarola, R. Alfieri, F. Quaini, A. Falco, D. Madeddu, S. La Monica, D. Cretella and A. Ravelli (2017). "Combined Inhibition of CDK4/6 and PI3K/AKT/mTOR Pathways Induces a Synergistic Anti-Tumor Effect in Malignant Pleural Mesothelioma Cells." Neoplasia **19**(8): 637-648.

Britschgi, A., R. Andraos, H. Brinkhaus, I. Klebba, V. Romanet, U. Müller, M. Murakami, T. Radimerski and M. Bentires-Alj (2012). "JAK2/STAT5 inhibition circumvents resistance to PI3K/mTOR blockade: a rationale for cotargeting these pathways in metastatic breast cancer." Cancer cell **22**(6): 796-811.

Brooks, A. N., E. Kilgour and P. D. Smith (2012). "Molecular pathways: fibroblast growth factor signaling: a new therapeutic opportunity in cancer." Clinical cancer research **18**(7): 1855-1862.

Brown, K. K. and A. Toker (2015). "The phosphoinositide 3-kinase pathway and therapy resistance in cancer." F1000prime reports **7**.

Carneiro, B. A., J. J. Meeks, T. M. Kuzel, M. Scaranti, S. A. Abdulkadir and F. J. Giles (2015). "Emerging therapeutic targets in bladder cancer." Cancer Treatment Reviews **41**(2): 170-178.

Carracedo, A., L. Ma, J. Teruya-Feldstein, F. Rojo, L. Salmena, A. Alimonti, A. Egia, A. T. Sasaki, G. Thomas and S. C. Kozma (2008). "Inhibition of mTORC1 leads to MAPK pathway activation through a PI3K-dependent feedback loop in human cancer." The Journal of clinical investigation **118**(9): 3065-3074.

Chakrabarty, A., V. Sánchez, M. G. Kuba, C. Rinehart and C. L. Arteaga (2012). "Feedback upregulation of HER3 (ErbB3) expression and activity attenuates antitumor effect of PI3K inhibitors." Proceedings of the National Academy of Sciences **109**(8): 2718-2723.

Chan, K. S., I. Espinosa, M. Chao, D. Wong, L. Ailles, M. Diehn, H. Gill, J. Presti, H. Y. Chang and M. van de Rijn (2009). "Identification, molecular characterization, clinical prognosis, and therapeutic targeting of human bladder tumor-initiating cells." Proceedings of the National Academy of Sciences **106**(33): 14016-14021.

Chen, J., Y. Cui, P. Li, L. Liu, C. Li and X. Zu (2017). "Expression and clinical significance of androgen receptor in bladder cancer: A meta‐analysis." Molecular and clinical oncology **7**(5): 919-927.

Chia, S., S. Gandhi, A. Joy, S. Edwards, M. Gorr, S. Hopkins, J. Kondejewski, J. Ayoub, N. Califaretti and D. Rayson (2015). "Novel agents and associated toxicities of inhibitors of the pi3k/Akt/mtor pathway for the treatment of breast cancer." Current oncology **22**(1): 33.

Choi, S. Y. C., D. Lin, P. W. Gout, C. C. Collins, Y. Xu and Y. Wang (2014). "Lessons from patient-derived xenografts for better in vitro modeling of human cancer." Advanced drug delivery reviews **79**: 222-237.

Choi, W., S. Porten, S. Kim, D. Willis, E. Plimack, J. Hoffman-Censits, B. Roth, T. Cheng, M. Tran, I. Lee, J. Melquist, J. Bondaruk, T. Majewski, S. Zhang, S. Pretzsch, K. Baggerly, A. Siefker-Radtke, B. Czerniak, C. Dinney and D. McConkey (2014). "Identification of Distinct Basal and Luminal Subtypes of Muscle-Invasive Bladder Cancer with Different Sensitivities to Frontline Chemotherapy." Cancer Cell **25**(2): 152-165.

Choi, W., S. Porten, S. Kim, D. Willis, E. R. Plimack, J. Hoffman-Censits, B. Roth, T. Cheng, M. Tran, I. L. Lee, J. Melquist, J. Bondaruk, T. Majewski, S. Zhang, S. Pretzsch, K. Baggerly, A. Siefker-Radtke, B. Czerniak, C. P. Dinney and D. J. McConkey (2014). "Identification of distinct basal and luminal subtypes of muscle-invasive bladder cancer with different sensitivities to frontline chemotherapy." Cancer Cell **25**(2): 152-165.

Chou, R., S. S. Selph, D. I. Buckley, K. S. Gustafson, J. C. Griffin, S. E. Grusing and J. L. Gore (2016). "Treatment of muscle-invasive bladder cancer: A systematic review." Cancer **122**(6): 842-851.

Chou, T.-C. (2010). "Drug combination studies and their synergy quantification using the Chou-Talalay method." Cancer research **70**(2): 440-446.

Christian, B. J., L. J. Loretz, T. D. Oberley and C. A. Reznikoff (1987). "Characterization of human uroepithelial cells immortalized in vitro by simian virus 40." Cancer research **47**(22): 6066-6073.

Ciamporcero, E., H. Shen, S. Ramakrishnan, S. Y. Ku, S. Chintala, L. Shen, R. Adelaiye, K. M. Miles, C. Ullio and S. Pizzimenti (2016). "YAP activation protects urothelial cell carcinoma from treatment-induced DNA damage." Oncogene **35**(12): 1541.

Cirone, P., C. J. Andresen, J. R. Eswaraka, P. B. Lappin and C. M. Bagi (2014). "Patient-derived xenografts reveal limits to PI3K/mTOR-and MEK-mediated inhibition of bladder cancer." Cancer chemotherapy and pharmacology **73**(3): 525-538.

Damrauer, J. S., K. A. Hoadley, D. D. Chism, C. Fan, C. J. Tiganelli, S. E. Wobker, J. J. Yeh, M. I. Milowsky, G. Iyer and J. S. Parker (2014). "Intrinsic subtypes of high-grade bladder cancer reflect the hallmarks of

breast cancer biology." Proceedings of the National Academy of Sciences **111**(8): 3110-3115.

Darden, T., D. York and L. Pedersen (1993). "Particle mesh Ewald: An N· log (N) method for Ewald sums in large systems." The Journal of chemical physics **98**(12): 10089-10092.

Dasari, S. and P. B. Tchounwou (2014). "Cisplatin in cancer therapy: molecular mechanisms of action." European journal of pharmacology **740**: 364-378.

Dawson, M. A., R. K. Prinjha, A. Dittmann, G. Giotopoulos, M. Bantscheff, W.-I. Chan, S. C. Robson, C.-w. Chung, C. Hopf and M. M. Savitski (2011). "Inhibition of BET recruitment to chromatin as an effective treatment for MLL-fusion leukaemia." Nature **478**(7370): 529.

Delmore, J. E., G. C. Issa, M. E. Lemieux, P. B. Rahl, J. Shi, H. M. Jacobs, E. Kastritis, T. Gilpatrick, R. M. Paranal and J. Qi (2011). "BET bromodomain inhibition as a therapeutic strategy to target c-Myc." Cell **146**(6): 904-917.

Dey, N., B. Leyland-Jones and P. De (2015). "MYC-xing it up with PIK3CA mutation and resistance to PI3K inhibitors: summit of two giants in breast cancers." American journal of cancer research **5**(1): 1.

Dhalluin, C., J. E. Carlson, L. Zeng, C. He, A. K. Aggarwal and M.-M. Zhou (1999). "Structure and ligand of a histone acetyltransferase bromodomain." Nature **399**(6735): 491.

Di Martino, E., C. L'hôte, W. Kennedy, D. Tomlinson and M. Knowles (2009). "Mutant fibroblast growth factor receptor 3 induces intracellular signaling and cellular transformation in a cell type-and mutation-specific manner." Oncogene **28**(48): 4306.

Dobin, A., C. A. Davis, F. Schlesinger, J. Drenkow, C. Zaleski, S. Jha, P. Batut, M. Chaisson and T. R. Gingeras (2013). "STAR: ultrafast universal RNA-seq aligner." Bioinformatics **29**(1): 15-21.

Dobruch, J., S. Daneshmand, M. Fisch, Y. Lotan, A. P. Noon, M. J. Resnick, S. F. Shariat, A. R. Zlotta and S. A. Boorjian (2016). "Gender and bladder cancer: a collaborative review of etiology, biology, and outcomes." European urology **69**(2): 300-310.

Drayton, R. M., E. Dudziec, S. Peter, S. Bertz, A. Hartmann, H. E. Bryant and J. W. Catto (2014). "Reduced expression of miRNA-27a modulates cisplatin resistance in bladder cancer by targeting the cystine/glutamate exchanger SLC7A11." Clinical cancer research **20**(7): 1990-2000.

Earl, J., D. Rico, E. Carrillo-de-Santa-Pau, B. Rodríguez-Santiago, M. Méndez-Pertuz, H. Auer, G. Gómez, H. B. Grossman, D. G. Pisano and W. A.

Schulz (2015). "The UBC-40 Urothelial Bladder Cancer cell line index: a genomic resource for functional studies." BMC genomics **16**(1): 403.

Edmonson, M. N., J. Zhang, C. Yan, R. P. Finney, D. M. Meerzaman and K. H. Buetow (2011). "Bambino: a variant detector and alignment viewer for next-generation sequencing data in the SAM/BAM format." Bioinformatics **27**(6): 865-866.

Elbanna, M., S. Chintala, E. Ciamporcero, R. Adelayie, A. Orillion, S. Arisa, N. Damayanti, M. Grimard, T. Puls and S. Harbin (2017). In vitro modeling of patient derived bladder cancer cell lines in 3D culture systems, AACR.

Eriksson, P., C. Rovira, F. Liedberg, G. Sjödahl and M. Höglund (2018). "A validation and extended description of the Lund taxonomy for urothelial carcinoma using the TCGA cohort." Scientific reports **8**(1): 3737.

Fijalkowska, I., W. Xu, S. A. Comhair, A. J. Janocha, L. A. Mavrakis, B. Krishnamachary, L. Zhen, T. Mao, A. Richter and S. C. Erzurum (2010). "Hypoxia inducible-factor1α regulates the metabolic shift of pulmonary hypertensive endothelial cells." The American journal of pathology **176**(3): 1130-1138.

Filippakopoulos, P., J. Qi, S. Picaud, Y. Shen, W. B. Smith, O. Fedorov, E. M. Morse, T. Keates, T. T. Hickman and I. Felletar (2010). "Selective inhibition of BET bromodomains." Nature **468**(7327): 1067.

Fiser, A. and A. Šali (2003). "Modeller: generation and refinement of homology-based protein structure models." Methods in enzymology **374**: 461-491.

Fletcher, R. and M. J. Powell (1963). "A rapidly convergent descent method for minimization." The computer journal **6**(2): 163-168.

Galluzzi, L., L. Senovilla, I. Vitale, J. Michels, I. Martins, O. Kepp, M. Castedo and G. Kroemer (2012). "Molecular mechanisms of cisplatin resistance." Oncogene **31**(15): 1869.

Gu, J. and X. Wu (2011). "Genetic susceptibility to bladder cancer risk and outcome." Personalized medicine **8**(3): 365-374.

Gui, Y., G. Guo, Y. Huang, X. Hu, A. Tang, S. Gao, R. Wu, C. Chen, X. Li and L. Zhou (2011). "Frequent mutations of chromatin remodeling genes in transitional cell carcinoma of the bladder." Nature genetics **43**(9): 875-878.

Guo, Y., Y. Chekaluk, J. Zhang, J. Du, N. S. Gray, C. L. Wu and D. J. Kwiatkowski (2013). "TSC1 involvement in bladder cancer: diverse effects and therapeutic implications." The Journal of pathology **230**(1): 17-27.

Hess, B., H. Bekker, H. J. Berendsen and J. G. Fraaije (1997). "LINCS: a linear constraint solver for molecular simulations." Journal of computational chemistry **18**(12): 1463-1472.

Hess, B., C. Kutzner, D. Van Der Spoel and E. Lindahl (2008). "GROMACS 4: algorithms for highly efficient, load-balanced, and scalable molecular simulation." Journal of chemical theory and computation **4**(3): 435-447.

Hnisz, D., B. J. Abraham, T. I. Lee, A. Lau, V. Saint-André, A. A. Sigova, H. A. Hoke and R. A. Young (2013). "Super-enhancers in the control of cell identity and disease." Cell **155**(4): 934-947.

Hochstein, C., S. Arnesen and J. Goshorn (2007). "Environmental health and toxicology resources of the United States National Library of Medicine." Medical reference services quarterly **26**(3): 21-45.

Horstmann, M., R. Witthuhn, M. Falk and A. Stenzl (2008). "Gender-specific differences in bladder cancer: a retrospective analysis." Gender medicine **5**(4): 385-394.

Houédé, N. and P. Pourquier (2015). "Targeting the genetic alterations of the PI3K–AKT–mTOR pathway: Its potential use in the treatment of bladder cancers." Pharmacology & therapeutics **145**: 1-18.

Howlader, N., A. Noone, M. Krapcho, J. Garshell, D. Miller and S. Altekruse (2012). SEER cancer statistics review, 1975–2013. Bethesda, MD: National Cancer Institute; April 2016.

Hughes, L. A., V. Melotte, J. De Schrijver, M. De Maat, V. T. Smit, J. V. Bovée, P. J. French, P. A. Van Den Brandt, L. J. Schouten and T. De Meyer (2013). "The CpG island methylator phenotype: what's in a name?" Cancer research.

Huw, L., C. O'brien, A. Pandita, S. Mohan, J. Spoerke, S. Lu, Y. Wang, G. Hampton, T. Wilson and M. Lackner (2013). "Acquired PIK3CA amplification causes resistance to selective phosphoinositide 3-kinase inhibitors in breast cancer." Oncogenesis **2**(12): e83.

Ilic, N., T. Utermark, H. R. Widlund and T. M. Roberts (2011). "PI3K-targeted therapy can be evaded by gene amplification along the MYC-eukaryotic translation initiation factor 4E (eIF4E) axis." Proceedings of the National Academy of Sciences **108**(37): E699-E708.

Inoue, T., N. Terada, T. Kobayashi and O. Ogawa (2017). "Patient-derived xenografts as in vivo models for research in urological malignancies." Nature Reviews Urology **14**(5): 267.

Irizarry, R. A., C. Ladd-Acosta, B. Wen, Z. Wu, C. Montano, P. Onyango, H. Cui, K. Gabo, M. Rongione and M. Webster (2009). "The human colon cancer methylome shows similar hypo-and hypermethylation at conserved tissue-specific CpG island shores." Nature genetics **41**(2): 178.

Iyer, G., A. J. Hanrahan, M. I. Milowsky, H. Al-Ahmadie, S. N. Scott, M. Janakiraman, M. Pirun, C. Sander, N. D. Socci and I. Ostrovnaya (2012). "Genome sequencing identifies a basis for everolimus sensitivity." Science **338**(6104): 221-221.

Jäger, W., H. Xue, T. Hayashi, C. Janssen, S. Awrey, A. W. Wyatt, S. Anderson, I. Moskalev, A. Haegert and M. Alshalalfa (2015). "Patient-derived bladder cancer xenografts in the preclinical development of novel targeted therapies." Oncotarget **6**(25): 21522.

Jain, A. N. (2003). "Surflex: fully automatic flexible molecular docking using a molecular similarity-based search engine." Journal of medicinal chemistry **46**(4): 499-511.

Jang, M. K., K. Mochizuki, M. Zhou, H.-S. Jeong, J. N. Brady and K. Ozato (2005). "The bromodomain protein Brd4 is a positive regulatory component of P-TEFb and stimulates RNA polymerase II-dependent transcription." Molecular cell **19**(4): 523-534.

Janku, F., A. M. Tsimberidou, I. Garrido-Laguna, X. Wang, R. Luthra, D. S. Hong, A. Naing, G. S. Falchook, J. W. Moroney and S. A. Piha-Paul (2011). "PIK3CA mutations in patients with advanced cancers treated with PI3K/AKT/mTOR axis inhibitor." Molecular cancer therapeutics: molcanther. 0994.2010.

Janku, F., J. J. Wheler, A. Naing, G. S. Falchook, D. S. Hong, V. M. Stepanek, S. Fu, S. A. Piha-Paul, J. J. Lee and R. Luthra (2013). "PIK3CA mutation H1047R is associated with response to PI3K/AKT/mTOR signaling pathway inhibitors in early-phase clinical trials." Cancer research **73**(1): 276-284.

Jiang, B., E.-H. Li, Y.-Y. Lu, Q. Jiang, D. Cui, Y.-F. Jing and S.-J. Xia (2012). "Inhibition of fatty-acid synthase suppresses P-AKT and induces apoptosis in bladder cancer." Urology **80**(2): 484. e489-484. e415.

Johnson, M., I. Zaretskaya, Y. Raytselis, Y. Merezhuk, S. McGinnis and T. L. Madden (2008). "NCBI BLAST: a better web interface." Nucleic acids research **36**(suppl_2): W5-W9.

Joseph, S. B., B. A. Laffitte, P. H. Patel, M. A. Watson, K. E. Matsukuma, R. Walczak, J. L. Collins, T. F. Osborne and P. Tontonoz (2002). "Direct and indirect mechanisms for regulation of fatty acid synthase gene expression

by liver X receptors." Journal of Biological Chemistry **277**(13): 11019-11025.

Juanpere, N., L. Agell, M. Lorenzo, S. de Muga, L. López-Vilaró, R. Murillo, S. Mojal, S. Serrano, J. A. Lorente and J. Lloreta (2012). "Mutations in FGFR3 and PIK3CA, singly or combined with RAS and AKT1, are associated with AKT but not with MAPK pathway activation in urothelial bladder cancer." Human pathology **43**(10): 1573-1582.

Juvekar, A., L. N. Burga, H. Hu, E. P. Lunsford, Y. H. Ibrahim, J. Balmañà, A. Rajendran, A. Papa, K. Spencer and C. A. Lyssiotis (2012). "Combining a PI3K inhibitor with a PARP inhibitor provides an effective therapy for BRCA1-related breast cancer." Cancer discovery **2**(11): 1048-1063.

Kamat, A. M., N. M. Hahn, J. A. Efstathiou, S. P. Lerner, P.-U. Malmström, W. Choi, C. C. Guo, Y. Lotan and W. Kassouf (2016). "Bladder cancer." The Lancet **388**(10061): 2796-2810.

Kashiwagi, E., H. Ide, S. Inoue, T. Kawahara, Y. Zheng, L. O. Reis, A. S. Baras and H. Miyamoto (2016). "Androgen receptor activity modulates responses to cisplatin treatment in bladder cancer." Oncotarget **7**(31): 49169.

Kenny, H. A., M. Lal-Nag, E. A. White, M. Shen, C.-Y. Chiang, A. K. Mitra, Y. Zhang, M. Curtis, E. M. Schryver and S. Bettis (2015). "Quantitative high throughput screening using a primary human three-dimensional organotypic culture predicts in vivo efficacy." Nature communications **6**: 6220.

Kidger, A. M., J. Sipthorp and S. J. Cook (2018). "ERK1/2 inhibitors: New weapons to inhibit the RAS-regulated RAF-MEK1/2-ERK1/2 pathway." Pharmacology & therapeutics.

Kim, J., R. Akbani, C. J. Creighton, S. P. Lerner, J. N. Weinstein, G. Getz and D. J. Kwiatkowski (2015). "Invasive bladder cancer: genomic insights and therapeutic promise." Clinical Cancer Research **21**(20): 4514-4524.

Kim, J., K. W. Mouw, P. Polak, L. Z. Braunstein, A. Kamburov, G. Tiao, D. J. Kwiatkowski, J. E. Rosenberg, E. M. Van Allen and A. D D'Andrea (2016). "Somatic ERCC2 mutations are associated with a distinct genomic signature in urothelial tumors." Nature genetics **48**(6): 600.

Kim, J. H., A. Sharma, S. S. Dhar, S. H. Lee, B. Gu, C. H. Chan, H. K. Lin and M. G. Lee (2014). "UTX and MLL4 coordinately regulate transcriptional programs for cell proliferation and invasiveness in breast cancer cells." Cancer Res **74**(6): 1705-1717.

Kitchen, M. O., R. T. Bryan, R. D. Emes, J. R. Glossop, C. Luscombe, K. Cheng, M. P. Zeegers, N. D. James, A. J. Devall and C. A. Mein (2016). "Quantitative genome-wide methylation analysis of high-grade non-muscle invasive bladder cancer." Epigenetics **11**(3): 237-246.

Knowles, M. A. (2008). "Molecular pathogenesis of bladder cancer." International journal of clinical oncology **13**(4): 287-297.

Knowles, M. A. and C. D. Hurst (2015). "Molecular biology of bladder cancer: new insights into pathogenesis and clinical diversity." Nature Reviews Cancer **15**(1): 25-41.

Knowles, M. A., F. M. Platt, R. L. Ross and C. D. Hurst (2009). "Phosphatidylinositol 3-kinase (PI3K) pathway activation in bladder cancer." Cancer and Metastasis Reviews **28**(3-4): 305-316.

Kompier, L. C., I. Lurkin, M. N. van der Aa, B. W. van Rhijn, T. H. van der Kwast and E. C. Zwarthoff (2010). "FGFR3, HRAS, KRAS, NRAS and PIK3CA mutations in bladder cancer and their potential as biomarkers for surveillance and therapy." PloS one **5**(11): e13821.

Lai, Y., X. Wei, S. Lin, L. Qin, L. Cheng and P. Li (2017). "Current status and perspectives of patient-derived xenograft models in cancer research." Journal of hematology & oncology **10**(1): 106.

Lauss, M., M. Aine, G. Sjödahl, S. Veerla, O. Patschan, S. Gudjonsson, G. Chebil, K. Lövgren, M. Fernö and W. Månsson (2012). "DNA methylation analyses of urothelial carcinoma reveal distinct epigenetic subtypes and an association between gene copy number and methylation status." Epigenetics **7**(8): 858-867.

Lee, J.-E., Y.-K. Park, S. Park, Y. Jang, N. Waring, A. Dey, K. Ozato, B. Lai, W. Peng and K. Ge (2017). "Brd4 binds to active enhancers to control cell identity gene induction in adipogenesis and myogenesis." Nature communications **8**(1): 2217.

Lee, J.-E., C. Wang, S. Xu, Y.-W. Cho, L. Wang, X. Feng, A. Baldridge, V. Sartorelli, L. Zhuang and W. Peng (2013). "H3K4 mono-and di-methyltransferase MLL4 is required for enhancer activation during cell differentiation." Elife **2**: e01503.

Leow, J. J., W. Martin-Doyle, P. S. Rajagopal, C. G. Patel, E. M. Anderson, A. T. Rothman, R. J. Cote, Y. Urun, S. L. Chang and T. K. Choueiri (2014). "Adjuvant chemotherapy for invasive bladder cancer: a 2013 updated systematic review and meta-analysis of randomized trials." European urology **66**(1): 42-54.

Li, H. and R. Durbin (2009). "Fast and accurate short read alignment with Burrows–Wheeler transform." Bioinformatics **25**(14): 1754-1760.

Li, H., B. Handsaker, A. Wysoker, T. Fennell, J. Ruan, N. Homer, G. Marth, G. Abecasis and R. Durbin (2009). "The sequence alignment/map format and SAMtools." Bioinformatics **25**(16): 2078-2079.

Li, P., J. Chen and H. Miyamoto (2017). "Androgen receptor signaling in bladder cancer." Cancers **9**(2): 20.

Liang, X., J. Potter, S. Kumar, N. Ravinder and J. D. Chesnut (2017). "Enhanced CRISPR/Cas9-mediated precise genome editing by improved design and delivery of gRNA, Cas9 nuclease, and donor DNA." Journal of biotechnology **241**: 136-146.

Liu, P., H. Cheng, S. Santiago, M. Raeder, F. Zhang, A. Isabella, J. Yang, D. J. Semaan, C. Chen and E. A. Fox (2011). "Oncogenic PIK3CA-driven mammary tumors frequently recur via PI3K pathway–dependent and PI3K pathway–independent mechanisms." Nature medicine **17**(9): 1116.

Liu, T.-J., D. Koul, T. LaFortune, N. Tiao, R. J. Shen, S.-M. Maira, C. Garcia-Echevrria and W. A. Yung (2009). "NVP-BEZ235, a novel dual phosphatidylinositol 3-kinase/mammalian target of rapamycin inhibitor, elicits multifaceted antitumor activities in human gliomas." Molecular cancer therapeutics **8**(8): 2204-2210.

Liu, W., Q. Ma, K. Wong, W. Li, K. Ohgi, J. Zhang, A. K. Aggarwal and M. G. Rosenfeld (2013). "Brd4 and JMJD6-associated anti-pause enhancers in regulation of transcriptional pause release." Cell **155**(7): 1581-1595.

Liu, X., V. Ory, S. Chapman, H. Yuan, C. Albanese, B. Kallakury, O. A. Timofeeva, C. Nealon, A. Dakic and V. Simic (2012). "ROCK inhibitor and feeder cells induce the conditional reprogramming of epithelial cells." The American journal of pathology **180**(2): 599-607.

Lobo, N., C. Mount, K. Omar, R. Nair, R. Thurairaja and M. S. Khan (2017). "Landmarks in the treatment of muscle-invasive bladder cancer." Nature Reviews Urology **14**(9): 565.

Lombard, A. P. and M. Mudryj (2015). "The emerging role of the androgen receptor in bladder cancer." Endocrine-related cancer **22**(5): R265-R277.

LoRusso, P. M. (2016). "Inhibition of the PI3K/AKT/mTOR pathway in solid tumors." Journal of Clinical Oncology **34**(31): 3803-3815.

Love, M. I., W. Huber and S. Anders (2014). "Moderated estimation of fold change and dispersion for RNA-seq data with DESeq2." Genome biology **15**(12): 550.

Lovén, J., H. A. Hoke, C. Y. Lin, A. Lau, D. A. Orlando, C. R. Vakoc, J. E. Bradner, T. I. Lee and R. A. Young (2013). "Selective inhibition of tumor oncogenes by disruption of super-enhancers." Cell **153**(2): 320-334.

Luo, W., M. S. Friedman, K. Shedden, K. D. Hankenson and P. J. Woolf (2009). "GAGE: generally applicable gene set enrichment for pathway analysis." BMC bioinformatics **10**(1): 161.

Malats, N. and F. X. Real (2015). "Epidemiology of bladder cancer." Hematology/oncology clinics **29**(2): 177-189.

Martin, L. P., T. C. Hamilton and R. J. Schilder (2008). "Platinum resistance: the role of DNA repair pathways." Clinical cancer research **14**(5): 1291-1295.

Massari, F., C. Ciccarese, M. Santoni, R. Iacovelli, R. Mazzucchelli, F. Piva, M. Scarpelli, R. Berardi, G. Tortora and A. Lopez-Beltran (2016). "Metabolic phenotype of bladder cancer." Cancer treatment reviews **45**: 46-57.

Massihnia, D., A. Galvano, D. Fanale, A. Perez, M. Castiglia, L. Incorvaia, A. Listì, S. Rizzo, G. Cicero and V. Bazan (2016). "Triple negative breast cancer: shedding light onto the role of pi3k/akt/mtor pathway." Oncotarget **7**(37): 60712.

Matkar, S., P. Sharma, S. Gao, B. Gurung, B. W. Katona, J. Liao, A. B. Muhammad, X.-C. Kong, L. Wang and G. Jin (2015). "An epigenetic pathway regulates sensitivity of breast cancer cells to HER2 inhibition via FOXO/c-Myc axis." Cancer cell **28**(4): 472-485.

McCleland, M. L., K. Mesh, E. Lorenzana, V. S. Chopra, E. Segal, C. Watanabe, B. Haley, O. Mayba, M. Yaylaoglu and F. Gnad (2016). "CCAT1 is an enhancer-templated RNA that predicts BET sensitivity in colorectal cancer." The Journal of clinical investigation **126**(2): 639-652.

Mertz, J. A., A. R. Conery, B. M. Bryant, P. Sandy, S. Balasubramanian, D. A. Mele, L. Bergeron and R. J. Sims (2011). "Targeting MYC dependence in cancer by inhibiting BET bromodomains." Proceedings of the National Academy of Sciences **108**(40): 16669-16674.

Mikeska, T. and J. M. Craig (2014). "DNA methylation biomarkers: cancer and beyond." Genes **5**(3): 821-864.

Miled, N., Y. Yan, W.-C. Hon, O. Perisic, M. Zvelebil, Y. Inbar, D. Schneidman-Duhovny, H. J. Wolfson, J. M. Backer and R. L. Williams (2007). "Mechanism of two classes of cancer mutations in the phosphoinositide 3-kinase catalytic subunit." science **317**(5835): 239-242.

Mitra, K. and J. Lippincott-Schwartz (2010). "Analysis of mitochondrial dynamics and functions using imaging approaches." Current protocols in cell biology **46**(1): 4.25. 21-24.25. 21.

Morrison, C. D., P. Liu, A. Woloszynska-Read, J. Zhang, W. Luo, M. Qin, W. Bshara, J. M. Conroy, L. Sabatini and P. Vedell (2014). "Whole-genome sequencing identifies genomic heterogeneity at a nucleotide and chromosomal level in bladder cancer." Proceedings of the National Academy of Sciences **111**(6): E672-E681.

Mostafa, M. H., S. Sheweita and P. J. O'Connor (1999). "Relationship between schistosomiasis and bladder cancer." Clinical microbiology reviews **12**(1): 97-111.

Muellner, M. K., I. Z. Uras, B. V. Gapp, C. Kerzendorfer, M. Smida, H. Lechtermann, N. Craig-Mueller, J. Colinge, G. Duernberger and S. M. Nijman (2011). "A chemical-genetic screen reveals a mechanism of resistance to PI3K inhibitors in cancer." Nature chemical biology **7**(11): 787.

Munster, P., R. Aggarwal, D. Hong, J. H. Schellens, R. Van Der Noll, J. Specht, P. O. Witteveen, T. L. Werner, E. C. Dees and E. Bergsland (2015). "First-in-human phase I study of GSK2126458, an oral pan-class I phosphatidylinositol-3-kinase inhibitor, in patients with advanced solid tumor malignancies." Clinical Cancer Research.

Nakanishi, Y., K. Walter, J. M. Spoerke, C. O'Brien, L. Y. Huw, G. M. Hampton and M. R. Lackner (2016). "Activating mutations in PIK3CB confer resistance to PI3K inhibition and define a novel oncogenic role for p110β." Cancer research: canres. 2201.2015.

Network, C. G. A. R. (2014). "Comprehensive molecular characterization of urothelial bladder carcinoma." Nature **507**(7492): 315.

Nicodeme, E., K. L. Jeffrey, U. Schaefer, S. Beinke, S. Dewell, C.-w. Chung, R. Chandwani, I. Marazzi, P. Wilson and H. Coste (2010). "Suppression of inflammation by a synthetic histone mimic." Nature **468**(7327): 1119.

O'Reilly, K. E., F. Rojo, Q.-B. She, D. Solit, G. B. Mills, D. Smith, H. Lane, F. Hofmann, D. J. Hicklin and D. L. Ludwig (2006). "mTOR inhibition induces upstream receptor tyrosine kinase signaling and activates Akt." Cancer research **66**(3): 1500-1508.

Olkhov-Mitsel, E., A. J. Savio, K. J. Kron, V. V. Pethe, T. Hermanns, N. E. Fleshner, B. W. van Rhijn, T. H. van der Kwast, A. R. Zlotta and B. Bapat (2017). "Epigenome-wide DNA methylation profiling identifies differential methylation biomarkers in high-grade bladder cancer." Translational oncology **10**(2): 168-177.

Ong, C.-T. and V. G. Corces (2011). "Enhancer function: new insights into the regulation of tissue-specific gene expression." Nature Reviews Genetics **12**(4): 283.

Oostenbrink, C., A. Villa, A. E. Mark and W. F. Van Gunsteren (2004). "A biomolecular force field based on the free enthalpy of hydration and solvation: the GROMOS force-field parameter sets 53A5 and 53A6." Journal of computational chemistry **25**(13): 1656-1676.

Osthus, R. C., H. Shim, S. Kim, Q. Li, R. Reddy, M. Mukherjee, Y. Xu, D. Wonsey, L. A. Lee and C. V. Dang (2000). "Deregulation of glucose transporter 1 and glycolytic gene expression by c-Myc." Journal of Biological Chemistry **275**(29): 21797-21800.

Pan, C.-x., H. Zhang, C. G. Tepper, T.-y. Lin, R. R. Davis, J. Keck, P. M. Ghosh, P. Gill, S. Airhart and C. Bult (2015). "Development and characterization of bladder cancer patient-derived xenografts for molecularly guided targeted therapy." PloS one **10**(8): e0134346.

Park, M. C., H. Jeong, S. H. Son, Y. Kim, D. Han, P. C. Goughnour, T. Kang, N. H. Kwon, H. E. Moon and S. H. Paek (2016). "Novel morphologic and genetic analysis of cancer cells in a 3D microenvironment identifies STAT3 as a regulator of tumor permeability barrier function." Cancer research **76**(5): 1044-1054.

Patching, S. G. (2014). "Surface plasmon resonance spectroscopy for characterisation of membrane protein–ligand interactions and its potential for drug discovery." Biochimica et Biophysica Acta (BBA)-Biomembranes **1838**(1): 43-55.

Paulsen, J. L. and A. C. Anderson (2009). "Scoring ensembles of docked protein: ligand interactions for virtual lead optimization." Journal of chemical information and modeling **49**(12): 2813-2819.

Pearlman, D. A., D. A. Case, J. W. Caldwell, W. S. Ross, T. E. Cheatham III, S. DeBolt, D. Ferguson, G. Seibel and P. Kollman (1995). "AMBER, a package of computer programs for applying molecular mechanics, normal mode analysis, molecular dynamics and free energy calculations to simulate the structural and energetic properties of molecules." Computer Physics Communications **91**(1-3): 1-41.

Peng, D.-J., J. Wang, J.-Y. Zhou and G. S. Wu (2010). "Role of the Akt/mTOR survival pathway in cisplatin resistance in ovarian cancer cells." Biochemical and biophysical research communications **394**(3): 600-605.

Pérez-Salvia, M. and M. Esteller (2017). "Bromodomain inhibitors and cancer therapy: from structures to applications." Epigenetics **12**(5): 323-339.

Petrylak, D. P., C. M. Tangen, P. J. Van Veldhuizen, J. W. Goodwin, P. W. Twardowski, J. N. Atkins, S. R. Kakhil, M. K. Lange, M. Mansukhani and E. D. Crawford (2010). "Results of the Southwest Oncology Group phase II evaluation (study S0031) of ZD1839 for advanced transitional cell carcinoma of the urothelium." BJU international **105**(3): 317-321.

Philips, G., S. Halabi, B. Sanford, D. Bajorin, E. Small, Cancer and L. G. B (2009). "A phase II trial of cisplatin (C), gemcitabine (G) and gefitinib for advanced urothelial tract carcinoma: results of Cancer and Leukemia Group B (CALGB) 90102." Annals of oncology **20**(6): 1074-1079.

Piunti, A. and A. Shilatifard (2016). "Epigenetic balance of gene expression by Polycomb and COMPASS families." Science **352**(6290): aad9780.

Platt, F. M., C. D. Hurst, C. F. Taylor, W. M. Gregory, P. Harnden and M. A. Knowles (2009). "Spectrum of phosphatidylinositol 3-kinase pathway gene alterations in bladder cancer." Clinical cancer research **15**(19): 6008-6017.

Ploussard, G., F. Dubosq, H. Soliman, J. Verine, F. Desgrandchamps and P. Mongiat-Artus (2010). "Prognostic Value of Loss of Heterozygosity at Chromosome 9p in Non–muscle-invasive Bladder Cancer." Urology **76**(2): 513. e513-513. e518.

Priolo, C., S. Pyne, J. Rose, E. R. Regan, G. Zadra, C. Photopoulos, S. Cacciatore, D. Schultz, N. Scaglia and J. E. McDunn (2014). "AKT1 and MYC induce distinctive metabolic fingerprints in human prostate cancer." Cancer research: canres. 1490.2014.

Pruthi, R. S., M. Nielsen, S. Heathcote, E. M. Wallen, W. K. Rathmell, P. Godley, Y. Whang, J. Fielding, H. Schultz and G. Grigson (2010). "A phase II trial of neoadjuvant erlotinib in patients with muscle-invasive bladder cancer undergoing radical cystectomy: clinical and pathological results." BJU international **106**(3): 349-354.

Rebouissou, S., I. Bernard-Pierrot, A. de Reyniès, M.-L. Lepage, C. Krucker, E. Chapeaublanc, A. Hérault, A. Kamoun, A. Caillault and E. Letouzé (2014). "EGFR as a potential therapeutic target for a subset of muscle-invasive bladder cancers presenting a basal-like phenotype." Science translational medicine **6**(244): 244ra291-244ra291.

Reuter, V. E. (2006). "The pathology of bladder cancer." Urology **67**(3): 11-17.

Robertson, A. G., J. Kim, H. Al-Ahmadie, J. Bellmunt, G. Guo, A. D. Cherniack, T. Hinoue, P. W. Laird, K. A. Hoadley and R. Akbani (2017). "Comprehensive molecular characterization of muscle-invasive bladder cancer." Cell **171**(3): 540-556. e525.

Rozen, S. and H. Skaletsky (2000). Primer3 on the WWW for general users and for biologist programmers. Bioinformatics methods and protocols, Springer**:** 365-386.

Sada, K., T. Nishikawa, D. Kukidome, T. Yoshinaga, N. Kajihara, K. Sonoda, T. Senokuchi, H. Motoshima, T. Matsumura and E. Araki (2016). "Hyperglycemia induces cellular hypoxia through production of mitochondrial ROS followed by suppression of aquaporin-1." PloS one **11**(7): e0158619.

Sánchez-Carbayo, M. (2012). "Hypermethylation in bladder cancer: biological pathways and translational applications." Tumor Biology **33**(2): 347-361.

SchuÈttelkopf, A. W. and D. M. Van Aalten (2004). "PRODRG: a tool for high-throughput crystallography of protein–ligand complexes." Acta Crystallographica Section D: Biological Crystallography **60**(8): 1355-1363.

Seront, E., S. Rottey, B. Sautois, J. Kerger, L. D'hondt, V. Verschaeve, J.-L. Canon, C. Dopchie, J. Vandenbulcke and N. Whenham (2012). "Phase II study of everolimus in patients with locally advanced or metastatic transitional cell carcinoma of the urothelial tract: clinical activity, molecular response, and biomarkers." Annals of oncology **23**(10): 2663-2670.

Serra, V., P. J. Eichhorn, C. García-García, Y. H. Ibrahim, L. Prudkin, G. Sánchez, O. Rodríguez, P. Antón, J.-L. Parra and S. Marlow (2013). "RSK3/4 mediate resistance to PI3K pathway inhibitors in breast cancer." The Journal of clinical investigation **123**(6): 2551-2563.

Serra, V., M. Scaltriti, L. Prudkin, P. J. Eichhorn, Y. H. Ibrahim, S. Chandarlapaty, B. Markman, O. Rodriguez, M. Guzman and S. Rodriguez (2011). "PI3K inhibition results in enhanced HER signaling and acquired ERK dependency in HER2-overexpressing breast cancer." Oncogene **30**(22): 2547.

Shah, J. B., D. J. McConkey and C. P. Dinney (2011). "New strategies in muscle-invasive bladder cancer: on the road to personalized medicine." Clinical Cancer Research **17**(9): 2608-2612.

Siegel, R. L., K. D. Miller and A. Jemal (2018). "Cancer statistics, 2018." CA Cancer J Clin **68**(1): 7-30.

Sjödahl, G., M. Lauss, S. Gudjonsson, F. Liedberg, C. Halldén, G. Chebil, W. Månsson, M. Höglund and D. Lindgren (2011). "A systematic study of gene mutations in urothelial carcinoma; inactivating mutations in TSC2 and PIK3R1." PloS one **6**(4): e18583.

Sjödahl, G., M. Lauss, K. Lövgren, G. Chebil, S. Gudjonsson, S. Veerla, O. Patschan, M. Aine, M. Fernö and M. Ringnér (2012). "A molecular

taxonomy for urothelial carcinoma." Clinical cancer research **18**(12): 3377-3386.

Smith, M. C., M. M. Mader, J. A. Cook, P. Iversen, R. Ajamie, E. Perkins, L. Bloem, Y. Y. Yip, D. A. Barda and P. P. Waid (2016). "Characterization of LY3023414, a novel PI3K/mTOR dual inhibitor eliciting transient target modulation to impede tumor growth." Molecular cancer therapeutics **15**(10): 2344-2356.

Spruck, C. H., P. F. Ohneseit, M. Gonzalez-Zulueta, D. Esrig, N. Miyao, Y. C. Tsai, S. P. Lerner, C. Schmütte, A. S. Yang and R. Cote (1994). "Two molecular pathways to transitional cell carcinoma of the bladder." Cancer research **54**(3): 784-788.

Stine, Z. E., Z. E. Walton, B. J. Altman, A. L. Hsieh and C. V. Dang (2015). "MYC, metabolism, and cancer." Cancer discovery **5**(10): 1024-1039.

Stratikopoulos, E. E., M. Dendy, M. Szabolcs, A. J. Khaykin, C. Lefebvre, M.-M. Zhou and R. Parsons (2015). "Kinase and BET inhibitors together clamp inhibition of PI3K signaling and overcome resistance to therapy." Cancer cell **27**(6): 837-851.

Stratikopoulos, E. E. and R. E. Parsons (2016). "Molecular Pathways: Targeting the PI3K Pathway in Cancer—BET Inhibitors to the Rescue." Clinical Cancer Research **22**(11): 2605-2610.

Suh, Y. S., K.-C. Jeong, S.-J. Lee and H. K. Seo (2017). "Establishment and application of bladder cancer patient-derived xenografts as a novel preclinical platform." Translational Cancer Research **6**(4): S733-S743.

Sundararajan, S. and N. J. Vogelzang (2015). "Anti-PD-1 and PD-L1 therapy for bladder cancer: what is on the horizon?" Future Oncology **11**(16): 2299-2306.

Sverrisson, E. F., P. N. Espiritu and P. E. Spiess (2013). "New therapeutic targets in the management of urothelial carcinoma of the bladder." Research and reports in urology **5**: 53.

Thomas, P. and T. G. Smart (2005). "HEK293 cell line: a vehicle for the expression of recombinant proteins." Journal of pharmacological and toxicological methods **51**(3): 187-200.

Tögel, L., R. Nightingale, A. C. Chueh, A. Jayachandran, H. Tran, T. Phesse, R. Wu, O. M. Sieber, D. Arango and A. S. Dhillon (2016). "Dual targeting of bromodomain and extraterminal domain proteins, and WNT or MAPK signaling, inhibits c-MYC expression and proliferation of colorectal cancer cells." Molecular cancer therapeutics **15**(6): 1217-1226.

Trapnell, C., L. Pachter and S. L. Salzberg (2009). "TopHat: discovering splice junctions with RNA-Seq." Bioinformatics **25**(9): 1105-1111.

Turner, P. (2005). "XMGRACE, Version 5.1. 19." Center for Coastal and Land-Margin Research, Oregon Graduate Institute of Science and Technology, Beaverton, OR.

Van Kessel, K. E., T. C. Zuiverloon, A. R. Alberts, J. L. Boormans and E. C. Zwarthoff (2015). "Targeted therapies in bladder cancer: an overview of in vivo research." Nature reviews Urology **12**(12): 681.

Volkmer, J.-P., D. Sahoo, R. K. Chin, P. L. Ho, C. Tang, A. V. Kurtova, S. B. Willingham, S. K. Pazhanisamy, H. Contreras-Trujillo and T. A. Storm (2012). "Three differentiation states risk-stratify bladder cancer into distinct subtypes." Proceedings of the National Academy of Sciences **109**(6): 2078-2083.

von Rundstedt, F.-C., K. Rajapakshe, J. Ma, J. M. Arnold, J. Gohlke, V. Putluri, R. Krishnapuram, D. B. Piyarathna, Y. Lotan and D. Gödde (2016). "Integrative pathway analysis of metabolic signature in bladder cancer: a linkage to the cancer genome atlas project and prediction of survival." The Journal of urology **195**(6): 1911-1919.

Wagle, N., B. C. Grabiner, E. M. Van Allen, A. Amin-Mansour, A. Taylor-Weiner, M. Rosenberg, N. Gray, J. A. Barletta, Y. Guo and S. J. Swanson (2014). "Response and acquired resistance to everolimus in anaplastic thyroid cancer." New England Journal of Medicine **371**(15): 1426-1433.

Wan, J., V. F. Oliver, G. Wang, H. Zhu, D. J. Zack, S. L. Merbs and J. Qian (2015). "Characterization of tissue-specific differential DNA methylation suggests distinct modes of positive and negative gene expression regulation." BMC genomics **16**(1): 49.

Wang, K., M. Li and H. Hakonarson (2010). "ANNOVAR: functional annotation of genetic variants from high-throughput sequencing data." Nucleic acids research **38**(16): e164-e164.

Wang, L., S. Wang and W. Li (2012). "RSeQC: quality control of RNA-seq experiments." Bioinformatics **28**(16): 2184-2185.

Wei, L., S. Chintala, E. Ciamporcero, S. Ramakrishnan, M. Elbanna, J. Wang, Q. Hu, S. T. Glenn, M. Murakami and L. Liu (2016). "Genomic profiling is predictive of response to cisplatin treatment but not to PI3K inhibition in bladder cancer patient-derived xenografts." Oncotarget **7**(47): 76374.

Wolff, E. M., Y. Chihara, F. Pan, D. J. Weisenberger, K. D. Siegmund, K. Sugano, K. Kawashima, P. W. Laird, P. A. Jones and G. Liang (2010). "Unique DNA methylation patterns distinguish noninvasive and invasive

urothelial cancers and establish an epigenetic field defect in premalignant tissue." Cancer research **70**(20): 8169-8178.

Wong, C., Y. Qian and J. Yu (2017). "Interplay between epigenetics and metabolism in oncogenesis: mechanisms and therapeutic approaches." Oncogene **36**(24): 3359.

Wong, Y., S. Litwin, E. Plimack, D. Vaughn, W. Song, S. Cohen, J. Lee, M. Dabrow, H. Tuttle and G. Hudes (2011). "Effect of EGFR inhibition with cetuximab on the efficacy of paclitaxel in previously treated metastatic urothelial cancer." Journal of Clinical Oncology **29**(7_suppl): 243-243.

Wong, Y., S. Litwin and D. Vaughn (2013). "Phase II Trial of Cetuximab With or Without Paclitaxel in Patients With Advanced Urothelial Tract Carcinoma (vol 30, pg 3545, 2012)." JOURNAL OF CLINICAL ONCOLOGY **31**(28): 3612-3612.

Wu, X.-R. (2005). "Urothelial tumorigenesis: a tale of divergent pathways." Nature Reviews Cancer **5**(9): 713.

Xiong, Q., S. Mukherjee and T. S. Furey (2014). "GSAASeqSP: a toolset for gene set association analysis of RNA-Seq data." Scientific reports **4**: 6347.

Zhang, S., M. Hosaka, T. Yoshihara, K. Negishi, Y. Iida, S. Tobita and T. Takeuchi (2010). "Phosphorescent light–emitting iridium complexes serve as a hypoxia-sensing probe for tumor imaging in living animals." Cancer research: 0008-5472. CAN-0009-3948.

Zhang, Y. (2013). "Understanding the gender disparity in bladder cancer risk: the impact of sex hormones and liver on bladder susceptibility to carcinogens." Journal of Environmental Science and Health, Part C **31**(4): 287-304.

Zhao, G., W. T. McMillen, S. Cai, B. Zhao, M. Whitesell, W. Wu, K. Huss, B. Anderson, X.-J. Yuan and S. Jaken (2017). Identifying high quality, potent and selective pyrimidinylthienopyrrolone inhibitors of ERK1/2 kinase: LY3214996, AACR.

Zhao, J. J., Z. Liu, L. Wang, E. Shin, M. F. Loda and T. M. Roberts (2005). "The oncogenic properties of mutant p110α and p110β phosphatidylinositol 3-kinases in human mammary epithelial cells." Proceedings of the National Academy of Sciences of the United States of America **102**(51): 18443-18448.

Zhao, L. and P. K. Vogt (2008). "Helical domain and kinase domain mutations in p110α of phosphatidylinositol 3-kinase induce gain of function by different

mechanisms." Proceedings of the National Academy of Sciences **105**(7): 2652-2657.

Zheng, S. S., J. G. Gao, Z. J. Liu, X. H. Zhang, S. Wu, B. W. Weng, Y. L. Wang, S. C. Hou and B. Jiang (2016). "Downregulation of fatty acid synthase complex suppresses cell migration by targeting phospho‐AKT in bladder cancer." Molecular medicine reports **13**(2): 1845-1850.

Zhitomirsky, B. and Y. G. Assaraf (2016). "Lysosomes as mediators of drug resistance in cancer." Drug Resistance Updates **24**: 23-33.

Zhu, J., J. Blenis and J. Yuan (2008). "Activation of PI3K/Akt and MAPK pathways regulates Myc-mediated transcription by phosphorylating and promoting the degradation of Mad1." Proceedings of the National Academy of Sciences **105**(18): 6584-6589.

Zuber, J., J. Shi, E. Wang, A. R. Rappaport, H. Herrmann, E. A. Sison, D. Magoon, J. Qi, K. Blatt and M. Wunderlich (2011). "RNAi screen identifies Brd4 as a therapeutic target in acute myeloid leukaemia." Nature **478**(7370): 524.

CURRICULUM VITAE

May F. M. Elbanna

EDUCATION

PhD in Pharmacology

Department of Pharmacology and Toxicology

Indiana University, Indianapolis, IN – *Graduated: March 2019*

MSc in Cancer Biology

University College London, London, UK – *Graduated: July 2013*

MSc in Clinical Oncology and Nuclear Medicine

Mansoura University, Mansoura, Egypt – *Graduated: May 2012*

Bachelor of Medicine and Surgery (M.B.B.Ch)

Very Good with Honors

Faculty of Medicine, Mansoura University, Egypt – *Graduated: November 2006*

PROFESSIONAL EXPERIENCE

Graduate Research Assistant – Department of Pharmacology and Toxicology, Indiana University School of Medicine, Indianapolis, IN - *August 2015 – December 2018*

Graduate Research Assistant – Department of Pharmacology and Molecular Cancer Therapeutics, Roswell Park Cancer Institute, Buffalo, NY- *August 2013 – August 2015*

Resident Doctor – Department of Clinical Oncology and Nuclear Medicine, Mansoura University, Mansoura, Egypt - *October 2008 - July 2012*

General Practitioner – Al-Montazah Primary Healthcare unit- Egyptian Department of Health, New Damietta, Egypt- *March 2008 - October 2008*

Medical Intern (Transitional Internship Year-PGY1) – Demerdash University Hospital – Ain Shams University, Cairo, Egypt- *March 2007 - March 2008*

RESEARCH EXPERIENCE

PhD Candidate – Supervisor: Professor. Dr. Roberto Pili

Department of Pharmacology and Toxicology – IU Simon Cancer Center , Department of Hematology/Oncology, Indiana University School of Medicine, Indianapolis, IN - *August 2015 – December 2018*

Research Focus:

- Drug Development in Bladder cancer management (Mechanisms of resistance to PI3K targeted therapy in bladder cancer- in collaboration with Lilly)
- Development of antibodies that target tumor associated macrophages (+/- androgen blockade therapy) in the management of prostate cancer-in collaboration with Syndax
- Diet studies in syngeneic mice models of various GU malignancies (prostate/Renal) to study the effect of diet on enhancing the therapeutic efficiency of immunotherapies

Graduate Research Assistant – Supervisor: Assistant. Professor. Hannelore Heemers

Department of Pharmacology and Molecular Cancer Therapeutics, Roswell Park Cancer Institute, Buffalo, NY- *December 2013 – April 2014*

Research Focus:

- Validate the role of serum response factor in driving resistance to Androgen Deprivation Therapy in prostate cancer cell lines.

Graduate Research Assistant – Supervisor: Professor. Candace Johnson

Department of Pharmacology and Molecular Cancer Therapeutics, Roswell Park Cancer Institute, Buffalo, NY- *July 2013 – December 2013*

Research Focus:

- Study the role of Vitamin D in sensitizing bladder cancer cell lines to cisplatin treatment.

Research Assistant – Supervisor: Professor. Sibylle Mittnacht

University College London, London, UK – *July 2012 - July 2013*

Research Focus:

- Validation of Ki-67 as a clinically applicable readout for the synergistic combination of PD-0332991 with crizotinib in the treatment of a panel of cancer cell lines

Research Assistant – Supervisor: Professor. Hanem Sakr

Department of Clinical Oncology and Nuclear Medicine, Faculty of Medicine, Mansoura, Egypt – *October 2008 – April 2012*

Research Focus:

- Retrospective literature Review **-** Problems In Pediatric Tumors management (late effects of radiation therapy and survivorship issues)

TEACHING EXPERIENCE

Mentoring masters and summer rotation students. Department of Pharmacology and Toxicology, Indiana University School of Medicine, Indianapolis, IN – *August 2015 – December 2018*

Techniques taught:

- In vivo mouse models handling
- Molecular Biology Techniques (Western Blotting, qPCR)
- Immunohistochemistry
- In vitro tissue culture training

PUBLICATIONS

- **Elbanna, M**., Chintala, S., Ciamporcero, E., Adelayie, R., Orillion, A., Arisa, S., ... & Pili, R. (2019). Therapeutic targeting of the PI3K/RAS/MYC axis in muscle invasive bladder cancer. *Molecular cancer therapeutics. (Under Preparation)*
- **Elbanna, M.**, Orillion, A., Damayanti, N., Adelaiye-Ogala, R., ….&Pili, R. (2019). Dual inhibition of angiopoietin-TIE2 and MET alters the tumor microenvironment and prolongs survival in a metastatic model of renal cell carcinoma. *Molecular cancer therapeutics. (Under Review)*
- Jerde, TJ., Xia, H., McGeown, J., McIlwain, D., **Elbanna, M**., Craft, A., Sandusky, GE., Kaimakliotis, H., Althouse, S., Pili, R., Kelley, MR., Fishel, ML.. Anti-tumor activity and characterization of APE1/Ref-1 inhibitors in bladder cancer (2019). *Molecular cancer therapeutics. (Under Preparation)*
- Orillion, A., Damayanti, N., Shen, L.,…, **Elbanna, M.**, ….., and Pili,R. (2018). Dietary protein restriction reprograms tumor associated macrophages and enhances immunotherapy. *Clinical Cancer Research*, 24(24): p. 6383-6395.

- Damayanti, N., Budka, J.,……. **Elbanna, M.,** …..& Pili, R. (2018). Therapeutic targeting of TFE3/IRS-1/PI3K/mTOR axis in translocation renal cell carcinoma. *Clinical Cancer Research, 24(23): 5977-5989.*
- Damayanti, N., Budka, J.,……. **Elbanna, M.,** …..& Pili, R. (2018). Therapeutic targeting of TFE3/IRS-1/PI3K/mTOR axis in translocation renal cell carcinoma. *Clinical Cancer Research, 24(23): 5977-5989.*
- Wei, L., Chintala, S., Ciamporcero, E., Ramakrishnan, S., **Elbanna, M.,** Wang, J., ... & Gomez, E. C. (2016). Genomic profiling is predictive of response to cisplatin treatment but not to PI3K inhibition in bladder cancer patient-derived xenografts. *Oncotarget, 7(47), 76374., 2015, 58, 5015-5027*
- **Elbanna, M.,** & Heemers, H. V. (2014). Alternative approaches to prevent androgen action in prostate cancer: are we there yet*. Discovery medicine, 17(95), 267-274.*

PUBLISHED ABSTRACTS

- **Elbanna, M.,** Damayanti,N., Chintala,S., Pili.,R.. PIK3CA E542K mutation in bladder cancer confers resistance to PI3K targeted therapy but synergy with BET inhibition. *Proceedings of the American Association for Cancer Research Annual Meeting 2018. 2018, Jul; 78(13 Suppl): Abstract nr 1825.*
- **Elbanna, M.,** Chintala, S., Ciamporcero, E., Adelayie, R., Orillion, A., Arisa, S., ... & Pili, R. (2017). In vitro modeling of patient derived bladder

cancer cell lines in 3D culture systems [abstract]. *Proceedings of the American Association for Cancer Research Annual Meeting 2017; 2017 Apr 1-5; Washington, DC. Philadelphia (PA): AACR; Cancer Res 2017; 77(13 Suppl): Abstract nr 5783.*

- **Elbanna, M.,** Ciamporcero, E., Adelaiye, R., Orillion, A., Chintala, S., & Pili, R. (2016). Differential response to a dual PI3K/mTOR inhibitor in PIK3CA mutant urothelial cancer patient derived xenografts. [abstract]. *In: Proceedings of the 107th Annual Meeting of the American Association for Cancer Research; 2016 Apr 16-20; New Orleans, LA. Philadelphia (PA): AACR; Cancer Res 2016; 76(14 Suppl): Abstract nr 384.*
- **Elbanna, M.,** Ciamporcero, E., Ramakrishnan, S., Adelaiye, R., Shen, L., Orillion, A., . . . Pili, R. (2015).Characterization of patient-derived bladder cancer xenografts: role of xCT in response to cisplatin. [abstract]. In: *Proceedings of the 106th Annual Meeting of the American Association for Cancer Research; 2015 Apr 18-22; Philadelphia, PA. Philadelphia (PA): AACR; Cancer Res 2015; 75(15 Suppl): Abstract nr 1462.*

POSTER PRESENTATIONS

- **Elbanna, M.,** Chintala, S., Ciamporcero, E., ... & Pili (2017).Understanding epigenetic determinants of response to PI3K targeted therapy in PIK3CA driven bladder cancer. Poster presented at **IU Cancer Research Day 2017. <u>Best poster award (4th Place), Basic Science section.</u>**

- **Elbanna, M.,** Chintala, S., Ciamporcero, E., Adelayie, R., Orillion, A., Arisa, S., ... & Fishel, M. In vitro modeling of patient derived bladder cancer cell lines in 3D culture systems (2017). Poster presented at **AACR 2017**. **Best 3D culture poster award, Corning**.
- **Elbanna, M.,** Ciamporcero, E., Adelaiye, R., Orillion, A., Chintala, S., & Pili, R. (2016). Differential response to a dual PI3K/mTOR inhibitor in PIK3CA mutant urothelial cancer patient derived xenografts. Poster presented at **AACR 2016 and IU Cancer Research Day 2016**. **Best Poster award (3rd Place), translational Science Section**
- **Elbanna, M.,** Ciamporcero, E., Ramakrishnan, S., Adelaiye, R., Shen, L., Orillion, A., ... & Pili, R. (2015). Characterization of patient-derived bladder cancer xenografts: role of xCT in response to cisplatin. **Poster presented at AACR 2015.**

ORAL PRESENTATIONS

- **Elbanna, M. (July 2017).** Differential response to a dual PI3K/mTOR inhibitor in PI3KCA mutant urothelial cancer patient derived xenografts. Indiana Basic Urologic Research (IBUR) meeting. Indianapolis, IN.
- **Elbanna, M. (October 2016).** Understanding resistance to PI3K targeted therapy in bladder cancer Management. MD Anderson Cancer Center. ”Symposium on Cancer Evolution: Mechanisms of Vulnerability and Resistance.” Houston, TX.

- **Elbanna, M. (October 2014).** Student Seminar presentation. Paper discussion: Rebouissou, S., et al. (2014). "EGFR as a potential therapeutic target for a subset of muscle-invasive bladder cancers presenting a basal-like phenotype." Science translational medicine 6(244): 244ra291-244ra291. Roswell Park Cancer Institute, Buffalo, NY.
- **Elbanna, M. (March 2014).** Student Seminar presentation. Paper discussion: Korpal, M., et al. (2013). "An F876L mutation in androgen receptor confers genetic and phenotypic resistance to MDV3100 (enzalutamide)." Cancer discovery 3(9): 1030-1043. Roswell Park Cancer Institute, Buffalo, NY.

PROFESSIONAL MEMBERSHIPS

2014- Present	Member, The American Association of Cancer Research (AACR)
2014- Present	Member, The American Society of Clinical Oncology (ASCO)
2007-Present	Member, Egyptian Medical Syndicate (EMS)

FELLOWSHIPS AND AWARDS

- **Paradise Travel Award-** Department of Pharmacology and Toxicology, IUSM- *January 2018*
- **Best Poster Award-** IU Cancer Research Day (3rd place, Translational science section)- *May 2018*

- **Best Poster Award-** IU Cancer Research Day (4th place, Basic science section)- *May 2017*
- **Fulbright Foreign student Award-** Fellowship to conduct doctoral research in the United States- *August 2013-2016*
- **O'Brien Fellowship for biological microscopy (IU)-** Fellowship towards training and free usage of IU confocal microscopy facilities for imaging of 3D culture developed for Bladder cancer- *July2016-2018*
- **Nominated by IU for the HHMI pre-doctoral Award-** *November 2016*
- **Young Investigator Travel Fellowship-** MD Anderson Cancer Center. "Symposium on Cancer Evolution: Mechanisms of Vulnerability and Resistance" Houston, TX- *October 2016*
- **Best Poster Award Best Poster Award-** IU Cancer Research Day (3rd place, translational science section)- *May 2016*
- **University College London-Global Excellence Award-** Award for MSc Degree tuition expenses- *August 2012-2013*
- **Arab-British Chamber Charitable Foundation (ABCCF) Bursary-** Award for MSc Degree tuition expenses- *August 2012-2013*
- **Certificate of excellence as Intern/PGY1-** Department of Pediatrics; Neonatology Division, Ain Shams university, Cairo, Egypt- *May 2008*
- **Fellowship from the International Federation of Medical Students Associations (IFMSA)-** to conduct clinical clerkship training in Department of Ophthalmology, Oviedo, Spain- *August 2004*

- **Fellowship from the International Federation of Medical Students Associations (IFMSA)-** to conduct clinical clerkship training in Department of Pediatrics, Pisa, Italy- *July 2003*

EXTRACURRICULAR ACTIVITIES

Volunteer translator at Dar Al Tarjama- *March 2007- September 2008*

- An initiative concerned with translating remarkable Arabic works to English and vice versa as means of mutual cultural understanding.

Volunteer at Bridges foundation- *March 2007- September 2008*

- An initiative concerned with creating bridges between nations through outreach workshops and cultural events.
- I volunteered in organization of workshops and in translating their website into French.

Volunteer in the organization of the Arab universities' youth week held in Mansoura University, Egypt- *January 2006*

Volunteer in the organization of the Egyptian universities' youth week held in Mansoura University, Egypt- *January 2005*

COMMUNITY SERVICES AND OUTREACH PROGRAMS

Fund raising in department of clinical oncology, Mansoura University Hospitals, Mansoura, Egypt- *April 2011*

- Fundraising was initiated for buying new treatment chairs in the outpatient chemotherapy unit and buying a new Gamma camera at our center)

Outreach cancer screening campaign, Mansoura University Hospitals, Mansoura, Egypt- *January 2010*

- Arranged by the faculty of medicine, Mansoura university (Egypt) in ''Meniet Elnasr; rural region in our province''

Volunteer at the ''Dakahliya Cancer Patients' Association'', Mansoura, Egypt- *October 2008-2012*

- **Responsibilities:** One on one assessment of individual cancer cases that need financial and/or psychological support.

Volunteer at ''Mazeed Charitable Organization'', Cairo, Egypt- *March 2007- 2008*

- Concerned with providing financial and social support for the less privileged areas of Cairo as in Elzawya elhamra and Ezbet Khairallah.

Outreach medical campaign, faculty of medicine, Mansoura University – *Mansoura, Egypt-* *March 2006*

- The campaign offered primary medical care to border regions in southern Egypt (Marsa Alam, Halayeb and Shalateen)